

72-469

CASPERSON, Lee Wendel, 1944-
MODES AND SPECTRA OF HIGH GAIN LASERS.

California Institute of Technology, Ph.D.,
1971
Physics, optics

University Microfilms, A XEROX Company, Ann Arbor, Michigan

(c) 1971

Lee Wendel Casperson

ALL RIGHTS RESERVED

MODES AND SPECTRA
OF
HIGH GAIN LASERS

Thesis by
Lee Wendel Casperson

In Partial Fulfillment of the Requirements
For the Degree of
Doctor of Philosophy

California Institute of Technology
Pasadena, California

1971

PLEASE NOTE:

**Some Pages have indistinct
print. Filmed as received.**

UNIVERSITY MICROFILMS

Acknowledgments

The author is pleased to acknowledge the interest and support in this research from Professor Amnon Yariv. I have also enjoyed many stimulating discussions with Mr. Desmond Armstrong in addition to his excellent technical assistance. I am grateful too to the other people associated with the Quantum Electronics Laboratory for occasional helpful discussions and for tolerance when my research required more than its fair share of the laboratory equipment.

I also wish to acknowledge financial support during the course of this work from the Tektronix Foundation, the NASA Foundation, and Caltech.

Abstract

This research has dealt with various problems related to high gain lasers including: gain and dispersion focusing of the transverse modes, mode pulling and mode splitting of the longitudinal modes, ultrashort pulse propagation, relaxation oscillations, spectral narrowing, dispersion effects on the oscillation line width, and a saturation and power formalism for high gain lasers. Most of these subjects had not been treated previously and it is found that the properties of high gain lasers may differ drastically from the properties of similar low gain lasers. Besides the theoretical treatment of these subjects, experimental verification has been obtained whenever possible. The experiments were conducted using 3.51 micron xenon lasers.

Table of Contents

Part	Title	Page
I	Introduction	1
II	Saturation Theory	
	2.1 Introduction	5
	2.2 The coherent rate equations	5
	2.3 The incoherent rate equations	11
	2.4 Steady state solutions	16
	2.5 Homogeneous broadening	26
	2.6 Inhomogeneous broadening	29
	2.7 Spectral hole burning	37
	2.8 Conclusion	46
	Bibliography	48
III	The 3.51 Micron Xenon Laser	
	3.1 Introduction	50
	3.2 Homogeneous linewidth	52
	3.3 Inhomogeneous linewidth	54
	3.4 Hyperfine structure	56
	3.5 Isotope shifts	65
	3.6 Conclusion	68
	Bibliography	70
IV	Longitudinal Modes	
	4.1 Introduction	72
	4.2 Inhomogeneous broadening	73
	4.3 Homogeneous broadening	80

Part	Title	Page
IV	Longitudinal Modes (con't.)	
	4.4 Saturation effects	83
	4.5 Experiment	89
	4.6 Profile effects	98
	4.7 Conclusion	102
	Bibliography	103
V	Transverse Modes	
	5.1 Introduction	104
	5.2 Beam modes	106
	5.3 The beam parameter	114
	5.4 Lenslike media	117
	5.5 Beam matrices	125
	5.6 Resonator modes	129
	5.7 Gain Focusing experiment	140
	5.8 Dispersion focusing theory	146
	5.9 Dispersion focusing experiment	158
	5.10 The cylindrical laser	163
	5.11 Conclusion	172
	Bibliography	173
VI	Relaxation Oscillations	
	6.1 Introduction	174
	6.2 The inhomogeneous frequency equation	175
	6.3 Solutions of the frequency equation	183
	6.4 Time domain experiment	191
	6.5 Frequency domain experiment	201

Part	Title	Page
VI	Relaxation Oscillations (con't.)	
	6.6 Coherence effects	208
	Bibliography	216
VII	Oscillation Line Width	
	7.1 Introduction	218
	7.2 Oscillation line width	220
	7.3 Dispersion effects	229
	7.4 Saturation effects	233
	7.5 Experiment	240
	7.6 Conclusion	244
	Bibliography	245
VIII	Spectral Narrowing	
	8.1 Introduction	246
	8.2 Unsaturated amplifiers	248
	8.3 Saturation effects	257
	8.4 Oscillators	266
	8.5 Conclusion	269
	Bibliography	270
IX	Ultrashort Pulses	
	9.1 Introduction	271
	9.2 Mode locking theory	273
	9.3 Mode locking experiment	276
	9.4 Pulse propagation	286
	9.5 Conclusion	290

Part	Title	Page
IX	Ultrashort Pulses (con't)	
	Bibliography	292
X	Power in Laser Oscillators	
	10.1 Introduction	293
	10.2 Zero dimensions	295
	10.3 One dimension	300
	10.4 Gaussian modes in three-dimensional lasers	311
	10.5 Experiment	318
	10.6 Conclusion	322
	Bibliography	323

I. Introduction

A conventional laser oscillator consists basically of a medium which amplifies light located in a mirror arrangement which provides positive feedback. The most important ingredient is the amplifying medium, and it is necessary that the gain of this amplifier exceed the losses of the optical cavity. The first lasers employed very high-Q cavities enclosing media with single-pass gains of at most a few percent.

Since the early lasers were low gain devices, the corresponding theoretical developments are mostly suitable only for analysis of the properties of such low gain lasers. It turns out that the assumption of small single pass gain leads to a dramatic simplification of the equations governing laser performance. More recently a variety of lasers have been developed which have single-pass gains of several orders of magnitude. For the most part, the low gain theories can not be applied to high gain lasers with any assurance of even qualitative agreement.

The purpose of this thesis is to set down in a fairly systematic and rigorous fashion a theoretical treatment of some of the more interesting and important aspects of the behavior of high gain lasers. As far as possible the conclusions are verified experimentally using a high gain xenon laser. In many cases high gain lasers may exhibit new effects which could not be anticipated from the low gain theories and experiments. The subject of high gain lasers is extremely broad and this treatment is not intended to be exhaustive. We have attempted to demonstrate the basic principles underlying a variety of significant

high gain laser problems.

In Chapter II are derived the basic saturation equations for the gain and index of refraction, which are useful for the theoretical work of the succeeding chapters. It is precisely the unusual properties of the gain and index of refraction in high gain media which lead to the interesting optical behavior of lasers containing such media. This chapter is included because many of the specialized saturation treatments in the literature are either so elementary as to miss important effects or so general as to be mostly unintelligible.

Chapter III is an investigation of some of the properties of the high gain 3.51 micron transition in xenon. This is one of the highest gain gas laser transitions known, and all of our experiments were conducted using a xenon laser. Because of its narrow line width, the 3.51 micron transition also exhibits extreme anomalous dispersion. On the basis of these investigations it is concluded that greater gain should be attainable in a properly designed xenon laser than has yet been reported.

The remaining chapters contain theoretical and experimental results relevant to specific high gain laser phenomena. The theory is specialized as necessary to show the effects of interest with a minimum of mathematical obfuscation. Supporting experimental evidence is included. Because of the relative independence of these chapters, there is a brief concluding section with each but no concluding chapter at the end of the thesis. Also, there is no particular significance to the ordering of the chapters.

Chapter IV is a discussion of the effects of strong anomalous

dispersion on the longitudinal modes of a laser oscillator. In ordinary low gain lasers mode pulling effects may either be ignored or treated as a perturbation. In high gain lasers, on the other hand, the longitudinal mode spectra may be entirely different from the spectra of low gain lasers. A new mode splitting effect is anticipated in which three different frequencies occur at the same wavelength in the laser medium. Experimentally, we have observed a much greater mode pulling than has previously been reported in good agreement with the theory.

The effects of a simple radial gain profile on the transverse laser modes are investigated in Chapter V with particular emphasis on gain and dispersion focusing effects. We have also obtained experimental verification of the focusing theory. A useful matrix method for calculating the modes of a resonator containing a lenslike medium is described in some detail. A discussion is also included on the modes of a new and potentially useful cylindrical resonator geometry.

In Chapter VI is a fairly thorough consideration of relaxation oscillations in laser oscillators including the effects of inhomogeneous broadening. The observation of undamped relaxation oscillations in a xenon laser is also reported. Experiments have been conducted in both the time and frequency domains, and good agreement with the theory has been obtained.

A treatment of the oscillation linewidth of a high gain laser is given in Chapter VII. Previous analyses of the laser linewidth have all assumed that the gain per pass was small. Here we derive the linewidth of a high gain laser including dispersion. A line broadening effect resulting from hole burning is discussed qualitatively, and supporting

experimental evidence is presented.

The basic ideas of spectral narrowing in laser amplifiers are well known, but a reasonably detailed theoretical study has not been given previously. In Chapter VIII is an analysis of spectral narrowing in homogeneous and inhomogeneous amplifiers including the effects of saturation. It is found that saturation slows the narrowing in a homogeneous amplifier and causes a broadening of the spectrum in an inhomogeneous amplifier.

In Chapter IX are reported some experiments with the spontaneous mode-locking of the xenon laser. Ultrashort pulses have been observed with a wide range of pulse widths and repetition rates in agreement with theory. These pulses are found to propagate through the xenon amplifier with velocities less than the vacuum speed of light by as much as a factor of 2.5 in good agreement with the theoretical group velocity of a dispersive medium. Previous experiments using low gain lasers had only shown a deviation from the speed of light of less than a part in a thousand.

Conventional treatments of the power in saturated laser oscillators usually assume that the radiation fields and amplifying media are spatially uniform. This is an extremely poor approximation in high gain lasers. In Chapter X we derive some useful conservation rules and saturation formulas which are valid in high gain lasers. Simple expressions are obtained for the output power of a high gain laser oscillator, and experimental evidence is included.

II. Saturation Theory

2.1 Introduction

The purpose of this chapter is to develop the gain and saturation formalism which will be the basis for most of the calculations of the succeeding chapters. Initially the treatment is quite general. Rate equations are developed for the interaction of a time varying electromagnetic field with a laser medium having an arbitrary coherence time and an arbitrary inhomogeneous line width. For most of the situations which we have studied the coherence effects may be neglected. The coherent rate equations should, however, be useful in other applications such as the study of short pulse propagation.

The coherent rate equations reduce to the much simpler incoherent rate equations if the fields vary sufficiently slowly. The basic results for the gain and index of refraction of a saturating high gain laser medium are obtained from the steady state solutions of the incoherent rate equations. The importance of level degeneracy is discussed. The results are then specialized to the forms that will be useful in later chapters with considerations of the limits of homogeneous and inhomogeneous broadening. A section is also included on spectral hole burning.

2.2 The coherent rate equations

The purpose of this section is to develop the equations governing the population inversion and electromagnetic field in a laser, including the effects of atomic coherence and inhomogeneous broadening. In terms of the familiar density matrix formalism for a two level system, the equations governing the atoms in states a and b in the presence of the

electric field $E(t, z)$ may be written

$$\frac{\partial}{\partial t} (\rho_{aa} - \rho_{bb}) = p - \frac{2i\mu E(t, z)}{\hbar} (\rho_{ab} - \rho_{ba}) - \frac{(\rho_{aa} - \rho_{bb})}{T_1} \quad (2.2-1)$$

$$\frac{\partial}{\partial t} \rho_{ab} = -i\omega \rho_{ab} - \frac{i\mu E(t, z)}{\hbar} (\rho_{aa} - \rho_{bb}) - \frac{\rho_{ab}}{T_2} \quad (2.2-2)$$

$$\rho_{ba} = \rho_{ab}^* \quad (2.2-3)$$

Here T_1 and T_2 may be regarded as phenomenological relaxation times. T_1 represents the spontaneous decay time of the excited state and T_2 is the transverse coherence time. p is the rate of excitation and $\mu = e r_{ab}$ is the dipole matrix element. Equations (2.2-1) to (2.2-3) hold for any particular class of atoms in an inhomogeneously broadened medium. These equations are similar to equations (25) and (26) of Lamb except for the notation and inclusion of a pumping term. The restriction to a two level system is only done by convention for convenience. Some generalizations will be treated in later sections.

If the atoms are distributed in frequency according to the function $f(\omega)$, then the macroscopic polarization is given by

$$P' = \mu N \int_0^\infty d\omega f(\omega) [\rho_{ab}(\omega, t, z) + \rho_{ba}(\omega, t, z)] \quad (2.2-4)$$

where N is the total density of atoms and the frequency is related to the energy levels by $\omega = (E_a - E_b)/\hbar$. The electric field and polarization are assumed to be time harmonic at the frequency ω_ℓ in the form

$$E(t, z) = E(t, z) \cos(kz - \omega_\ell t) \quad (2.2-5)$$

$$P'(t, z) = S(t, z) \sin(kz - \omega_\ell t) + C(t, z) \cos(kz - \omega_\ell t) \quad (2.2-6)$$

where $E(t, z)$, $S(t, z)$, and $C(t, z)$ are slowly varying functions of time and space. In writing the field and polarization in this form we implicitly assume that the phase is constant. This approximation will be considered later. Also, only a one dimensional geometry is considered. Some effects of spatial variations are treated in chapters V and X.

Equation (2.2-2) is a linear first order differential equation which can be integrated^(2.2) to obtain

$$\rho_{ab} = -\frac{i\mu}{2\hbar} \int_{-\infty}^t e^{-\frac{t-t'}{T^2}} e^{-i\omega(t-t')} E(t', z) (\rho_{aa} - \rho_{bb}) dt' \quad (2.2-7)$$

Substituting equation (2.2-5) in equation (2.2-7) and neglecting nonsynchronous terms leads to

$$\rho_{ab} = -\frac{i\mu}{2\hbar} e^{i(kz - \omega_\ell t)} \int_{-\infty}^t E(t', z) e^{-\frac{t-t'}{T^2}} e^{-i(\omega - \omega_\ell)(t-t')} (\rho_{aa} - \rho_{bb}) dt' \quad (2.2-8)$$

Then from equation (2.2-4) the macroscopic polarization is found to be

$$P' = \frac{\mu^2 N}{\hbar} \int_0^\infty d\omega f(\omega) \int_{-\infty}^t E(t', z) e^{-\frac{t-t'}{T^2}} \sin[(kz - \omega_\ell t) - (\omega - \omega_\ell)(t-t')] (\rho_{aa} - \rho_{bb}) dt' \quad (2.2-9)$$

Therefore, the sine component $S(t, z)$ and cosine component $C(t, z)$ of the polarization are given by

$$S(t, z) = \frac{\mu^2 N}{\pi} \int_0^\infty d\omega f(\omega) \int_{-\infty}^t E(t', z) e^{-\frac{T-t'}{2}} \cos[(\omega - \omega_\ell)(t-t')] (\rho_{aa} - \rho_{bb}) dt' \quad (2.2-10)$$

$$C(t, z) = -\frac{\mu^2 N}{\pi} \int_0^\infty d\omega f(\omega) \int_{-\infty}^t E(t', z) e^{-\frac{T-t'}{2}} \sin[(\omega - \omega_\ell)(t-t')] (\rho_{aa} - \rho_{bb}) dt' \quad (2.2-11)$$

The response of the electromagnetic field to the polarization of equations (2.2-10) and (2.2-11) is determined by the one-dimensional wave equation, which in mks units may be written

$$-\frac{\partial^2 E}{\partial z^2} + \frac{1}{c'^2} \frac{\partial^2 E}{\partial t^2} = -\frac{1}{\epsilon c'^2} \frac{\partial^2 P'}{\partial t^2} \quad (2.2-12)$$

where c' is the velocity of light in the medium neglecting resonance effects associated with the transition. Substituting equations (2.2-5) and (2.2-6) leads to

$$k = \frac{\omega_\ell}{c'} \sqrt{1 + \frac{c}{\epsilon E}} \approx \frac{\omega_\ell}{c} \left(n_0 + \frac{n_0 c}{2\epsilon E} \right) = \frac{\omega_\ell n}{c} \quad (2.2-13)$$

and

$$\frac{\partial E}{\partial z} + \frac{n_0}{c} \frac{\partial E}{\partial t} = \frac{\omega_\ell n_0 S}{2\epsilon c} \quad (2.2-14)$$

where the field and polarization components are assumed to vary slowly in time compared to an optical cycle and slowly in space compared to a wavelength. The free space speed of light is c , the nonresonant index of refraction is n_0 , and the total index of refraction is n . Evidently

the propagation "constant" k is generally a function of E , whereas in our derivation it was assumed to be constant. This additional approximation which is believed to be valid for our work, essentially involves the neglect of small fluctuating phase terms as discussed by Close^(2.3,2.4). Moreover, for radiation at line center the in-phase component of polarization vanishes identically as we now show.

If equation (2.2-8) is substituted in equation (2.2-1) and nonsynchronous terms are neglected, one finds that the excitation is governed by

$$\frac{\partial}{\partial t}(\rho_{aa} - \rho_{bb}) = p - \frac{u^2}{\hbar^2} E(t, z) \int_{-\infty}^t E(t', z) e^{-\frac{|t-t'|}{T^2}} \cos[(\omega - \omega_\ell)(t-t')] (\rho_{aa} - \rho_{bb}) dt' \frac{\rho_{aa} - \rho_{bb}}{T_1} \quad (2.2-15)$$

Therefore, the excitation density is symmetrical about the optical frequency ω_ℓ . Then if the atomic distribution $f(\omega)$ is also symmetrical about ω_ℓ , $C(t, z)$ will be zero according to equation (2.2-11) because $\sin(\omega - \omega_\ell)(t-t')$ is antisymmetric about ω_ℓ . Thus for radiation at the center of a symmetric pumping line the phase is constant. The stability of this situation has been considered by Hopf and Scully^(2.5).

Equations (2.2-10), (2.2-11), (2.2-13), and (2.2-14) may be combined to yield

$$\frac{\partial E}{\partial z} + \frac{n_0}{c} \frac{\partial E}{\partial t} = \frac{\omega_\ell n_0 u^2 N}{2\epsilon c \hbar} \int_0^\infty d\omega f(\omega) \int_{-\infty}^t E(t', z) e^{-\frac{|t-t'|}{T^2}} \cos[(\omega - \omega_\ell)(t-t')] (\rho_{aa} - \rho_{bb}) dt' \quad (2.2-16)$$

$$n-n_0 = -\frac{n_0^2 N}{2\epsilon E \hbar} \int_0^\infty d\omega f(\omega) \int_{-\infty}^t E(t', z) e^{-\frac{T^2}{2}} \sin[(\omega - \omega_\ell)(t-t')] (\rho_{aa} - \rho_{bb}) dt' \quad (2.2-17)$$

It is useful to change to the frequency variable v and to introduce

the population inversion density $n(v, t, z) = Nf(v)[\rho_{aa}(v, t, z) - \rho_{bb}(v, t, z)]$,

the frequency independent "Einstein coefficient" $B_0 = \frac{n_0^2 \mu^2}{2c\epsilon \hbar^2}$, and the

pumping rate $P(v) = pNf(v)$. The same letter n is used to designate both the population inversion and the index of refraction, but the refractive index appears only in the $n-n_0$ on the left side of the equations so that confusion is unlikely. In terms of these definitions equations (2.2-15) to (2.2-17) become respectively

$$\frac{\partial}{\partial t} n(v, t, z) = P(v) - \frac{2cB_0 \epsilon E(t, z)}{n_0} \int_{-\infty}^t E(t', z) e^{-\frac{T^2}{2}} \cos[2\pi(v - v_\ell)(t-t')] n(v, t', z) dt' - \frac{n(v, t, z)}{T_1} \quad (2.2-18)$$

$$\frac{\partial E}{\partial z} + \frac{n_0}{c} \frac{\partial E}{\partial t} = B_0 h v_\ell \int_0^\infty dv \int_{-\infty}^t E(t', z) e^{-\frac{T^2}{2}} \cos[2\pi(v - v_\ell)(t-t')] n(v, t', z) dt' - \frac{\alpha E}{2} \quad (2.2-19)$$

$$n-n_0 = -\frac{cB_0 h}{E} \int_0^\infty dv \int_{-\infty}^t E(t', z) e^{-\frac{T^2}{2}} \sin[2\pi(v - v_\ell)(t-t')] n(v, t', z) dt' \quad (2.2-20)$$

A loss term has been included in equation (2.2-19).

Equations (2.2-18) to (2.2-20) are the primary results of this section. We refer to them as the inhomogeneous coherent rate equations

because they may be regarded as a generalization of the more familiar rate equations to include inhomogeneous broadening and coherence effects. These equations should be useful in problems involving short pulse propagation, echoes, and high frequency relaxation phenomena. This form of the results has a greater intuitive appeal than the equations of Hopf and Scully^(2.5) involving symmetric and antisymmetric susceptibility functions. Evidently the inversion, gain, and refractive index depend on the history of the system for a time of roughly T_2 into the past.

2.3 The incoherent rate equations

For slowly varying fields the rate equations simplify greatly. In this section the conditions are considered under which these simplifications can be made. Also, the results are generalized to include four level laser media interacting with optical fields at many frequencies.

The exponentials in equations (2.2-18) to (2.2-20) cut off the time integrations for times much greater than T_2 into the past. Consequently, if the field and inversion vary negligibly in the time T_2 , they may be brought outside of the time integrals. The remaining integrals can be performed according to

$$\begin{aligned} & \int_{-\infty}^t e^{-\frac{t-t'}{T_2}} \cos[2\pi(v-v_\ell)(t-t')] dt' \quad \tau = t - t' \\ &= \int_0^\infty e^{-\frac{\tau}{T_2}} \cos[2\pi(v-v_\ell)\tau] d\tau = \frac{T_2}{1 + [2\pi(v-v_\ell)T_2]^2} \end{aligned} \quad (2.3-1)$$

and

$$\begin{aligned}
 & \int_{-\infty}^{t - \frac{t-t'}{T_2}} e^{-\frac{t-t'}{T_2}} \sin[2\pi(v-v_g)(t-t')] dt' \\
 &= \int_0^{\infty} e^{-\frac{\tau}{T_2}} \sin[2\pi(v-v_g)\tau] d\tau \\
 &= \frac{[2\pi(v-v_g)T_2]T_2}{1 + [2\pi(v-v_g)T_2]^2} \tag{2.3-2}
 \end{aligned}$$

It is also useful to define the homogeneous line width Δv_h as

$$\Delta v_h = \frac{1}{\pi T_2} \tag{2.3-3}$$

and the frequency dependent Einstein coefficient

$$B(v, v_g) = B_0 \frac{\left(\frac{2}{\pi \Delta v_h}\right)}{1 + \left[\frac{2(v - v_g)}{\Delta v_h}\right]^2} \tag{2.3-4}$$

Use of equations (2.3-1) to (2.3-4) reduces the coherent rate equations (2.2-18) to (2.2-20) to the much simpler form

$$\frac{\partial n}{\partial t}(v, t, z) = P(v) - \frac{ce E^2}{n_0} n(v, t, z) B(v, v_g) - \frac{n(v, t, z)}{T_1} \tag{2.3-5}$$

$$\frac{\partial E}{\partial z} + \frac{n_0}{c} \frac{\partial E}{\partial t} = \frac{hv_g E}{2} \int_0^{\infty} n(v, t, z) B(v, v_g) dv - \frac{\alpha E}{2} \tag{2.3-6}$$

$$n - n_0 = - \frac{ch}{4\pi} \int_0^{\infty} n(v, t, z) B(v, v_g) \left(\frac{2(v - v_g)}{\Delta v_h} \right) dv \tag{2.3-7}$$

We refer to these as the incoherent rate equations. It is useful further to introduce the intensity $I = \frac{c\epsilon E^2}{n_0}$ and to write the lifetime as $T_1 = \tau$. With these definitions equations (2.3-5) to (2.3-7) become

$$\frac{\partial n}{\partial t}(v, t, z) = P(v) - B(v, v_\ell) I(t, z) n(v, t, z) - \frac{n(v, t, z)}{\tau} \quad (2.3-8)$$

$$\frac{\partial I(t, z)}{\partial z} + \frac{n_0}{c} \frac{\partial I(t, z)}{\partial t} = hv_\ell I(t, z) \int_0^\infty B(v, v_\ell) n(v, t, z) dv - \alpha I(t, z) \quad (2.3-9)$$

$$n - n_0 = - \frac{ch}{4\pi} \int_0^\infty B(v, v_\ell) n(v, t, z) \left(\frac{2(v-v_\ell)}{\Delta v_h} \right) dv \quad (2.3-10)$$

Equations (2.3-8) to (2.3-10) govern the interaction between a two level population inversion and a monochromatic radiation field which varies slowly compared to the homogeneous line width. One can also show that near threshold these results still hold if the variations are only slow compared to the total line width.

The rate equations may be extended to include the interaction of several radiation fields with a four level system. This cannot be done rigorously in a straightforward fashion, so we make an approximation which is valid for all of our work. We assume that equations (2.3-9) and (2.3-10) remain correct for any particular field even when other fields are present. The population inversion $n(v, t, z)$ of equation (2.3-8) will, of course, be influenced by the other fields. By making this approximation coherence effects are again neglected.

Close^(2.3) has shown that the inversion actually may be modulated by the beats between the various frequencies. The result of this

modulation is a frequency mixing with resultant combination tone generation. The present theory will not predict combination tone generation. However, in most laser situations this modulation of the inversion is completely unimportant. Combination tones have only been observed in rather special circumstances. They require a small number of intense monochromatic radiation fields separated in frequency by less than the homogeneous line width. Even then the amplitudes of such tones are usually negligible compared to the amplitudes of the saturating fields^(2.6). In important applications involving widely separated lines or continuous spectra the inversion modulation may be neglected.

In accordance with the previous discussion and equations (2.3-8) to (2.3-10), the rate equations for a four level laser may be written

$$\begin{aligned} \frac{\partial n_3}{\partial t}(v, t, z) = & P_3(v) - n_3(v, t, z)[A_3 + \sum_n B(v, v_n)I_n] \\ & + n_2(v, t, z) \sum_n B(v, v_n)I_n \end{aligned} \quad (2.3-11)$$

$$\begin{aligned} \frac{\partial n_2}{\partial t}(v, t, z) = & P_2(v) + n_3(v, t, z)[A_{32} + \sum_n B(v, v_n)I_n] \\ & - n_2(v, t, z)[A_2 + \sum_n B(v, v_n)I_n] \end{aligned} \quad (2.3-12)$$

$$\begin{aligned} \frac{\partial I_\ell}{\partial z} + \frac{n_0}{c} \frac{\partial I_\ell}{\partial t} = & h\nu_\ell I_\ell \int_0^\infty B(v, v_\ell) [n_3(v, t, z) \\ & - n_2(v, t, z)] dv - \alpha I_\ell \end{aligned} \quad (2.3-13)$$

$$n - n_0 = - \frac{ch}{4\pi} \int_0^{\infty} B(v, v_{\ell}) [n_3(v, t, z) - n_2(v, t, z)] \left(\frac{2(v-v_{\ell})}{\Delta v_h} \right) dv \quad (2.3-14)$$

Equations (2.3-11) and (2.3-12) are a generalization of equations given by Gordon, White, and Rigden^(2.7), and the meaning of the coefficients is obvious. If equation (2.3-12) is subtracted from equation (2.3-11), one obtains a result for the population difference $n = n_3 - n_2$ which, except for the spontaneous emission terms, is similar in form to equation (2.3-8).

2.4 Steady state solutions

The only application in this work of the general time dependent rate equations will be to the problem of relaxation oscillations discussed in Chapter VI, although the equations should be useful for other problems such as pulse propagation. In this section we obtain the basic solutions to the rate equations in the limit of steady state. At steady state equations (2.3-11) and (2.3-12) may be solved for the population inversion with the result

$$n_3(v, z) - n_2(v, z) = \frac{\frac{P_3(v)}{A_3} - \frac{P_3(v) A_{32} + P_2(v) A_3}{A_2 A_3}}{1 + \left(\frac{A_3 - A_{32}}{A_2 A_3} + \frac{1}{A_3} \right) \sum_n B(v, v_n) I_n(z)} \quad (2.4-1)$$

We only consider here the special case where the pump spectrum is the Gaussian function

$$P_i(v) = P_{i0} e^{-\frac{2(v-v_0)^2}{\Delta v_D^2} \ln 2} \quad (2.4-2)$$

This is the most important pump spectrum in practice. In particular, it applies to the Doppler broadening of gas lasers such as the 3.51 micron xenon laser. Δv_D is the Doppler width of the atomic transition centered at the frequency v_0 .

The rate equations (2.3-13) and (2.3-14) may be written using equations (2.3-4), (2.4-1), and (2.4-2) in the form

$$\frac{dI_\lambda}{dz} = gI_\lambda \int_0^\infty \frac{\frac{2}{\pi\Delta\nu_h} e^{-[\frac{2(v-v_0)}{\Delta\nu_D}]^2 \ln 2}}{1 + s \sum_n \frac{I_n}{1 + [\frac{2(v-v_n)}{\Delta\nu_h}]^2}} dv - \alpha I_\lambda \quad (2.4-3)$$

$$n - n_0 = -\frac{cg}{4\pi\nu_\lambda} \int_0^\infty \frac{\frac{2}{\pi\Delta\nu_h} e^{-[\frac{2(v-v_0)}{\Delta\nu_D}]^2 \ln 2}}{1 + s \sum_n \frac{I_n}{1 + [\frac{2(v-v_n)}{\Delta\nu_h}]^2}} \left[\frac{2(v-v_\lambda)}{\Delta\nu_h} \right] dv \quad (2.4-4)$$

where s is a saturation parameter given by

$$s = \frac{2B_0}{\pi\Delta\nu_h} \left[\frac{A_3 - A_{32}}{A_2 A_3} + \frac{1}{A_3} \right] \quad (2.4-5)$$

and g is defined by

$$g = h\nu_\lambda B_0 \left[\frac{P_{30}}{A_3} - \frac{P_{30}A_{32} + P_{20}A_3}{A_2 A_3} \right] \quad (2.4-6)$$

It will become evident later that g represents the small signal line center incremental intensity gain for an inhomogeneously broadened medium.

Equations (2.4-3) and (2.4-4) simplify further to

$$\frac{dI_\lambda}{dz} = \frac{gI_\lambda}{\pi} \int_0^\infty \frac{e^{-\epsilon^2(z-z_0)^2}}{[1+(z-z_\lambda)^2][1+s \sum_n \frac{I_n}{1+(z-z_n)^2}]} dz - \alpha I_\lambda \quad (2.4-7)$$

$$n-n_0 = -\frac{cg}{4\pi^2 v_\lambda} \int_0^\infty \frac{e^{-\epsilon^2(z-z_0)^2}}{[1+(z-z_\lambda)^2][1+s \sum_n \frac{I_n}{1+(z-z_n)^2}]} (z-z_\lambda) dz \quad (2.4-8)$$

using the new frequency parameter $z_i = 2v_i/\Delta v_h$ and the natural damping ratio (2.8)

$$\epsilon = \frac{\Delta v_h}{\Delta v_D} \sqrt{\ln 2}$$

which measures the relative importance of the homogeneous and inhomogeneous broadening. The frequency parameter is not to be confused with the distance in the spatial derivative which is also called z to conserve alphabet. These equations are the primary results of this section. It is often possible to expand integrals of this type and express the results in terms of the tabulated error function of complex argument or the plasma dispersion function. However, in most practical situations it is more useful to assume that the laser medium is predominantly either homogeneously or inhomogeneously broadened. In these limits the integrals simplify greatly as is demonstrated in the next two sections.

Sometimes it is necessary to regard the saturation as being due to a continuum of radiation frequencies rather than discrete lines. Then equations (2.4-7) and (2.4-8) go over in an obvious fashion to the expressions

$$\frac{dI(z_\ell)}{dz} = \frac{gI(z_\ell)}{\pi} \int_0^\infty \frac{e^{-\epsilon^2(z-z_0)^2}}{[1+(z-z_\ell)^2][1+s \int_0^\infty \frac{I(z_n)dz_n}{1+(z-z_n)^2}]} dz - \alpha I(z_\ell) \quad (2.4-9)$$

$$n-n_0 = -\frac{cg}{4\pi^2 v_\ell} \int_0^\infty \frac{e^{-\epsilon^2(z-z_0)^2} (z-z_\ell) dz}{[1+(z-z_\ell)^2][1+s \int_0^\infty \frac{I(z_n)dz_n}{1+(z-z_n)^2}]} \quad (2.4-10)$$

Here $I(z_\ell)$ is the spectral density at the frequency z_ℓ .

So far we have assumed that the energy levels of the laser transition are nondegenerate. In practice the energy levels commonly are degenerate, so we discuss here the generalization of the preceding results to the important situation of degenerate levels and linearly polarized radiation. According to Dienes^(2.9), this generalization would lead to the replacement of equations (2.4-7) and (2.4-8) by

$$\frac{dI_\ell}{dz} = \frac{gI_\ell}{\pi} \sum_m C_{m,m}^2 \int_0^\infty \frac{e^{-\epsilon^2(z-z_0)^2}}{[1+(z-z_\ell)^2][1+sC_{m,m}^2 \sum_n \frac{I_n}{1+(z-z_n)^2}]} dz - \alpha I_\ell \quad (2.4-11)$$

$$n-n_0 = -\frac{cg}{4\pi v_\ell} \sum_m C_{m,m}^2 \int_0^\infty \frac{e^{-\epsilon^2(z-z_0)^2} (z-z_\ell) dz}{[1+(z-z_\ell)^2][1+sC_{m,m}^2 \sum_n \frac{I_n}{1+(z-z_n)^2}]} \quad (2.4-12)$$

The coefficients for the transition from level 3 to level 2 of the four

level system are

$$c_{m,m}^2 = \frac{3}{2j_3+1} [\langle j_2, 1, m, 0 | j_2, 1, j_3, m \rangle]^2 \quad (2.4-13)$$

The factor in the brackets is a Clebsch-Gordan coefficient, coupling an angular momentum j_2 having a z-component m with an angular momentum of unity having a z-component of zero (corresponding to the linearly polarized photon) to form a resultant angular momentum of j_3 having a z-component of m . In the summations of equations (2.4-11) and (2.4-12) m takes on all integer values between $-j_3$ and $+j_3$.

Equation (2.4-13) may be rewritten in terms of the "Wigner 3j-symbol" (2.10) as

$$c_{m,m}^2 = 3 \left(\begin{array}{ccc} j_3 & j_2 & 1 \\ m & -m & 0 \end{array} \right)^2 \quad (2.4-14)$$

For the various possible transitions the 3j-symbols can be evaluated and the final results are

$$j_3 = j_2 + 1 \quad c_{m,m}^2 = \frac{6(j_3+m)(j_3-m)}{(2j_3-1)(2j_3)(2j_3+1)} \quad (2.4-15)$$

$$j_3 = j_2 = j \quad c_{m,m}^2 = \frac{12m^2}{2j(2j+1)(2j+2)} \quad (2.4-16)$$

$$j_3 = j_2 - 1 \quad c_{m,m}^2 = \frac{6(j_3+1+m)(j_3+1-m)}{(2j_3+1)(2j_3+2)(2j_3+3)} \quad (2.4-17)$$

These coefficients may be shown to satisfy the relation $c_{m,m}^2 = c_{-m,-m}^2$ and the condition $\sum_m c_{m,m}^2 = 1$.

The degeneracy coefficients are evaluated in Table 2.1 for j_3 values up to 5. For much of the discussion of later chapters only a qualitative understanding of the saturation process is required. The summation over m in the saturation equations (2.4-11) and (2.4-12) is an added complication which turns out to be unnecessary for our purposes. In particular, for $j_3 = j_2 \pm 1$ and for fairly small values of j_3 it is evident from Table 2.1 that the degeneracy coefficients do not vary much with the permissible values of m (except for the diagonal of zeros). Therefore, a reasonable approximation to equations (2.4-15) and (2.4-17) is to assume that the coefficients are independent of m . Then retaining the relation $\sum_m c_{m,m}^2 = 1$ leads to the approximate degeneracy factors

$$j_3 = j_2 + 1 \quad -(j_3-1) < m < (j_3-1) \quad c_{m,m}^2 = \frac{1}{2j_3-1} \quad (2.4-18)$$

$$j_3 = j_2 - 1 \quad -j_3 < m < j_3 \quad c_{m,m}^2 = \frac{1}{2j_3+1} \quad (2.4-19)$$

Also, for the case $j_3 = j_2$ it is evident from Table 2.1 that the coefficient for $m = j_3$ is much larger than for the other values of m provided that j_3 is not too large. Therefore, these two terms dominate the summation, and a reasonable approximation to equation (2.4-14) is

$$j_3 = j_2 = m \quad c_{m,m}^2 = \frac{1}{2} \quad (2.4-20)$$

These results are satisfactory for j_3 values of less than about four or five.

Table 2.1: Degeneracy coefficients $C_{m,m}^2$ from (a) equation (2.4-15);
 (b) equation (2.4-16); and (c) equation (2.4-17)

		(a)										
		0	1/2	1	3/2	2	5/2	3	7/2	4	9/2	5
$j_3^{\pm m}$	3/2		1/2		0							
	2	2/5		3/10		0						
	5/2		3/10		1/5		0					
	3	9/35		8/35		1/7		0				
	7/2		3/14		5/28		3/28		0			
	4	4/21		5/28		1/7		1/12		0		
	9/2		1/6		3/20		7/60		1/15		0	
	5	5/33		3/20		7/55		16/165		3/55		0

		(b)										
		0	1/2	1	3/2	2	5/2	3	7/2	4	9/2	5
$j_3^{\pm m}$	1/2		1/2									
	1	0		1/2								
	3/2		1/20		9/20							
	2	0		1/10		2/5						
	5/2		1/70		9/70		25/70					
	3	0		1/28		1/7		9/28				
	7/2		1/168		3/56		25/168		7/24			
	4	0		1/60		1/15		3/20		4/15		
	9/2		1/330		3/110		5/66		49/330		27/110	
	5	0		1/110		2/55		9/110		8/55		5/22

(c)

$\frac{1}{2}$	0	1/2	1	3/2	2	5/2	3	7/2	4	9/2	5
$\frac{1}{2}$		$1/2$									
1		$2/5$		$3/10$							
$\frac{3}{2}$			$3/10$		$1/5$						
2		$9/35$		$8/35$		$1/7$					
$\frac{5}{2}$			$3/14$		$5/28$		$3/28$				
3		$4/21$		$5/28$		$1/7$		$1/2$			
$\frac{7}{2}$			$1/6$		$3/20$		$7/60$		$1/15$		
4		$5/33$		$8/55$		$7/55$		$16/165$		$3/55$	
$\frac{9}{2}$			$3/22$		$7/55$		$6/55$		$9/110$		$1/22$
5		$18/143$		$35/286$		$16/143$		$27/286$		$10/143$	$1/26$

With the above approximations the degeneracy summations in equations (2.4-11) and (2.4-12) may be performed with the obvious results

$$\frac{dI_\ell}{dz} = \frac{gI_\ell}{\pi} \int_0^\infty \frac{e^{-\epsilon^2(z-z_0)^2}}{[1+(z-z_\ell)^2][1+sC_{m,m}^2 \sum_n \frac{I_n}{1+(z-z_\ell)^2}]} dz - \alpha I_\ell \quad (2.4-21)$$

$$n - n_0 = - \frac{cg}{4\pi v_\ell} \int_0^\infty \frac{e^{-\epsilon^2(z-z_0)^2}}{[1+(z-z_\ell)^2][1+sC_{m,m}^2 \sum_n \frac{I_n}{1+(z-z_\ell)^2}]} (z-z_\ell) dz \quad (2.4-22)$$

Thus the primary effect of the degeneracy is to modify the saturation parameter provided that the total angular momentum quantum number j_3 is small. Equations (2.4-21) and (2.4-22) would be identical to equations (2.4-7) and (2.4-8) if the saturation parameter s in the earlier equations were replaced by $s' = sC_{m,m}^2$.

The approximate equations (2.4-21) and (2.4-22) are adequate for all our experimental work. The 3.51 micron transition in xenon (Chapter III) is characterized by $j_3 = 3$ and $j_2 = 2$. Then from Table 2.1 and equation (2.4-18) it is apparent that the approximation involves replacing $9/35$, $8/35$, and $5/35$ by $7/35$. This accuracy is satisfactory and we use equations (2.4-7) and (2.4-8) as our basic results. The saturation parameter s is regarded as an experimentally determinable number.

Only the four-level laser has been considered in detail here. However, from equation (2.3-8) it is evident that the steady state population inversion in a two level system has the same form as equation

(2.4-1). In the important homogeneously broadened three level lasers the inversion again takes the same form^(2.11). Thus, equations (2.4-11) and (2.4-12) are quite generally valid. It is only the gain, saturation and degeneracy parameters which depend on the details of the atomic model. These details are not of interest here.

In this section we have obtained the basic equations governing the steady state gain and index of refraction of a laser medium. The corrections for degeneracy of the laser levels have been considered and the appropriate coefficients tabulated. Many treatments of the gain and saturation neglect the dependence of the strength of the transition on the m values and include only the degeneracy factors. Such treatments are in error.

2.5 Homogeneous broadening

Here we consider the important limit of predominantly homogeneous line broadening. In this limit the homogeneous line width $\Delta\nu_h$ becomes much greater than the inhomogeneous Doppler line width $\Delta\nu_D$ so that the natural damping ratio

$$\epsilon = \frac{\Delta\nu_h}{\Delta\nu_D} \sqrt{\ln 2}$$

becomes large. For large ϵ the integrands of equations (2.4-7) and (2.4-8) vanish except for frequencies near $z = z_0$. Thus the slowly varying terms may be brought outside of the integrals with the results

$$\frac{dI_\ell}{dz} = \frac{gI_\ell}{\pi} \frac{1}{[1 + (z_0 - z_\ell)^2][1 + s \sum_n \frac{I_n}{1 + (z_0 - z_n)^2}]} \int_0^\infty e^{-\epsilon^2(z-z_0)^2} dz - \alpha I_\ell \quad (2.5-1)$$

$$n - n_0 = - \frac{cg}{4\pi^2 v_\ell} \frac{(z_0 - z_\ell)}{[1 + (z_0 - z_\ell)^2][1 + s \sum_n \frac{I_n}{1 + (z_0 - z_n)^2}]} \int_0^\infty e^{-\epsilon^2(z-z_0)^2} dz \quad (2.5-2)$$

The value of the integrals is $\sqrt{\pi}/\epsilon$ so equations (2.5-1) and (2.5-2) may be written simply as

$$\frac{dI_\ell}{dz} = g'I_\ell \frac{1}{(1 + y_\ell^2)(1 + s \sum_n \frac{I_n}{1 + y_n^2})} - \alpha I_\ell \quad (2.5-3)$$

$$n - n_0 = \frac{cg'}{4\pi v_\ell} \frac{y_\ell}{(1 + y_\ell^2)(1 + s \sum_n \frac{I_n}{1 + y_n^2})} \quad (2.5-4)$$

where $g' = g/(\sqrt{\pi}\epsilon)$ is the unsaturated line center incremental intensity

gain for homogeneous broadening and $y_n = z_n - z_0$ is the homogeneous frequency difference.

If saturation is due to a continuum of frequencies rather than discrete lines, then equations (2.5-3) and (2.5-4) are replaced by

$$\frac{dI(y_\lambda)}{dz} = g' I(y_\lambda) \frac{1}{(1+y_\lambda^2)(1+s \int_{-\infty}^{\infty} \frac{I(y_n) dy_n}{1+y_n^2})} - \alpha I_\lambda \quad (2.5-5)$$

$$n - n_0 = \frac{cg'}{4\pi v_\lambda} \frac{y_\lambda}{(1+y_\lambda^2)(1+s \int_{-\infty}^{\infty} \frac{I(y_n) dy_n}{1+y_n^2})} \quad (2.5-6)$$

If saturation is due to a single monochromatic radiation field, then equations (2.5-3) and (2.5-4) simplify to the results

$$\frac{dI_\lambda}{dz} = g' I_\lambda \frac{1}{1+y_\lambda^2 + sI_\lambda} - \alpha I_\lambda \quad (2.5-7)$$

$$n - n_0 = \frac{cg'}{4\pi v_\lambda} \frac{y_\lambda}{1+y_\lambda^2 + sI_\lambda} \quad (2.5-8)$$

In this section expressions have been obtained for the gain and index of refraction of a homogeneously broadened laser medium. In all cases the gain profile is Lorentzian in shape. The width of this Lorentzian may be found by writing equation (2.5-3) as

$$\frac{dI_\ell}{dz} = g' I_\ell \frac{1}{(1+y_\ell)^2 (1+s \sum_{n \neq \ell} \frac{I_n}{1+y_n^2}) + s I_\ell} - \alpha I_\ell$$

$$= \frac{g' I_\ell}{1+s \sum_{n \neq \ell} \frac{I_n}{1+y_n^2}} \frac{1}{(1+\frac{s I_\ell}{1+s \sum_{n \neq \ell} \frac{I_n}{1+y_n^2}})+y_\ell^2} - \alpha I_\ell \quad (2.5-9)$$

Thus the line width is

$$\Delta v = \Delta v_h \sqrt{1 + \frac{s I_\ell}{1+s \sum_{n \neq \ell} \frac{I_n}{1+y_n^2}}} \quad (2.5-10)$$

2.6 Inhomogeneous broadening

The purpose of this section is to obtain expressions for the gain and index of refraction of a laser medium in which the Doppler line width $\Delta\nu_D$ is much greater than the homogeneous line width $\Delta\nu_h$ so that the natural damping ratio $\epsilon = (\Delta\nu_h / \Delta\nu_D) \sqrt{\ln 2}$ becomes small. We consider first the important special case where the spacing between the saturating lines is much greater than the homogeneous line width associated with each line.

In the limit of weakly interacting fields each line only depletes the population inversion over a limited frequency range. Consequently the integrals in equations (2.4-7) and (2.4-8) may be broken up into several integrals over the important regions of the Doppler spectrum. The appropriate way to do this is

$$\frac{dI_\ell}{dz} = \frac{gI_\ell}{\pi} \left\{ \int_0^\infty \frac{e^{-\epsilon^2(z-z_0)^2}}{1+sI_\ell + (z-z_\ell)^2} dz - \sum_{n \neq \ell} \left[\int_{z_n - \delta n}^{z_n + \delta n} \frac{e^{-\epsilon^2(z-z_0)^2}}{(z-z_\ell)^2} \cdot \left(1 - \frac{\frac{1}{sI_n}}{1 + \frac{sI_n}{1 + (z-z_n)^2}} \right) dz \right] \right\} - \alpha I_\ell \quad (2.6-1)$$

$$n - n_0 = - \frac{cg}{4\pi^2 v_\ell} \left\{ \int_0^\infty \frac{e^{-\epsilon^2(z-z_0)^2}}{1+sI_\ell + (z-z_\ell)^2} \cdot \frac{(z-z_\ell) dz}{(z-z_\ell)^2} - \sum_{n \neq \ell} \left[\int_{z_n - \delta n}^{z_n + \delta n} \frac{e^{-\epsilon^2(z-z_0)^2}}{(z-z_\ell)^2} \left(1 - \frac{\frac{1}{sI_n}}{1 + \frac{sI_n}{1 + (z-z_n)^2}} \right) dz \right] \right\} \quad (2.6-2)$$

The first integrals on the right sides of equations (2.6-1) and (2.6-2) are just the single frequency limits of equations (2.4-7) and (2.4-8). The other integrals provide corrections to the single frequency results due to depletion of the inversion in narrow regions in the vicinity of the other frequencies. These integrals are assumed to extend only over the narrow depleted regions. The condition for the validity of this approximation is that the frequency spacing be much greater than the saturated homogeneous widths $\Delta v_h \sqrt{1+sI_i}$ of two neighboring lines.

All of the factors in the correction integrals except the last are approximately constant in the immediate vicinity of a laser field, so they may be removed from the integrals with the results

$$\frac{1}{I_\ell} \frac{dI_\ell}{dz} = \frac{-x_\ell^2}{(1+sI_\ell)^{1/2}} - \frac{2\epsilon g}{\pi^{1/2}} [1 - 2x_\ell F(x_\ell)] - \frac{\epsilon g}{\pi} \sum_{n \neq \ell} \frac{e^{-x_n^2}}{(x_n - x_\ell)^2} \int_{-\infty}^{\infty} \left(\frac{\epsilon^2 s I_n}{\epsilon^2 (1 + s I_n) + (x - x_n)^2} \right) dx - \alpha \quad (2.6-3)$$

$$n - n_0 = \frac{cg F(x_\ell)}{2\pi^{3/2} v_\ell} - c\epsilon g (1 + s I_\ell)^{1/2} x_\ell e^{-x_\ell^2} - \frac{cg}{4\pi^2 v_\ell} \sum_{n \neq \ell} \frac{e^{-x_n^2}}{(x_n - x_\ell)^2} \int_{-\infty}^{\infty} \left(\frac{\epsilon^2 s I_n}{\epsilon^2 (1 + s I_n) + (x - x_n)^2} \right) dx \quad (2.6-4)$$

Here we have adapted the single frequency results of Close^(2.3) for evaluation of the first integrals and introduced the useful inhomogeneous frequency parameter $x_n = \epsilon(z_n - z_0)$. The range of integration has been extended to infinity without appreciable error, since the

integrand vanishes at frequencies far from x_n .

The function $F(x)$ appearing in equations (2.6-3) and (2.6-4) is sometimes referred to as Dawson's integral^(2.12), and it may be written as

$$F(x) = e^{-x^2} \int_0^x e^{t^2} dt \quad (2.6-5)$$

Because of its importance in the mode pulling investigations of Chapter IV, we consider here some of the basic properties of this integral. Dawson's integral has been tabulated^(2.12,2.13). For small values of x it may be expanded as^(2.14)

$$F(x) = x - \frac{2}{3} x^3 + \frac{2}{3 \cdot 5} x^5 - \frac{2^3}{3 \cdot 5 \cdot 7} x^7 + \dots \quad (2.6-6)$$

For large x the asymptotic expansion is^(2.13)

$$F(x) = \frac{1}{2x} + \frac{1}{2^2 x^3} + \frac{1 \cdot 3}{2^3 x^5} + \frac{1 \cdot 3 \cdot 5}{2^4 x^7} + \dots \quad (2.6-7)$$

An approximation to $F(x)$ which agrees with the first order terms of both series is

$$F(x) \approx \frac{x}{1 + 2x^2} \quad (2.6-8)$$

A better approximation which agrees with the second order terms of both series may be found by a bit of algebra and is

$$F(x) \approx \frac{x + (\frac{2}{3})x^2}{1 + (\frac{4}{3})x^2 + (\frac{4}{3})x^4} \quad (2.6-9)$$

Equation (2.6-5) and the approximate equations (2.6-8) and (2.6-9) for

Dawson's integral are plotted in Figure 2.1. For most applications the approximations are satisfactory. $F(x)$ also satisfies the easily verified relations

$$\frac{d}{dx} F(x) = -2x F(x) + 1, \quad F(-x) = -F(x) \quad (2.6-10)$$

The integrations in equations (2.6-3) and (2.6-4) may be performed and one obtains finally

$$\begin{aligned} \frac{1}{I_\lambda} \frac{dI_\lambda}{dz} &= \frac{ge^{-x_\lambda^2}}{(1+sI_\lambda)^{1/2}} - \frac{2\epsilon g}{\pi^{1/2}} [1 - 2x_\lambda F(x_\lambda)] \\ &\quad - \epsilon^2 g \sum_{n \neq \lambda} \frac{sI_n e^{-x_n^2}}{(x_n - x_\lambda)^2 (1+sI_n)^{1/2}} - \alpha \end{aligned} \quad (2.6-11)$$

$$\begin{aligned} n - n_0 &= \frac{cg F(x_\lambda)}{2\pi^{3/2} v_\lambda} - \frac{c\epsilon g}{2\pi v_\lambda} (1+sI_\lambda)^{1/2} x_\lambda e^{-x_\lambda^2} \\ &\quad - \frac{\epsilon cg}{4\pi v_\lambda} \sum_{n \neq \lambda} \frac{sI_n e^{-x_n^2}}{(x_n - x_\lambda)(1+sI_n)^{1/2}} \end{aligned} \quad (2.6-12)$$

These equations include the first order corrections to the gain and index of refraction at the frequency v_λ due to saturating fields at the frequency v_λ and at the distant frequencies v_n . The interaction correction to the gain is within the approximation of widely spaced lines due to the small factor $\epsilon^2 (x_n - x_\lambda)^{-2}$. The corresponding refraction correction may be important as is shown in Chapter IV. If the parameter ϵ is sufficiently small these equations reduce to

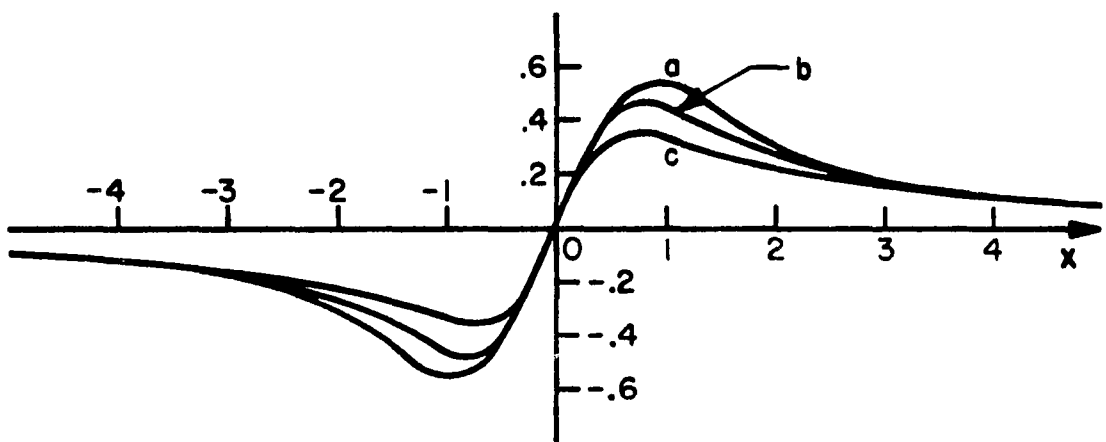


Figure 2.1 Dawson's integral according to (a) exact equation (2.6-5),
(b) equation (2.6-9), (c) equation (2.6-8).

- 34 -

$$\frac{1}{I_\lambda} \frac{dI_\lambda}{dz} = \frac{ge^{-x_\lambda^2}}{(1+sI_\lambda)^{1/2}} - \alpha \quad (2.6-13)$$

$$n - n_0 = \frac{cg F(x_\lambda)}{2\pi^{3/2} v_\lambda} \quad (2.6-14)$$

It becomes apparent that the parameter g was chosen to correspond to the small signal incremental gain for an inhomogeneously broadened medium.

It should be pointed out that the approximations used in the preceding derivation break down for sufficiently intense fields. The homogeneous widths associated with the various fields eventually overlap, and ultimately the entire gain line becomes effectively homogeneously broadened. In the single frequency case the medium may be regarded as inhomogeneously broadened only as long as the Doppler width is much greater than the homogeneous width $\Delta v_h \sqrt{1 + sI_\lambda}$.

So far only the special case of widely spaced lines has been considered. The opposite limit of a reasonably continuous spectral distribution is also important. This limit is appropriate to the problem of spectral narrowing, for example, which is treated in Chapter VIII. If the intensity spectrum $I(z_n)$ is nearly uniform over a spectral region of width Δv_h , then $I(z_n)$ may be removed from the denominator integrals of equations (2.4-9) and (2.4-10) leaving

$$\frac{1}{I(z_\lambda)} \frac{dI(z_\lambda)}{dz} = \frac{g}{\pi} \int_0^\infty \frac{e^{-\epsilon^2(z-z_0)^2}}{[1+(z-z_\lambda)^2][1+sI(z)]} dz - \alpha \quad (2.6-15)$$

$$n - n_0 = - \frac{cg}{4\pi^2 v_\ell} \int_0^\infty \frac{e^{-\epsilon^2(z-z_0)^2} (z-z_\ell) dz}{[1+(z-z_\ell)^2][1+sI(z)] \int_0^\infty \frac{dz}{1+(z-z_n)^2}} \quad (2.6-16)$$

The value of the integrals in the denominator is π so that equations (2.6-15) and (2.6-16) simplify to

$$\frac{1}{I(z_\ell)} \frac{dI(z_\ell)}{dz} = \frac{g}{\pi} \int_0^\infty \frac{e^{-\epsilon^2(z-z_0)^2} dz}{[1+(z-z_\ell)^2][1+\pi sI(z)]} - \alpha \quad (2.6-17)$$

$$n - n_0 = - \frac{cg}{4\pi^2 v_\ell} \int_0^\infty \frac{e^{-\epsilon^2(z-z_0)^2} (z-z_\ell) dz}{[1+(z-z_\ell)^2][1+\pi sI(z)]} \quad (2.6-18)$$

$I(z)$ is assumed to vary negligibly over the homogeneous line width, so the last factor in the denominators of equations (2.6-17) and (2.6-18) may be taken outside the integrals, leaving

$$\frac{1}{I(z_\ell)} \frac{dI(z_\ell)}{dz} = \frac{g}{\pi[1+\pi sI(z_\ell)]} \int_0^\infty \frac{e^{-\epsilon^2(z-z_0)^2} dz}{1+(z-z_\ell)^2} - \alpha \quad (2.6-19)$$

$$n - n_0 = - \frac{cg}{4\pi^2 v_\ell [1+\pi sI(z_\ell)]} \int_0^\infty \frac{e^{-\epsilon^2(z-z_0)^2} (z-z_\ell) dz}{1+(z-z_\ell)^2} \quad (2.6-20)$$

The integrals in these equations are analogous to the first integrals appearing in equations (2.6-1) and (2.6-2), and one obtains the final results

$$\frac{1}{I(x_\lambda)} \frac{dI(x_\lambda)}{dz} = \frac{ge^{-x_\lambda^2}}{1 + \pi s \epsilon I(x_\lambda)} - \frac{2\epsilon g [1 - 2x_\lambda F(x_\lambda)]}{\pi^{1/2} [1 + \pi s \epsilon I(x_\lambda)]} - \alpha \quad (2.6-21)$$

$$n - n_0 = \frac{cg F(x_\lambda)}{2\pi^{3/2} v_\lambda [1 + \pi s \epsilon I(x_\lambda)]} - \frac{c\epsilon g x_\lambda e^{-x_\lambda^2}}{2\pi v_\lambda [1 + \pi s \epsilon I(x_\lambda)]} \quad (2.6-22)$$

for a line which is predominantly inhomogeneously broadened. The relation $I(z) = \epsilon I(x)$ was used in writing the saturation terms in these equations.

If the first order correction is unimportant, then equations (2.6-21) and (2.6-22) reduce to

$$\frac{1}{I(x_\lambda)} \frac{dI(x_\lambda)}{dz} = \frac{ge^{-x_\lambda^2}}{1 + \pi s \epsilon I(x_\lambda)} - \alpha \quad (2.6-23)$$

$$n - n_0 = \frac{cg F(x_\lambda)}{2\pi^{3/2} v_\lambda [1 + \pi s \epsilon I(x_\lambda)]} \quad (2.6-24)$$

Thus the form of the line center continuum gain saturation, equation (2.6-23) for inhomogeneous broadening, is identical to the line center monochromatic field result for homogeneous broadening, equation (2.5-7), except for a factor of $\pi \epsilon$.

Results have been obtained in this section for laser media in which the inhomogeneous line width is much greater than the homogeneous line width. The limit of discrete lines spaced widely compared to the homogeneous width and the opposite limit of radiation spectra which are uniform over the homogeneous width have been considered in some detail.

2.7 Spectral hole burning

The concept of "hole burning" was introduced by Bennett^(2.15). The population inversion or gain in an inhomogeneously broadened medium may be depleted over a localized spectral region as a result of a strongly saturating monochromatic field. The depleted region is referred to as a "hole." Discussions of this subject are generally rather qualitative. However, a rigorous treatment of hole burning is straightforward using the formalism of the preceding sections of this chapter. The results will be useful in later chapters.

It is necessary to distinguish clearly between the hole burned in the population inversion spectrum and the hole burned in the gain spectrum by a saturating field. From equations (2.4-1), (2.4-2), (2.4-5), and (2.4-6) the population inversion may be written

$$n_3 - n_2 = \frac{g}{hv_i B_0} \frac{\frac{-\epsilon^2(z-z_0)^2}{e}}{1 + \frac{sI_i}{1 + (z-z_i)^2}} \quad (2.7-1)$$

where only a single field at the frequency z_i is considered. If the medium is strongly inhomogeneous ($\epsilon \rightarrow 0$), then the population inversion in the vicinity of the field is

$$n_3 - n_2 = \frac{\frac{-\epsilon^2(z_i z_0)^2}{g e}}{hv_i B_0} \left(1 - \frac{sI_i}{1 + sI_i + (z-z_i)^2}\right) \quad (2.7-2)$$

The second factor in the parentheses corresponds to the hole which is subtracted from the unsaturated population inversion. Evidently the hole is a Lorentzian of width

$$\Delta v_{inv} = \Delta v_h \sqrt{1 + sI_i} \quad (2.7-3)$$

We define the "normalized" population inversion as

$$\Delta n^* = 1 - \frac{sI_i}{1 + sI_i + \delta^2} \quad (2.7-4)$$

which is the ratio of $n_3 - n_2$ in the presence of the field I_i to that existing when $I_i = 0$. Here $\delta = z - z_i$ measures the frequency difference to the center of the hole. A plot of this function for various values of sI_i is given in Figure 2.2.

To study the gain and dispersion spectra in the vicinity of a hole it is necessary to consider two radiation fields. One is a fixed intense field I_i at the frequency z_i which creates the hole, and the other is a weak field I_ℓ of the frequency z_ℓ which samples the gain and dispersion. Equations (2.4-7) and (2.4-8) become

$$\frac{dI_\ell}{dz} = \frac{gI_\ell}{\pi} \int_0^\infty \frac{e^{-\epsilon^2(z-z_0)^2}}{[1 + (z-z_\ell)^2][1 + \frac{sI_i}{1 + (z-z_i)^2}]} dz \quad (2.7-5)$$

$$n - n_0 = - \frac{cg}{4\pi^2 v_\ell} \int_0^\infty \frac{e^{-\epsilon^2(z-z_0)^2}(z-z_\ell)}{[1 + (z-z_\ell)^2][1 + \frac{sI_i}{1 + (z-z_i)^2}]} dz \quad (2.7-6)$$

For strong inhomogeneous broadening these equations may be written for frequencies near z_i as

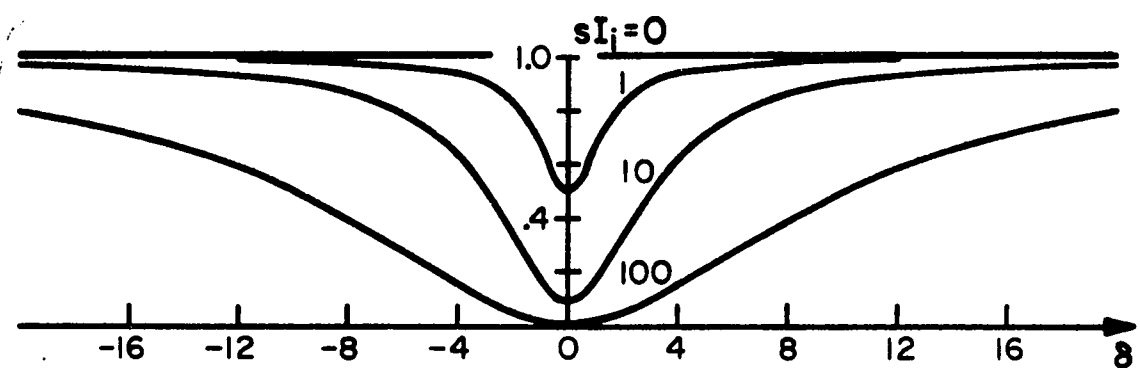


Figure 2.2 Normalized population inversion versus δ for various values of sI_1 .

$$\frac{dI}{dz} = \frac{gI_\ell}{\pi} \left[\int_0^\infty \frac{e^{-\epsilon^2(z-z_0)^2}}{1+(z-z_\ell)^2} - e^{-\epsilon^2(z_i-z_0)^2} \int_0^\infty \frac{1}{1+(z-z_\ell)^2} \left(1 - \frac{1}{1 + \frac{sI_i}{1+(z-z_i)^2}} \right) dz \right] \quad (2.7-7)$$

$$n - n_0 = - \frac{cg}{4\pi^2 v_\ell} \left[\int_0^\infty \frac{e^{-\epsilon^2(z-z_0)^2}}{1+(z-z_\ell)^2} \frac{(z-z_\ell)}{dz} dz - e^{-\epsilon^2(z_i-z_0)^2} \int_0^\infty \frac{(z-z_\ell)}{1+(z-z_\ell)^2} \left(1 - \frac{1}{1 + \frac{sI_i}{1+(z-z_i)^2}} \right) dz \right] \quad (2.7-8)$$

We write the equations in this form so as to confine the effects of the hole to the last integrals. For a weak saturating field I_i these integrals obviously vanish and there is no hole. In the following analysis we evaluate these integrals. The results will be presented in pairs with the first corresponding to the gain hole and the second to the dispersion hole.

The last integrals of equations (2.7-7) and (2.7-8) may be written

$$\int_{-\infty}^{\infty} \frac{dy}{[1+y^2][1+sI_i+(y+\delta)^2]} \quad (2.7-9)$$

$$\int_{-\infty}^{\infty} \frac{y dy}{[1+y^2][1+sI_i+(y+\delta)^2]} \quad (2.7-10)$$

where $y = z - z_\ell$, $\delta = z_\ell - z_i$ measures the frequency difference from the center of the hole and the factor sI_i has been removed. The integrals may be expanded by partial fractions as

$$\begin{aligned}
 & \frac{sI_1 + \delta^2}{(sI_1 + \delta^2)^2 + 4\delta^2} \int_{-\infty}^{\infty} \frac{dy}{1+y^2} - \frac{2\delta}{(sI_1 + \delta^2)^2 + 4\delta^2} \int_{-\infty}^{\infty} \frac{ydy}{1+y^2} \\
 & - \frac{(sI_1 + \delta^2) - 4\delta^2}{(sI_1 + \delta^2)^2 + 4\delta^2} \int_{-\infty}^{\infty} \frac{dy}{1+sI_1 + \delta^2 + 2\delta y + y^2} \\
 & + \frac{2\delta}{(sI_1 + \delta^2)^2 + 4\delta^2} \int_{-\infty}^{\infty} \frac{ydy}{1+sI_1 + \delta^2 + 2\delta y + y^2} \quad (2.7-11)
 \end{aligned}$$

and

$$\begin{aligned}
 & \frac{2\delta}{(sI_1 + \delta^2)^2 + 4\delta^2} \int_{-\infty}^{\infty} \frac{dy}{1+y^2} + \frac{sI_1 + \delta^2}{(sI_1 + \delta^2)^2 + 4\delta^2} \int_{-\infty}^{\infty} \frac{ydy}{1+y^2} \\
 & - \frac{2\delta(1+sI_1 + \delta^2)}{(sI_1 + \delta^2)^2 + 4\delta^2} \int_{-\infty}^{\infty} \frac{dy}{1+sI_1 + \delta^2 + 2\delta y + y^2} \\
 & - \frac{sI_1 + \delta^2}{(sI_1 + \delta^2)^2 + 4\delta^2} \int_{-\infty}^{\infty} \frac{ydy}{1+sI_1 + \delta^2 + 2\delta y + y^2} \quad (2.7-12)
 \end{aligned}$$

These integrals are all well known and the results are, term by term

$$\begin{aligned}
 & \left(\frac{sI_1 + \delta^2}{(sI_1 + \delta^2)^2 + 4\delta^2} \right) \pi - 0 - \left(\frac{(sI_1 + \delta^2) - 4\delta^2}{(sI_1 + \delta^2)^2 + 4\delta^2} \right) \frac{\pi}{\sqrt{1+sI_1}} \\
 & - \left(\frac{2\delta^2}{(sI_1 + \delta^2)^2 + 4\delta^2} \right) \frac{\pi}{\sqrt{1+sI_1}} \quad (2.7-13)
 \end{aligned}$$

$$\begin{aligned} & \left(\frac{2\delta}{(sI_i + \delta^2)^2 + 4\delta^2} \right) \pi + 0 - \left(\frac{2\delta(1 + sI_i + \delta^2)}{(sI_i + \delta^2)^2 + 4\delta^2} \right) \frac{\pi}{\sqrt{1 + sI_i}} \\ & + \left(\frac{\delta(sI_i + \delta^2)}{(sI_i + \delta^2)^2 + 4\delta^2} \right) \frac{\pi}{\sqrt{1 + sI_i}} \end{aligned} \quad (2.7-14)$$

Combining the terms yields

$$\frac{\pi}{(sI_i + \delta^2)^2 + 4\delta^2} \left[sI_i + \delta^2 - \frac{sI_i - \delta^2}{\sqrt{1 + sI_i}} \right] \quad (2.7-15)$$

$$\frac{\pi\delta}{(sI_i + \delta^2)^2 + 4\delta^2} \left[2 - \frac{2 + sI_i + \delta^2}{\sqrt{1 + sI_i}} \right] \quad (2.7-16)$$

Consideration of equations (2.6-13), (2.6-14), (2.7-7), (2.7-8), (2.7-15), and (2.7-16) shows that the final expressions for the gain and index of refraction of a laser medium with a single spectral hole may be written

$$\frac{1}{I_\ell} \frac{dI_\ell}{dz} = g \left\{ e^{-x_\ell^2} - \frac{sI_i e^{-x_i}}{(sI_i + \delta^2)^2 + 4\delta^2} \left[sI_i + \delta^2 - \frac{sI_i - \delta^2}{\sqrt{1 + sI_i}} \right] \right\} \quad (2.7-17)$$

$$n - n_0 = \frac{cg}{4\pi v_\ell} \left\{ \frac{2F(x_\ell)}{\pi} + \frac{sI_i \delta e^{-x_i^2}}{(sI_i + \delta^2)^2 + 4\delta^2} \left[2 - \frac{2 + sI_i + \delta^2}{\sqrt{1 + sI_i}} \right] \right\} \quad (2.7-18)$$

where again $x = \epsilon(z-z_0)$. If there are many widely spaced holes, there will be many corresponding correction terms of the form of those included in equations (2.7-17) and (2.7-18). We define the "normalized" gain and

index of refraction as

$$g^* = 1 - \frac{sI_i}{(sI_i + \delta^2)^2 + 4\delta^2} \left[sI_i + \delta^2 - \frac{sI_i - \delta^2}{\sqrt{1 + sI_i}} \right] \quad (2.7-19)$$

$$(n - n_o)^* = \frac{sI_i \delta}{(sI_i + \delta^2)^2 + 4\delta^2} \left[2 - \frac{2 + sI_i + \delta^2}{\sqrt{1 + sI_i}} \right] \quad (2.7-20)$$

These are the ratios of the saturated gain and index of refraction to their unsaturated values. Plots of g^* and $(n - n_o)^*$ appear in Figures 2.3 and 2.4 for various values of sI_i .

Comparison of Figures 2.2 and 2.3 shows that the inversion and gain holes are qualitatively similar. Quantitatively, however, the gain hole is wider and shallower than the corresponding inversion hole due to the interaction width of the sampling signal. The depth of the hole in the gain curve may be readily determined. With $\delta = 0$ equation (2.7-17) reduces to

$$\frac{1}{I} \frac{dI_\ell}{dz} = ge^{-x_\ell^2} \left\{ 1 - \left[1 - \frac{1}{\sqrt{1 + sI_i}} \right] \right\} = \frac{ge^{-x_\ell^2}}{\sqrt{1 + sI_i}} \quad (2.7-21)$$

For $\delta = 0$ the test signal I_ℓ and the saturating signal I_i , see the same gain. The hole depth is clearly

$$\text{hole depth} = ge^{-x_\ell^2} \left[1 - \frac{1}{\sqrt{1 + sI_i}} \right] \quad (2.7-22)$$

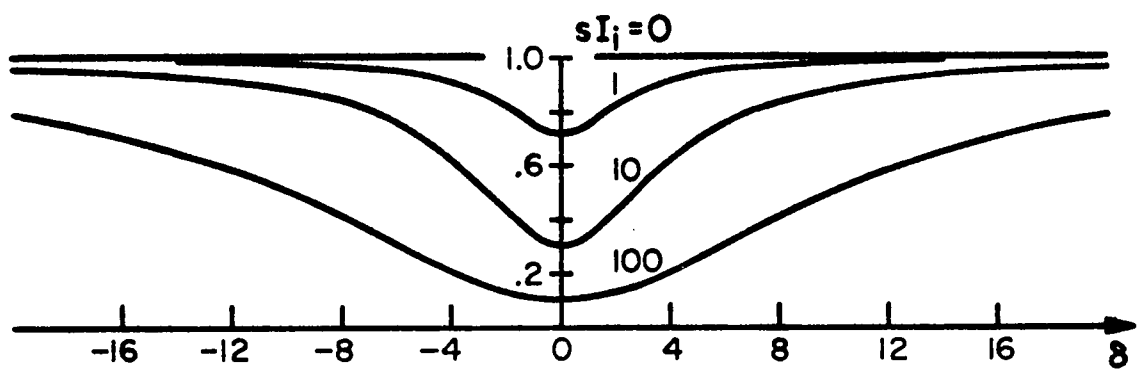


Figure 2.3 Normalized gain versus δ for various values of sI_j .

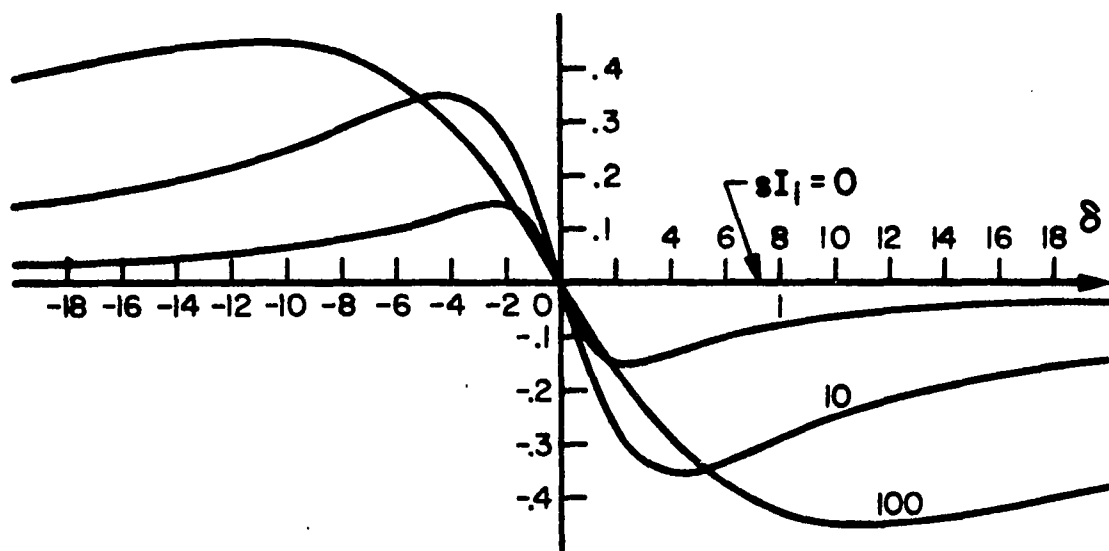


Figure 2.4 Normalized index of refraction versus δ for various values of sI_i .

The width of the hole in the gain profile may now be found by setting the hole depth at the frequency $\delta_{\frac{1}{2}}$ from equation (2.7-17) equal to one half of the line center hole depth from equation (2.7-22) or

$$\frac{sI_i}{(sI_i + \delta_{\frac{1}{2}}^2)^2 + 4\delta_{\frac{1}{2}}^2} \left[sI_i + \delta_{\frac{1}{2}}^2 - \frac{sI_i - \delta_{\frac{1}{2}}^2}{\sqrt{1 + sI_i}} \right] = \frac{1}{2} \left[1 - \frac{1}{\sqrt{1 + sI_i}} \right] \quad (2.7-23)$$

The result after some algebra is

$$\delta_{\frac{1}{2}} = 1 + \sqrt{1 + sI_i} \quad (2.7-24)$$

Thus the full width at half depth is

$$\Delta\nu_{\text{gain}} = \Delta\nu_h (1 + \sqrt{1 + sI_i}) \quad (2.7-25)$$

This is the reasonable result that the hole width is equal to the width of the hole in the inversion profile $\Delta\nu_h \sqrt{1 + sI_i}$ plus the interaction width $\Delta\nu_h$ of the sampling signal. Equation (2.7-25) has been given without proof by Close^(2.16). Our expression for the depth of the hole, equation (2.7-22), is in disagreement with the corresponding result of Close. Bennett^(2.15) and other authors make no clear distinction between the inversion hole and the gain hole.

In this section analytical expressions have been obtained for the spectral holes burned in the population inversion, gain, and index of refraction profiles of a strongly inhomogeneous laser medium.

2.8 Conclusion

In this chapter a general set of coherent rate equations was

developed from the familiar density matrix formalism. These results were then specialized to the much simpler incoherent rate equations for slowly varying fields and finally to the limit of steady state. Degeneracy effects were shown to be qualitatively unimportant in most laser applications. The steady state solutions were considered in the limits of homogeneous and inhomogeneous broadening, and various special cases were treated in detail. In particular, an analytical investigation of the important aspects of spectral hole burning was included. The results of this chapter form the basis of most of the theoretical considerations of the succeeding chapters.

Bibliography

- 2.1 W.E. Lamb, Jr., Physical Review 134, No. 6A, page A1429, 15 June 1964.
- 2.2 W. Kaplan, Ordinary Differential Equations, Addison-Wesley, Palo Alto, 1962, equation (2-58).
- 2.3 D.H. Close, Physical Review 153, No. 2, page 360, 10 January 1967.
- 2.4 D.H. Close, Ph.D. Thesis, California Institute of Technology, 1965.
- 2.5 F.A. Hopf and M.O. Scully, Physical Review 179, No. 2, page 399, 10 March 1969.
- 2.6 A. Dienes, Physical Review 174, No. 2, page 400, 10 October 1968, section 4B.
- 2.7 E.I. Gordon, A.D. White, and J.D. Rigden, Symposium on Optical Masers, Polytechnic Institute of Brooklyn, page 309, 1963.
- 2.8 A.C.G. Mitchell and M.W. Zemansky, Resonance Radiation and Excited Atoms, Cambridge, 1961, page 101.
- 2.9 A. Dienes, Physical Review 174, No. 2, page 414, 10 October 1968, section 4B.
- 2.10 L.D. Landau and E.M. Lifshitz, Quantum Mechanics, second edition, Addison-Wesley, Palo Alto, 1965, chapter XIV.
- 2.11 A. Yariv, Quantum Electronics, Wiley, New York, equation 15.3-5.
- 2.12 Handbook of Mathematical Functions, edited by M. Abramowitz and I.A. Stegun (U.S. Department of Commerce, National Bureau of Standards, Washington, D.C., 1964), Applied Mathematics Series 55, page 298.

- 2.13 B. Lohmander and S. Rittsten, Kungl. Fysiografiska Sällskapets i Lund Förhandlingar 28, No. 6, page 45, 1958.
- 2.14 This series is obtained by expanding the exponentials in the definition of $F(x)$ of equation (2.6-5), performing the integration, and multiplying together the two resultant series. The result is in disagreement with equation (214) of Mitchell and Zemansky, op. cit.
- 2.15 W.R. Bennett, Jr., Physical Review 126, No. 2, page 580, 15 April 1962.
- 2.16 D.H. Close, Ph.D. Thesis, op. cit., section 6.51.

III. The 3.51 Micron Xenon Laser

3.1 Introduction

Most of our experiments have been carried out using a xenon laser. The 3.51 micron transition in xenon exhibits extremely high optical gain, so that this medium is ideal for studying a variety of gain and saturation effects. Helium-xenon lasers may have unsaturated gains of 400 dB/m ^(3.1), while the gain in pure xenon may be up to 70 dB/m ^(3.2). The pure xenon laser is somewhat easier to fill and maintain than the helium-xenon laser, so we did not introduce helium. Also, the gain using pure xenon proved to be adequate for our purposes.

A simplified energy level diagram for the 3.51 micron transition is shown in Figure 3.1. The first subscript on the energy level designation represents the intermediate quantum number k less $\frac{1}{2}$, and the second subscript is the total angular momentum in this modified Racah notation^(3.3). The details of the inversion and decay mechanisms have been studied by Freiberg and Weaver^(3.4). Essentially, the upper laser level $5d_{33}$ is excited from the ground state by electron impact while the lower laser level $6p_{22}$ is populated only by the radiative decay of higher lying s and d levels. The natural lifetimes of the laser levels have been calculated by Clark^(3.5) using the Bates and Damgaard^(3.6) coulomb approximation. The results are that the lifetime of the upper level is 1.35 microseconds and the lifetime of the lower level is only 44 nanoseconds. Essentially the same results were also obtained in a later calculation by Allen et al^(3.7). It is this favorable lifetime ratio

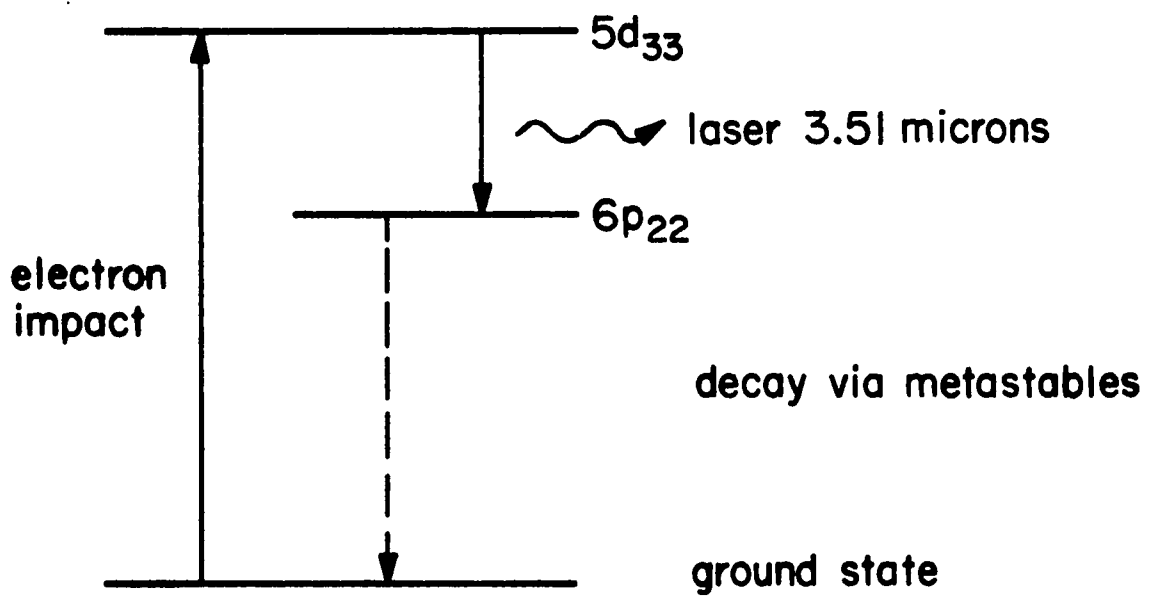


Figure 3.1 Schematic energy level diagram for the 3.51 micron transition.

and the selective pumping which lead to the large gains which have been observed at 3.51 microns in xenon. In the following sections some of the details of the gain spectrum are considered.

3.2 Homogeneous line width

There are two line widths associated with the 3.51 micron transition. The first of these is the unsaturated homogeneous line width resulting from the finite phase coherence lifetime of the excited states of identical atoms. This lifetime is determined by the natural decay rates of the states and possibly also by the collision lifetime (pressure broadening). The natural line width depends on the lifetimes of the energy levels^(3.8), and for this case it may be written

$$\Delta\nu_n < \frac{1}{2\pi} \left(\frac{1}{\tau_3} + \frac{1}{\tau_2} \right) \quad (3.2-1)$$

where $\tau_3 \approx 1.35\mu s$ is the calculated lifetime of the upper state and $\tau_2 \approx 44ns$ is the lifetime of the lower state^(3.5). The less-than sign results from the fact that a portion of the decay goes directly from the upper level to the ground state although the branching ratio is very nearly equal to unity^(3.1). According to equation (3.2-1) the natural line width is about 3.73 MHz.

The Holtsmark pressure broadening line width may be written roughly as^(3.9)

$$\Delta\nu_\ell = 1.95 \cdot 10^{19} \ p \sqrt{\frac{4R}{\pi TM}} \ \sigma_\ell^2 \quad (3.2-2)$$

where we consider that Holtsmark broadening is but a special case of Lorentz broadening. Here p is the pressure in mm., R is the universal gas constant, T is the temperature, M is the atomic weight, and σ_{ℓ}^2 is the Lorentz cross section. At a pressure of 5 microns as used in our experiments, and with $M = 131.3$ g/mole, $T = 300^\circ\text{k}$, $R = 8.31 \cdot 10^7$ erg/mole $\cdot^\circ\text{k}$, and $\sigma_{\ell}^2 \approx 10^{-14} \text{ cm}^2$ one finds

$$\Delta v_{\ell} \approx .05 \text{ MHz} \quad (3.2-3)$$

The value of σ_{ℓ}^2 was obtained by a rough extrapolation to xenon of the data of Mitchell and Zemansky's Table 21.

On the basis of the above considerations we would expect the pressure broadening to be negligible, and the overall homogeneous line width should be about

$$\Delta v_h = \Delta v_n + \Delta v_{\ell} \approx 3.7 \text{ MHz} \quad (3.2-4)$$

Schlossberg and Javan^(3.10) have obtained the "rough estimate" $\Delta v_h = 1.0 \text{ MHz}$ from a Zeeman effect measurement of the 3.51 micron line. The Lamb dip measurement described in section 5.9 yielded a threshold dip width of about 6 MHz in agreement with the width of 5 MHz reported by Wang et al.^(3.11) This width should be equal to twice the homogeneous width of about 3 MHz, which is in reasonable agreement with equation (3.2-4). For most of our work the precise value of the homogeneous line width is unimportant and we simply assume the width to be of the order of 4 MHz.

In the article of Wang et al. the theoretical homogeneous line

width is incorrectly given as 2 MHz. Also, we don't understand the reason for those authors using both a high pressure helium-xenon discharge and a low pressure xenon discharge in the same cavity when investigating the Lamb dip. From Figure 5.10 we have obtained a dip depth about twice as great as their "enhanced" dip of only 10 percent. The asymmetry shown in Figure 5.10 could be removed by using a cavity arrangement in which dispersion focusing is unimportant.

3.3 Inhomogeneous line width

Inhomogeneous broadening results whenever the atoms involved in the laser transition are not identical. Doppler broadening due to the relative motions of the atoms in the xenon discharge causes the gain spectrum of a xenon laser to be inhomogeneously broadened. The Doppler spectrum is a Gaussian^(3.12). The Doppler width $\Delta\nu_D$ may be written

$$\Delta\nu_D = \frac{2}{\lambda} \sqrt{\frac{2RT}{M}} \ln 2 \quad (3.3-1)$$

where λ is the wavelength, R is the gas constant, T is the temperature, and M is the atomic weight. $\Delta\nu_D$ is plotted as a function of T in Figure 3.2 for $\lambda = 3.51 \cdot 10^{-4}$ cm, $R = 8.31 \cdot 10^7$ ergs/mole·°k, and $M = 131.3$ g/mole.

Patel^(3.13) has derived the value $T = 515^\circ$ k for a xenon discharge independent of pressure and discharge condition based on measurements of the line width of the 2.026 micron laser transition. This result seems a little high and could be due partly to isotope shifts. For our experiments the discharge tube walls only became perceptibly warm at

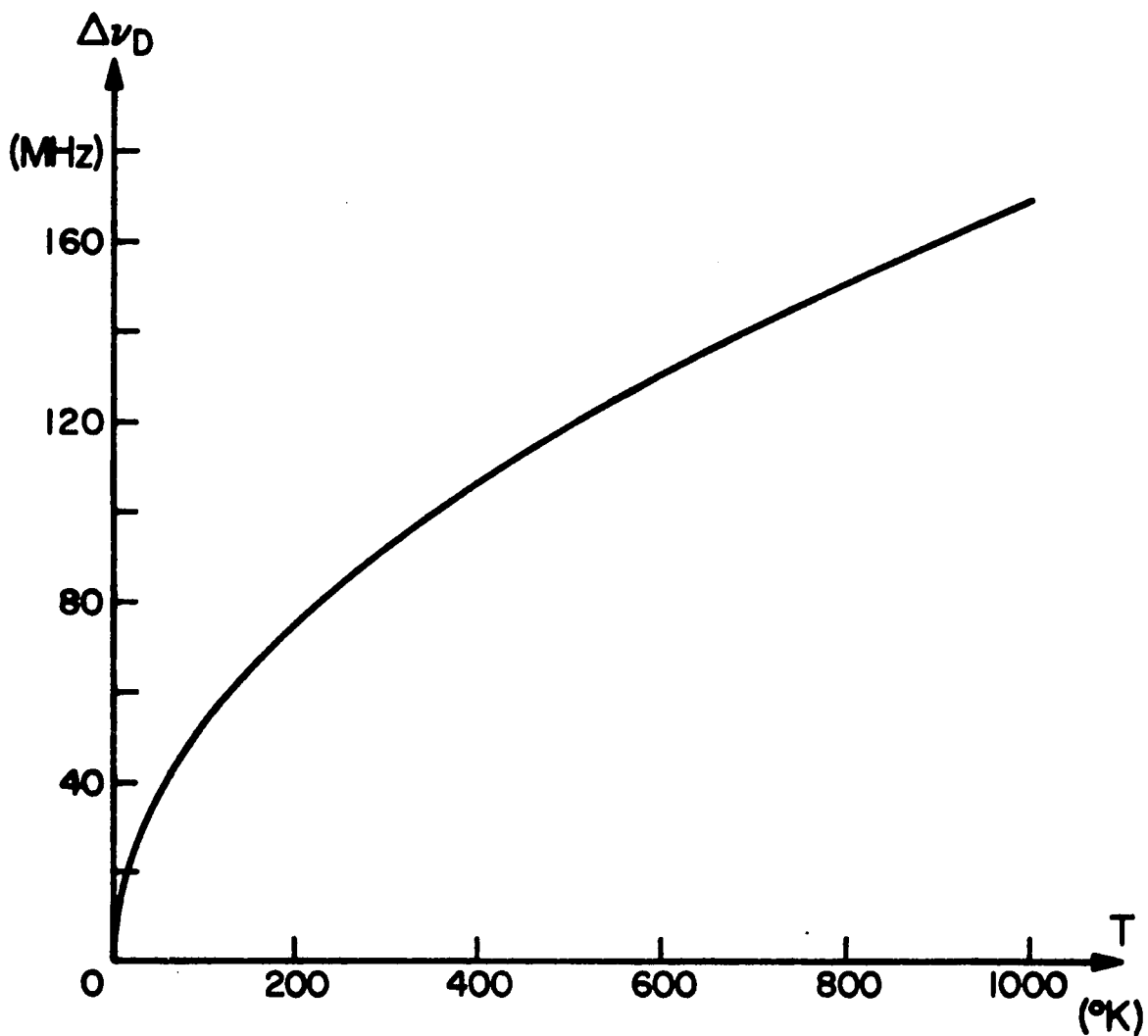


Figure 3.2 Doppler width versus temperature for the 3.51 micron transition.

the higher discharge currents. The Doppler line width is not a very sensitive function of temperature, and we choose for our calculations the approximate value 100 MHz, which corresponds to a temperature of about 350°k.

We have not obtained a direct experimental measurement of the Doppler width. Various indirect measurements seem to suggest a larger value for the line width. The mode pulling measurements of section 4.5, for example, suggest a Doppler width of about 160 MHz. There are several possible reasons for this discrepancy which are discussed elsewhere in this work.

3.4 Hyperfine structure

If Doppler broadening were the only mechanism causing the atoms in a xenon discharge to be nonidentical, then the gain spectrum would be a simple Gaussian function with a width of about 100 MHz as discussed in the previous section. However, magnetic hyperfine splitting has been found to be important for two of the naturally occurring isotopes of xenon, so the situation is more complicated. The atomic weights, percent abundances, and nuclear spins of the natural xenon isotopes are listed in Table 3.1.^(3.14)

The energy shift of the hyperfine levels is governed by the equation^(3.15)

$$E = E_0 + \frac{a_1}{2} [f(f+1) - i(i+1) - j(j+1)] \quad (3.4-1)$$

if the electric quadrupole interaction is neglected. The letters f, i,

Weight	% abund.	spin
124	.096	0
126	.090	0
128	1.92	0
129	26.44	1/2
130	4.08	0
131	21.18	3/2
132	26.89	0
134	10.44	0
136	8.87	0

Table 3.1 Atomic weights, relative abundances, and nuclear
spins of the stable isotopes of xenon.

and j are the quantum numbers associated respectively with the total angular momentum vector of the atom \vec{F} , the nuclear spin vector \vec{I} , and the electronic angular momentum \vec{J} . The coefficients a_j are the magnetic hyperfine coupling constants. Sakurai and Shimoda^(3.16) have measured the coupling coefficients for the 3.51 micron transition for isotope 131 and obtained the frequency values $a_3 = 174 \pm 15$ MHz and $a_2 = 96 \pm 15$ MHz. The nuclear spin of this isotope is $i = 3/2$. Then using equation (3.4-1) the hyperfine energy terms and the relative hyperfine frequencies can be calculated. The coupling coefficients for isotope 129 are related to those for isotope 131 by the ratio of the nuclear magnetic moments. According to Sakurai and Shimoda this ratio is $\mu_i(129)/\mu_i(131) = -1.10$ (although the C.R.C. data^(3.17) leads to the value -1.12). Thus for isotope 129 the coupling coefficients are $a_3 = -191$ MHz and $a_2 = -106$ MHz. The even isotopes have zero spin and consequently, since $f = j$, there is no hyperfine splitting.

The relative intensities of the hyperfine components can also be calculated. The results have been tabulated by White and Eliason^(3.18). The values relevant to the 3.51 micron transition are listed in Table 3.2 together with the relative frequencies from equation (3.4-1). They are graphed in Figure 3.3 as corrected for the percent abundances from Table 3.1. This graph differs in some particulars from a similar graph by Sakurai and Shimoda, but ours is believed to be correct.

The shape of the overall theoretical gain curve can be obtained by assigning to each of the hyperfine lines of Figure 3.3 a Gaussian of width 100 MHz. The result is shown in Figure 3.4. Similarly, the overall dispersion curve may be calculated by assigning to each line

Isotope 131

f → f'	rel. freq. MHz	rel. int.
9/2 - 7/2	495	100
7/2 - 7/2	-288	11.4
7/2 - 5/2	48	68.6
5/2 - 7/2	-897	.6
5/2 - 5/2	-561	14.6
5/2 - 3/2	-321	44.8
3/2 - 5/2	-996	.8
3/2 - 3/2	-756	11.2
3/2 - 1/2	-612	28.0

Isotope 129

f → f'	rel. freq. MHz	rel. int.
7/2 - 5/2	-182	100
5/2 - 5/2	490	5.0
5/2 - 3/2	225	70.0

Table 3.2. Relative frequencies and intensities of the 3.51 micron xenon hyperfine transitions.

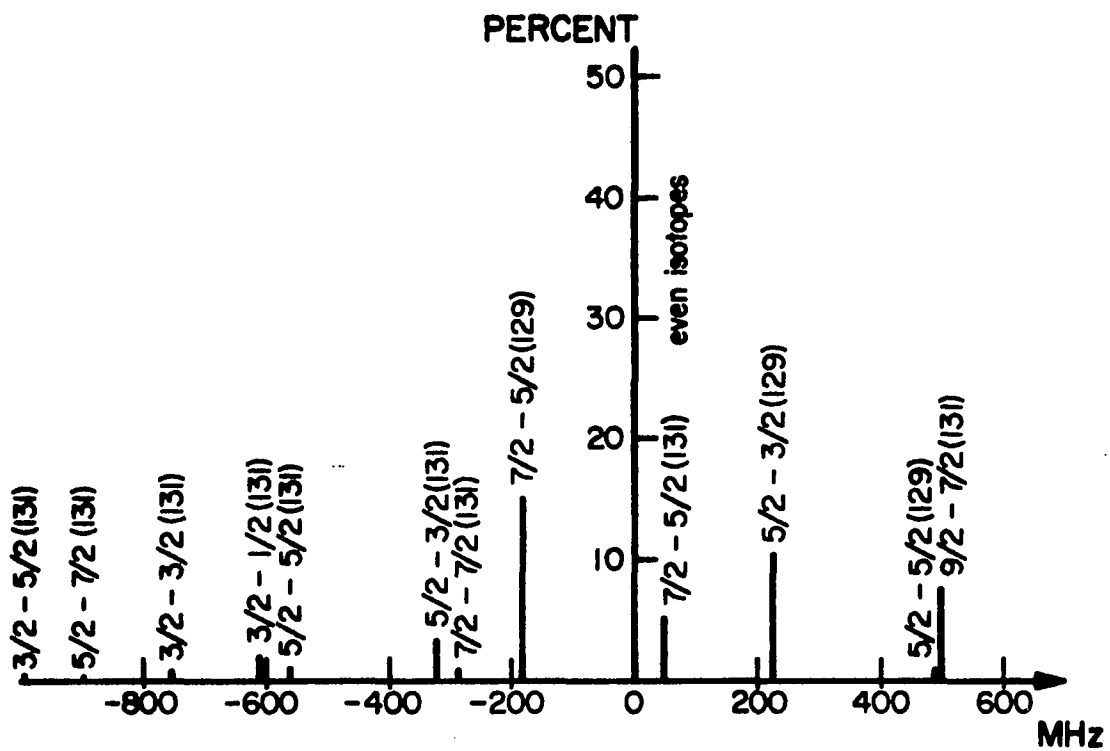


Figure 3.3 Hyperfine structure of the 3.51 micron transition

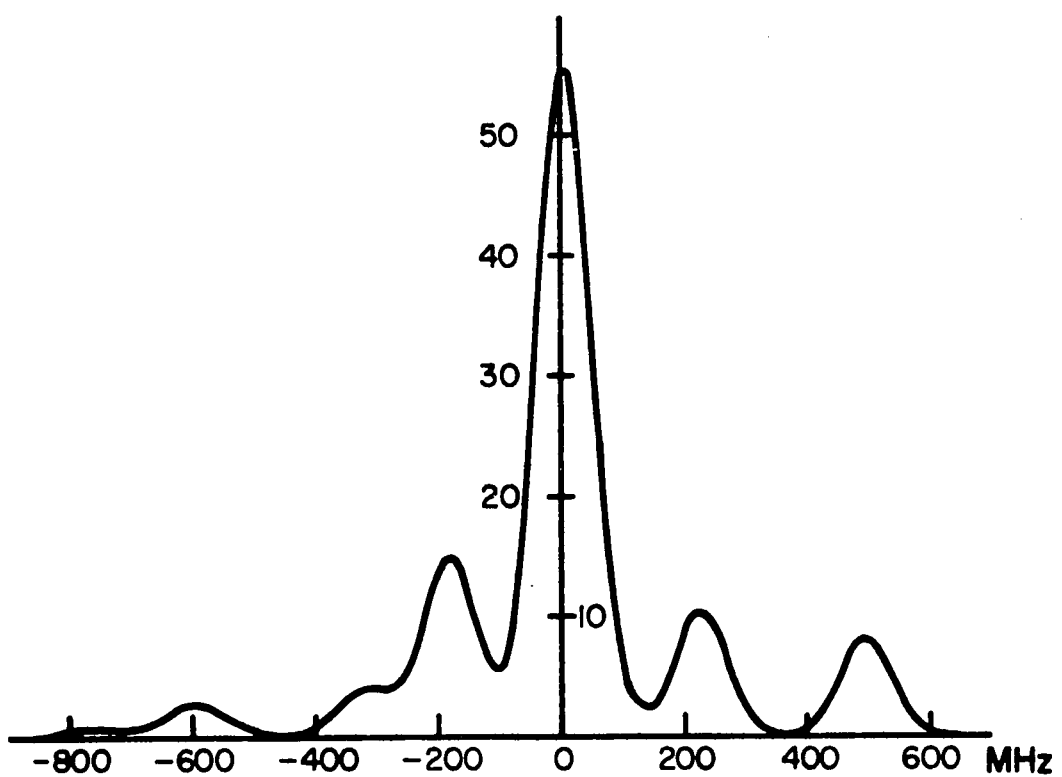


Figure 3.4 Theoretical gain spectrum including hyperfine structure.

Dawson's integral $F(x)$ as given approximately by equation (2.6-9). The result is shown in Figure 3.5. In Figure 3.6 is an expanded view near line center of the gain and dispersion curves as compared to the results which would be obtained if the odd isotopes were not present. Clearly, the odd isotopes contribute negligibly in a high loss laser and may be ignored. A practical consequence of this result is that a laser filled with even isotopic xenon should have twice the incremental gain of a laser filled with natural xenon and operated under identical conditions. In other words, a 400 dB/m helium-xenon laser would become an 800 dB/m laser.

We have performed experiments using both naturally occurring xenon and pure xenon 136. The results, as indicated in section 4.5, are that the gain is about 30 percent greater and the line width is about 30 percent less when the monoisotopic xenon was used. It is satisfying that the apparent "area" of the gain spectrum remained unchanged for a fixed discharge level, but the magnitude of the gain enhancement was much less than the above considerations would have led us to expect. The reason for this discrepancy is unknown. We obtained a mass spectrogram of the xenon to verify that it was indeed 91 percent xenon 136 as specified by its manufacturer (Monsanto). Two other obvious explanations are that either we erred in our experimental measurements or else the hyperfine coupling constants of Sakurai and Shimoda^(3.16) are incorrect.

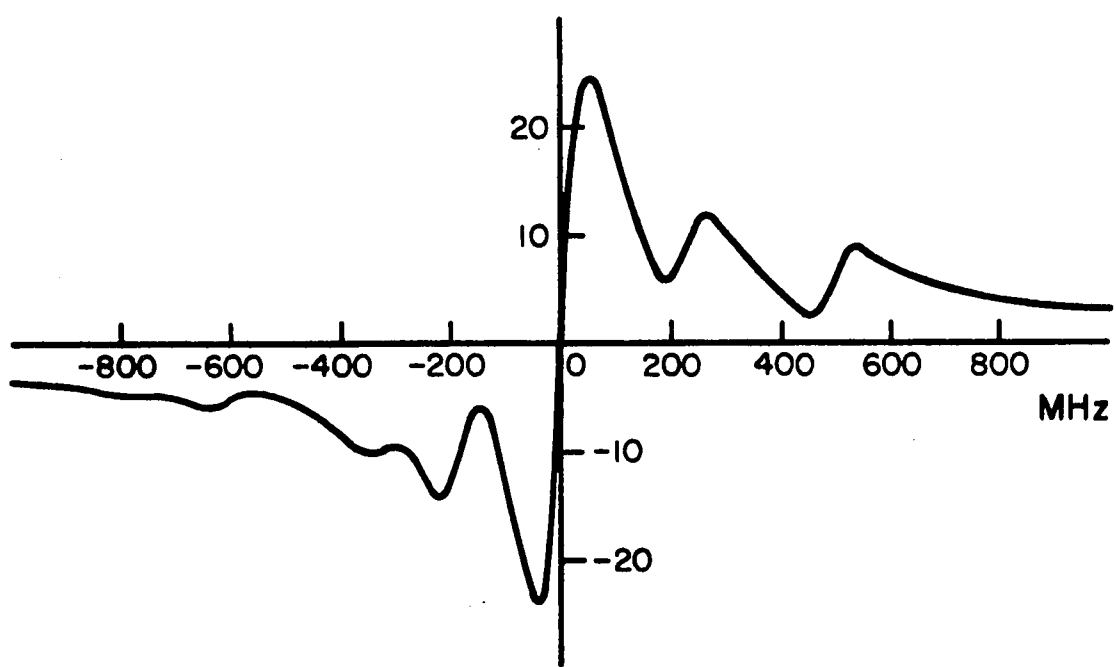


Figure 3.5 Theoretical dispersion spectrum including hyperfine structure.

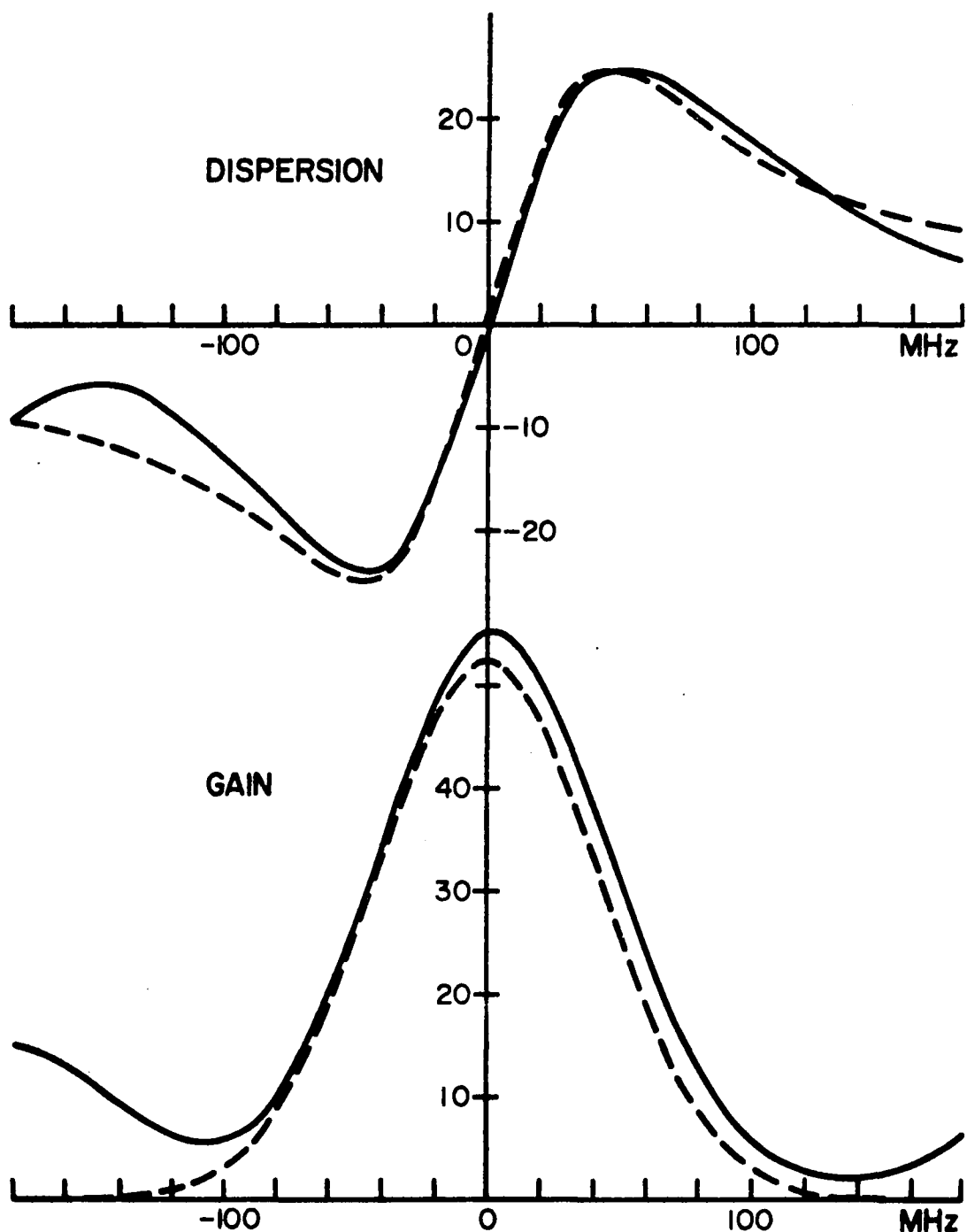


Figure 3.6 Line center gain and dispersion curves including all isotopes (solid lines) and only even isotopes (dashed lines).

3.5 Isotope shifts

With the discrepancy between theory and experiment which was described in the previous section it is perhaps pointless to investigate in detail the possibility of isotope shifts of the 3.51 micron transition. Nevertheless, we assume here that the preceding analysis is correct and include some basic considerations which might be useful in later work. It was shown that the gain and dispersion profiles near line center in a xenon laser should be determined primarily by the even isotopes. On that basis one would expect the gain in an unsaturated laser to be given essentially by a Gaussian of 100 MHz width. It turns out, however, that the even isotopes themselves do not all occur at precisely the same frequency because of isotope shift effects.

Isotope shifts are described in detail in section I-IV of Kopfermann^(3.19), and shifts in the rare gases have been discussed by Stone^(3.20). Here we only give some elementary considerations based mainly on the work of those authors. There are two basic types of isotope shifts known as the mass effect and the volume effect. The mass effect has two main contributions. The normal mass effect results because the reduced mass of the electron depends slightly on the nuclear mass. The specific mass effect results from an electron pair interaction with the nucleus.

We consider first the normal mass effect. The hydrogenic term values are

$$T_n = \frac{R_{\infty} Z^2}{n^2} \frac{m_n}{m_n + m_e} \quad (3.5-1)$$

where R_∞ is the Rydberg constant, Z is the appropriate atomic number in this Bohr atom model, n is the principal quantum number, and m_e and m_n are respectively the electronic and nuclear masses. From equation (3.5-1) it follows in a straightforward fashion that the Bohr frequency shift is given approximately by

$$\Delta\nu_B \approx \frac{m_e}{m_p} \frac{M_2 - M_1}{M_1 \cdot M_2} \nu \quad (3.5-2)$$

where m_p is the proton mass and M_2 and M_1 are the atomic weights of two isotopes. Equation (3.5-2) describes the most important isotope shift effect for light atoms.

For values appropriate to the 3.51 micron transition equation (3.5-2) becomes

$$\Delta\nu_B = 4.66 \cdot 10^4 \left(\frac{M_2 - M_1}{M_1 \cdot M_2} \right) \text{ MHz} \quad (3.5-3)$$

The heavier atoms are resonant at higher frequencies than the lighter atoms. From Table 2.1 the dominant even isotope has the weight 132. Assuming $M_1 \approx M_2 \approx 132$, equation (3.5-2) simplifies to

$$\Delta\nu_B \approx 2.68 \Delta M \text{ MHz} \quad (3.5-4)$$

Thus the frequency difference between isotopes 132 and 134 would be about 5 MHz. Shifts of this magnitude would result in a slightly broadened gain profile which was still essentially Gaussian in shape.

The specific mass effect is due to the term $\left(\frac{1}{M}\right) \sum_{k>\ell} \bar{P}_k \cdot \bar{P}_\ell$

in the electronic Hamiltonian, where M is the nuclear mass and the summation is over pairs of electrons. Evaluation of the specific mass shift involves some complicated integrations of electronic wave functions which we have not attempted. The procedure is given by Stone^(3.20).

The volume effect isotope shift results whenever the orbital electronic charge density overlaps the nuclear volume. The electrons are bound more weakly the larger the nuclear volume if the total nuclear charge is constant. But the nuclear volume increases for increasing isotopic weight. Thus the term value shifts are given approximately by

$$\Delta T \approx C' \Delta M \quad (3.5-5)$$

where the constant C' depends on the details of the nuclear model and the electronic configuration. The term spacings are nearly uniform as indicated by equation (3.5-5) provided that quadrupole effects are unimportant. The overlap is only appreciable for the s and $p_{\frac{1}{2}}$ electrons (in jj coupling). The lower state $6p_{22}$ of the 3.51 micron transition (intermediate coupling) has some $6p_{\frac{1}{2}}$ character so that volume effect shifts are to be expected.

From equation (3.5-5) the frequency shifts for this transition should be governed by the equation

$$\Delta v_v = - C \Delta M \quad (3.5-6)$$

where $C = C'/h$ and h is Planck's constant. Thus the volume effect shifts have the opposite sign to the Bohr shifts with the heavier isotopes

occurring here at lower frequencies than the lighter isotopes. These arguments have been oversimplified, of course, and we make no attempt at the difficult problem of calculating the constant C.

In xenon the Bohr shift is negligible but both the specific mass effect and the volume effect are appreciable. Volume effect shifts have been shown experimentally to be dominant for transitions to the 6s level^(3.21). For the 3.51 micron transition the specific mass effect is most important and a shift of 78.9 MHz has been measured by Vetter^(3.22) between isotopes 132 and 136. If the isotope frequency spacings were equal (not always a good assumption), then the shift constant would be 19.7 MHz/amu. Our information on the isotope shifts in xenon is not sufficiently detailed to justify plotting theoretical gain and dispersion curves for the even isotopes. However, from the data of Vetter it is apparent that the effective line width should be somewhat greater than the Doppler width estimated in section 3.3. These shifts might also lead to an asymmetry in the gain spectrum. As mentioned in the previous section, our experiments indicate an increase in height and a decrease in width of the gain spectrum when the laser is operated with pure xenon 136. This effect is due to the elimination of both the hyperfine structure and the isotope shifts.

3.6 Conclusion

In this chapter it has been shown that reasonable values for the homogeneous and inhomogeneous line widths of the 3.51 micron xenon transition are 4 MHz and 100 MHz respectively. These results will be

used in the succeeding chapters. Also, it has been shown that the odd isotopes of xenon are split up by the magnetic hyperfine interaction into several weak components which should not contribute significantly to the gain in a high loss laser.

Isotope shifts are probably also important in xenon with a magnitude on the order of 20 MHz per amu. If these interpretations were correct, then the laser gain would be determined primarily by isotope 132, which has only a 27 percent natural abundance. Consequently a laser using only xenon 132 would, in principle, have about three times the incremental gain of an equivalent laser using natural xenon. Thus c.w. gains in excess of 1000 dB/m should be readily obtainable. The highest gain previously reported for a gas laser is 630 dB/m^(3.23) for a pulsed lead vapor system. Experiments with a monoisotopic xenon laser show an increase in gain of only about 30 percent. The reason for this discrepancy is not known.

Another tactic which is familiar in plasma work but which evidently has not been employed in gas laser studies is the cooling of the gas discharge. If all other factors were unchanged, cooling the discharge should lead to a narrower line width and a larger line center gain. In particular, at 77°k the line width would be halved and the gain doubled from their room temperature values.

Bibliography

- 3.1 J. W. Klüver, Journal of Applied Physics 37, No. 8, page 2987, July 1966.
- 3.2 P. O. Clark, Journal of Quantum Electronics QE-1, No. 3, page 109, June 1965.
- 3.3 American Institute of Physics Handbook (McGraw-Hill Book Co., Inc., New York, 1957), page 7-58.
- 3.4 R. J. Freiberg and L. A. Weaver, Journal of Applied Physics 38, No. 1, page 250, January 1967.
- 3.5 P. O. Clark, R. A. Huback, and J. Y. Wada, JPL Contract No. 950803, Final Report, April 1965.
- 3.6 D. R. Bates and A. Damgaard, Royal Society of London Philosophical Transactions 242, page 101, 1949.
- 3.7 L. Allen, D. G. C. Jones, and D. G. Schofield, Journal of the Optical Society of America 59, No. 7, page 842, July 1969.
- 3.8 A. C. G. Mitchell and M. W. Zemansky, Resonance Radiation and Excited Atoms, Cambridge University Press, page 100, equation (36), 1961.
- 3.9 Ibid., page 170, equation (105).
- 3.10 H. R. Schlossberg and A. Javan, Physical Review Letters 17, No. 25, page 1242, 19 December 1966.
- 3.11 S. C. Wang, R. L. Byer, and A. E. Siegman, Applied Physics Letters 17, No. 3, page 120, 1 August 1970.
- 3.12 A. Yariv, Quantum Electronics, John Wiley and Sons, Inc., New York, page 457, 1967.

- 3.13 C. K. N. Patel, Physical Review 131, No. 4, page 1582, 15 August 1963.
- 3.14 Handbook of Chemistry and Physics, forty-ninth edition, The Chemical Rubber Co., Cleveland, Ohio, pages B-44 and E-73, 1968.
- 3.15 H. Kopfermann and E. E. Schneider, Nuclear Moments, Academic Press Inc., New York, page 16, equation (4.2), 1958.
- 3.16 K. Sakurai and K. Shimoda, Journal of the Physical Society of Japan 21, page 1214, 1966.
- 3.17 Handbook of Chemistry and Physics, op. cit., page E-73.
- 3.18 H. E. White and A. Y. Eliason, Physical Review 44, page 753, 1933.
- 3.19 H. Kopfermann and E. E. Schneider, op. cit., page 161.
- 3.20 A. P. Stone, Proceedings of the Physical Society of London 74, page 424, 1959.
- 3.21 J. Koch and E. Rasmussen, Physical Review 77, page 722, 1950.
- 3.22 R. Vetter, C. R. Acad. Sc. Paris 265, Series B, page 1415, 18 December 1967.
- 3.23 W. T. Silfvast and J. S. Deech, Applied Physics Letters 11, No. 3, page 97, August 1967.

IV. Longitudinal Modes

4.1 Introduction

The arrangement of longitudinal modes in a high gain laser oscillator may differ substantially from those in more conventional lasers where anomalous dispersion effects are unimportant^(4.1). The basic features of mode pulling in low gain lasers are well known^(4.2 - 4.5). In particular, it is found that modes near the center of the gain spectrum of the amplifying medium are pulled toward the gain center and repelled from each other. These effects result from the anomalous dispersion associated with the gain line, and for most purposes they are negligible. In typical low gain lasers the mode spacing may be reduced by at most a small fraction of a percent from its empty resonator spacing.

In a high gain helium-xenon laser, on the other hand, the mode spacing may in principle be reduced by more than an order of magnitude. Also, in a high gain laser oscillation may be obtained in the wings of the gain line. Dispersion effects near the wings are different from the effects expected near line center. The modes may split and display an increase in frequency with decreasing mode order. In other words, the frequency of radiation propagating through a highly dispersive medium may increase with increasing wave length. We present here a theoretical analysis of mode pulling in high gain lasers which are predominantly either homogeneously or inhomogeneously broadened. Saturation effects are included. Some of the conclusions are verified experimentally using a high gain xenon laser. We have observed a

saturation dependent reduction in mode spacing by a factor of 2.5 in approximate agreement with the theory.

4.2 Inhomogeneous broadening

The laser systems in which the mode structure distortion is likely to be most important are all inhomogeneously broadened. In an inhomogeneously broadened laser the homogeneous line width is much less than the overall gain line width. In particular, we consider here Doppler broadened gas lasers, where the combination of high gain and narrow line width makes anomalous dispersion effects especially significant.

As our starting point we use equation (2.6-14) for the frequency dependent index of refraction of an unsaturated Doppler broadened amplifying medium with a negligible homogeneous line width. This equation for a low pressure gas laser is

$$n(v) = 1 + \frac{cg F(x)}{2\pi^{3/2} v} \quad (4.2-1)$$

where $F(x)$ is Dawson's integral given by equation (2.6-5). The frequency is measured by $x = \frac{2(v-v_0)}{\Delta v_D} \sqrt{\ln 2}$ and g is the small signal incremental gain constant at line center. Equation (4.2-1) is valid so long as $\epsilon(1+si)^{\frac{1}{2}} \ll 1$ where $\epsilon = \frac{\Delta v_h}{\Delta v_D} \sqrt{\ln 2}$ is the natural damping ratio, s is the saturation parameter, and I is the intensity. Saturation effects are considered in Section 4.4.

The phase condition which must be satisfied by any oscillating mode is that the real round trip phase delay be an integral multiple of 2π , or

$$2\pi m = \int \gamma dz \\ = \frac{2\pi v}{c} \int n(v, z) dz \quad (4.2-2)$$

where γ is the real part of the propagation constant. If the cavity length is L and the length of the active medium is ℓ , then equation (4.2-2) becomes

$$2\pi m = \frac{4\pi v L}{c} \left[1 + \frac{\ell}{L} (\bar{n}(v) - 1) \right] \quad (4.2-3)$$

where $\bar{n}(v)$ is the spatially averaged index of refraction of the medium. In terms of the empty resonator mode frequencies $v_m = \frac{mc}{2L}$, equation (4.2-3) may be written

$$v_m = v \left[1 + \frac{\ell}{L} (\bar{n}(v) - 1) \right] \quad (4.2-4)$$

This is the general result for the mode frequencies of a laser containing a dispersive amplifying medium.

Using equation (4.2-1), equation (4.2-4) becomes

$$v_m - v = \frac{\ell}{L} \frac{cg}{2\pi^{3/2}} F(x)$$

or

$$x_m - x = \beta F(x) \quad (4.2-5)$$

where we define the dispersion parameter β as

$$\beta = \frac{\ell}{L} \frac{cg \sqrt{\ln 2}}{\pi^{3/2} \Delta v_D} \quad (4.2-6)$$

Equation (4.2-5) may be used to determine the oscillation frequencies of a laser in which the amplifying medium is predominantly Doppler broadened.

For lines near gain center ($x \ll 1$), Dawson's integral simplifies to $F(x) \approx x$ according to equation (2.6-6). With this approximation equation (4.2-5) may be solved with the result

$$x = \frac{x_m}{1 + \beta} \quad (4.2-7)$$

The mode spacing is reduced from its empty resonator value according to

$$\Delta\nu = \frac{\Delta\nu_0}{1 + \beta} \quad (4.2-8)$$

For example, in a typical helium-neon laser at 6328 \AA the Doppler line width is about 1800 MHz and the gain may be $g = .1 \text{ m}^{-1}$. Then from equation (4.2-6) the dispersion parameter is roughly $\beta = .2 \cdot 10^{-2}$ so that mode pulling reduces the mode spacing by only about .2 percent. On the other hand, in a high gain helium-xenon laser at 3.51 microns the Doppler line width is about 100 MHz (Section 3.3) and the gain may be $400 \text{ dB/m}^{4.6}$ or $g = 92$. In this case the dispersion parameter is about $\beta = 40$ and the mode spacing is reduced by more than an order of magnitude from its empty resonator value.

For low gain lasers near threshold one finds that β is approximately the ratio of the cavity line width $\Delta\nu_c$ to the Doppler line width. Then equation (4.2-7) may be used to write an expression for the oscillation frequency

$$\nu = \frac{\Delta\nu_D v_m + \Delta\nu_c v_0}{\Delta\nu_D + \Delta\nu_c} \quad (4.2-9)$$

This result has been given by Bennett (4.2). It is not as general as equation (4.2-7) which applies even for high gain lasers where perturbation treatments are not valid. The first order saturation corrections to equation (4.2-7) will be given in Section 4.4.

So far attention has been restricted to frequencies near gain center where the dispersion is linear. However, in high gain lasers oscillation may be obtained in the wings of a resonance line where the dispersion effects are strikingly different. Equation (4.2-5) may be written

$$F(x) = \frac{x_m - x}{\beta} \quad (4.2-10)$$

Perhaps the simplest way to see the qualitative implications of this equation is by a graphical solution. In Figure 4.1 graphical solutions of equation (4.2-10) are shown for three values of β and for $\Delta x_m = 2$. For $\beta = 0$ dispersion is unimportant and the mode frequencies have their empty resonator values x_m — for indeed the condition $\beta = 0$ means that the resonator is empty. When $\beta = 1$ there is a "pulling" of the modes near gain center. For $\beta = 10$ the mode structure bears little resemblance to its empty cavity form. Some of the modes split and occur at three different frequencies as indicated by the circled intersections in Figure 4.1c. In other words there may be three frequencies which all correspond to the same number of half wavelengths between the mirrors. Moreover, the modes occurring between approximately $x = 1$ and $x = 2.5$ are in reverse order with the higher frequency modes having longer average wavelengths inside the resonator than lower frequency modes.

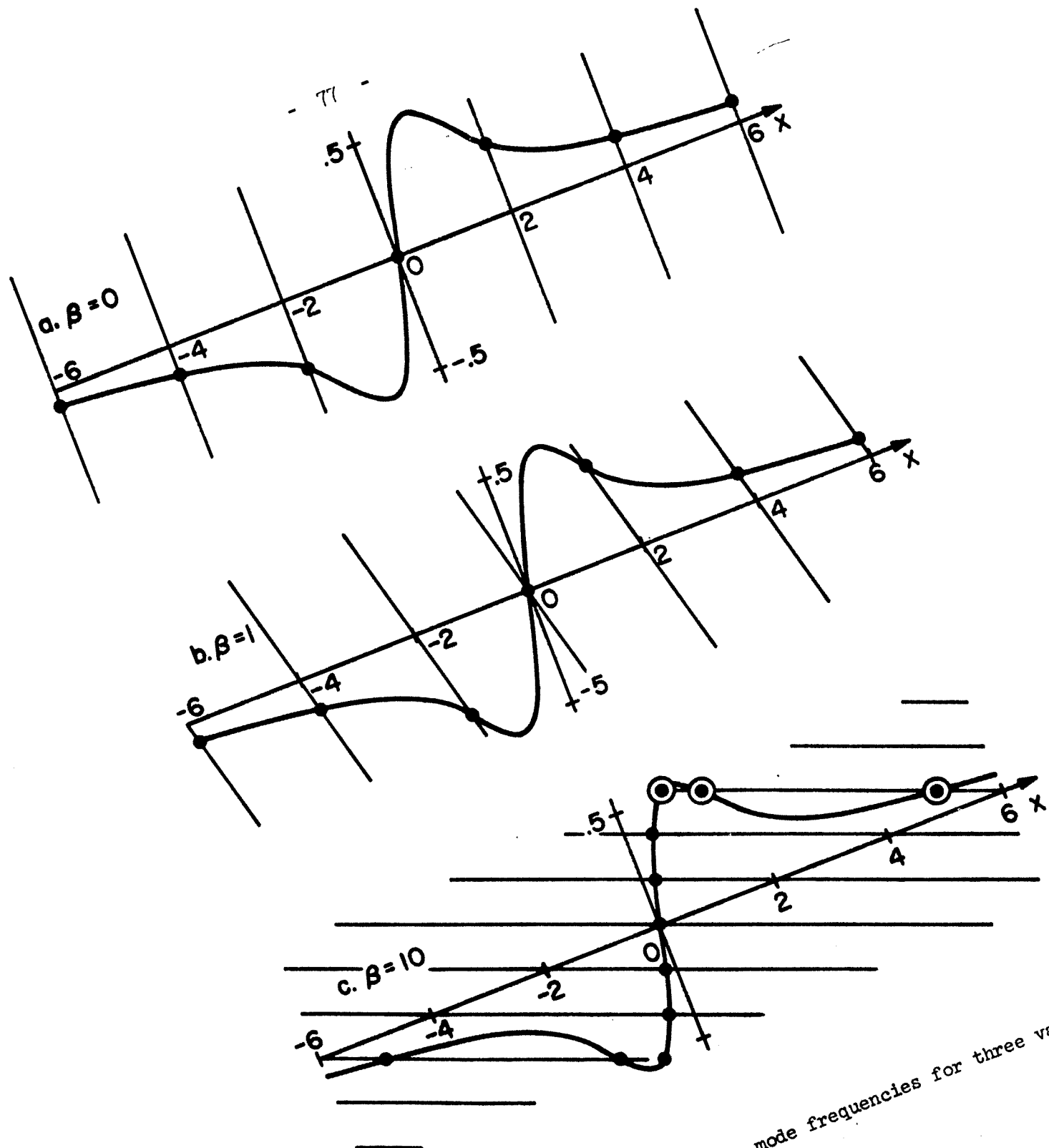


Figure 4.1 Graphical solution for mode frequencies for three values of β

All of the features of Figure 4.1c should be obtainable in a helium-xenon laser. From the figure it is clear that the condition for mode splitting to be possible is that the slope of Dawson's integral at the outer inflection points be less $-1/\beta$ or

$$\left. \frac{dF}{dx} \right|_{x_{\text{inf}}} < -\frac{1}{\beta} \quad (4.2-11)$$

Using equation (2.6-10) , this result may be written

$$\beta > \frac{1}{2[xF(x)]_{x_{\text{inf}}} - 1} \quad (4.2-12)$$

The value of $xF(x)$ at the inflection point ^(4.7) is 0.64237 so that the condition for mode splitting becomes

$$\beta > 3.51 \quad (4.2-13)$$

This condition is readily satisfied in xenon and helium-xenon at 3.51 microns. In fact these are believed to be the only continuous lasers in which mode splitting could presently be observed.

For completeness we consider the possibility of oscillation far in the wings of the resonance line. In this region Dawson's integral simplifies to $F(x) \approx \frac{1}{2}x$ according to equation (2.6-7) . Then equation (4.2-5) becomes

$$x_m - x = \frac{\beta}{2x} \quad (4.2-14)$$

or approximately

$$x \approx x_m - \frac{\beta}{2x_m} \quad (4.2-15)$$

Thus, even in the wings there is a pulling of the modes toward line center. This pulling becomes less important for increasing values of $|x_m|$. Oscillation cannot be obtained arbitrarily far into the wings, of course, since the gain is falling off as e^{-x^2} in this region.

These mode pulling effects have important consequences for laser stability. It is evident from the foregoing that an order of magnitude reduction in mode spacing implies an order of magnitude improvement in stability with respect to mirror displacement. Specifically, if the stability S is defined as the rate of change of frequency with mirror position, then

$$S = \frac{S_0}{1 + \beta} \quad (4.2-16)$$

where S_0 is the rate in a similar laser which lacks dispersion. This result is, of course, only valid in the linear region of the dispersion curve near line center.

Also, any frequency dependent peculiarity in the output spectrum of a laser can often be employed in a feedback arrangement to stabilize the laser. We propose here a stabilization scheme for a xenon laser making use of the mode splitting described above. Consider a high gain laser ($\beta = 10$) of such a length as to support only the resonant frequencies shown circled in Figure 4.1c. Suppose further that the highest of the three frequencies is below threshold. The output then will consist of two lines, the spacing between which will be a very sensitive function of the cavity length. Shortening the cavity would reduce the beat frequency

between the two lines, and lengthening the cavity would increase the beat frequency. Moreover, the beat frequency would go to zero and oscillation would abruptly cease if the cavity were shortened too much and the lines of Figure 4.1c ceased to intersect. Arrangements to sense the beat frequency and correct the mirror positions would yield an absolute frequency standard. Such a feedback system would be simpler than some schemes which have been employed ^(4.8). Continuous vibration of one of the mirrors is not required, and long term stability would be limited by changes in the Doppler profile due, for example, to temperature fluctuations. It would, however, be necessary to either operate the laser very near to threshold or else maintain a constant saturation power because of possible repulsion effects between the components of the split mode.

4.3 Homogeneous broadening

Here we consider some consequences of anomalous dispersion in homogeneously broadened laser oscillators. For the most part homogeneous lasers have either too small a gain or too large a line width for dispersion effects to be of much importance. The principal application of these results would probably be to strongly saturated high gain Doppler lines in gas lasers. Saturation may cause such lines to appear homogeneously broadened.

According to equation (2.5-8) the index of refraction of an unsaturated homogeneously broadened material is

$$n(v) = 1 + \frac{cg'}{4\pi v} \frac{y}{1+y^2} \quad (4.3-1)$$

where $g' = \frac{g}{\frac{\pi^2}{L^2} \epsilon}$ is the line center gain and $y = \frac{2(v - v_o)}{\Delta v_h}$ is a frequency parameter. Substituting this expression in equation (4.2-4) yields

$$v_m - v = \frac{L}{L} \frac{cg'}{4\pi} \frac{y}{1+y^2}$$

or

$$y_m - y = \beta' \frac{y}{1+y^2} \quad (4.3-2)$$

where we define the dispersion parameter β' as

$$\beta' = \frac{L}{L} \frac{cg'}{2\pi\Delta v_h} = \frac{\beta}{2\epsilon} \quad (4.3-3)$$

Equation (4.3-2) is the general expression for the oscillation frequencies of an unsaturated homogeneously broadened laser. The effects of saturation are considered in Section 4.4.

Equation (4.3-2) may be written

$$y^3 - y_m y^2 + (1 + \beta') y - y_m = 0 \quad (4.3-4)$$

A similar equation could be written for inhomogeneously broadened lasers using the approximate form of Dawson's integral given in equation (2.6-8). This is a cubic equation which may have either one or three real roots. The case of three real roots corresponds to a splitting of a particular mode into three frequencies, as discussed previously. Equation (4.3-4) may, with some difficulty, be solved analytically for all of the oscillation frequencies in a particular laser configuration.

We do not do so here. Graphical solutions are of course possible as before, but qualitatively they are no different from the solutions of Figure 4.1 for an inhomogeneous line and are also omitted.

Near gain center ($y^2 \ll 1$) equation (4.3-2) becomes

$$y = \frac{y_m}{1 + \beta'} \quad (4.3-5)$$

This is the linear mode pulling approximation analogous to equation (4.2-7) for inhomogeneous broadening. For large values of y it is convenient to write equation (4.3-2) as

$$y_m - y = \frac{\beta'}{y(1 + \frac{1}{y^2})} \quad (4.3-6)$$

Then the mode frequencies far in the wings are given approximately by

$$y = y_m - \frac{\beta'}{y_m} \quad (4.3-7)$$

in analogy with equation (4.2-15).

The condition for mode splitting to be possible may be written as before

$$\frac{dy}{dy} \left(\frac{y}{1 + y^2} \right) < - \frac{1}{\beta'}, \quad (4.3-8)$$

One finds after a little algebra that the inflection point occurs at $y = \sqrt{3}$ where the value of the derivative is $-1/8$. Therefore, equation (4.3-8) yields

$$\beta' > 8 \quad (4.3-9)$$

As an example of these results we consider the case of the homogeneously broadened 1.06 micron YAlG laser. In YAlG the unsaturated line center gain may be about $g' = 3 \text{ m}^{-1}$ and the homogeneous line width is approximately 1500 MHz. Then according to equation (4.3-3) the dispersion parameter is at most about $\beta = .1$. Thus from equation (4.3-5) a reduction in the mode spacing of about 10 percent is the most that could be expected in a short unsaturated YAlG laser.

4.4 Saturation effects

In the preceding sections of this chapter saturation effects have been assumed to be negligible. The purpose of this section is to investigate the influence of saturation on the location of the longitudinal mode frequencies. Expressions are developed for saturation dependent mode pulling which are roughly appropriate to the experiments with a xenon laser which are described in section 4.5.

First we consider the important limit of predominantly inhomogeneous broadening ($\epsilon \ll 1$). As our starting point for this case we have equation (2.6-12) for the index of refraction at the frequency v_ℓ of a medium containing several weakly interacting radiation fields

$$n(v_\ell) = 1 + \frac{cgF(x_\ell)}{2\pi^{3/2}v_\ell} - \frac{c\epsilon g}{2\pi v_\ell} (1 + sI_\ell)^{\frac{1}{2}} x_\ell e^{-x_\ell^2} - \frac{\epsilon cg}{4\pi v_\ell} \sum_{n \neq \ell} \frac{sI_n e^{-x_n^2}}{(x_n - x_\ell)(1 + sI_n)^{\frac{1}{2}}} \quad (4.4-1)$$

Equation (4.4-1) is valid so long as the holes burned in the population inversion by the various lines do not overlap significantly.

Using equation (4.2-4), the coupled equations governing the mode frequencies x_n may be written

$$x_{\ell o} = \bar{x}_{\ell} + \beta \left[F(\bar{x}_{\ell}) - \frac{1}{\pi^2 \epsilon} \frac{\bar{x}_{\ell}^2}{(1 + sI_{\ell})^{1/2}} x_{\ell} e^{-x_{\ell}^2} \right. \\ \left. - \frac{\pi^2 \epsilon}{2} \sum_{n \neq \ell} \frac{sI_n}{(1 + sI_n)^{1/2}} \frac{e^{-x_n^2}}{(x_{\ell} - x_n)} \right] \quad (4.4-2)$$

where $x_{\ell o}$ is an empty resonator mode frequency and the bars indicate spatial averages. These equations are generally difficult to solve. Since we only seek qualitative agreement with experiment, several additional approximations are helpful.

The equations are simplified by assuming that all of the modes are fairly near to gain center ($|x_n| \lesssim 1$). Then according to equation (2.6-6) Dawson's integral can be approximated by $F(x) \approx x$ and equation (4.4-2) reduces to

$$x_{\ell o} = \bar{x}_{\ell} \left[1 + \beta \left(1 - \frac{1}{\pi^2 \epsilon} \frac{\bar{x}_{\ell}^2}{(1 + sI_{\ell})^{1/2}} \right) \right] \\ - \frac{\beta \pi^2 \epsilon}{2} \sum_{n \neq \ell} \frac{sI_n}{(1 + sI_n)^{1/2}} \frac{1}{(x_{\ell} - x_n)} \quad (4.4-3)$$

To proceed with the solution, we now make the simplest possible assumption consistent with our mode pulling experiments. We assume that there are two equal modes of intensity I which are disposed

exactly symmetrically about a Gaussian gain profile. Then equation (4.4-3) becomes

$$x_{10} = x_1 \left[1 + \beta \left(1 - \frac{1}{\pi^{\frac{1}{2}}} \epsilon \overline{(1 + sI)^{\frac{1}{2}}} \right) \right] - \frac{\beta \pi^{\frac{1}{2}} \epsilon}{2} \frac{\overline{sI}}{(1 + sI)^{\frac{1}{2}}} \frac{1}{(x_1 - x_2)}$$

(4.4-4)

$$x_{20} = x_2 \left[1 + \beta \left(1 - \frac{1}{\pi^{\frac{1}{2}}} \epsilon \overline{(1 + sI)^{\frac{1}{2}}} \right) \right] - \frac{\beta \pi^{\frac{1}{2}} \epsilon}{2} \frac{\overline{sI}}{(1 + sI)^{\frac{1}{2}}} \frac{1}{(x_2 - x_1)}$$

(4.4-5)

The generalization for a nonsymmetric mode arrangement is straightforward but the solutions are more difficult to obtain.

Ordinarily each mode would burn two holes in the population inversion spectrum due to the interaction by the left and right traveling wave components with the Doppler broadened medium. By assuming that the two modes are exactly symmetric about the line center, however, the problem is simplified so that there are only two holes burned in the gain profile altogether. This is the assumption made to obtain equations (4.4-4) and (4.4-5). Experimentally the oscillation line widths are many MHz wide and the mode pulling is found to be rather independent of the actual mode locations (mirror position). Thus the equations are expected to agree qualitatively with experiments. They would be more correct in a one-way traveling wave ring laser where each mode burns only one hole.

The mode spacing $\Delta x = x_2 - x_1$ is found by subtracting equation

(4.4-4) from equation (4.4-5) with the result

$$\Delta x_o = \Delta x \left[1 + \beta \left(1 - \pi^{\frac{1}{2}} \epsilon (1 + sI)^{\frac{1}{2}} \right) \right] - \beta \pi^{\frac{1}{2}} \epsilon \frac{sI}{(1 + sI)^{\frac{1}{2}}} \frac{1}{\Delta x} \quad (4.4-6)$$

Equation (4.4-6) is a quadratic equation for x which may be solved yielding

$$\Delta x = \frac{\Delta x_o}{2 \left[1 + \beta \left(1 - \pi^{\frac{1}{2}} \epsilon (1 + sI)^{\frac{1}{2}} \right) \right]} + \frac{1}{2} \sqrt{\left(\frac{\Delta x_o}{1 + \beta \left(1 - \pi^{\frac{1}{2}} \epsilon (1 + sI)^{\frac{1}{2}} \right)} \right)^2 + \frac{4 \pi^{\frac{1}{2}} \beta \epsilon \frac{sI}{(1 + sI)^{\frac{1}{2}}}}{1 + \beta \left(1 - \pi^{\frac{1}{2}} \epsilon (1 + sI)^{\frac{1}{2}} \right)}} \quad (4.4-7)$$

If saturation effects are weak, as assumed in deriving equation (4.4-1), then the square root may be expanded to obtain

$$\Delta x = \frac{\Delta x_o}{1 + \beta \left(1 - \pi^{\frac{1}{2}} \epsilon (1 + sI)^{\frac{1}{2}} \right)} + \frac{\beta \pi^{\frac{1}{2}} \epsilon \frac{sI}{(1 + sI)^{\frac{1}{2}}}}{\Delta x_o} \quad (4.4-8)$$

This result could have been obtained from equation (4.4-6) by a single iteration. The first term on the right side of equation (4.4-8) can also be expanded yielding

$$\Delta x = \frac{\Delta x_o}{1 + \beta} + \frac{\Delta x_o \beta \pi^{\frac{1}{2}} \epsilon}{(1 + \beta)^2} \frac{1}{(1 + sI)^{\frac{1}{2}}} + \frac{\beta \pi^{\frac{1}{2}} \epsilon \frac{sI}{(1 + sI)^{\frac{1}{2}}}}{\Delta x_o} \quad (4.4-9)$$

The first term on the right side of equation (4.4-9) is the unsaturated mode pulling result given by equation (4.2-8). The second term represents self-saturation due to the effect of each line on the index of refraction which it sees itself. The last term represents the interaction of each line on the other.

If the laser medium is strongly saturated ($sI \gg 1$) over much of its length, then equation (4.4-9) becomes

$$\Delta x = \frac{\Delta x_0}{1 + \beta} + \beta \pi^{\frac{1}{2}} \epsilon (sI)^{\frac{1}{2}} \left(\frac{\Delta x_0}{(1 + \beta)^2} + \frac{1}{\Delta x_0} \right) \quad (4.4-10)$$

Thus saturation weakens the mode pulling effect. It is perhaps worth mentioning that the width of the holes burned in the inversion spectrum is given in this limit by $\Delta v_{\text{hole}} = \Delta v_h (sI)^{\frac{1}{2}}$ according to equation (2.7-3). Thus the magnitude of the saturation term is proportional to the average hole width. Saturation must not be so strong, of course, that the entire Doppler line is "burned up", or else the original equation (4.4-1) becomes invalid. Hence we have the two conditions on equation (4.4-10): $sI \gg 1$, $\epsilon(1 + sI)^{\frac{1}{2}} \ll 1$. In our experiments ϵ is approximately $\epsilon \sim .03$ so that these conditions are not inconsistent.

For completeness we consider the opposite limit of strongly saturating fields $\epsilon(1 + sI)^{\frac{1}{2}} \gg 1$ where the entire Doppler line is affected. The index of refraction in this homogeneous limit is given by equation (2.5-4) as

$$n = 1 + \frac{cg'}{4\pi\nu_l} \frac{y_l}{(1 + y_l)^2 \left(1 + \sum_n \frac{sI_n}{1 + y_n^2} \right)} \quad (4.4-11)$$

Then using equation (4.2-4), the coupled equations governing the mode frequencies y_n may be written

$$y_{\ell o} = y_{\ell} + \frac{\beta' y_{\ell}}{1 + y_{\ell}^2} \frac{1}{1 + \sum_n \frac{sI_n}{1 + y_n^2}} \quad (4.4-12)$$

For fields near to line center ($y_n^2 \ll 1$) this equation may be solved yielding

$$x_{\ell} = \frac{x_{\ell o}}{1 + \beta' \frac{1}{1 + \sum_n sI_n}} \quad (4.4-13)$$

where we have switched to the inhomogeneous frequency parameter $x = \epsilon y$.

As before we assume that there are two equal lines symmetrically disposed about gain center. Then the mode spacing from equation (4.4-13) is

$$\Delta x = \frac{\Delta x_o}{1 + \beta' \frac{1}{1 + 2sI}} \quad (4.4-14)$$

The condition of strong saturation leads to

$$\Delta x = \Delta x_o \left(1 - \frac{\beta}{4\epsilon} (sI)^{-1} \right) \quad (4.4-15)$$

For sufficiently high intensities the gain line is evidently completely "burned down" and the mode spacing returns to its empty resonator value as we should expect.

4.5 Experiment

In this section we describe an experiment which has been done to verify the theory of saturation dependent mode pulling. The apparatus used is shown schematically in Figure 4.2. The mirrors were flat. The left mirror was highly reflecting while the right mirror reflected only about four percent. No confinement of the beam was necessary since diffraction losses are small compared to other losses. The left mirror could be uniformly translated along the axis of the laser at one micron per second using a motor drive assembly. The active region of the pure xenon discharge was 1.1 meters long and 5.5 mm in diameter. The pressure was maintained at about five microns using a liquid nitrogen trap^(4.9). The detector was germanium doped with mercury and cooled by liquid hydrogen.

With the arrangement shown in Figure 4.2, the oscilloscope displays the beat spectrum of the laser output. Synchronous detection was used to extract the weak signal from noise. A typical oscilloscope display showing a mode spacing of about 45 MHz is given in Figure 4.3. The dispersion is 5 MHz per centimeter. The null at D.C. on this spectrum results from the decreasing sensitivity of the spectrum analyzer (Tektronix Type 1L20) below 10 MHz. The length of the cavity is 1.36 meters so that, except for dispersion, the mode spacing would be $c/2L = 110$ MHz.

In Figure 4.4 the mode spacing as a function of the square root of the output power is given for a discharge current of 75 ma. These beat frequency data were obtained from oscilloscope displays like Figure 4.3. The power measurements were made by running the signal

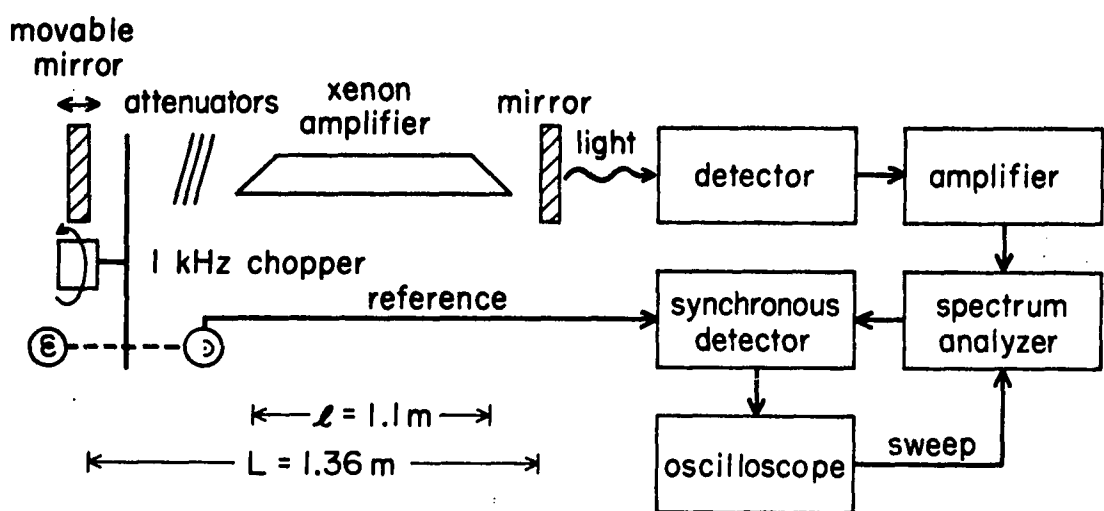


Figure 4.2 Experimental setup

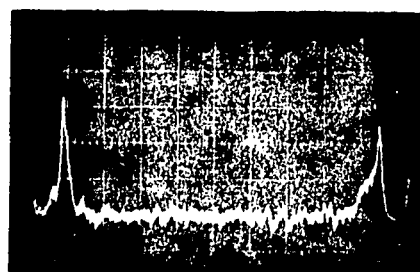


Figure 4.3 Output beat spectrum at 62 ma discharge current. Dispersion is 5 mc per centimeter with D.C. at the right edge of the display.

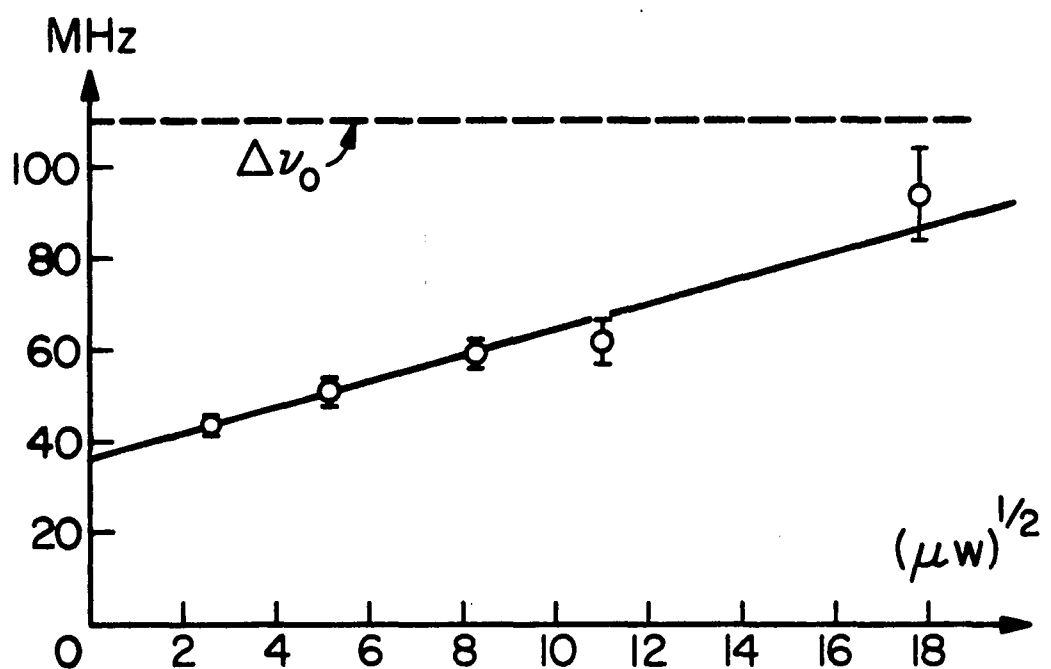


Figure 4.4 Mode spacing versus the square root of output power with a 75 ma discharge.

from the amplifier (HP 461A) of Figure 4.2 directly into the synchronous detector (PAR Model HR-8). The output power was varied at fixed discharge current by varying the attenuation in the cavity. The power calibration indicated on the figure was obtained with an Eppley thermopile.

Errors in the frequency measurements are typically about ± 2 MHz due primarily to the large oscillation line width (up to 10 MHz). Also, the power output varied by about 10 percent as the modes were swept across the gain line and the indicated results are the maximum values obtained for each setting of current and attenuation. In the vicinity of $14(\mu\text{w})^{1/2}$ the uncertainty in the frequency measurements was much greater as the beat spectrum became sensitive to mirror position and a third mode began to oscillate. Consequently data for this region are omitted. At higher outputs the beat frequency again became stable. The mode spacing approached its empty resonator value as it should according to equation (4.4-15).

The features apparent from Figure 4.4 are that the mode spacing may be much less than its empty cavity value, and that the spacing increases with increasing power. These results are qualitatively in agreement with equation (4.4-10). The mode spacing has roughly a square root dependence on output power over two orders of magnitude of power variations as suggested by the line drawn through the data. There are presently too many uncertainties to attempt a detailed analysis of this saturation behavior. The output power is not related simply to the average of the square root of the intensity in the cavity needed for comparison with equation (4.4-10), and the saturation parameter is not

accurately known. However, Figure 4.4 suggests that at the minimum power at which measurements could be made, saturation only increases the mode spacing by about 15 percent. Hence we now neglect saturation and consider in detail the gain dependence of the mode spacing at low output intensities.

If saturation effects are neglected, the mode frequencies are governed in accordance with equation (4.4-2) by

$$x_{lo} = x_l + \beta [F(x_l) - \pi^{1/2} \epsilon x_l e^{-x_l^2}] \quad (4.5-1)$$

In Section 3.2 the homogeneous line width is estimated at $\Delta\nu_h = 4.0$ MHz and from Section 3.3 the Doppler line width is about $\Delta\nu_D = 100$ MHz. Therefore the natural damping ratio is about $\epsilon \approx .03$ and the last term in equation (4.5-1) is negligible.

At the lower currents the condition on the mode frequencies $x \ll 1$ begins to break down, so it is necessary to retain higher order terms in Dawson's integral $F(x)$. From equation (2.2-6) the appropriate approximation is

$$F(x) \approx x - \frac{2}{3} x^3 \quad (4.5-2)$$

Using equation (4.5-2), equation (4.5-1) may be solved for β yielding

$$\beta = \frac{\frac{x_o}{x_l} - 1}{1 - \frac{2}{3} x_l^2} \quad (4.5-3)$$

If two modes are assumed to be symmetrically spaced on the Doppler line (which is the condition for maximum mode pulling), then equation (4.5-3) may be written in terms of the mode spacing as

$$\beta = \frac{\frac{\Delta x_o}{\Delta x} - 1}{1 - \frac{2}{3} \left(\frac{\Delta x}{2} \right)^2} \quad (4.5-4)$$

Equation (4.5-4) has been compared with the beat frequency data using

$$\Delta x = \frac{2\Delta v}{\Delta v_D} \sqrt{\ln 2}$$

The resulting plot of β versus discharge current is in Figure 4.5. Also in Figure 4.5 is a plot of the line center gain constant g versus discharge current obtained by introducing a known attenuation in the laser cavity and reducing the current until oscillation ceased. It is essential in performing these threshold measurements to scan one of the mirrors. Otherwise the lines may not be centered properly on the Doppler curve, and the threshold current will be too large.

From equation (4.2-6) with the values appropriate to our experiment we find the theoretical result $\beta = .36g$ (mks). Examination of the data of Figure 4.5 shows that at the lower currents β is very nearly proportional to g but that the proportionality constant is approximately .16 rather than .36. In other words, the implied Doppler width is about 225 MHz rather than 100 MHz. This result is partially explained by the fact that saturation effects are not negligible, even at the lowest measurable output powers. Much of the discrepancy, however, is due to the isotope shifts and hyperfine structure discussed in Chapter III. These shifts have the effect of broadening the Doppler gain line. Also shown in Figure 4.5 is some later data obtained using mono-isotopic xenon 136. An analysis of these results shows that the gain is increased by about 30 percent and the effective Doppler width is reduced by about 30 percent to 162 MHz.

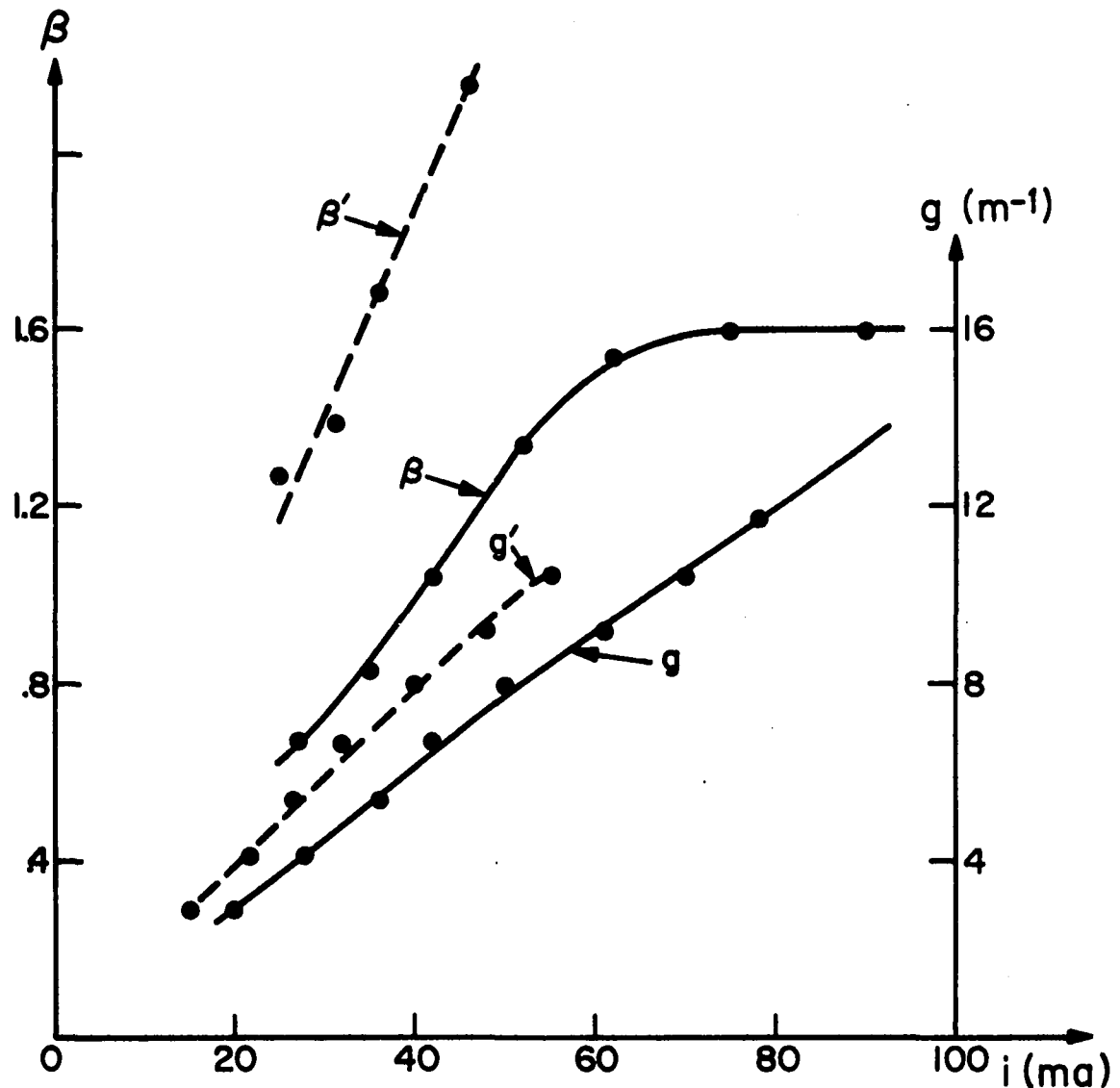


Figure 4.5 The dispersion parameter β and gain g as functions of the discharge current i . Solid lines are for natural xenon and dashed lines are for xenon 136.

when the mono-isotopic xenon is used.

At high currents the parameter β appears to saturate. A possible explanation is that at the higher gains amplified spontaneous emission is significantly depleting the central portion of the Doppler gain curve. This flattening of the gain curve can be regarded roughly as an effective increase in the Doppler width.

To show that spontaneous emission is able to partially saturate the gain, we operated the laser as a single mirror superradiant source. The output power of this source at a current of 90 ma was 265 μw , which is greater than the saturation power $P_s \approx 100 \mu\text{w}$ ^(4.10). Thus at the higher currents we should expect a significant distortion of the gain spectrum as evidenced by the β data.

4.6 Profile effects

Throughout this chapter we have assumed that the laser had only one dimension. In practice, of course, lasers have three dimensions, and it is important to consider the possible effects of profiles of the beam and of the laser medium. The experiment described in Section 4.5, for example, employed a plane parallel resonator in which the beam confinement was accomplished entirely by the gain profile of the medium. The interpretation of those results is only valid if profile effects can be shown to be negligible. In this section we consider the effects of gain and beam profiles on the longitudinal modes of a plane parallel laser of the sort described in the previous section. The analysis of profile effects in any other laser configuration would be similar.

In this investigation we make use of some results of Chapter V. Equation (5.3-7) describes the electric field of a gain-confined beam. Using this expression, one finds that the phase condition on the longitudinal modes which is given in equation (4.2-2) should be replaced by

$$2\pi m = \oint \gamma dz + \text{Re } P \quad (4.6-1)$$

where γ is the real part of the propagation constant and P is an additional phase correction. From equations (5.2-25) and (5.3-6) P is related to the beam parameter q by

$$\frac{dP}{dz} = - \frac{i(2p + \lambda + 1)}{q} \quad (4.6-2)$$

where p and ℓ are the indices of a Laguerre-Gaussian beam. We assume in writing equation (4.6-2) that the medium has no z variations. The beam parameter is defined in equation (5.3-6), and with this definition the real part of P for the fundamental Gaussian beam ($p = \ell = 0$) is simply

$$\text{Re } P = - \oint \frac{\lambda}{\pi w^2} dz \quad (4.6-3)$$

where w is the spot size of the beam. Therefore, equation (4.6-1) becomes

$$2\pi m = \oint \left(\gamma - \frac{\lambda}{\pi w^2} \right) dz \quad (4.6-4)$$

To proceed with this derivation, an expression is needed for the spot size. Equation (5.6-13) gives the spot size of a simple gain-focused beam as

$$\frac{\lambda}{\pi w^2} = \frac{1}{2} \sqrt{\frac{\alpha_2 \lambda}{\pi}} \quad (4.6-5)$$

where α_2 is the coefficient of the quadratic term in the gain profile. Equation (4.6-5) neglects dispersion focusing; but, as shown in Section 5.8, dispersion focusing has only a small effect on the spot size. For our purposes here dispersion is unimportant, and its neglect simplifies the mathematics. For a gas laser α_2 is related to α_0 by equation (5.7-1), and equation (4.6-5) becomes

$$\frac{\lambda}{\pi w^2} = \frac{1}{2r_0} \sqrt{\frac{2.88 \alpha_0 \lambda}{\pi}} \quad (4.6-6)$$

or in terms of the actual frequency dependent intensity gain

$$\frac{\lambda}{\pi w^2} = \frac{1}{2r_o} \sqrt{\frac{1.44 g_o \lambda}{\pi}} e^{-x^2/2} \quad (4.6-7)$$

where g_o is the line center incremental intensity gain.

With equation (4.6-7) for the spot size, equation (4.6-4) may be written

$$2\pi m = \int \left(\frac{2\pi v n(v)}{c} - \frac{1}{2r_o} \sqrt{\frac{1.44 g_o \lambda}{\pi}} e^{-x^2/2} \right) dz$$

or

$$2\pi m = \frac{2\pi v}{c} \int \left(n(v) - \frac{c}{4\pi r_o v} \sqrt{\frac{1.44 g_o \lambda}{\pi}} e^{-x^2/2} \right) dz \quad (4.6-8)$$

where $n(v)$ is the frequency dependent index of refraction. Following the derivation of Section 4.2, we obtain finally the result that the mode frequencies are governed by

$$v_m - v = \frac{\ell}{L} \frac{cg_o F(x)}{2\pi^{3/2}} - \frac{c}{4\pi r_o} \sqrt{\frac{1.44 g_o \lambda}{\pi}} e^{-x^2/2} \quad (4.6-9)$$

where we have made the approximation that the spot size is constant even outside the laser medium. This equation should be valid for ℓ nearly equal to L . In terms of the dispersion parameter β of equation (4.2-6) the result may be rewritten as

$$x_m - x = \beta \left[F(x) - \frac{L}{2r_o \ell} \sqrt{\frac{1.44 \lambda}{g_o}} e^{-x^2/2} \right] \quad (4.6-10)$$

Equation (4.6-10) is the general equation governing the longitudinal mode frequencies of a gain focused laser. Near line center ($x \rightarrow 0$) it reduces to

$$x = \frac{1}{1 + \beta} \left(x_m + \frac{\beta L}{2r_o \ell} \sqrt{\frac{1.44 \lambda}{g_o}} \right) \quad (4.6-11)$$

Thus, we find that the primary effect of the beam profile is to shift the mode frequencies upward slightly. This frequency shift would be unimportant for all of our work. The mode spacing would be given by

$$\Delta\nu = \frac{\Delta\nu_0}{1 + \beta} \quad (4.6-12)$$

which is the same as equation (4.2-8). We conclude therefore that the neglect of profile effects is justified.

4.7 Conclusion

A general theory has been developed for determining the longitudinal mode frequencies of high gain lasers. It is found that the mode configuration may differ drastically from that which would be expected if dispersion effects were ignored. In particular, power dependent mode pulling has been investigated theoretically and experimentally. Semi-quantitative agreement between experiment and theory has been obtained in the limit of weak saturation. The rather complicated results for saturation effects have been verified qualitatively. Because of the small empty resonator mode spacing and possible saturation by spontaneous emission, the present laser system is not well suited to investigation of the extreme mode pulling and mode splitting which should be observable in xenon and helium-xenon systems. Additional experimental work in this area would probably be justified.

Bibliography

- 4.1 L. W. Caspenson and A. Yariv, *Applied Physics Letters* 17, No. 6, page 259, 15 September 1970.
- 4.2 W. R. Bennett, Jr., *Physical Review* 126, No. 2, page 580, 1962.
- 4.3 R. A. McFarlane, *Physical Review* 135A, page 543, 1964.
- 4.4 R. L. Fork and M. A. Pollack, *Physical Review* 139A, page 1408, 1965.
- 4.5 B. K. Garside, *Journal of Quantum Electronics* QE-5, No. 2, page 97, February 1969.
- 4.6 J. W. Klüver, *Journal of Applied Physics* 37, No. 8, page 2987, July 1966.
- 4.7 B. Lohmander and S. Rittsten, *Kungl. Fysiografiska Sällskapets i Lund Förhandlingar* 28, No. 6, page 45, 1958.
- 4.8 G. Birnbaum, *Proceedings of the IEEE* 55, No. 6, page 1015, June 1967.
- 4.9 D. Armstrong, *Journal of Quantum Electronics* QE-4, No. 11, page 968, November 1968.
- 4.10 P. O. Clark, *Journal of Quantum Electronics* QE-1, No. 3, page 109, June 1965. The saturation power for our laser was estimated from Clark's Figures 2 and 3.

V. Transverse Modes

5.1 Introduction

The purpose of this chapter is to investigate the effects of gain on the transverse structure of laser modes. In the preceding chapter it was shown that the presence of a high gain medium within the resonator cavity could have a drastic effect on the longitudinal modes of a laser oscillator. Similarly, it will be shown here that a high gain medium can significantly alter the transverse modes of a laser. In particular, a gain focusing effect is studied which can be important in media having a radial gain profile^(5.1,5.2). A dispersion focusing effect is also described which can have important consequences for Lamb dip measurements in high gain lasers.

First the beam mode solutions of the wave equation are obtained for lenslike media having at most a quadratic variation of the gain and index of refraction with distance from the beam axis. Lenslike media are common in practice. Experimentally, care may be necessary to prevent gain saturation which would distort the gain profile and possibly the refraction profile as well. The propagation characteristics of the beams through such media and through other simple optical elements are studied by means of beam matrices. These matrix techniques are then applied to the problem of determining the transverse modes of simple laser resonators containing lenslike media. Finally, experiments are described which verify some of the conclusions concerning gain focusing and dispersion focusing.

A section is also included on a new cylindrical cavity geometry.

The analysis procedure for these radially propagating waves is essentially identical to that described for the more conventional lasers. The cylindrical laser is of theoretical interest, and it may also find some practical applications because of the extremely high fields which should result at the center of the laser resonator.

5.2 Beam modes

The scalar wave equation for a harmonically varying electric field may be written

$$\nabla^2 E + k^2 E = 0 \quad (5.2-1)$$

where k is the propagation constant defined by

$$k = \omega \sqrt{\epsilon \mu} \quad (5.2-2)$$

In a medium including an atomic resonance the dielectric permittivity ϵ is in general complex so that k is also complex. A lenslike medium is defined as one in which k has a weak quadratic variation with distance from the axis of propagation described by

$$k = k_0 - \frac{1}{2} k_2 r^2 \quad (5.2-3)$$

Kogelnik^(5.3) has considered the propagation of the fundamental Gaussian beam through such media, and the notation used here will agree as much as possible with his.

In all practical lasers the propagation constant varies by at most a few percent over the cross section of the beam so that equation (5.2-1) may be written

$$\nabla^2 E + k_0^2 E - k_0 k_2 r^2 E = 0 \quad (5.2-4)$$

where equation (5.2-3) has been used. The solution for the beam modes now involves a sequence of substitutions. This solution is most easily performed in the conventional cylindrical or rectangular Cartesian coordinates. Many important lasers have a predominantly

axial symmetry, so the solutions in cylindrical coordinates are most useful. The solutions in Cartesian coordinates will be considered later.

One is interested mostly in waves which are nearly plane, and a reasonable substitution is (following Kogelnik)

$$E = \psi e^{-i \int k_o dz} \quad (5.2-5)$$

Then equation (5.2-4) becomes

$$\frac{1}{r} \frac{\partial}{\partial r} (r \frac{\partial \psi}{\partial r}) + \frac{1}{r^2} \frac{\partial^2 \psi}{\partial \phi^2} - 2ik_o \frac{\partial \psi}{\partial z} - i\psi \frac{dk_o}{dz} - k_o k_2 r^2 \psi = 0 \quad (5.2-6)$$

where the second derivative of ψ with respect to z is assumed to be negligible.

Only beams of finite transverse extent are of interest and a useful substitution is

$$\psi = S e^{-i \frac{Q}{2} r^2} \quad (5.2-7)$$

where $Q(z)$ and $S(r, \phi, z)$ are in general complex. Then equation (5.2-6) becomes

$$\begin{aligned} \frac{\partial^2 S}{\partial r^2} + (\frac{1}{r} - 2iQr) \frac{\partial S}{\partial r} - 2iQS - Q^2 r^2 S + \frac{1}{r^2} \frac{\partial^2 S}{\partial \phi^2} \\ - 2ik_o \frac{\partial S}{\partial z} - k_o \frac{dQ}{dz} r^2 S - i \frac{dk_o}{dz} S - k_o k_2 r^2 S = 0 \end{aligned} \quad (5.2-8)$$

The sum of the terms in $r^2 S$ may be set equal to zero, since Q has not been specified. This results in the two equations

$$Q^2 + k_o \frac{dQ}{dz} + k_o k_2 = 0 \quad (5.2-9)$$

$$\frac{r^2 \partial^2 S}{\partial r^2} + r(1 - 2iQr^2) \frac{\partial S}{\partial r} - 2iQr^2 S + \frac{\partial^2 S}{\partial \phi^2} - 2ik_o r^2 \frac{\partial S}{\partial z} - \frac{ik_o}{dz} r^2 S = 0 \quad (5.2-10)$$

Equation (5.2-9) is called the beam parameter equation and is considered in Section 5.4.

Equation (5.2-10) is simplified by the change of variables

$$\rho = iQr^2 \quad (5.2-11)$$

becoming

$$\rho \frac{\partial^2 S}{\partial \rho^2} + (1 - \rho) \frac{\partial S}{\partial \rho} - \frac{S}{2} + \frac{1}{4\rho} \frac{\partial^2 S}{\partial \phi^2} - \frac{k_o}{2Q} \frac{\partial S}{\partial z} - \frac{1}{4Q} \frac{dk_o}{dz} S = 0 \quad (5.2-12)$$

Now a useful substitution is

$$S(\rho, \phi, z) = R(\rho) \Phi(\phi) Z(z) \quad (5.2-13)$$

which leads to

$$\frac{\rho}{R} \frac{d^2 R}{d\rho^2} + \frac{(1 - \rho)}{R} \frac{dR}{d\rho} - \frac{1}{2} + \frac{1}{4\rho\Phi} \frac{d^2 \Phi}{d\phi^2} - \frac{k_o}{2QZ} \frac{dZ}{dz} - \frac{1}{4Q} \frac{dk_o}{dz} = 0 \quad (5.2-14)$$

This equation may be separated into the three equations

$$\frac{d^2 \Phi}{d\phi^2} + \ell^2 \Phi = 0 \quad (5.2-15)$$

$$\rho \frac{d^2 R}{d\rho^2} + (1 - \rho) \frac{dR}{d\rho} - \frac{\ell^2 R}{4\rho} + (\rho + \frac{\ell}{2}) R = 0 \quad (5.2-16)$$

$$k_o \frac{dZ}{dz} + \frac{1}{2} \frac{dk_o}{dz} Z + (2\rho + \ell + 1) QZ = 0 \quad (5.2-17)$$

where ℓ and ρ are separation constants.

The solutions of equation (5.2-15) may be written within

multiplicative constants as

$$\phi = \begin{cases} \sin \\ \cos \end{cases} \ell \phi \quad (5.2-18)$$

so that ℓ must be an integer. Thus the field has a sinusoidal variation about the axis of propagation.

It is helpful to make the substitution

$$R = \rho^{-\ell/2} L \quad (5.2-19)$$

in equation (5.2-16) with the result

$$\rho \frac{\partial^2 L}{\partial \rho^2} + (1 + \ell - \rho) \frac{\partial L}{\partial \rho} + \rho L = 0 \quad (5.2-20)$$

This is the Laguerre differential equation (5.4), and one has the final result for the radial variation

$$R = \rho^{-\ell/2} L_p^\ell(\rho) \quad (5.2-21)$$

where $L_p^\ell(\rho)$ is an associated Laguerre polynomial. Since the coordinate ρ is complex, one finds that the radial part R of the field is also complex. However, one is usually most interested in the field distribution on a surface of constant phase. On the axis ($\rho = 0$) the radial part is real. Away from the axis the field on a phase surface may be obtained by setting the imaginary part of R equal to zero. This result is mathematically equivalent to the replacement of ρ by ρ_r where the subscript r will mean the real part and the subscript i will mean the imaginary part. Using equation (5.2-11) one finds

$$\rho + \rho_r = - Q_1 r^2 \quad (5.2-22)$$

so that the radial amplitude distribution equation (5.2-21) becomes

$$R = (-Q_1 r^2)^{\lambda/2} L_p^\lambda(-Q_1 r^2) \quad (5.2-23)$$

The z dependence is most conveniently written in terms of a complex phase parameter P given by

$$Z = e^{-iP} \quad (5.2-24)$$

With this substitution equation (5.2-17) becomes

$$\frac{dP}{dz} = -i \left[\frac{(2p + \lambda + 1)Q}{k_o} + \frac{1}{2k_o} \frac{dk_o}{dz} \right] \quad (5.2-25)$$

This result will be referred to as the phase parameter equation.

Collecting together equations (5.2-5), (5.2-7), (5.2-13), (5.2-18), (5.2-23) and (5.2-24), one finds that the beam modes in lenslike media expressed in cylindrical coordinates are within multiplicative constants given by

$$E(r, z, \phi) = \begin{cases} \sin & \\ \cos & \end{cases} \lambda \phi (-Q_1 r^2)^{\lambda/2} L_p^\lambda(-Q_1 r^2) e^{-\frac{10r^2}{2}} e^{-iP} e^{-i \int k_o dz} \quad (5.2-26)$$

where Q and P are given by equations (5.2-9) and (5.2-25) respectively. These are usually referred to as Laguerre-Gaussian modes and are the principal result of this section. The propagation of these modes is determined entirely by the z dependence of the parameters P and Q .

The beam modes considered so far are useful in lasers having an axial symmetry. Some lasers, however, have a degree of rectangular symmetry due to apertures, windows, etc. and then a different family of modes is likely to arise. By an analysis entirely analogous to the

preceding, one finds that the field distribution of these rectangular modes is given by

$$E(x, y, z) = H_m(\sqrt{-Q_1}x) H_n(\sqrt{-Q_1}y) e^{-\frac{Q}{2}(x^2 + y^2)} e^{-ip} e^{-i \int k_o dz} \quad (5.2-27)$$

where H_m and H_n are the well known Hermite polynomials. The beam parameter Q is again governed by equation (5.2-9) and the phase parameter is given by

$$\frac{dp}{dz} = -i \left[\frac{(m+n+1)Q}{k_o} + \frac{1}{2k_o} \frac{dk_o}{dz} \right] \quad (5.2-28)$$

The fields given by equation (5.2-27) are usually referred to as Hermite-Gaussian modes.

All of the modes considered above have simple spherical phase fronts. These results can be generalized to modes having phase fronts with different radii of curvature in the x and y directions. The propagation constant is also permitted to have differing variations in the two directions. The interested reader (if extant) may readily show that the electric field for this case would be given by

$$E = H_m(\sqrt{-Q_x}x) H_n(\sqrt{-Q_y}y) e^{-\frac{1}{2}(Q_x x^2 + Q_y y^2)} e^{-ip} e^{-i \int k_o dz} \quad (5.2-29)$$

where the beam parameters are determined from the two equations

$$Q_x^2 + k_o \frac{dQ_x}{dz} + k_o k_{2x} = 0 \quad (5.2-30)$$

$$Q_y^2 + k_o \frac{dQ_y}{dz} + k_o k_{2y} = 0 \quad (5.2-31)$$

and the phase parameter is described by

$$\frac{dP}{dz} = -i \left[\frac{(m + \frac{1}{2})Q_x + (n + \frac{1}{2})Q_y}{k_o} + \frac{1}{2k_o} \frac{dk_o}{dz} \right] \quad (5.2-32)$$

These astigmatic results might be useful in lasers containing asymmetric lenslike media, Brewster windows, or other optical elements having differing properties in the x and y directions. It is difficult to visualize applications where astigmatism would actually be desirable.

An amusing special case of the above result would be the situation where no variations are permitted in the y direction. Then $Q_y = 0$ and the fields are confined, more or less, to a plane rather than to an axis. The results are

$$E = H_m (\sqrt{-Q_{xi}} x) e^{-\frac{iQ_x^2}{2}} e^{-ip} e^{-ik_o dz} \quad (5.2-33)$$

with the beam parameter equation

$$Q_x^2 + k_o \frac{dQ_x}{dz} + k_o k_{2x} = 0 \quad (5.2-34)$$

and the phase equation

$$\frac{dP}{dz} = -i \left[\frac{(m + \frac{1}{2})Q_x}{k_o} + \frac{1}{2k_o} \frac{dk_o}{dz} \right] \quad (5.2-35)$$

Elliptical mirrors and lenses exist and it is possible that these results could be useful.

In this section the forms of the electric field modes relevant to several simple types of lenslike media have been considered. The propagation of these modes through various optical systems is considered in the following sections. It should be emphasized that in all of the rather diverse laser geometries mentioned above the beam parameter equations are essentially identical as are also the phase

equations. Consequently, in the investigations of beam propagation the results will apply to all of the different beam geometries.

5.3 The beam parameter

As shown in the previous section, the propagation of the important Laguerre-Gaussian and Hermite-Gaussian beams is governed by the z dependence of the complex parameters Q and P . It is useful to express the beam parameter Q in terms of some more familiar features of the wave. The evolution of Q as a function of z will then be considered in the following section.

First it is useful to consider a simple scalar outgoing spherical wave in a homogeneous medium with propagation constant k_0 . The amplitude and phase of such a wave are governed within constants by

$$E(r, \phi, z) = \frac{1}{R} e^{-ik_0 R}, \quad R = \sqrt{r^2 + z^2} \quad (5.3-1)$$

where R is the radius of curvature of the phase fronts of the wave and cylindrical coordinates are used. If only a narrow region about the positive z axis ($r \ll z$) is of interest, then R may be written approximately

$$\begin{aligned} R &= z \sqrt{1 + \frac{r^2}{z^2}} \\ &\approx z + \frac{r^2}{2R} \end{aligned} \quad (5.3-2)$$

and the spherical wave of equation (5.3-1) becomes

$$E = \frac{1}{R} e^{-ik_0 z} e^{-i \frac{k_0 r^2}{2R}} \quad (5.3-3)$$

But the Laguerre-Gaussian modes of equation (5.2-26) and the Hermite-Gaussian modes of equation (5.2-27) contain the factor $e^{(-iQr^2)/2}$. Thus the real part of Q is related to the radius of curvature of the phase fronts of the narrow Gaussian beams by

$$\frac{Q_r}{k_o} = \frac{1}{R} \quad (5.3-4)$$

The imaginary part of Q characterizes the decrease in amplitude away from the z axis. This dependence is Gaussian and hence the beams are referred to as Gaussian beams. Clearly one may write

$$\frac{Q_r}{k_o} = -\frac{2}{k_o w^2} = -\frac{\lambda_m}{\pi w^2} \quad (5.3-5)$$

where w is the "spot size" or radius at which the amplitude falls to $1/e$ of its value on the z axis and λ_m is the wavelength in the medium. Thus one may define a new quantity q given by

$$\frac{1}{q} = \frac{Q_r}{k_o} = \frac{1}{R} - i \frac{\lambda_m}{\pi w^2} \quad (5.3-6)$$

Often q is referred to as the beam parameter rather than Q . The above considerations assumed that the real part of k_o is much greater than the imaginary part. This assumption is valid in all practical lasers, since the gain per wavelength is small.

Now the field distributions can be written in a somewhat more familiar form. The Laguerre-Gaussian modes of equation (5.2-26) become

$$E(r, z, \phi) = \begin{cases} \sin \phi & \text{for } \ell = 0 \\ \cos \phi & \text{for } \ell \neq 0 \end{cases} \left(\frac{2r^2}{w^2} \right)^{\ell/2} L_p^{\ell} \left(\frac{2r^2}{w^2} \right) e^{-\frac{ik_o r^2}{2R}} e^{-r^2/w^2} e^{-ip} e^{-i \int k_o dz} \quad (5.3-7)$$

and the Hermite-Gaussian modes of equation (5.2-27) become

$$E(x, y, z) = H_m \left(\frac{\sqrt{2}x}{w} \right) H_n \left(\frac{\sqrt{2}y}{w} \right) e^{-\frac{ik_o(x^2+y^2)}{2R}} e^{-\frac{(x^2+y^2)}{w^2}} e^{-ip} \times e^{-i \int k_o dz} \quad (5.3-8)$$

In these expressions the plane wave amplitude and phase are governed by $\int k_0 dz$. The parameter P provides corrections to the amplitude and phase resulting from the finite extent of the beam and the phase front curvature.

5.4 Lenslike media

In this section the propagation of the beam parameter through lenslike media is considered and the stability condition for long distances is derived. The behavior of Q in other simple optical systems will be treated in terms of beam matrices in the next section. The starting point for this discussion is the beam parameter equation (5.2-9)

$$Q^2 + k_o \frac{dQ}{dz} + k_o k_2 = 0 \quad (5.4-1)$$

Following Kogelnik^(5.3), this Riccati equation may be transformed to a second order linear equation by the substitution

$$Q = k_o \frac{1}{x} \frac{dx}{dz} \quad (5.4-2)$$

with the result

$$(k_o x')' + k_2 x = 0 \quad (5.4-3)$$

Equation (5.4-3) cannot be solved analytically for an arbitrary z dependence of k_o and k_2 . However, in most practical laser media these parameters are roughly constant. Then equation (5.4-3) may be rewritten as

$$x'' + \frac{k_2}{k_o} x = 0 \quad (5.4-4)$$

The solution of equation (5.4-4) for propagation through a distance d is

$$x_2 = a \cos \sqrt{\frac{k_2}{k_o}} d + b \sin \sqrt{\frac{k_2}{k_o}} d \quad (5.4-5)$$

Matching boundary conditions at the input yields

$$x_2 = x_1 \cos \sqrt{\frac{k_2}{k_o}} d + \left. \frac{dx}{dz} \right|_1 \sqrt{\frac{k_o}{k_2}} \sin \sqrt{\frac{k_2}{k_o}} d \quad (5.4-6)$$

Substituting this expression in equation (5.4-2) gives a simple (in appearance at least) formula for the evolution of Q

$$\frac{Q_2}{k_o} = \frac{-\sqrt{\frac{k_2}{k_o}} \sin \sqrt{\frac{k_2}{k_o}} d + \frac{Q_1}{k_o} \cos \sqrt{\frac{k_2}{k_o}} d}{\cos \sqrt{\frac{k_2}{k_o}} d + \frac{Q_1}{k_o} \sqrt{\frac{k_o}{k_2}} \sin \sqrt{\frac{k_2}{k_o}} d} \quad (5.4-7)$$

Equation (5.4-7) may be written in terms of the beam parameter q using equation (5.3-6) with the result

$$q_2 = \frac{q_1 \cos \sqrt{\frac{k_2}{k_o}} d + \sqrt{\frac{k_o}{k_2}} \sin \sqrt{\frac{k_2}{k_o}} d}{-q_1 \sqrt{\frac{k_2}{k_o}} \sin \sqrt{\frac{k_2}{k_o}} d + \cos \sqrt{\frac{k_2}{k_o}} d} \quad (5.4-8)$$

Equation (5.4-8) suggests that q_2 is a periodic function of position. However, both k_o and k_2 may in general be complex, so the interpretation of this result isn't so easy. The circular functions of complex argument are

$$\cos(a + ib) = \cos a \cosh b - i \sin a \sinh b \quad (5.4-9)$$

$$\sin(a + ib) = \sin a \cosh b + i \cos a \sinh b \quad (5.4-10)$$

Thus equation (5.4-8) represents a sort of damped non-sinusoidal oscillatory behavior which may be characterized by a period p and a damping length δ given by

$$p = \frac{2\pi}{\left| \operatorname{Re} \sqrt{\frac{k_2}{k_0}} \right|}, \quad \delta = \frac{1}{\left| \operatorname{Im} \sqrt{\frac{k_2}{k_0}} \right|} \quad (5.4-11)$$

We write k in terms of its real and imaginary parts as

$$k = \beta + i\alpha \quad (5.4-12)$$

The real part β is related to the refractive index by $\beta = 2\pi n/\lambda$ and the imaginary part is the plane wave electric field gain constant.

By using the easily verified result

$$\sqrt{a + ib} = \frac{1}{\sqrt{2}} \left(\sqrt{\sqrt{a^2 + b^2} + a} + i \sqrt{\sqrt{a^2 + b^2} - a} \right) \quad (5.4-13)$$

equations (5.4-11) can be written explicitly as

$$p = 2\pi \left| \sqrt{\frac{2\beta_0}{\sqrt{\frac{\beta^2}{2} + \frac{\alpha^2}{2}} + \beta_2}} \right|, \quad \delta = \left| \sqrt{\frac{2\beta_0}{\sqrt{\frac{\beta^2}{2} + \frac{\alpha^2}{2}} - \beta_2}} \right| \quad (5.4-14)$$

provided the gain per wavelength is small ($\alpha_0 \ll \beta_0$).

Two important special cases are of interest. The first occurs when there is no gain profile or $\alpha_2 = 0$. Then equation (5.4-14) becomes

$$p = 2\pi \left| \sqrt{\frac{\beta_0}{\beta_2}} \right|, \quad \delta \Rightarrow \infty \quad (5.4-15)$$

for $\beta_2 > 0$. Thus when there is only a refractive index profile, the oscillations of the beam parameter are undamped. The other special case occurs when there is only a gain profile. Equation (5.4-14) becomes

$$p = 2\pi \left| \sqrt{\frac{2\beta_o}{\alpha_2}} \right|, \quad \delta = \left| \sqrt{\frac{2\beta_o}{\alpha_2}} \right| \quad (5.4-16)$$

for $\alpha_2 > 0$ so that the period of oscillation is equal to 2π times the damping length.

It is interesting to inquire what happens to the beam parameter at distances much greater than the damping length ($d \gg \delta$). At large distances

$$\cosh(\text{Im} \sqrt{\frac{k_2}{k_o}} d) = \frac{e^{\pm \text{Im} \sqrt{\frac{k_2}{k_o}} d}}{2}, \quad \sinh(\text{Im} \sqrt{\frac{k_2}{k_o}} d) = \pm \frac{e^{\pm \text{Im} \sqrt{\frac{k_2}{k_o}} d}}{2} \quad (5.4-17)$$

where the upper sign is used if $\text{Im} \sqrt{\frac{k_2}{k_o}} > 0$ and the lower sign when $\text{Im} \sqrt{\frac{k_2}{k_o}} < 0$. Now equations (5.4-8) to (5.4-10) and (5.4-17) may be combined yielding at large distances

$$\begin{aligned} q_2 &= \frac{q_1 [\cos(\text{Re} \sqrt{\frac{k_2}{k_o}} d) \mp i \sin(\text{Re} \sqrt{\frac{k_2}{k_o}} d)] + \sqrt{\frac{k_o}{k_2}} [\sin(\text{Re} \sqrt{\frac{k_2}{k_o}} d) \pm i \cos(\text{Re} \sqrt{\frac{k_2}{k_o}} d)]}{-q_1 \sqrt{\frac{k_2}{k_o}} [\sin(\text{Re} \sqrt{\frac{k_2}{k_o}} d) \pm i \cos(\text{Re} \sqrt{\frac{k_2}{k_o}} d)] + [\cos(\text{Re} \sqrt{\frac{k_2}{k_o}} d) \mp i \sin(\text{Re} \sqrt{\frac{k_2}{k_o}} d)]} \\ &= \frac{q_1 e^{\pm i \text{Re} \sqrt{\frac{k_2}{k_o}} d} \pm i \sqrt{\frac{k_o}{k_2}} e^{\pm i \text{Re} \sqrt{\frac{k_2}{k_o}} d}}{-iq_1 \sqrt{\frac{k_2}{k_o}} e^{\pm i \text{Re} \sqrt{\frac{k_2}{k_o}} d} + e^{\pm \text{Re} \sqrt{\frac{k_2}{k_o}} d}} \\ &= \frac{q_1 \pm i \sqrt{\frac{k_o}{k_2}}}{\mp iq_1 \sqrt{\frac{k_2}{k_o}} + 1} = \pm i \sqrt{\frac{k_o}{k_2}} \quad (5.4-18) \end{aligned}$$

Thus at large distances the beam parameter becomes a constant independent of the initial beam parameter.

Next there is the question of stability. It is not immediately obvious in what situations equation (5.4-18) implies a finite confined beam. This equation may be rewritten using equation (5.3-6) as

$$\frac{1}{q} = \frac{1}{R} - i \frac{\lambda_m}{\pi w^2} = \mp i \sqrt{\frac{k_2}{k_0}} \quad (5.4-19)$$

A finite beam must have a real spot size, so that from equation (5.4-19) the stability condition may be written

$$\operatorname{Re} \pm \sqrt{\frac{k_2}{k_0}} > 0 \quad (5.4-20)$$

From equation (5.4-20) and the sign convention adopted previously, it is evident that stability results only when the real and imaginary parts of $\sqrt{k_2/k_0}$ are either both positive or both negative, but not otherwise. But the real and imaginary parts of the square root of a complex number have the same sign only if the number itself lies in the first two quadrants of an Argand diagram. Thus the stability condition is

$$\operatorname{Im} \frac{k_2}{k_0} > 0 \quad (5.4-21)$$

Written in terms of the real and imaginary parts of the wave number, this condition becomes

$$0 \lessdot \operatorname{Im} \frac{\beta_2 + i\alpha_2}{\beta_0} \quad (5.4-22)$$

or simply

$$\alpha_2 > 0 \quad (5.4-23)$$

where the gain per wavelength has been assumed to be small ($\beta_0 \gg \alpha_0$). Thus if the gain does not fall off with increasing radius, the amplifier is unstable, and the spot size of an incident beam will eventually increase without bound as the beam propagates. Equations analogous to equations (5.4-15) and (5.4-16) may be written for $\alpha_2 < 0$ or $\beta_2 < 0$ but then, of course, the "damping" length will correspond to an exponential growth constant.

In one degenerate case the preceding stability analysis does not apply. That is the situation where the input beam parameter is given exactly by

$$q_1 = \pm i \sqrt{\frac{k_0}{k_2}} \quad (5.4-24)$$

Then from equation (5.4-8) one obtains

$$q_2 = \pm i \sqrt{\frac{k_0}{k_2}} \quad (5.4-25)$$

independent of d . Thus if the input is exactly "matched" the beam parameter remains a constant. In any practical laser, however, the input cannot be exactly matched, so the stability arguments of the preceding paragraphs are important.

Kogelnik^(5.3) obtained the matching input parameter differently. The steady state beam modes may be obtained by setting dQ/dz equal to zero in the original beam equation with the result

$$Q = \mp i \sqrt{k_0 k_2} \quad (5.4-26)$$

or

$$q = \pm i \sqrt{\frac{k_0}{k_2}} \quad (5.4-27)$$

which is the same as equation (5.4-25). It is impossible to tell from the steady state solution obtained in this way whether or not the limiting value of the spot size in a long laser amplifier is finite. For this purpose one must use equation (5.4-21).

It is perhaps worth while to consider briefly the important special case of propagation through free space. Then $k_2 = 0$ and equation (5.4-1) simplifies to

$$\frac{dQ}{Q^2} = - \frac{dz}{k_o} \quad (5.4-28)$$

with the solution

$$\frac{1}{Q(z)} - \frac{1}{Q(0)} = \int_0^z \frac{dz}{k_o} \quad (5.4-29)$$

If k_o is independent of z , this equation may be written

$$q = q_o + z \quad (5.4-30)$$

Equation (5.4-30) together with the definition of q given in equation (5.3-6) implies that the free space propagation of the spot size and phase front curvature are governed by the well known equations

$$\frac{\pi w^2}{\lambda} = z_o [1 + (\frac{z}{z_o})^2] \quad (5.4-31)$$

$$R = z [1 + (\frac{z_o}{z})^2] \quad (5.4-32)$$

where $z_o = \frac{\pi w_o^2}{\lambda}$ and distance is measured from the beam waist.

In this section the problem of the propagation of Gaussian beams through general lenslike media has been studied in detail. In

particular, the stability of such waveguides has been investigated. It was shown that the spot size either oscillates periodically or grows without bound unless the medium has a positive gain profile ($\alpha_2 > 0$). The amplification and damped focusing possible in high gain media would be desirable properties for long distance beam propagation.

5.5 Beam matrices

In passing through any simple optical element such as a lens, mirror, or lenslike medium, the complex beam parameter transforms according to the relation

$$q_2 = \frac{A_1 q_1 + B_1}{C_1 q_1 + D_1} \quad (5.5-1)$$

where the coefficients depend on the details of the optical element in question. Later in this section the values of the coefficients will be determined for some particular elements of interest. Kogelnik^(5.3) refers to equation (5.5-1) as the ABCD law. If an element governed by this equation is followed by a second element with the transformation

$$q_3 = \frac{A_2 q_2 + B_2}{C_2 q_2 + D_2} \quad (5.5-2)$$

then it is a matter of simple arithmetic to show that the net transformation is

$$q_3 = \frac{(A_2 A_1 + B_2 C_1) q_1 + (A_2 B_1 + B_2 D_1)}{(A_1 C_2 + C_1 D_2) q_1 + (B_1 C_2 + D_1 D_2)} \quad (5.5-3)$$

This is again a transformation of the form (5.5-1).

It turns out to be useful to collect these coefficients into two by two matrices. Suppose one takes the ordered product of the matrices corresponding to equations (5.5-1) and (5.5-2) as follows

$$\begin{vmatrix} A_2 & B_2 \\ C_2 & D_2 \end{vmatrix} \times \begin{vmatrix} A_1 & B_1 \\ C_1 & D_1 \end{vmatrix} = \begin{vmatrix} A_2 A_1 + B_2 C_1 & A_2 B_1 + B_2 D_1 \\ A_1 C_2 + C_1 D_2 & B_1 C_2 + D_1 D_2 \end{vmatrix} \quad (5.5-4)$$

The coefficients of the product matrix are seen to be just the same as those of the net transformation equation (5.5-3). By induction the procedure is obvious for obtaining the net transformation for an arbitrary sequence of lens elements. One merely writes the transformation coefficients for each element in the form of a matrix and then multiplies together the matrices to obtain the coefficients for the net transformation. The order of multiplication is important, and the correct arrangement is to have the element first encountered by the beam correspond to the matrix farthest right. These matrix methods are not essential. They are merely a formalism for simplifying the algebra required in investigating beam propagation.

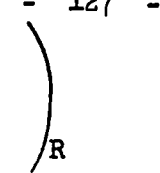
The matrices corresponding to various basic optical components likely to be encountered in laser problems are shown in Figure 5.1. The direction of propagation is always taken to be the positive z direction and in the figure beams are incident from the left. The radius of curvature of a surface is taken to be positive if the center of curvature occurs at a smaller value of z than does the surface itself.

Diffraction effects may be assumed to be negligible in thin lenses, mirrors, and across interfaces. Then the beam matrices for these elements may be obtained immediately from well known results of geometrical optics^(5.5). The result for a spherical mirror, when expressed in terms of the radii of curvature of the phase fronts is

$$\frac{1}{R_2} = \frac{1}{R_1} - \frac{2}{R} \quad (5.5-5)$$

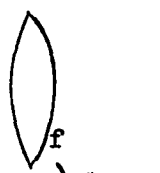
Since the spot size of the beam does not change in reflection from the mirror, this can be written using equation (5.3-6) as

a. Mirror



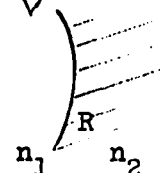
$$\begin{vmatrix} 1 & 0 \\ -\frac{2}{R} & 1 \end{vmatrix}$$

b. Thin Lens



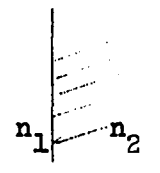
$$\begin{vmatrix} 1 & 0 \\ -\frac{1}{f} & 1 \end{vmatrix}$$

c. Spherical Interface



$$\begin{vmatrix} 1 & 0 \\ \frac{n_2 - n_1}{n_2 R} & \frac{n_1}{n_2} \end{vmatrix}$$

d. Plane Interface



$$\begin{vmatrix} 1 & 0 \\ 0 & \frac{n_1}{n_2} \end{vmatrix}$$

e. Lenslike Medium

$$k = k_o - \frac{1}{2} k_2 r^2$$

(complex profile)

$$\begin{vmatrix} \cos \sqrt{\frac{k_2}{k_o}} d & \sqrt{\frac{k_o}{k_2}} \sin \sqrt{\frac{k_2}{k_o}} d \\ -\sqrt{\frac{k_2}{k_o}} \sin \sqrt{\frac{k_2}{k_o}} d & \cos \sqrt{\frac{k_2}{k_o}} d \end{vmatrix}$$

f. Lenslike Medium

$$n = n_o - \frac{1}{2} n_2 r^2$$

(real profile)

$$\begin{vmatrix} \cos \sqrt{\frac{n_2}{n_o}} d & \sqrt{\frac{n_o}{n_2}} \sin \sqrt{\frac{n_2}{n_o}} d \\ -\sqrt{\frac{n_2}{n_o}} \sin \sqrt{\frac{n_2}{n_o}} d & \cos \sqrt{\frac{n_2}{n_o}} d \end{vmatrix}$$

g. Short Medium

$$d \rightarrow 0$$

$$\begin{vmatrix} 1 & d \end{vmatrix}$$

$$k_o \rightarrow \infty$$

$$\begin{vmatrix} \frac{k_2}{k_o} d & 1 \end{vmatrix}$$

$$\text{or Weak Profile}$$

$$k_2 \rightarrow 0$$

h. Uniform Medium

$$k_2 = 0$$

$$\begin{vmatrix} 1 & d \\ 0 & 1 \end{vmatrix}$$

Figure 5.1 Beam matrices for some basic optical elements.

$$\frac{1}{q_2} = \frac{1}{q_1} - \frac{2}{R} \quad (5.5-6)$$

or

$$q_2 = \frac{q_1}{\frac{2}{R} q_1 + 1} \quad (5.5-7)$$

Using equation (5.5-1), the beam matrix for the mirror shown in Figure 5.1a follows immediately. The formula for the thin lens is obtained in the same way with $R/2$ replaced by f .

For the curved interface the optics formula is

$$\frac{1}{R_2} = \frac{n_1}{n_2} \frac{1}{R_1} + \frac{(n_2 - n_1)}{n_2 R} \quad (5.5-8)$$

Therefore,

$$q_2 = \frac{q_1}{\frac{n_2 - n_1}{n_2 R} + \frac{n_1}{n_2}} \quad (5.5-9)$$

remembering that λ_m in equation (5.3-6) is the wavelength in the medium. The matrix of Figure 5.1c follows from equation (5.5-9) and the matrix for a plane interface is just the obvious special case $R = \infty$.

The matrix for a general lenslike medium follows immediately from equation (5.4-8). The last three matrices are special cases of the medium matrix.

In this section matrix methods have been described for studying the propagation of Gaussian beams through simple optical systems. The results are very useful in laser problems such as the calculation of the transverse resonator modes described in the next section. There

are relations between the beam matrices described here and the familiar ray propagation theory of geometrical optics. The ray theory is not of interest in our work so we omit it.

5.6 Resonator modes

In the previous section a matrix method has been described for studying the propagation of Gaussian beams through sequences of simple optical elements. Using that method, it is straightforward to calculate the transverse modes of an optical resonator. The resonator is regarded as a closed sequence of such elements, and the modes are obtained from a self-consistency requirement which we now describe.

The mode calculation procedure is most easily shown by means of an example. Consider the simple empty half-symmetric resonator of Figure 5.2 with the input and output beam parameters as indicated. The total matrix corresponding to one round trip through this resonator is

$$\begin{pmatrix} A & B \\ C & D \end{pmatrix} = \begin{pmatrix} 1 & d \\ 0 & 1 \end{pmatrix} \begin{pmatrix} 1 & 0 \\ 0 & 1 \end{pmatrix} \begin{pmatrix} 1 & d \\ 0 & 1 \end{pmatrix} \begin{pmatrix} 1 & 0 \\ -2/R & 1 \end{pmatrix} = \begin{pmatrix} 1 - \frac{4d}{R} & 2d \\ -\frac{2}{R} & 1 \end{pmatrix} \quad (5.6-1)$$

Requiring that $q_2 = q_1 = q$ and solving equation (5.5-1) yields

$$\frac{1}{q} = \frac{D-A}{2B} \mp \frac{1}{2B} \sqrt{-4BC - (D-A)^2} \quad (5.6-2)$$

The sign must be chosen so that a confined beam is obtained.

The value of the beam parameter at the left mirror is found by substituting equation (5.6-1) into equation (5.6-2). The result is

$$\frac{1}{q} = \frac{1}{R} - i \frac{\sqrt{\frac{R}{d} - 1}}{R} \quad (5.6-3)$$

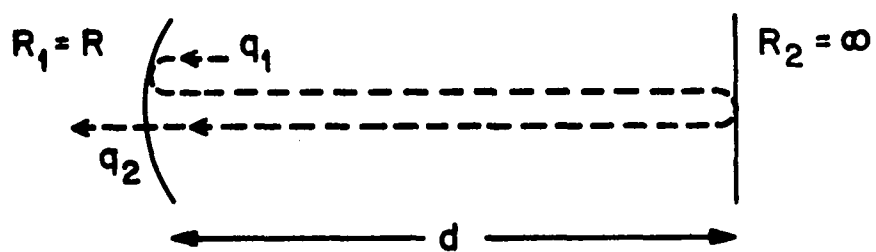


Figure 5.2 Half-symmetric resonator.

With the definition of the beam parameter given by equation (5.3-6) one obtains the familiar expression for the mirror spot size of a half-symmetric resonator

$$\frac{\lambda}{\pi w^2} = \frac{\sqrt{\frac{R}{d} - 1}}{R} \quad (5.6-4)$$

The beam parameter at any other location in the resonator may be found by a similar derivation using a different reference plane. Alternatively the result given by equation (5.6-3) may be used together with a free space matrix transformation to the plane of interest. These matrix methods are useful for lasers containing any of the optical elements described in the previous section.

The modes determined by equation (5.6-2) satisfy the condition that the beam parameter repeat itself after one loop through the resonator. One may inquire whether additional modes might be possible which repeat only after two or more loops. The uniqueness of the modes can be established by substituting into equation (5.6-2) the matrix elements corresponding to n passes through the resonator. One finds that the resultant beam parameter is identical to that which is obtained when only a single pass is considered, and hence q is unique. The appropriate matrix elements are given by Yariv^(5.6).

Actually there may be some pathological cases where the beam parameter as given by equation (5.6-2) is not unique. These occur when either the real or imaginary parts of equation (5.6-2) reduce to zero divided by zero. For example, in a simple free space confocal resonator ($d = R$) one readily finds that neither the phase front curvature nor the spot size are well defined. This fact is believed to be

responsible for the instability and peculiar transient behavior of resonators which are exactly confocal.

The situation of greatest interest here is that of a laser resonator filled with an unsaturated lenslike medium which is describable by the matrix of Figure 5.1e. For the resonator of Figure 5.2 filled with such a medium the round trip beam matrix becomes

$$\begin{pmatrix} A & B \\ C & D \end{pmatrix} = \begin{pmatrix} \cos \sqrt{\frac{k_2}{k_0}} 2d - \frac{2}{R} \sqrt{\frac{k_0}{k_2}} \sin \sqrt{\frac{k_2}{k_0}} 2d & \sqrt{\frac{k_0}{k_2}} \sin \sqrt{\frac{k_2}{k_0}} 2d \\ -\sqrt{\frac{k_2}{k_0}} \sin \sqrt{\frac{k_2}{k_0}} 2d - \frac{2}{R} \cos \sqrt{\frac{k_2}{k_0}} 2d & \cos \sqrt{\frac{k_2}{k_0}} 2d \end{pmatrix} \quad (5.6-5)$$

The output beam parameter for this laser may be found from equations (5.6-2) and (5.6-5) with the result

$$\frac{1}{q} = \frac{1}{R} \mp \frac{i}{R} \sqrt{(R\sqrt{\frac{k_2}{k_0}})^2 + 2(R\sqrt{\frac{k_0}{k_2}}) \cot(\sqrt{\frac{k_2}{k_0}} 2d) - 1} \quad (5.6-6)$$

If both mirrors are flat ($R \rightarrow \infty$), equation (5.6-6) reduces to

$$\frac{1}{q} = \mp i \sqrt{\frac{k_2}{k_0}} \quad (5.6-7)$$

This equation is the same as equation (5.4-18). For the plane parallel laser filled with a lenslike medium the beam parameter is independent of position in the resonator.

Our primary interest here is in high gain lasers having a negligible index of refraction profile ($\beta_2 = 0$, $\beta_0 = \frac{2\pi}{\lambda}$). The limits of validity of this approximation will be considered later. Then if the gain per

wavelength is small ($\beta_0 \gg \alpha_0$) ,

$$\sqrt{\frac{k_2}{k_0}} \approx \sqrt{\frac{i\alpha_2}{\beta_0}} = \frac{1+i}{2} \sqrt{\frac{\lambda\alpha_2}{\pi}} \quad (5.6-8)$$

For a half-symmetric resonator equations (5.6-6) and (5.6-8) imply

$$\frac{1}{q} = \frac{1}{R} + \frac{i}{R} \sqrt{\frac{iR^2\lambda\alpha_2}{2\pi} + (1+i)R\sqrt{\frac{\lambda\alpha_2}{\pi}} \cot\left[(1+i)\sqrt{\frac{\lambda\alpha_2}{\pi}} d\right] - 1}. \quad (5.6-9)$$

The cotangent function may be expanded into its real and imaginary parts by means of

$$\cot(a+ib) = \frac{1}{2} \frac{\sin 2a - i \sinh 2b}{\cosh^2 b \sin^2 a + \cos^2 a \sinh^2 b} \quad (5.6-10)$$

Then with equation (5.3-6) the output spot size at the curved mirror can be written

$$\frac{\pi w^2}{\lambda} = \left[\operatorname{Re} \sqrt{\frac{1}{2Rx} \frac{\frac{2d}{x} + \sinh \frac{2d}{x}}{\cosh^2 \frac{d}{x} \sin^2 \frac{d}{x} + \cos^2 \frac{d}{x} \sinh^2 \frac{d}{x}} - \frac{1}{R^2}} \right. \\ \left. + i \left(\frac{1}{2x^2} + \frac{1}{2Rx} \frac{\sin \frac{2d}{x} - \sinh \frac{2d}{x}}{\cosh^2 \frac{d}{x} \sin^2 \frac{d}{x} + \cos^2 \frac{d}{x} \sinh^2 \frac{d}{x}} \right) \right]^{-1} \quad (5.6-11)$$

where $x = \sqrt{\frac{\pi}{\alpha_2 \lambda}}$. This is solvable using

$$\text{Re}\sqrt{a + ib} = \sqrt{\frac{a^2 + b^2 + a}{2}} \quad (5.6-12)$$

Plots of equation (5.6-11) are given in Figure 5.3 for three different resonator configurations. It is evident from the figure that for a sufficiently strong gain profile the spot size is independent of the mirror curvature in contrast to the usual free space results. In this limit the spot size may readily be shown to be governed by

$$\frac{\pi w^2}{\lambda} = 2\sqrt{\frac{\pi}{\alpha_2 \lambda}} \quad (5.6-13)$$

Even the unstable and high loss resonators are rendered stable by the amplifying medium. Low diffraction loss modes are thus possible in resonators which otherwise could not support them. In the limit of low gain the spot size approaches its empty resonator value. The asymptotic forms for the spot size in this limit may be obtained from a straightforward expansion of equation (5.6-11). The results are

$$\lim_{\alpha_2 \rightarrow 0} \frac{\pi w^2}{\lambda} = \begin{cases} \frac{4}{d} \sqrt{\frac{1 - \frac{R}{d}}{\left(\frac{4}{3} - \frac{R}{d}\right)}} \left(\frac{\pi}{\lambda \alpha_2} \right) & \frac{R}{d} < 1 \\ \sqrt{\frac{R}{d}} & \frac{R}{d} > 1 \end{cases} \quad (5.6-14)$$

$$= \begin{cases} \frac{4}{d} \sqrt{\frac{1 - \frac{R}{d}}{\left(\frac{4}{3} - \frac{R}{d}\right)}} \left(\frac{\pi}{\lambda \alpha_2} \right) & \frac{R}{d} < 1 \\ \sqrt{\frac{R}{d}} & \frac{R}{d} > 1 \end{cases} \quad (5.6-15)$$

Equation (5.6-14) describes the quadratically increasing behavior of Figure 5.3(a), while equation (5.6-15) is in agreement with the stable form of Figure 5.3(c). In the special case of the plane parallel laser shown in Figure 5.3(b) the spot size is always given by equation (5.6-13).

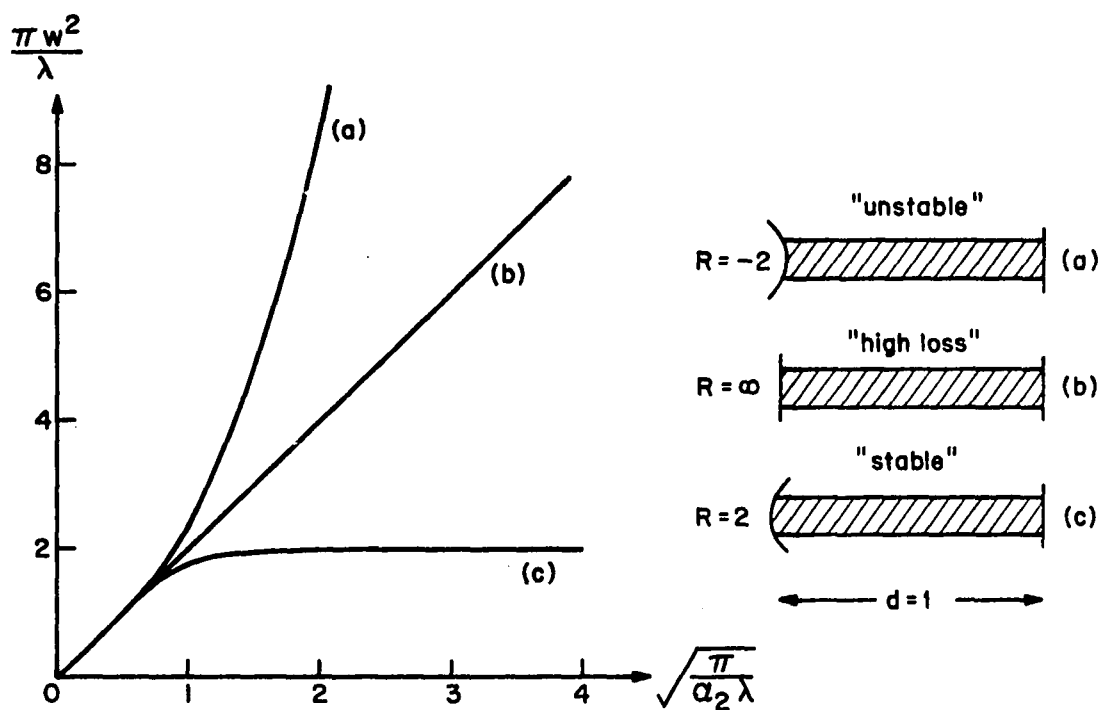


Figure 5.3 Theoretical curves showing the dependence of the beam radius at the left mirror on the gain constant α_2 .

The spot size changes from its large α_2 form to its small α_2 form at the value of α_2 given roughly by

$$\sqrt{\frac{\pi}{\alpha_2 \lambda}} = \begin{cases} \frac{d}{2} \frac{\left(\frac{4}{3} - \frac{R}{d}\right)}{\sqrt{1 - \frac{R}{d}}} & \frac{R}{d} < 1 \\ \frac{R}{2\sqrt{\frac{R}{d} - 1}} & \frac{R}{d} > 1 \end{cases} \quad (5.6-16)$$

$$(5.6-17)$$

These expressions were obtained from a comparison of equations (5.6-13) to (5.6-15). They may be used to estimate whether the gain focusing effect will be important for any particular laser system.

In the last few paragraphs we have assumed that the index of refraction profile is unimportant compared to the gain profile. However, it was shown in Chapter 2 that there is always anomalous dispersion associated with an amplifying transition. Consequently it is important to consider under what conditions the index effects are really negligible. To do this we consider the simplest case of the plane parallel laser. From equations (5.6-7) and (5.3-6) the spot size is governed approximately by

$$\frac{\lambda}{\pi w^2} = \text{Re} \sqrt{\frac{k_2}{k_0}} \approx \sqrt{\frac{\sqrt{\beta_2^2 + \alpha_2^2} + \beta_2}{2\beta_0}} \quad (5.6-18)$$

where equation (5.6-12) has been used and the gain per wavelength is assumed small.

From equation (5.6-18) it is clear that refraction focusing will be unimportant as long as the condition

$$\alpha_2 \gg \beta_2 = \frac{2\pi n_2}{\lambda} \quad (5.6-19)$$

is satisfied. For example, if the transition is homogeneously broadened then equations (2.5-7) and (2.5-8) imply

$$n_2(v) = \frac{cy}{2\pi v} \alpha_2(v) \quad (5.6-20)$$

where $y = \frac{2(v - v_o)}{\Delta v_h}$ is the homogeneous frequency difference. Therefore, equation (5.6-19) in the homogeneous limit becomes

$$y \ll 1$$

or

$$v - v_o \ll \frac{\Delta v_h}{2} \quad (5.6-21)$$

A similar condition is obtained for inhomogeneously broadened lasers. For this case equations (2.6-13) and (2.6-14) imply

$$n_2(v) = \frac{\lambda \alpha_2(v)}{\pi^{3/2}} F(x) e^{-x^2} \quad (5.6-22)$$

where $x = \frac{2(v - v_o)}{\Delta v_D} (\ln 2)^{\frac{1}{2}}$ is the inhomogeneous frequency difference, $F(x)$ is Dawson's integral, and saturation is assumed to be negligible. Therefore, equation (5.6-19) in the inhomogeneous limit is

$$\frac{\pi^{\frac{1}{2}}}{2} >> F(x)e^{-x^2}$$
$$>> x + \frac{x^3}{3!} + \frac{x^5}{5 \cdot 2!} + \frac{x^7}{7 \cdot 3!} + \frac{x^9}{9 \cdot 4!} + \dots \quad (5.6-23)$$

The power series expansion follows from equation (2.6-5) . A numerical solution of equation (5.6-23) leads to the condition

$$x << 732$$

or

$$v - v_o << 44 \Delta v_D \quad (5.6-24)$$

The interpretation of the conditions given in equations (5.6-21) and (5.6-24) is that for radiation reasonably near to line center gain focusing is more important than the associated anomalous dispersion focusing or defocusing effects. Nevertheless, dispersion can be important in some circumstances. Dispersion focusing is discussed in detail in section 5.8.

There are, of course, other types of refraction focusing effects which may sometimes be important. A matrix method of mode calculation identical to ours was used in a recent paper by Schlie and Verdeyen (5.7) to investigate the dependence of the transverse resonator modes on the dispersion profile associated with an adjacent absorbing transition in the 6401 Å helium-neon laser. These methods have also recently been applied by McCaul (5.8) in a study of the dependence of the resonator modes on the refraction associated with the free electron density in an HCN laser at 337 microns. Thermal lens effects may also be treated this way.

As an example of the application of the phase equation, one can calculate the minimum gain required for oscillation. For the plane parallel resonator with a fundamental Gaussian beam ($p = l = 0$) confined by the amplifying medium equations (5.2-25) and (5.4-26) imply

$$\frac{dP}{dz} = \mp \sqrt{\frac{k_2}{k_o}} \quad (5.6-25)$$

In a medium with only a positive gain profile the solution is

$$P = - \frac{(1 + i)}{2} \sqrt{\frac{\alpha_2 \lambda}{\pi}} z \quad (5.6-26)$$

Then according to equation (5.3-7) the amplitude of the beam is governed by

$$E \sim E_o e^{(\alpha_o - \frac{1}{2} \sqrt{\frac{\alpha_2 \lambda}{\pi}}) z} \quad (5.6-27)$$

The gain required for oscillation is

$$2\alpha_o - \sqrt{\frac{\alpha_2 \lambda}{\pi}} = - \frac{\ln R_1 R_2}{2d} \quad (5.6-28)$$

where R_1 and R_2 are the effective right and left mirror intensity reflectivities and d is the length of the resonator.

In this section matrix methods have been described which are useful for the systematic analysis of the transverse modes of optical resonators containing an assortment of lenses and lenslike elements. In particular, the modes of a resonator containing a medium with a gain profile have been derived, and the relative importance of the gain profile and the

associated dispersion profile has been investigated.

5.7 Gain focusing experiment

We have done an experiment to verify the conclusions of the previous section regarding gain focusing in a plane parallel laser. The apparatus is shown schematically in Figure 5.4. A D.C. xenon discharge may exhibit very high optical gain at 3.51 microns as discussed in Chapter III. The xenon pressure was maintained at about 5 microns by means of a liquid nitrogen trap^(5.9) on a side arm of the discharge tube. The right mirror was highly reflecting and the output beam came through the partly transmitting left mirror.

The spot size was determined by scanning the detector across the output and plotting the power as a function of radius. Readings were made using a PAR model HR-8 lock-in amplifier. It was necessary to operate the laser very near to threshold to avoid distortion of the gain profile by saturation. Threshold conditions were obtained by reducing the discharge current until the output intensity was only slightly larger than the superradiant output (obtained by misaligning the left mirror). The mirror position had to be corrected from time to time to ensure that the oscillating mode was near the center of the gain profile in accordance with the condition given in equation (5.6-24). Otherwise dispersion effects would not necessarily be negligible.

Typical experimental curves are shown in Figure 5.5. The beam is very nearly Gaussian and much smaller than the 5.5 mm discharge diameter. We use as the spot size the radius at which the difference between the

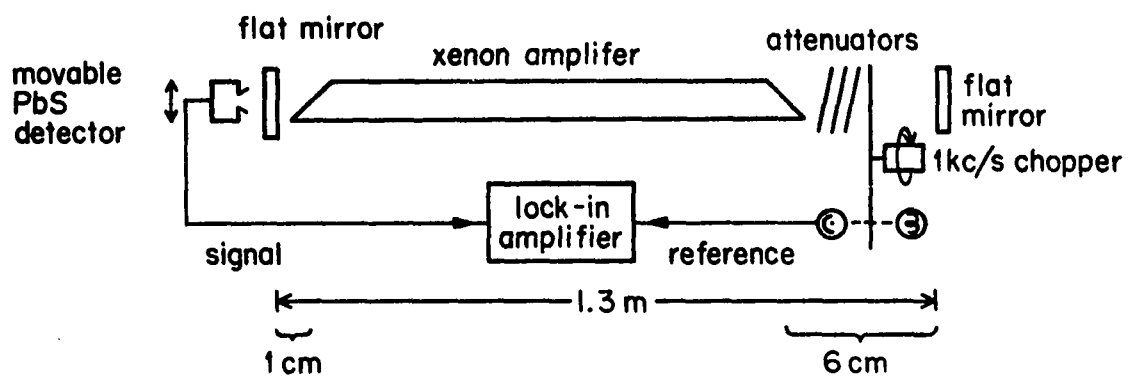


Figure 5.4 Experimental setup

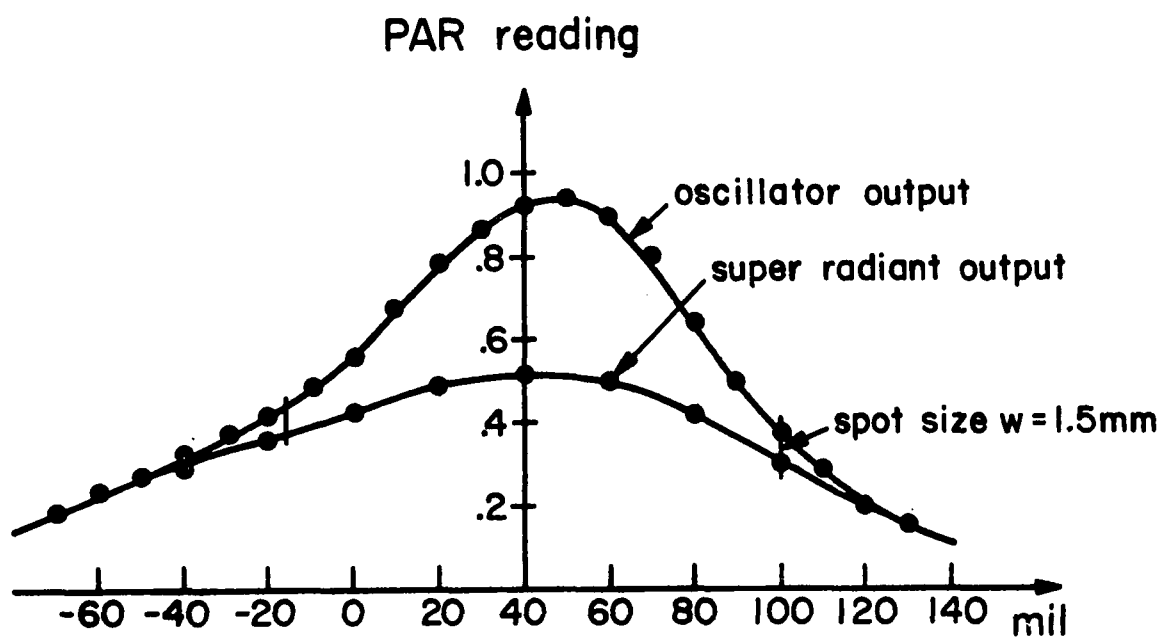


Figure 5.5 Typical experimental beam profiles.

resonator output intensity and the superradiant intensity falls to $1/c^2$ of its maximum value.

The reason that gain focusing occurs in xenon is that the gain is high near the center of the discharge and goes to zero at the tube walls. It has been shown⁽⁵¹⁰⁾ that in a gas discharge laser the radial variation of the gain constant is described by a zero order Bessel function if the excitation is low. If the Bessel function is approximated near the tube axis by a quadratic one finds

$$\alpha_2 = \alpha_o \frac{2.88}{r_o^2} \quad (5.7-1)$$

where r_o is the radius of the discharge and α_o is the gain at the axis.

In Figure 5.6 the experimental spot size data are compared with the theoretical plot of equation (5.6-13). The good agreement provides a verification of the theory. The gain constants were determined by measuring the losses in the cavity. According to equation (5.6-28) the gain required for oscillation may be written

$$2\alpha_o - \sqrt{\frac{\alpha_2 \lambda}{\pi}} = - \frac{\ln f}{2d} \quad (5.7-2)$$

where f is the fraction of the intensity left after a round trip through the losses in the resonator (attenuators, windows, mirrors). All of the losses can be measured. Equations (5.7-1) and (5.7-2) can be combined into a quadratic equation and solved for either α_o or α_2 for various levels of attenuation. We did not attempt an experimental

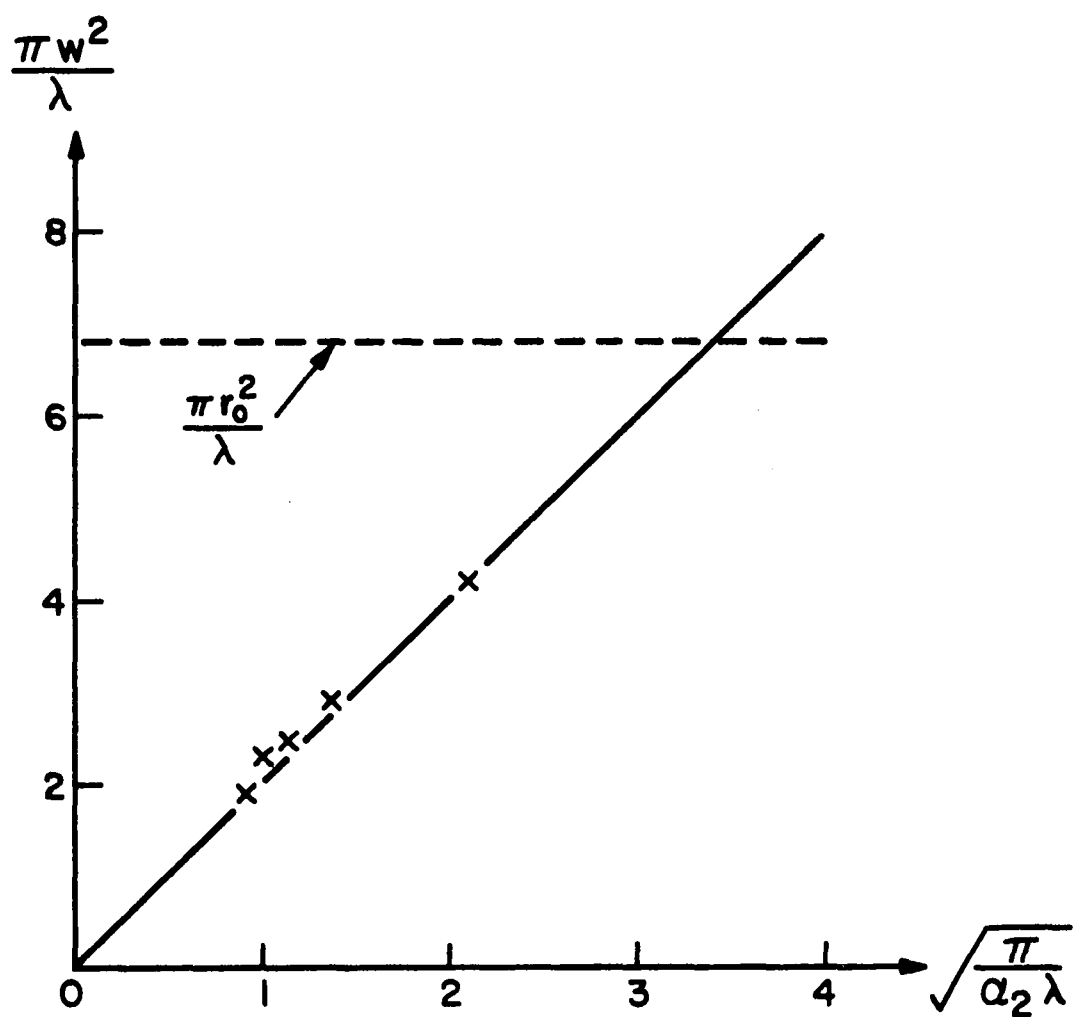


Figure 5.6 Experimental spot size data compared with the theoretical result.

investigation of curves of the sort shown in Figure 5.3(a) and Figure 5.3(c) because of the greater uncertainties involved.

In this section we have presented experimental verification of the theory of gain focusing in laser resonators. Good agreement was obtained.

5.8 Dispersion focusing theory

In the previous sections we have considered in some detail the focusing and defocusing effects which can result from profiles of the gain and index of refraction. For the most part it was assumed that these two types of profiles could occur independently of each other. However, it was pointed out in section 5.6 that whenever there is a gain spectrum there must also be an associated dispersion spectrum. Therefore, refraction focusing due to dispersion must always accompany gain focusing. Within the conditions given in equation (5.6-21) and (5.6-24) the spot size will be only slightly affected by this refraction effect. Nevertheless, there may be other significant consequences of dispersion. It is the purpose of this section to study more carefully the relative importance of gain and dispersion focusing. A simple experiment is also described which demonstrates the occurrence of dispersion focusing in a xenon laser.

The simplest laser geometry for studying focusing effects consists of a medium with no z variations which is positioned between a pair of plane mirrors. As shown previously, the beam spot size and phase front curvature are independent of position in such a configuration. From equation (5.6-18) the spot size is given by

$$\frac{\pi w^2}{\lambda_m} = 2\sqrt{\frac{\pi}{\alpha_2 \lambda_m}} \left(\sqrt{1 + \left(\frac{\beta_2}{\alpha_2}\right)^2} + \frac{\beta_2}{\alpha_2} \right)^{-\frac{1}{2}} \quad (5.8-1)$$

We have written the spot size in this form for comparison with the basic gain focusing result of equation (5.6-13). If dispersion is unimportant, β_2 will be much less than α_2 and equation (5.8-1) reduces to equation (5.6-13) as we should expect.

From equations (5.6-20) and (5.8-1) the spot size in a homogeneously broadened laser including both gain and dispersion focusing is

$$\frac{\pi w^2}{\lambda_m} = 2 \sqrt{\frac{\pi}{\alpha_2 \lambda_m}} \left(\sqrt{1 + y^2} + y \right)^{-\frac{1}{2}} \quad (5.8-2)$$

From equations (5.6-22) and (5.8-1) the corresponding result for an inhomogeneously broadened laser is

$$\frac{\pi w^2}{\lambda_m} = 2 \sqrt{\frac{\pi}{\alpha_2 \lambda_m}} \left(\sqrt{1 + \left(\frac{2F(x)e^x}{\pi^{\frac{1}{2}}} \right)^2} + \frac{2F(x)e^x}{\pi^{\frac{1}{2}}} \right)^{-\frac{1}{2}} \quad (5.8-3)$$

In the limit of small x equation (5.8-3) reduces to

$$\frac{\pi w^2}{\lambda_m} = 2 \sqrt{\frac{\pi}{\alpha_2 \lambda_m}} \left(\sqrt{1 + \left(\frac{2x}{\pi^{\frac{1}{2}}} \right)^2} + \frac{2x}{\pi^{\frac{1}{2}}} \right)^{-\frac{1}{2}} \quad (5.8-4)$$

Thus, the homogeneous and inhomogeneous limits of the spot size are qualitatively identical near line center.

For comparison with experiment we are most interested in the limit of inhomogeneous broadening. The results for homogeneous broadening are similar and will not be considered here. The gain $\alpha(v)$ in a Doppler broadened medium has a Gaussian spectrum. Therefore, in accordance with equation (5.8-3) the normalized spot size

$w^* \equiv w(x)/w(0)$ is

$$w^*(x) = e^{x^2/4} \sqrt{1 + \left(\frac{2F(x)e^{x^2}}{\pi^{1/2}}\right)^2 + \frac{2F(x)e^{x^2}}{\pi^{1/2}}}^{-1/4} \quad (5.8-5)$$

The exponential factor results from the frequency dependence of α_2 .

Equation (5.8-5) is plotted in Figure 5.7 using the approximation given in equation (2.6-9) for $F(x)$. Also plotted in the figure is the function $e^{x^2/4}$ which would represent the frequency dependence of the normalized spot size if dispersion focusing did not occur. From the graph it is apparent that dispersion focusing does not have a very drastic effect on the spot size. The difference between the spot size for the two theories is at most of the other of ten percent. Nevertheless, the dispersion focusing could, in principle, be detected directly by scanning the output beam profile of a laser if the oscillation frequency were known. We have not attempted this experiment.

Another aspect of Figure 5.7 is that the minimum spot size occurs at a frequency of about $x \approx .6$ rather than at $x = 0$ as it would if dispersion were neglected. This is due to the positive refraction profile (focusing) which occurs at positive frequencies. This asymmetry in the spot size spectrum leads to an asymmetry in the spectrum of the total output power. In particular, the maximum power output of the laser does not occur when the oscillation frequency is at gain center (neglecting the Lamb dip, of course) because the power output is a sensitive function of the spot size. The asymmetry in the power output is easily measured and provides a fairly direct indication of dispersion focusing.

There remains the problem of determining the output power

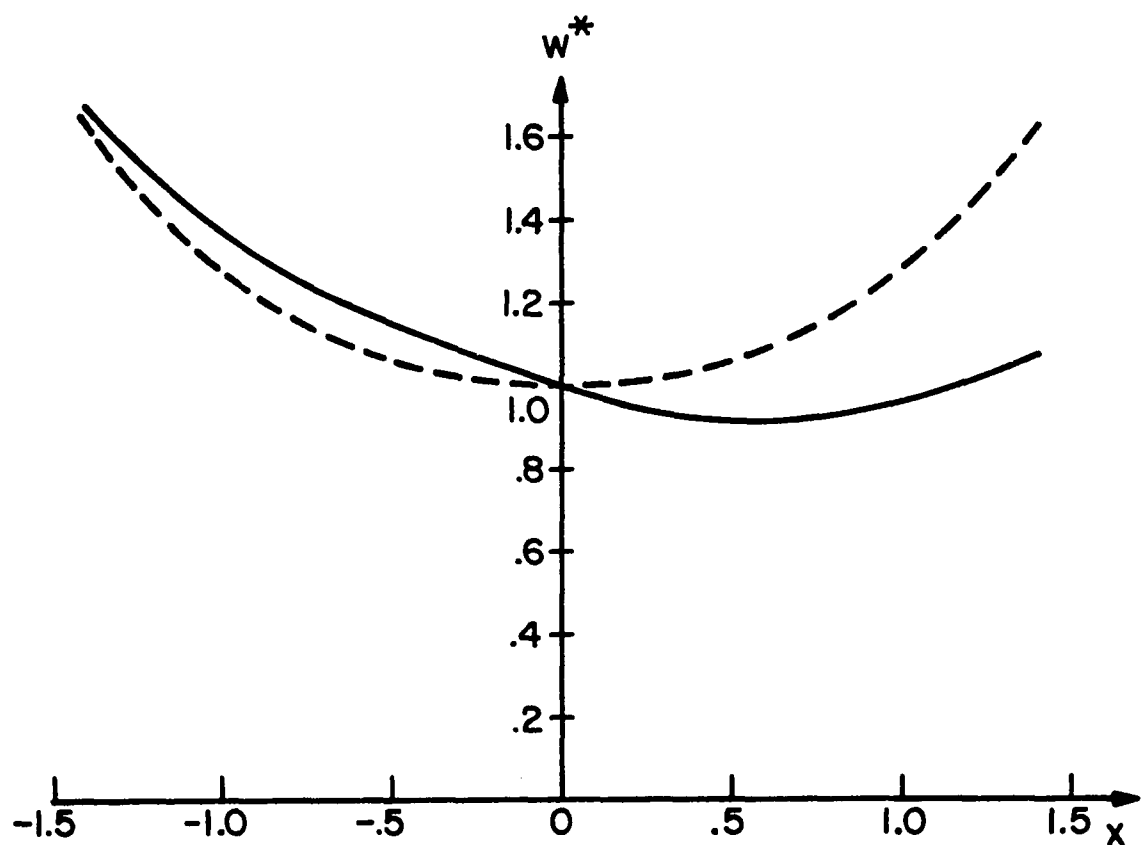


Figure 5.7 Solid line is the normalized spot size as a function of frequency. Dashed line is the spot size neglecting dispersion focusing.

spectrum of a laser oscillator including gain and dispersion focusing. This calculation makes use of some results of the power saturation formalism of Chapter X. According to equation (10.4-12), the total power P of a Gaussian beam in an inhomogeneously broadened medium with a quadratic gain profile is governed by

$$\begin{aligned} \frac{dP}{dz} = & \frac{g_0 \pi w^2}{s} \left[\left(1 + \frac{2sP}{\pi w^2} \right)^{\frac{1}{2}} - 1 \right] \\ & + \frac{g_2 \pi w^4}{4s} \left[\ln \frac{\left(1 + \frac{2sP}{\pi w^2} \right)^{\frac{1}{2}} + 1}{\left(1 + \frac{2sP}{\pi w^2} \right)^{\frac{1}{2}} - 1} + 2 - 2 \left(1 + \frac{2sP}{\pi w^2} \right)^{\frac{1}{2}} + \ln \frac{sP}{\pi w^2} \right] \end{aligned} \quad (5.8-6)$$

This equation can only be valid in this application as long as the saturation is very weak, because we are assuming that the beam is confined by the z -independent gain profile. Experimentally, this means that the laser must be operated very close to threshold. In this limit equation (5.8-6) can be greatly simplified.

For weak saturation equation (5.8-6) may be written to second order in P (after some algebra) as

$$\frac{dP}{dz} = g_0 P \left(1 - \frac{1}{2} \frac{sP}{\pi w^2} \right) - \frac{g_2 w^2 P}{4} \left(1 - \frac{1}{4} \frac{sP}{\pi w^2} \right) \quad (5.8-7)$$

This equation can be put in the more convenient approximate form

$$\frac{dp}{dz} = \frac{g_o P \left(1 - \frac{g_2}{g_o} \frac{w^2}{4}\right)}{1 + \frac{1}{2} \frac{sP}{\pi w^2} \left(\frac{1 - \frac{g_2}{g_o} \frac{w^2}{8}}{1 - \frac{g_2}{g_o} \frac{w^2}{4}} \right)} \quad (5.8-8)$$

In a gas laser of the sort used in our experiment g_2 is related to g_o by

$$g_2 = g_o \frac{2.88}{r_o^2} \quad (5.8-9)$$

according to equation (5.7-1). Therefore, the power is governed finally by

$$\frac{dp}{dz} = \frac{g_o P \left(1 - .72 \frac{w^2}{r_o^2}\right)}{1 + \frac{1}{2} \frac{sP}{\pi w^2} \left(\frac{1 - .36 \frac{w^2}{r_o^2}}{1 - .72 \frac{w^2}{r_o^2}} \right)} \quad (5.8-10)$$

Equation (5.8-10) is the general result for the weak saturation of a Gaussian beam in a gas laser. It can be solved analytically for the output power of a laser oscillator as a function of frequency by using equation (5.8-3) for the frequency dependent spot size. However, we first make one further approximation to simplify the mathematics. If the spot size is much less than the discharge radius, equation (5.8-10) reduces to

$$\frac{dP}{dz} = \frac{g_o P}{1 + \frac{1}{2} \frac{sP}{\pi w^2}} \quad (5.8-11)$$

This is not always a terribly good approximation, but it is believed to be adequate for our experiment and makes the results independent of the tube radius. Comparison with equation (10.4-14) shows that equation (5.8-11) is just the small signal limit (homogeneous limit) of the one dimension approximation for inhomogeneous broadening. The corresponding result for pure homogeneous broadening would lack the factor $\frac{1}{2}$.

If one mirror is highly reflecting, equation (5.8-11) can be integrated for one loop through the laser medium, and the result is

$$\frac{1}{2} \frac{s}{\pi w^2} (P_2 - P_1) = 2g_o \ell - \ln \frac{P_2}{P_1} \quad (5.8-12)$$

where ℓ is the length of the medium. If the reflectivity of the output mirror is R and the transmission is T , then equation (5.8-12) may be solved for the output power P_o as

$$P_o = \frac{2\pi w^2}{s} \left(\frac{T}{1-R} \right) (2g_o \ell + \ln R) \quad (5.8-13)$$

We are most interested here in the frequency dependence of P_o . Substituting equation (5.8-3) into equation (5.8-13) leads to

$$P_o(x) = \frac{4r_o}{s} \sqrt{\frac{\pi \lambda m}{1.44 g_o}} \left(\frac{T}{1-R} \right) (2g_o \ell + \ln R) \left(\sqrt{1 + \left(\frac{2F(x)e^{x^2}}{\pi^2} \right)^2} + \frac{2F(x)e^{x^2}}{\pi^2} \right)^{-\frac{1}{2}} \quad (5.8-14)$$

where equation (5.8-9) has been used to replace $g_2 = 2\alpha_2$ by g_o .

The gain on the axis of a gas laser is a Gaussian function of frequency of the form $g_o = g'_o e^{-x^2}$. With this substitution equation (5.8-14) may be written as

$$P_o(x) = \frac{8r_o \ell}{s} \sqrt{\frac{\pi \lambda_m g'_o}{1.44(1-R)}} \left(e^{-x^2} + \frac{\ln R}{2g'_o \ell} \right) e^{x^2/2} \left(\sqrt{1 + \left(\frac{2F(x)e^{x^2}}{\pi^{1/2}} \right)^2} + \frac{2F(x)e^{x^2}}{\pi^{1/2}} \right)^{-1/2} \quad (5.8-15)$$

This is the general expression for the frequency dependence of the output power of a laser oscillator (neglecting the Lamb dip). It is convenient to define the normalized power spectrum

$$P_o^*(x) = (e^{-x^2} - b) e^{x^2/2} \left(\sqrt{1 + \left(\frac{2F(x)e^{x^2}}{\pi^{1/2}} \right)^2} + \frac{2F(x)e^{x^2}}{\pi^{1/2}} \right)^{-1/2} \quad (5.8-16)$$

where

$$b = -\frac{\ln R}{2g'_o \ell} \quad (5.8-17)$$

is a threshold parameter.

Equation (5.8-16) is plotted in Figure 5.8 for various values of the parameter b . Evidently when the laser is above threshold, the greatest output occurs at a slightly negative frequency rather than at line center. The reason for this effect is that the spot size of the confined beam is larger at negative frequencies than at line center. Near threshold ($b \rightarrow 1$) this effect diminishes and the greatest output occurs near $x = 0$. Also plotted in Figure 5.8 is the gain spectrum e^{-x^2} .

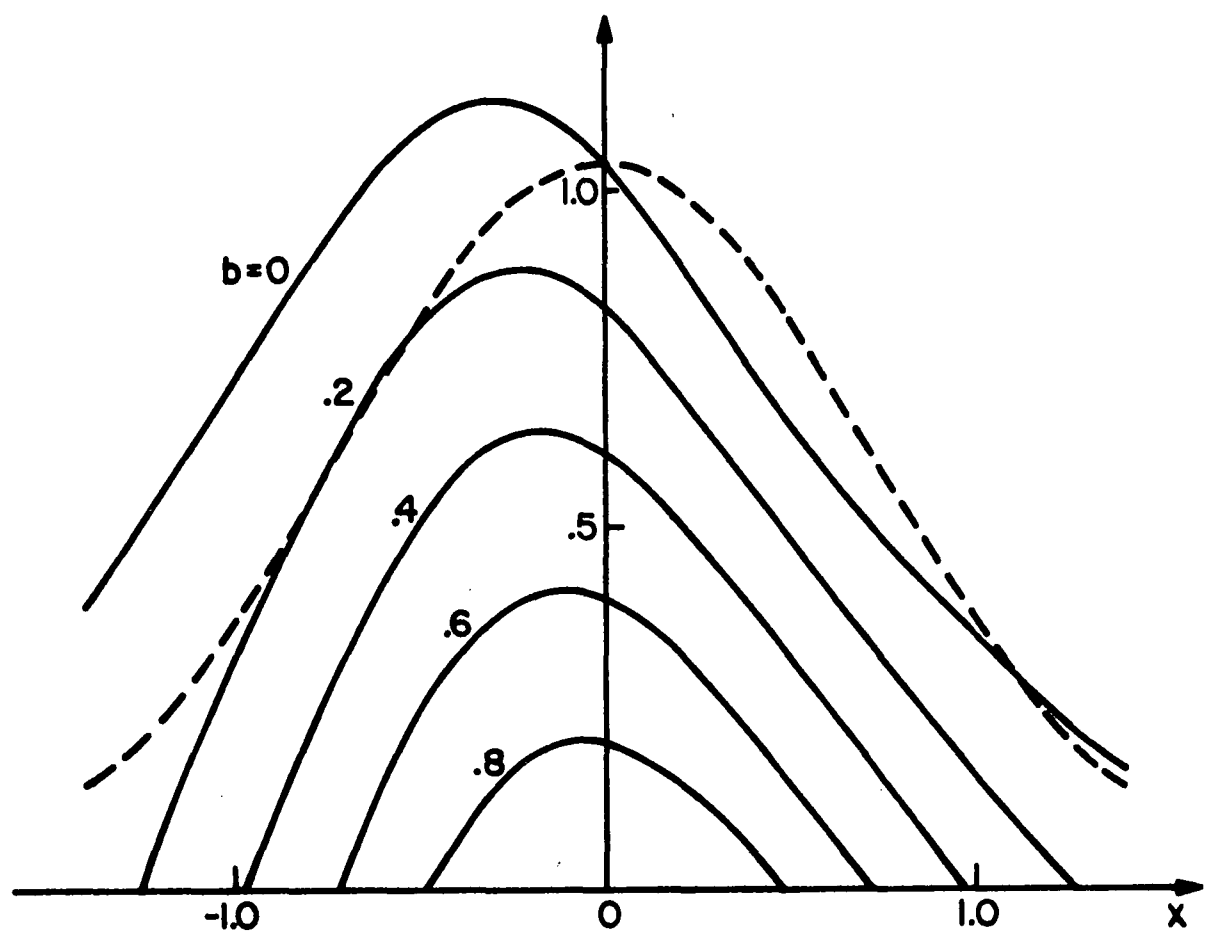


Figure 5.8 Normalized power output as a function of frequency
for various values of the threshold parameter.
Dashed line is the gain spectrum.

The asymmetry of the power spectrum is most conveniently characterized by the location in frequency of the power maximum. In Figure 5.9 is a plot of this frequency as a function of the threshold parameter b . The experimental points in the figure are discussed in Section 5.9. The plots in Figures 5.8 and 5.9. are not quantitatively correct for all values of b . From equation (5.8-13) this homogeneous approximation is only valid in an inhomogeneously broadened medium as long as the product $(1-R)(2g_0^{\frac{1}{2}}\ell + \ln R)$ is small compared to unity. In a high gain laser this is the same as requiring that b be nearly equal to unity. Nevertheless, these results are expected to be qualitatively correct for most values of b .

It is possible to obtain a simpler approximate expression for the output power as a function of frequency which is valid for small values of x . One finds after some algebra that equation (5.8-16) may be expanded to second order in x as

$$P_o^*(x) \approx (1-b) - \left(\frac{1-b}{\pi^{\frac{1}{2}}}\right)x + \left(\frac{1-b}{2\pi} - \frac{1+b}{2}\right)x^2 \quad (5.8-18)$$

The maximum of this spectrum occurs at the frequency

$$x_{\max} = \left(\pi^{-\frac{1}{2}} - \frac{1+b}{1-b}\pi^{\frac{1}{2}}\right)^{-1} \quad (5.8-19)$$

If b is nearly equal to unity, then the maximum is at

$$x_{\max} = -\frac{1-b}{2\pi^{\frac{1}{2}}} \quad (5.8-20)$$

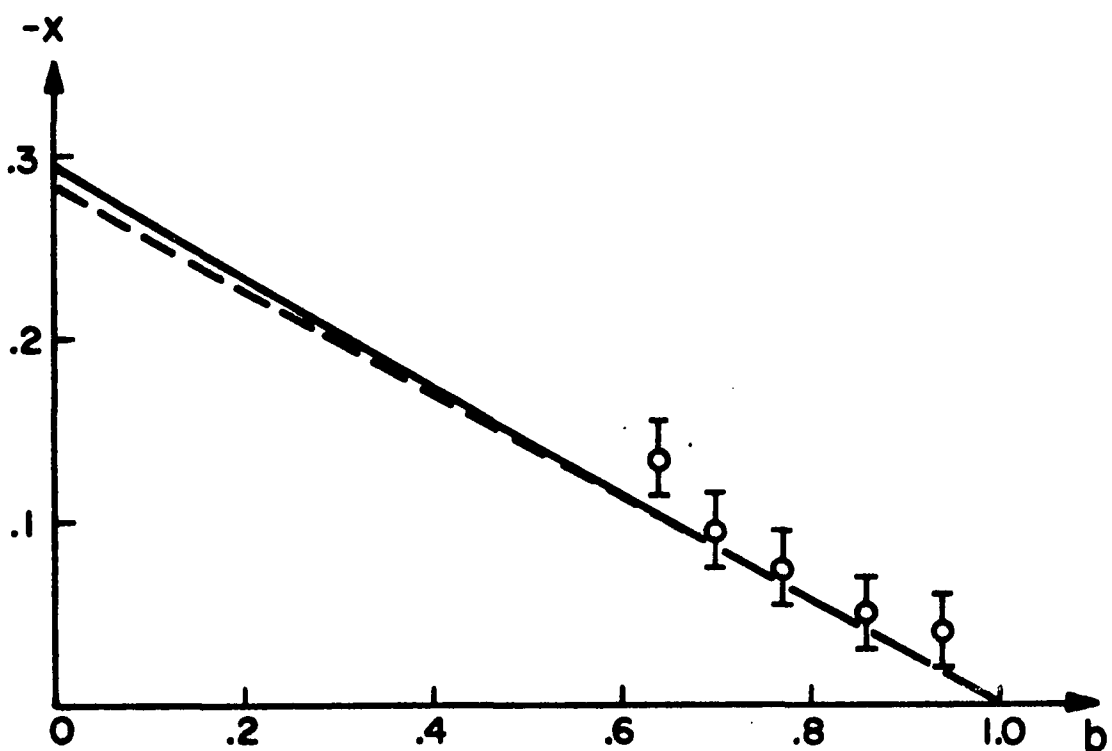


Figure 5.9 Frequency of the power maximum versus the threshold parameter b . The circles are experimental values.

This equation is plotted as a dashed line in Figure 5.9. The good agreement between the two lines in the figure is an indication that for most applications the approximate theory should provide sufficient accuracy.

In this section we have discussed a focusing effect which is due to the dispersion associated with a high gain laser transition. It was shown that the spot size of a waveguided beam is greater for frequencies below gain center than for frequencies greater than gain center. As a consequence of this focusing asymmetry, the power output maximum occurs at a frequency slightly below gain center. This shift in the power maximum may have a serious effect on the interpretation of Lamb dip measurements. Generally asymmetries in the power output of simple gas lasers are attributed to collisions between the atoms (5.11, 5.12). However, it is clear that in moderately high gain lasers dispersion focusing must be considered as well. An experimental verification of the theory is described in the next section.

5.9 Dispersion focusing experiment

In this section we describe an experiment which has been performed using a high gain xenon laser to verify the dispersion focusing theory of the previous section. The apparatus was similar to that used in the experiment of section 5.7, and most of the details are omitted here. Monoisotopic xenon 136 was used so that unnecessary asymmetries in the output would be avoided. The right mirror was highly reflecting and could be translated uniformly by means of a motor drive. The cavity length was 1.29 meters, so the empty cavity mode spacing would be about $\frac{c}{2L} = 116$ MHz.

A typical plot of the power output for decreasing cavity length is shown in Figure 5.10. The laser was operated very near threshold and the peaks represent successive longitudinal modes. These peaks are to be compared to the theoretical curves shown in Figure 5.8. In the experimental plot there is a dip in the output power on the high frequency side of the peak. This is the Lamb dip and it results from the interaction of the left and right traveling beams with atoms which have zero z-component of velocity. Thus the Lamb dip provides a convenient indication of the frequency $x = 0$.

Comparison of the experimental and theoretical plots shows that the power maximum is shifted down in frequency by roughly the amount predicted by the dispersion focusing theory. For a rigorous analysis it is necessary to take into account mode pulling. Suppose that the power shift indicated by a plot such as that in Figure 5.10 is $\Delta\nu_0$. Then in the notation of Chapter IV the actual power shift is $\Delta\nu_0/(1+\beta)$.

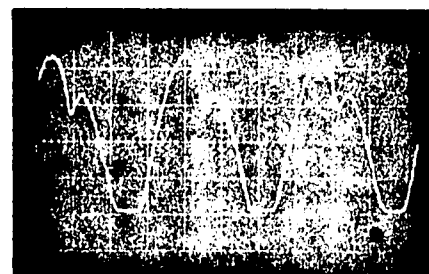


Figure 5.10 Power output for decreasing cavity length with a discharge current of 18 ma.

The values of β for various discharge currents were determined from mode pulling experiments like those described in Chapter IV. This mode pulling cannot be neglected because β is of the order of unity. The gain and the threshold parameter b were also determined as functions of discharge current. Using this information and plots like that shown in Figure 5.10, it was possible to determine the power shift as a function of the threshold parameter.

In Figure 5.9 are experimental values of the power shift versus b . The results are in agreement with the theory to within the estimated experimental errors. The pressure was low enough in these experiments (5 microns) that collision effects are believed to be completely unimportant. For use in section 3.2 we mention also that these experiments indicate that the threshold Lamb dip in xenon has a width of about 6 ± 1 MHz.

Another possible cause of asymmetry in the power measurements is the mass motion of the emitting atoms^(5.13). Particularly in a low pressure D.C. discharge one might expect a drift of the ions toward the cathode compensated by a drift of neutral atoms toward the anode. In a high gain laser the Doppler shifts resulting from this mass motion would result in an asymmetry of the output power spectrum. However, the asymmetry for light emerging from one end of the laser would be expected to be in the opposite direction to the asymmetry for light emerging from the other end. To check this possibility a resonator was constructed having equally transmitting mirrors at the two ends. It was found that the power spectrum was identical at the two ends of the laser indicating that for the conditions of our experiments drift of the atoms is complete-

ly unimportant.

The isotope shifts described in section 3.5 are another potential source of asymmetry. These experiments were conducted using "monoisotopic" xenon 136, but small quantities of the other isotopes were present nevertheless. Lamb dip measurements are fairly sensitive to small amounts of impurity isotopes, so it is conceivable that isotope shifts could affect the power spectrum. To check this possibility the composition of the gas in the laser was measured on a mass spectrometer. The results for the most important isotopes were: 136 - 91%, 134 - 5.5%, 132 - 1.3%, 131 - .8%, 130 - .1%, 129 - 1.1%. Thus the most important impurity is isotope 134. From the discussion in section 3.5 it is expected that the center frequency for isotope 136 would be about 40 MHz greater than the center frequency for isotope 134. Unfortunately this isotope shift leads to a power asymmetry which is similar in form to the asymmetry resulting from dispersion focusing.

The approximate effect of the isotope shift can readily be calculated. We assume that the dominant isotope has the relative abundance a_0 and occurs at the frequency $x = 0$ while the second isotope has the abundance a_2 and occurs at $x = \delta$. Then the net unsaturated gain spectrum has the form

$$g_0 = a_0 e^{-x^2} + a_2 e^{-(x-\delta)^2} \quad (5.9-1)$$

For small values of x and δ the gain is given roughly by the quadratic

$$g \approx (a_0 + a_2) + 2a_2\delta x - (a_0 + a_2)x^2 \quad (5.9-2)$$

This function has its maximum at the frequency

$$x_{\max} = \frac{a_2 \delta}{a_0 + a_2} \quad (5.9-3)$$

In ordinary frequency units this relation becomes

$$\nu_{\max} = \nu_0 + \frac{a_2}{a_0 + a_2} (\nu_2 - \nu_0) \quad (5.9-4)$$

Therefore for the numbers appropriate to our experiments ($a_2 \approx .055$, $\nu_2 - \nu_0 \approx -40$ MHz), we find that the gain maximum is shifted down by about 2.2 MHz due to isotope 134. This shift is small compared to the observed shift, so we conclude that dispersion focusing is the dominant source of asymmetry. Nevertheless, this isotope effect is not entirely negligible and it would probably be worthwhile to perform more extensive measurements of dispersion focusing using a purer sample of xenon 136.

5.10 The cylindrical laser

As a final example of the usefulness of the mode formalism developed in sections 5.2 to 5.6, we derive the optical modes of a new type of laser resonator. The mirror consists of a short cylinder which may be concave slightly toward the center of the resonator to provide confinement of the fields. The radiation propagates primarily in the radial r direction rather than in the axial z direction as in conventional lasers. A sketch of this arrangement is shown in Figure 5.11. Perhaps the most striking feature of such a laser is the high energy density which occurs on the axis of the resonator. The analysis will show that for low order modes essentially all of the power in the resonator flows within a wavelength of that axis.

The wave equation (5.2-4) in cylindrical coordinates appropriate to this problem including a lenslike variation in the z direction becomes

$$\frac{\partial^2 E}{\partial r^2} + \frac{1}{r} \frac{\partial E}{\partial r} + \frac{1}{r^2} \frac{\partial^2 E}{\partial \phi^2} + \frac{\partial^2 E}{\partial z^2} + k_o^2 E - k_o^2 k_2 z^2 E = 0 \quad (5.10-1)$$

The ϕ dependence can be separated out by means of the substitution

$$E = F(r, z) \Phi(\phi) \quad (5.10-2)$$

with the results

$$\frac{d^2 \Phi}{d\phi^2} + m^2 \Phi = 0 \quad (5.10-3)$$

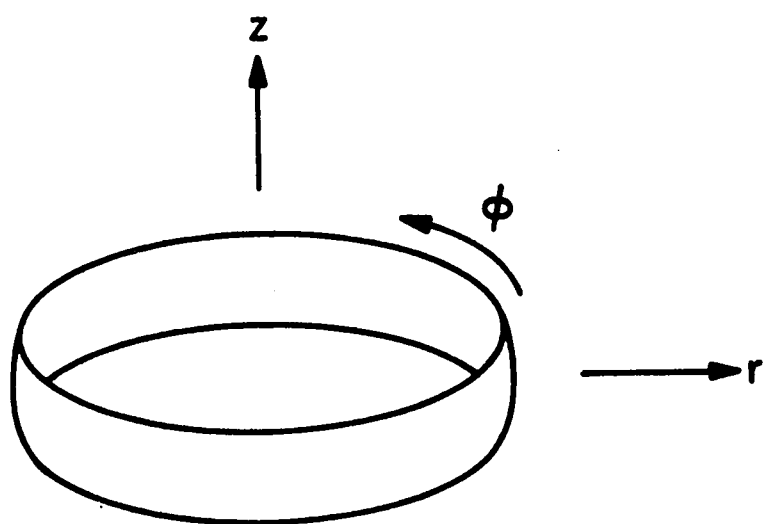


Figure 5.11 Convex cylindrical laser cavity.

$$\frac{\partial^2 F}{\partial r^2} + \frac{1}{r} \frac{\partial F}{\partial r} - \frac{m^2 F}{r^2} + \frac{\partial^2 F}{\partial z^2} + k_o^2 F - k_o k_2 z^2 F = 0 \quad (5.10-4)$$

where m is a separation constant. The solutions of equation (5.10-3) are given except for multiplicative constants by

$$\Phi = \begin{cases} \sin \\ \cos \end{cases} m\phi \quad (5.10-5)$$

The solutions to equation (5.10-4) are most easily obtained by solving in two regions and matching the solutions where these regions overlap. The first region is from the z axis out to a distance comparable to the z "thickness" of the beam. In this region diffraction is unimportant and the z variation can be ignored. Then equation (5.10-4) can be written

$$\frac{\partial^2 F}{2(k_o r)^2} + \frac{1}{k_o r} \frac{\partial F}{\partial (k_o r)} + \left(1 - \frac{m^2}{(k_o r)^2}\right) F = 0 \quad (5.10-6)$$

where we assume for simplicity that k_o is independent of r . But this is Bessel's equation, so the solution for outgoing waves can be expressed in terms of Hankel functions of the second kind

$$F = f(z) H_m^{(2)}(k_o r) \quad (5.10-7)$$

where $f(z)$ is an as yet undetermined slow function of z . This result is analogous to the beam modes described in section 5.2. The asymptotic form of this solution which will be useful later is

$$F \xrightarrow[r \rightarrow \infty]{} f(z) \sqrt{\frac{2}{\pi k_o r}} e^{-i(k_o r - \frac{m\pi}{2} - \frac{\pi}{4})} \quad (5.10-8)$$

To find the solution in the outer region, one may try the substitution

$$F = \psi e^{-ik_o r} \quad (5.10-9)$$

in equation (5.10-4) with the result

$$\frac{\partial^2 \psi}{\partial r^2} + \left(\frac{1}{r} - 2ik_o\right) \frac{\partial \psi}{\partial r} - \frac{ik_o \psi}{r} - \frac{m^2 \psi}{r^2} + \frac{\partial^2 \psi}{\partial z^2} - k_o k_2 z^2 \psi = 0 \quad (5.10-10)$$

If ψ is assumed to vary slowly with r ($\frac{\partial^2 \psi}{\partial r^2} \ll 2k_o \frac{\partial \psi}{\partial r}$) this equation may be written

$$-2ik_o \frac{\partial \psi}{\partial r} - \frac{ik_o \psi}{r} + \frac{\partial^2 \psi}{\partial z^2} - k_o k_2 z^2 \psi = 0 \quad (5.10-11)$$

at distances much greater than m^2 wavelengths from the z axis.

The substitution

$$\psi = S(r, z) e^{-\frac{iQ(r)z^2}{2}} \quad (5.10-12)$$

leads to

$$\frac{\partial^2 S}{\partial z^2} - 2iQz \frac{\partial S}{\partial z} - iQS - Q^2 z^2 S - 2ik_o \frac{\partial S}{\partial r} - k_o z^2 \frac{dQ}{dr} S - \frac{ik_o S}{r} - k_o k_2 S z^2 = 0 \quad (5.10-13)$$

Setting the coefficients of z^2 equal to zero yields the two equations

$$Q^2 + k_{odr} \frac{dQ}{dr} + k_o k_2 = 0 \quad (5.10-14)$$

$$\frac{\partial^2 S}{\partial z^2} - 2iQz \frac{\partial S}{\partial z} - iQS - 2ik_o \frac{\partial S}{\partial r} - i \frac{k_o}{r} S = 0 \quad (5.10-15)$$

Equation (5.10-14) is a beam parameter equation identical to equation (5.2-9), and the analysis of section 5.4 applies. Here, of course, any lenses and mirrors must wrap around the z axis.

The change of variables

$$\xi = \sqrt{iQ}z \quad (5.10-16)$$

simplifies equation (5.10-15) to

$$\frac{\partial^2 S}{\partial \xi^2} - 2\xi \frac{\partial S}{\partial \xi} - S - \frac{2k_o}{Q} \frac{\partial S}{\partial r} - \frac{k_o S}{Qr} = 0 \quad (5.10-17)$$

The substitution

$$S = T(\xi)U(r) \quad (5.10-18)$$

leads to the separation

$$\frac{d^2 T}{d\xi^2} - 2\xi \frac{dT}{d\xi} + 2nT = 0 \quad (5.10-19)$$

$$\frac{dU}{dr} + \frac{U}{2r} + \frac{(n + \frac{1}{2})QU}{k_o} = 0 \quad (5.10-20)$$

The acceptable solutions of equation (5.10-19) are the Hermite polynomials

$$T = H_n (\sqrt{-Q_1} z) \quad (5.10-21)$$

The substitution

$$U = v e^{-\frac{1}{2}P} \quad (5.10-22)$$

transforms equation (5.10-20) to the form

$$\frac{dv}{dr} + \frac{v}{2r} - iv \frac{dp}{dr} + \frac{(n + \frac{1}{2})Qv}{k_o} = 0 \quad (5.10-23)$$

which can be arbitrarily separated into

$$\frac{dp}{dr} = -i \frac{(n + \frac{1}{2})Q}{k_o} \quad (5.10-24)$$

$$\frac{dv}{dr} + \frac{v}{2r} = 0 \quad (5.10-25)$$

Equation (5.10-24) is a phase parameter equation of the form of equation (5.2-25). The integration can be performed when $Q(r)$ is known. Equation (5.10-25) has the solution

$$v \propto r^{-\frac{1}{2}} \quad (5.10-26)$$

Combining equations (5.10-9), (5.10-12), (5.10-18), (5.10-21), (5.10-22), and (5.10-26) yields the solution in the outer region in the form

$$F = \frac{1}{\sqrt{r}} e^{-ik_0 r} H_n(\sqrt{-Q_1} z) e^{-\frac{iQz^2}{2}} e^{-ip} \quad (5.10-27)$$

Comparison of equations (5.10-2), (5.10-5), (5.10-8), and (5.10-27) gives the solution valid everywhere

$$E(r, z, \phi) \approx \begin{cases} \sin \\ \cos \end{cases}(m\phi) H_m^{(2)}(k_0 r) H_n(\sqrt{-Q_1} z) e^{-\frac{iQz^2}{2}} e^{-ip} \quad (5.10-28)$$

with multiplicative constants omitted. In terms of the spot size w and phase front curvature R of equation (5.3-6) the beam parameter may be written

$$\frac{Q}{k_0} = \frac{1}{R} - i \frac{m}{\pi w^2} \quad (5.10-29)$$

and the field is

$$E(r, z, \phi) \approx \begin{cases} \sin \\ \cos \end{cases}(m\phi) H_m^{(2)}(k_0 r) H_n(\sqrt{2} \frac{z}{w}) e^{-\frac{k_0 z^2}{2R}} e^{-\frac{z^2}{w^2}} e^{-ip} \quad (5.10-30)$$

If m is sufficiently large that the inequality $k w_o >> m^2$ is not satisfied where w_o is the spot size on the z axis, then the two regions of solution don't overlap and equation (5.10-29) is not necessarily valid near the origin. Fields in the region $r >> m^2/k_0$ are always given by equation (5.10-29). Similarly the solutions

for incoming waves are given by

$$E(r, z, \phi) \approx \begin{cases} \sin \\ \cos \end{cases} (m\phi) H_m^{(1)}(k_0 r) H_n(\sqrt{-Q_1} z) e^{-\frac{i Q z^2}{2}} e^{-i P} \quad (5.10-31)$$

The parameters Q and P appearing in equation (5.10-28) are in general different from those in equation (5.10-30) in a given resonator if gain focusing is important.

Construction of such a cylindrical laser should not be unreasonably difficult. The simplest gas laser construction would probably involve a high gain medium pumped transversely to the optical plane by a D.C. discharge. Solid and liquid lasers can also be visualized which would be pumped from above and below the optical plane by means of flashlamps. Even semiconductor lasers of this style should be possible.

The most striking feature of the cylindrical laser is that all of the power of the fundamental mode flows within approximately one wavelength of the axis of the cavity. This fact follows from the well known asymptotic traveling-wave behavior of the Hankel functions in the outer region. Consequently, extremely high energy densities may be obtainable on the axis of the resonator without any additional focusing elements. These high energy standing waves might be useful for studying various nonlinear optical effects. Obviously, for this application a hole along the axis of the laser medium would be necessary. Moreover, the axis could be somewhat isolated from the laser itself if the resonator consisted of two concentric cylindrical mirrors. The output through the outside

mirror for the fundamental mode would consist of a plane of light.

In this section the modes of a new cylindrical type of laser resonator have been obtained from a solution of the wave equation. As in conventional lasers, the basic propagation characteristics of these modes are governed by beam parameter equations and the matrix methods of the previous sections.

5.11 Conclusion

The transverse optical beam modes appropriate to laser problems have been obtained as solutions of the wave equation. The analysis was sufficiently general to include the first order corrections for lenslike variations of gain and refractive index which commonly occur in practice. Matrix methods for studying the propagation of these modes through sequences of optical elements have been developed. In particular, the transverse modes of laser resonators have been derived for resonators containing a lenslike medium. Emphasis was placed on the analysis of the modes of a resonator containing a medium with a strong gain profile, since such an arrangement had not previously been studied. Experiments were performed which verified the theoretical conclusions regarding gain and dispersion focusing. A cylindrical laser geometry was also described.

Bibliography

- 5.1 L. Caspelson and A. Yariv, Applied Physics Letters 12, No. 10, page 355, 15 May 1968.
- 5.2 L. Caspelson and A. Yariv, Journal of Quantum Electronics QE-4, page 674, October 1968.
- 5.3 H. Kogelnik, Applied Optics 4, No. 12, page 1562, December 1965.
- 5.4 Handbook of Mathematical Functions, edited by M. Abramowitz and I. A. Stegun (U. S. Department of Commerce, National Bureau of Standards, Washington, D. C., 1964), Applied Mathematics Series 55, page 781, equation (22.6.15).
- 5.5 See for example B. Rossi, Optics, Chapter 2, Addison-Wesley, Reading, Massachusetts, 1957.
- 5.6 A. Yariv, Introduction to Optical Electronics, Holt, Rinehart and Winston, Inc., New York, equation (3.3-6), 1971.
- 5.7 L. A. Schlie and J. T. Verdeyen, Journal of Quantum Electronics, QE-5, No. 1, page 21, January 1969.
- 5.8 B. W. McCaul and A. L. Schawlow, Journal of Quantum Electronics QE-6, No. 3, page 178, March 1970, and private communication.
- 5.9 D. R. Armstrong, Journal of Quantum Electronics QE-4, No. 11, page 968, November 1968.
- 5.10 W. R. Bennett, Applied Optics Supplement 2, Chemical Lasers, page 3, 1965.
- 5.11 A. Szöke and A. Javan, Physical Review 145, No. 1, page 137, 6 May, 1966.
- 5.12 B. L. Gyorffy, M. Borenstein, and W. E. Lamb, Jr., Physical Review 169, No. 2, page 340, 10 May 1968.
- 5.13 A. D. White, Applied Physics Letters 10, No. 1, page 24, 1 Jan. 1967.

VI. Relaxation Oscillations

6.1 Introduction

Relaxation phenomena have been observed in essentially all types of lasers. Such effects are characterized by a pulsing of the laser power output on a time scale long compared to the cavity loop time. We have observed regular undamped oscillations in a simple atomic xenon gas laser system. The high gain xenon laser at 3.51 microns exhibits these pulsations at frequencies between 10^6 and 10^7 Hertz.

A rate equation model provides good agreement with most of the observed features of the oscillations. Conventional theories usually assume that all of the atoms are identical^(6.1,6.2). The validity of this assumption in gas lasers is not obvious, because the Doppler line width is often much greater than the homogeneous line width. In particular, in xenon the Doppler line width exceeds the natural line width by a factor of about thirty. Thus, the interaction between the atoms and the field is much weaker for atoms whose center frequency is far from the optical frequency than for those which are close.

The rate equations used here include the effects of inhomogeneous broadening. The consequences of the rate equation model are discussed in the following sections. Experiments have been conducted in both the time domain and the frequency domain, and satisfactory agreement with the theory has been obtained. The effects of coherence in homogeneously broadened lasers are considered in Section 6.6.

6.2 The inhomogeneous frequency equation

The purpose of this section is to investigate the effects of inhomogeneous broadening on relaxation phenomena in laser oscillators. Inhomogeneous broadening is common to many lasers, several of which are known to exhibit relaxation oscillations. In particular, we obtain an algebraic equation governing the complex frequency of small amplitude relaxation oscillations in inhomogeneously broadened lasers.

The starting point for this derivation is the pair of rate equations

$$\frac{dn(v)}{dt} = P(v) - qB(v, v_l) n(v) - \frac{n(v)}{\tau} \quad (6.2-1)$$

$$\frac{dq}{dt} = q \int_0^{\infty} B(v, v_l) n(v) dv - \frac{q}{t_c} \quad (6.2-2)$$

These equations are essentially the same as equations (2.3-8) and (2.3-9) except that the photon density q is used instead of the intensity I , and the frequency dependent Einstein B coefficient is slightly redefined. The pumping rate is $P(v)$; $n(v)$ is the population inversion density in the frequency range between v and $v + dv$; v_l is the laser frequency; τ is the inversion lifetime; and t_c is the average photon cavity lifetime. It is assumed that spontaneous emission does not contribute significantly to the photon density and that coupling to other atomic energy levels is unimportant. If the lifetime of the lower level of the laser transition were not negligible compared to the lifetime of the upper level, it would be necessary to write an additional rate equation governing the population density of the lower level. It is also assumed that spatial variations of the

electromagnetic fields, which are substantial in a high gain laser, do not affect the transient behavior of the laser. It has been shown by Globus et al^(6.3) and by Polloni and Svelto^(6.4) that the primary effect of nonuniform fields is a slight increase in damping.

Finally, equations (6.2-1) and (6.2-2) also neglect coherence effects. The observed pulsation period is sometimes shorter than the transverse relaxation time, which is equal to twice the lifetime τ in a low pressure gas system, so that coherence could be important. The rate equations may be generalized to include a finite coherence time as shown in Section 2.2, but solutions are more difficult to obtain. Near threshold the coherent rate equations may be shown to reduce to equations (6.2-1) and (6.2-2), and other coherent solutions which are derived in Section 6.6 do not differ qualitatively from the solutions of these equations. The incoherent equations provide satisfactory agreement with the experimental data obtained so far, and for simplicity we neglect coherence here.

The behavior of the solutions in the vicinity of the equilibrium point is of greatest interest, so equations (6.2-1) and (6.2-2) are linearized by the substitutions $q(t) = q_0 + q'(t)$, $n(v,t) = n_0(v) + n'(v,t)$. The primed quantities are regarded as small perturbations. The first order results are

$$\frac{dn'}{dt} = - (Bq_0 + \frac{1}{\tau})n' - Bn_0 q' + (P - Bn_0 q_0 - \frac{n_0}{\tau}) \quad (6.2-3)$$

$$\frac{dq'}{dt} = q_0 \int Bn' dv + (\int Bn_0 dv - \frac{1}{t_c}) q' + (q_0 \int Bn_0 dv - \frac{q_0}{t_c}) \quad (6.2-4)$$

This pair of linear first order equations is expected to have two

independent solutions. The equilibrium point is described by the steady state solutions

$$P = B n_o q_o + \frac{n_o}{\tau} \quad (6.2-5)$$

$$\frac{1}{t_c} = \int B n_o \, dv \quad (6.2-6)$$

Equations (6.2-5) and (6.2-6) may be combined to

$$\frac{1}{t_c} = \int \frac{P \, dv}{q_o + \frac{1}{B \tau}} \quad (6.2-7)$$

If the pumping spectrum is a Gaussian given by equation (2.4-2)

$$P(v) = P_o e^{-\left[\frac{2(v-v_o)}{\Delta v_D}\right]^2 \ln 2} \quad (6.2-8)$$

and the homogeneous line shape is a Lorentzian given by equation (2.3-4)

$$B(v, v_\ell) = B_o \frac{\frac{2}{\pi \Delta v_h}}{1 + \left[\frac{2(v-v_\ell)}{\Delta v_h}\right]^2} \quad (6.2-9)$$

then equation (6.2-7) may be rewritten as

$$\frac{1}{t_c} = P_o \int_0^\infty \frac{e^{-\left[\frac{2(v-v_o)}{\Delta v_D}\right]^2 \ln 2}}{1 + \left[\frac{2(v-v_\ell)}{\Delta v_h}\right]^2} dv + \frac{q_o + \frac{2B_o \tau}{\pi \Delta v_h}}{} \quad (6.2-10)$$

If the radiation is at line center ($v_o = v_\ell$) , this equation may be written in terms of the dimensionless frequency $z = \frac{2(v-v_o)}{\Delta v_h}$ as

$$\frac{1}{t_c} = \frac{P_o B_o \tau}{\pi} \int_{-\infty}^{\infty} \frac{-\varepsilon^2 z^2}{\frac{2q_o B_o \tau}{\pi \Delta v_h} + 1 + z^2} dz \quad (6.2-11)$$

where ε is the natural damping ratio $\varepsilon = \frac{\Delta v_h}{\Delta v_D} (\ln 2)^{1/2}$

The result of the integration is (6.5)

$$\frac{1}{t_c} = \frac{P_o B_o \tau}{\left(1 + \frac{2q_o B_o \tau}{\pi \Delta v_h}\right)^{1/2}} e^{(1 + \frac{2q_o B_o \tau}{\pi \Delta v_h})\varepsilon^2} \left\{ 1 - \operatorname{erf} \left[\left(1 + \frac{2q_o B_o \tau}{\pi \Delta v_h}\right)^{1/2} \varepsilon \right] \right\} \quad (6.2-12)$$

If the saturated homogeneous line width is much less than the Doppler line width $\left(1 + \frac{2q_o B_o \tau}{\pi \Delta v_h}\right)^{1/2} \varepsilon \ll 1$, then equation (6.2-12) simplifies to

$$\frac{1}{t_c} = \frac{P_o B_o \tau}{\left(1 + \frac{2q_o B_o \tau}{\pi \Delta v_h}\right)^{1/2}} \quad (6.2-13)$$

This result still applies for a laser field at the frequency $v_l \neq v_o$ if P_o is replaced by $P_l = P_o e^{-\varepsilon^2(v_l-v_o)^2}$. Solving equation (6.2-13) for q_o yields

$$q_o = \frac{\pi \Delta v_h}{2B_o \tau} [(P_l B_o \tau t_c)^2 - 1] = \frac{\pi \Delta v_h P_l t_c}{2a} (a^2 - 1) \quad (6.2-14)$$

where we define the dimensionless parameter $a = P_l B_o \tau t_c$. The threshold condition is clearly $a = 1$. Equation (6.2-14) will be used later in the derivation.

Using equations (6.2-5) and (6.2-6), equations (6.2-3) and (6.2-4) may be rewritten as

$$\frac{dn'}{dt} = -(Bq_0 + \frac{1}{\tau})n' - \frac{PBq'}{Bq_0 + \frac{1}{\tau}} \quad (6.2-15)$$

$$\frac{dq'}{dt} = q_0 \int Bn' dv \quad (6.2-16)$$

The solution of these equations is complicated by the presence of the variable n' under the frequency integral. Equations (6.2-15) and (6.2-16) may be combined into the second order equation

$$\frac{d^2n'}{dt^2} + (Bq_0 + \frac{1}{\tau}) \frac{dn'}{dt} = - \frac{PBq_0}{Bq_0 + \frac{1}{\tau}} \int Bn' dv \quad (6.2-17)$$

Substituting an exponential solution of the form $n'(v) = n''(v)e^{st}$ and solving for $n''(v)$ leads to

$$-n'' = \frac{PBq_0 \int Bn'' dv}{s(Bq_0 + \frac{1}{\tau})(s + Bq_0 + \frac{1}{\tau})} \quad (6.2-18)$$

Multiplying by $B(v)$, integrating over frequency, and canceling the factor $\int Bn'' dv$ gives

$$-1 = \int_0^\infty \frac{Pdv}{q_0 s [1 + \frac{1}{Bq_0} (\frac{1}{\tau})] [1 + \frac{1}{Bq_0} (s + \frac{1}{\tau})]} \quad (6.2-19)$$

This integration can be performed and the results expressed in terms of the error function of complex argument. The general solutions are complicated and probably not very useful, so we make the approximation that the line broadening is strongly inhomogeneous and replace $P(v)$ by P_ℓ , the value of the pumping coefficient near the laser line. Then using equation (6.2-9), equation (6.2-19) becomes

$$-1 = \frac{\Delta v_h P_\ell}{2q_o s} \int_{-\infty}^{\infty} \frac{dz}{\left[1 + \frac{1+z^2}{\frac{2B_o q_o \tau}{\pi \Delta v_h}} \right] \left[1 + \frac{1+z^2}{\frac{2B_o q_o \tau}{\pi \Delta v_h} \frac{1}{s\tau+1}} \right]} \quad (6.2-20)$$

where the dimensionless frequency $z = \frac{2(v-v_\ell)}{\Delta v_h}$ has been used. Using the definition $a = P_\ell B_o \tau t_c$ introduced in equation (6.2-14) and the new definition

$$b = \sqrt{1 + \frac{a^2 - 1}{s\tau + 1}}$$

equation (6.2-20) becomes

$$-1 = \frac{\Delta v_h P_\ell}{2q_o s} (a^2 - 1)(b^2 - 1) \int_{-\infty}^{\infty} \frac{dz}{(a^2 + z^2)(b^2 + z^2)} \quad (6.2-21)$$

Expanding the integrand in partial fractions leads to

$$-1 = \frac{\Delta v_h P_\ell}{2q_o s} (a^2 - 1)(b^2 - 1) \left[\frac{1}{b^2 - a^2} \int_{-\infty}^{\infty} \frac{dz}{a^2 + z^2} + \frac{1}{a^2 - b^2} \int_{-\infty}^{\infty} \frac{dz}{b^2 + z^2} \right] \quad (6.2-22)$$

Performing the integrations gives

$$\begin{aligned} -1 &= \frac{\Delta v_h P_\ell}{2q_o s} (a^2 - 1)(b^2 - 1) \left[\frac{\pi/a}{b^2 - a^2} + \frac{\pi/b}{a^2 - b^2} \right] \\ &= \frac{\pi \Delta v_h P_\ell}{2q_o s} \frac{(a^2 - 1)(b^2 - 1)}{ab(a + b)} \end{aligned} \quad (6.2-23)$$

Using equation (6.2-14) to eliminate q_o yields

$$-1 = \frac{1}{st_c} \left(\frac{b^2 - 1}{b(a+b)} \right)$$

or

$$b^2 - 1 + st_c b^2 = -st_c ab \quad (6.2-24)$$

With the definition $b = \sqrt{1 + \frac{a^2 - 1}{st + 1}}$ equation (6.2-24)

becomes

$$\frac{a^2 - 1}{st + 1} + st_c(1 + \frac{a^2 - 1}{st + 1}) = -st_c a \sqrt{1 + \frac{a^2 - 1}{st + 1}} \quad (6.2-25)$$

This then is the equation determining the natural frequencies of an inhomogeneously broadened laser oscillator. To solve it we square both sides and simplify. The general result finally, is the quartic equation

$$s^4 t_c^2 \tau^2 + s^3 t_c^2 \tau a^2 - 2s^2 t_c \tau - 2st_c a^2 - (a^2 - 1) = 0 \quad (6.2-26)$$

Two of the roots of this equation are nonphysical and result from the squaring operation. It is useful to reduce the number of parameters appearing in the frequency equation by introducing the dimensionless frequency $x = st$ and the ratio $c = \tau/t_c$. Then equation (6.2-26) becomes

$$x^4 + a^2 x^3 - 2cx^2 - 2a^2 cx - (a^2 - 1)c^2 = 0 \quad (6.2-27)$$

Equation (6.2-27) is the principal result of this section. It is valid for small amplitude fluctuations as long as the hole burned by the radiation field in the inhomogeneous spectrum is narrow compared to the overall line width. From equations (6.2-11) and (6.2-14) the hole width is

$$\Delta v_{\text{hole}} = \Delta v_h \left(1 + \frac{2q_o B_o \tau}{\pi \Delta v_h} \right)^{1/2} = a \Delta v_h \quad (6.2-28)$$

Then the condition that the frequency equation be valid for a Doppler broadened line is simply

$$a \ll \frac{\Delta\nu_D}{\Delta\nu_h} \quad (6.2-29)$$

In the xenon laser at 3.51 microns the ratio of the Doppler line width to the homogeneous line width is of the order of 30, and equation (6.2-29) is usually satisfied.

6.3 Solutions of the frequency equation

In this section we consider various solutions of the frequency equation. In principle, rigorous analytic solutions are obtainable for such a quartic equation. However, those solutions are generally sufficiently complicated as to be useless. Instead we present some computer solutions and some approximate analytical results which are adequate for most applications.

Equation (6.2-27) cannot be factored simply except in certain limits. For small values of a the cubic term may be neglected. In particular, for $x \ll 2c/a^2$ the cubic term is small compared to the quadratic term and for $x \gg a^2$ the cubic term is small compared to the quartic term. Combining these conditions, we find that for $a^4 \ll 2c$ the cubic term is unimportant for all x . The remaining equation may be factored approximately into

$$[x^2 - ax - c(a+1)] [x^2 + ax + c(a-1)] \approx 0 \quad (6.3-1)$$

where we also use the less stringent condition $a^2 \ll 2c$.

The left hand factor of equation (6.3-1) yields two real roots which are spurious. Thus for small a the natural frequencies are determined simply by the equation

$$x^2 + ax + c(a-1) = 0 \quad a \ll 4\sqrt{2c} \quad (6.3-2)$$

or in terms of the lifetimes

$$s^2 + \frac{as}{\tau} + \frac{1}{\tau t_c} (a-1) = 0 \quad a \ll 4\sqrt{\frac{2\tau}{t_c}} \quad (6.3-3)$$

But equation (6.3-3) is the same result that one would obtain for relaxation oscillations in a laser having purely homogeneous line broadening. To see this, one may solve equations (6.2-1) and (6.2-2) in the homogeneous limit. If $P(v)$ and $n(v)$ are strongly peaked at the frequency v_0 , then the rate equations may be written as

$$\frac{dN}{dt} = P - qBN - \frac{N}{\tau} \quad (6.3-4)$$

$$\frac{dq}{dt} = qBN - \frac{q}{t_c} \quad (6.3-5)$$

where $N = \int_0^\infty n(v) dv$, $P = \int_0^\infty P(v) dv$, and $B = B(v_0, v_\ell)$. The substitutions $N = N_0 + N'(t)$ and $q = q_0 + q'(t)$ lead to the linearization

$$\frac{dN'}{dt} = -(q_0 B + \frac{1}{\tau})N' - BN_0 q' + (P - q_0 BN_0 - \frac{N_0}{\tau}) \quad (6.3-6)$$

$$\frac{dq'}{dt} = q_0 BN' + (BN_0 - \frac{1}{t_c})q' + (q_0 BN_0 - \frac{q_0}{t_c}) \quad (6.3-7)$$

The steady state solutions of equations (6.3-6) and (6.3-7) are governed by the equations

$$P = q_0 BN_0 + \frac{N_0}{\tau} \quad (6.3-8)$$

$$BN_0 = \frac{1}{t_c} \quad (6.3-9)$$

and the natural frequencies are determined by the eigenvalue equation

$$\begin{vmatrix} -(q_0 B + \frac{1}{\tau}) - s & -BN_0 \\ q_0 B & (BN_0 - \frac{1}{t_c}) - s \end{vmatrix} = 0 \quad (6.3-10)$$

Using equations (6.3-8) and (6.3-9), equation (6.3-10) may be written as

$$s^2 + BP t_c s + \left(BP - \frac{1}{\tau t_c}\right) = 0 \quad (6.3-11)$$

With the definition $a = PB\tau t_c$ equation (6.3-11) becomes identical to equation (6.3-3). Thus, we will henceforth refer to equation (6.3-2) as the homogeneous limit of equation (6.2-27). This result is reasonable since for weak saturation the frequency region of the spectral line affected by the electromagnetic field is essentially $\Delta\nu_h$, the homogeneous line width, independent of the intensity; and the line is effectively homogeneous. The validity of this approximation will be clear from a consideration of Figure 6.1 later in this section.

The homogeneous frequency equation (6.3-2) is a simple quadratic and the solutions are

$$x = -\frac{a}{2} \pm i\sqrt{c(a-1) - \left(\frac{a}{2}\right)^2} \quad (6.3-12)$$

or

$$s = -\frac{a}{2\tau} \pm i\sqrt{\frac{a-1}{\tau t_c} - \left(\frac{a}{2\tau}\right)^2} \quad (6.3-13)$$

It is helpful to express the threshold parameter a in terms of the more familiar unsaturated gain coefficient g . From equation (6.2-2) as written for a steady state lossless amplifier rather than an oscillator, one finds

$$\frac{1}{I} \frac{dI}{dz} = g = \int \frac{nBdv}{c_m} \quad (6.3-14)$$

where I is the intensity and c_m is the speed of light in the amplifying medium. Then if saturation is neglected in equation (6.2-1) one finds $n = Pt$. Therefore, equation (6.3-14) becomes

$$g = \frac{\tau}{c_m} \int PB dv \quad (6.3-15)$$

If the Doppler line width is much greater than the homogeneous line width, equation (6.3-15) with equation (6.2-9) becomes simply

$$g = \frac{\tau P_\lambda B_0}{c_m} = \frac{a}{c_m t_c} = ag_{th} \quad (6.3-16)$$

where g_{th} is the threshold value of the gain. Thus the parameter a may be replaced by g/g_{th} or by $P_\lambda/P_{\lambda th}$ in the results which have been derived.

Using equation (6.3-16), equation (6.3-13) may be written

$$s = -\frac{gc_m t_c}{2\tau} \pm i\sqrt{\frac{gc_m}{\tau} - \frac{1}{\tau t_c} - \left(\frac{gc_m t_c}{2\tau}\right)^2} \quad (6.3-17)$$

In our experiment the last term under the radical is negligible. Thus, for small perturbations the fluctuations take the form of damped sinusoidal oscillations having a period

$$T_o = \frac{2\pi}{\sqrt{\frac{gc_m}{\tau} - \frac{1}{\tau t_c}}} \quad (6.3-18)$$

and a damping time

$$T_d = \frac{2\tau}{gc_m t_c} \quad (6.3-19)$$

One may obtain an estimate of the greatest number N_{max} of pulses which should be observable in a single time constant of the damped pulse train by maximizing the ratio $N = T_d/T_o$ with respect to the gain g . The maximum number occurs when the gain is twice its threshold value or $g_{opt} = 2/c_m t_c$. The result is

$$N_{\max} = \frac{1}{2\pi} \sqrt{\frac{\tau}{t_c}} \quad (6.3-20)$$

In our experiment $\tau \sim 1$ microsecond and $t_c \sim 1$ nanosecond so that $N_{\max} \sim 5$. This suggests that reasonably weak damping should be possible in a xenon laser.

If the laser system includes a broad band noise source, the dominant factor in the laser intensity fluctuation spectrum corresponding to equations (6.3-18) and (6.3-19) is^(6.6)

$$\Delta P(\omega) \sim \frac{1}{\left(\frac{gc_m}{\tau} - \frac{1}{\tau t_c} - \omega^2 \right)^2 + \omega^2 \left(\frac{gc_m t_c}{\tau} \right)^2} \quad (6.3-21)$$

This result is obtained from a Fourier transform solution of the rate equations. For weak damping the center frequency of the fluctuation spectrum is clearly

$$\omega_c = \sqrt{\frac{gc_m}{\tau} - \frac{1}{\tau t_c}} \quad (6.3-22)$$

and the width at half-height of the fluctuation spectrum about this center frequency is

$$\Delta\omega = \frac{gc_m t_c}{\tau} \quad (6.3-23)$$

So far only the near-threshold homogeneous limit of equation (6.2-27) has been considered. It turns out that the homogeneous approximation is valid in our experiments except at the highest powers. Far above threshold, however, hole burning becomes important, and the hole width is intensity dependent. Then if the intensity is oscillating the properties of the oscillations should be significantly different

from the homogeneous results. To investigate this situation we consider the opposite limit of large a . If the condition $a^2 \gg c/2$ is satisfied (for $c \gg 1$), then equation (6.2-27) can be factored approximately as

$$(x + a^2)(x^3 - 2cx - c^2) \approx 0 \quad (6.3-24)$$

The real root is spurious, so that in this limit the natural frequencies are governed by the cubic equation

$$x^3 - 2cx - c^2 = 0, \quad a^2 \gg c/2 \quad (6.3-25)$$

The solution of cubic equations is well known and the relevant results are

$$x = -\left(\frac{c^{2/3}}{2} + \frac{c^{1/2}}{3}\right) \pm i \frac{\sqrt{3}}{2} \left(c^{2/3} - \frac{2}{3} c^{1/3}\right), \quad a^2 \gg \frac{c}{2} \gg 1 \quad (6.3-26)$$

Thus, in this inhomogeneous limit the relaxation oscillations exhibit a strongly damped behavior which is independent of the threshold parameter a and hence independent of the pumping. This is in sharp contrast to the strong a dependence of the homogeneous limit given by equation (6.3-12).

In Figure 6.1 is a plot of the real and imaginary parts of x found from equation (6.2-27) for $c = 1080$, which is a reasonable value for our experiments with a xenon laser with no attenuators. The behavior in the homogeneous and inhomogeneous limits is apparent in the figure, where the limiting forms are determined from equations (6.3-12) and (6.3-26). The real and imaginary parts of the complex

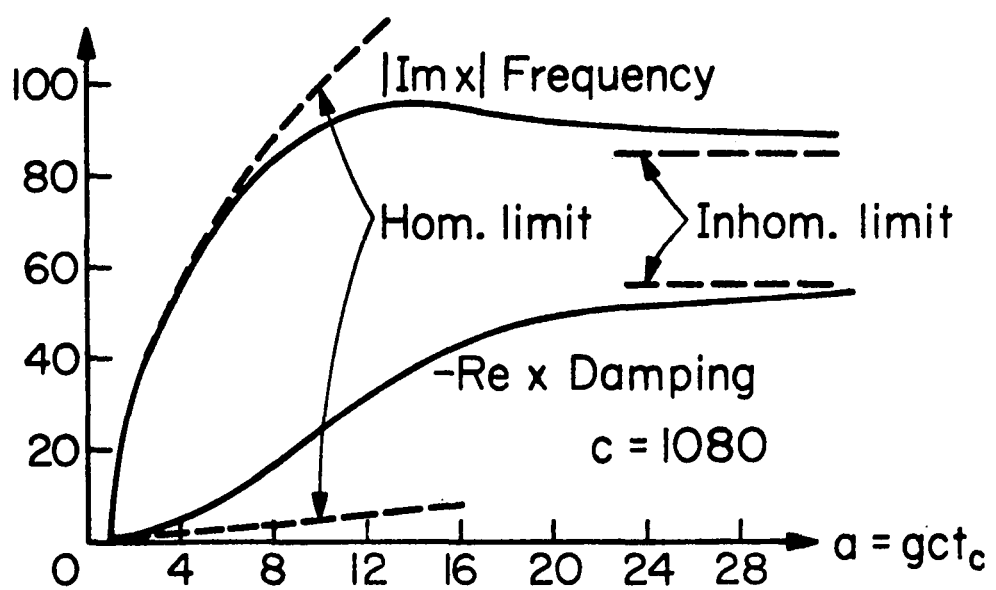


Figure 6.1 Real and imaginary parts of the complex frequency x versus a for $c = 1080$.

frequency χ are proportional respectively to the damping and frequency of small amplitude relaxation oscillations. Evidently the oscillation frequency reaches a maximum as the saturation is increased and then approaches the inhomogeneous limit. Eventually, of course, the width of the hole burned in the population inversion spectrum becomes comparable to the Doppler line width as the saturation is continuously increased. When this occurs, the oscillation behavior must return to a homogeneous limit, and the approximation of strongly inhomogeneous broadening made in equation (6.2-20) breaks down. Specifically, this failure occurs when the condition of equation (6.2-29) ceases to be satisfied.

In summary, we have obtained solutions for the small perturbation frequencies in an inhomogeneously broadened ($\Delta\nu_D \gg$ hole width) laser. The important "homogeneous" and "inhomogeneous" limits of this result were also considered. In our experiments we have used values of the parameter a between one and about seven. For this range Figure 6.1 shows that the homogeneous results should provide an adequate description of the oscillation frequency, whereas the general result would be needed to account for the damping. These conclusions are checked in the experiment sections of this chapter.

6.4 Time domain experiment

The apparatus used in the time domain studies is shown schematically in Figure 6.2. The mirrors were flat. The left mirror was highly reflecting while the right mirror reflected only about four percent. No confinement of the beam was necessary, since diffraction losses are small compared to other losses. The left mirror could be uniformly translated mechanically along the axis of the laser at slownesses exceeding 10 seconds per wavelength. The detector was germanium doped with mercury and cooled by liquid hydrogen. The detector bandpass was measured to be in excess of 60 MHz. The discharge diameter was 5.5 millimeters, and the pressure was about 5 microns (6.7).

An example of a pulsating output is shown in Figure 6.3. The photograph was obtained at a discharge current of 40 ma with no additional attenuation in the cavity. Many sweeps are recorded in the picture to give an indication of the degree of stability of the pulsing. Blurring at the left of the picture represents primarily amplifier noise, while the increasing fuzziness to the right of the picture shows that the pulsation period is not strictly constant in this example.

It was found that the stability of the pulsations depends on the length of the cavity. That is the reason the left mirror is movable. In particular, the undamped pulsations only occur when there is a longitudinal mode near the center of the gain curve. According to Section 3.3 the Doppler line width is about 100 MHz, and under pulsing conditions the laser can only support one or two longitudinal modes.

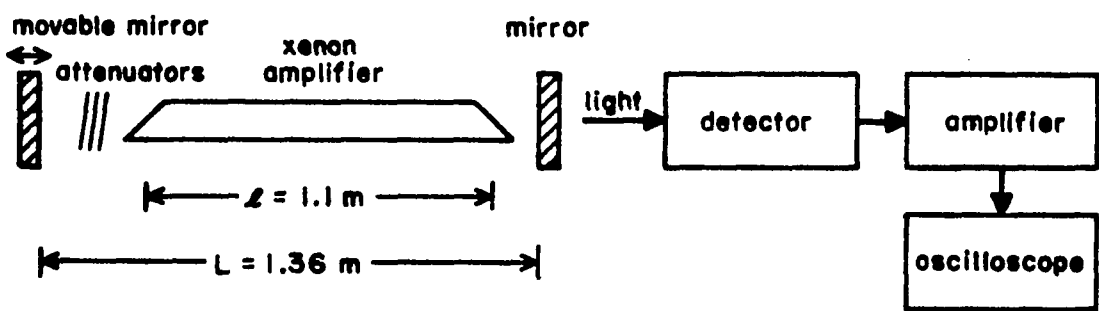


Figure 6.2 Experimental setup for time domain measurements.

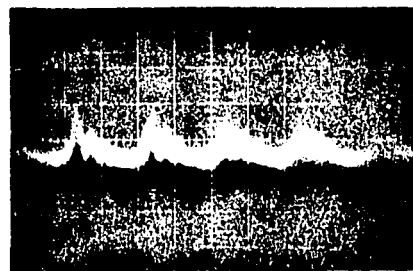


Figure 6.3 Relaxation oscillations at 40 ma and .2 μ s per division.

Hence the position of these modes can be inferred by monitoring the power output as the mirror is translated. The power is a maximum when a mode is near the center of the gain curve. The pulsation period decreases slightly as the mode approaches gain center, as expected from equation (6.3-18), and all of our data were taken near gain center.

In Figure 6.4 is another photograph of the pulsations having a period of .3 microseconds. Here the frequency stability is better than in Figure 6.3, and another effect is also apparent. The pulses alternate regularly in amplitude by about ten percent at half of the dominant pulse rate. This effect was occasionally observed and may be due to pulsation of two longitudinal modes at different pulse frequencies.

Also evident in Figures 6.3 and 6.4 are damped secondary pulses which always follow the dominant pulses. The period of the minor pulses is always about one-sixth of the major period, and the damping of the minor pulse train increases with increasing gain. The interpretation of these pulses is not clear. They may be due to the non-linearity of the rate equations, coupling to another laser level, transient mode pulling effects, or possibly to pulse breakup resulting from non-negligible coherence effects.

The depth of modulation is in excess of ninety percent as determined by periodically blocking the laser beam. The maximum average power output that could be obtained in the strongly pulsing regime was about 100 μ w as determined with an Eppley thermopile. The peak power was of the order of one mw. Pulse widths as short as 20 nanoseconds could be obtained at the higher currents.

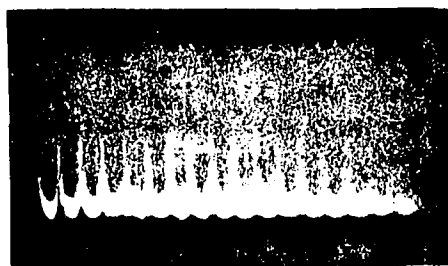


Figure 6.4 Relaxation oscillations at 50 ma and .5 μ s per division.

Typical experimental data are summarized in Figure 6.5. The data were obtained from oscilloscope displays like Figures 6.3 and 6.4. The pulse period is plotted as a function of the number of 50 percent transmission attenuators placed in the cavity for various values of discharge current. The solid lines are theoretical curves obtained by rewriting equation (6.3-18) as

$$T_o = \frac{2\pi}{\sqrt{\frac{c_m}{\tau} (g - g_n)}} \quad (6.4-1)$$

where g_n is the threshold value of gain for n attenuators, g is the actual gain at the indicated discharge current, and the lifetime is taken to be $\tau = 1.2$ microseconds. The values of gain are determined from Figure 6.6.

Figure 6.6 is a plot of gain g versus discharge current. The experimental values of gain were determined by placing in the cavity a known number of attenuators (indicated in the figure) and reducing the discharge current until threshold is reached. The gain can then be determined by considering the total amount of loss in the cavity. The gain turned out to be essentially proportional to current and a straight line was fitted to the data.

From Figure 6.5 it is apparent that the pulse period data depart significantly from the theory for low levels of discharge current and low loss. But this is just the regime where the pulsing is strongest as indicated in Figures 6.3 and 6.4. This discrepancy may be due to the linearization of the rate equations. When the

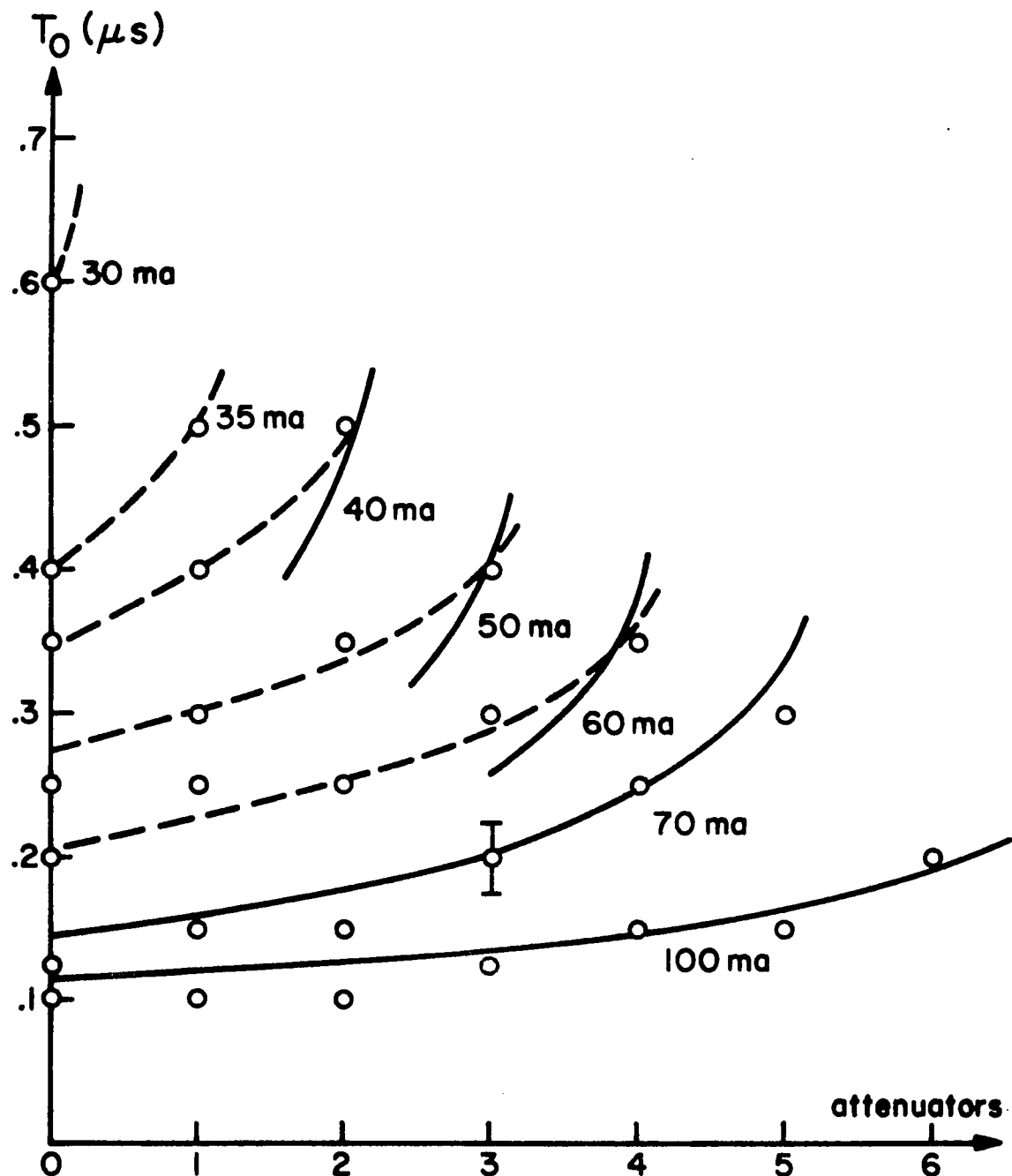


Figure 6.5 Pulsation period versus attenuation for various discharge currents. Solid lines are theoretical and dashed lines are fitted to the data points. A typical error bracket is shown.

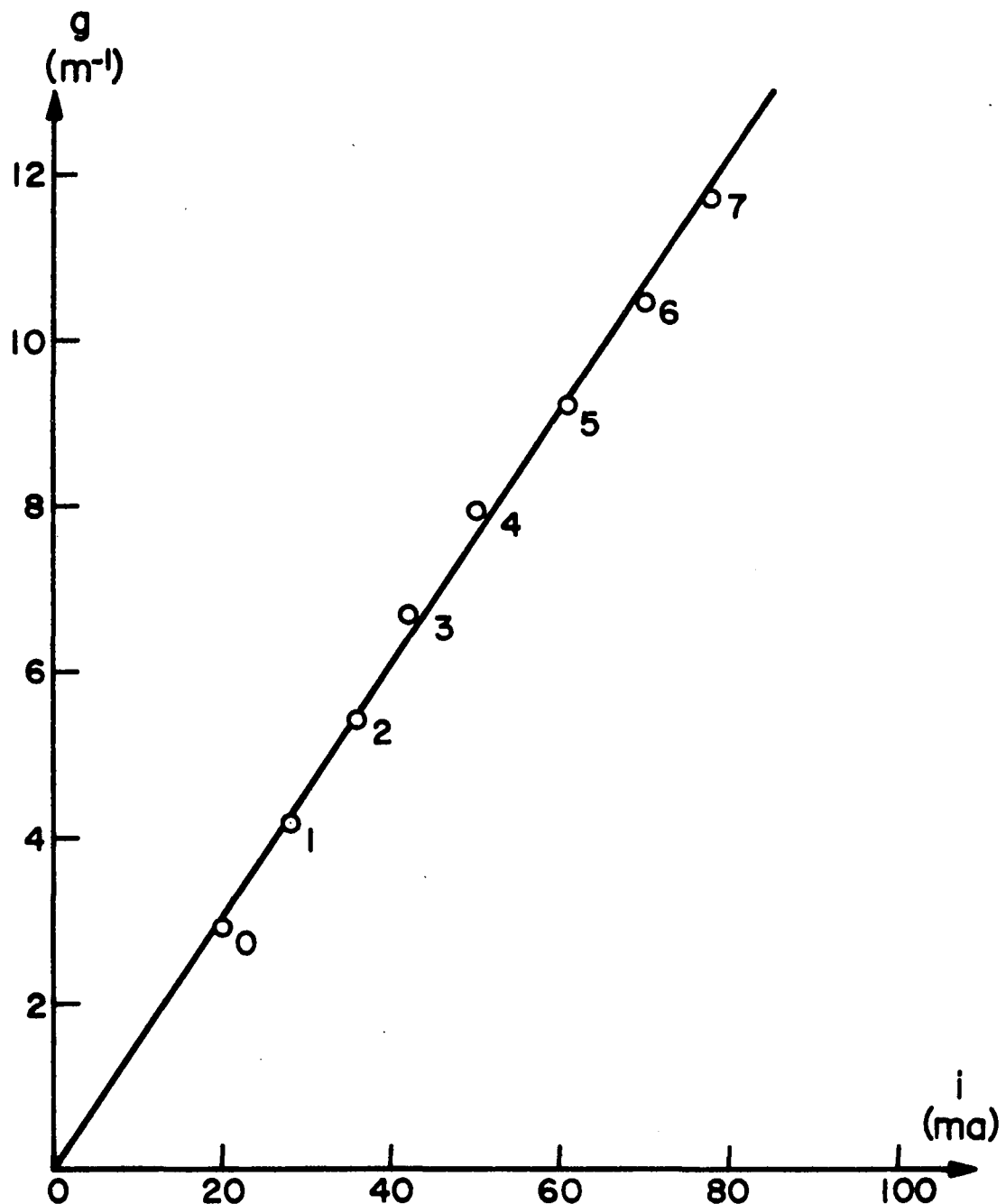


Figure 6.6 Gain versus discharge current. The number of attenuators is indicated.

linearization ceases to be valid, the pulsation period is expected to be greater than that predicted by the linear theory^(6.1). The fit is good near threshold where the pulsing is weak and at high currents where the pulsing is strongly damped.

In concluding this section we suggest that the rate equation model of equations (6.2-1) and (6.2-2) in the homogeneous limit provides an adequate description of the period of the observed relaxation oscillations in a high gain xenon laser as expected from the discussion in Section 6.3. Inhomogeneous broadening would only be important at higher saturation levels as shown in Figure 6.1. The value $\tau = 1.2$ microseconds used in fitting the experimental data in Figure 6.5 is in agreement with the value 1.35 microseconds calculated theoretically by Clark et al^(6.8) or 1.365 microseconds calculated recently by Allen et al^(6.9).

The theory predicts weakly damped oscillations, whereas experimentally the pulsing is sometimes apparently undamped. There are basically two possible explanations for the lack of damping. First, there may be some subtle effect in the high gain laser which we have not considered in the rate equations and which compensates for the expected damping, making the equations unstable. The equations as written may be shown by Liapounoff's second method^(6.10) to be always stable. Alternatively, the equations may be driven by some "white" noise source such as the quantum fluctuations or pump fluctuations discussed by McCumber^(6.6). One may distinguish between these possibilities by examining the frequency spectrum of the laser power output. If there is an instability in the rate equations, the output

spectrum should consist of well-defined lines at the pulsing frequency and its harmonics. However, if the rate equations are driven by noise, the output spectrum should resemble that given by equation (6.3-21). In the following section we describe an experiment in which the output spectrum has been measured.

6.5 Frequency domain experiment

The apparatus used in the frequency domain experiments is sketched in Figure 6.7. The mixer was used to shift the beat spectrum upward to a region with less interference. Synchronous detection was necessary because the signal to noise ratio was poor.

A typical spectrum for the case of pulsing at a discharge current of 40 ma is shown in Figure 6.8. The dispersion is 5 MHz per division and zero frequency is at the center of the display. Thus, the pulsation frequency is 2.5 MHz, and the spectrum corresponds to the pulsing shown in Figure 6.3. The spike expected at zero frequency saturated the spectrum analyzer (Tektronix Type 1L20) and is absent from the figure. Clearly the linear approximation to the rate equations is breaking down since six or seven harmonics of the fundamental frequency are visible in the photograph.

In Figure 6.9 is a typical spectrum for strongly damped pulsations. Here the spectrum is much broader and the higher harmonics are absent. Thus, the linear approximation is presumably valid, and the form of the spectrum is in excellent qualitative agreement with equation (6.3-21).

It is reasonable to inquire whether the rather discrete frequencies of oscillation suggested by the beat spectra of Figure 6.8 are associated in some way with the laser cavity modes. First, it is clear that the longitudinal mode coupling which has been suggested to explain relaxation oscillations in GaAs^(6.11) cannot apply here, since only one or two longitudinal modes are present. The other possibility is that the spectrum observed represents beats between various transverse modes.

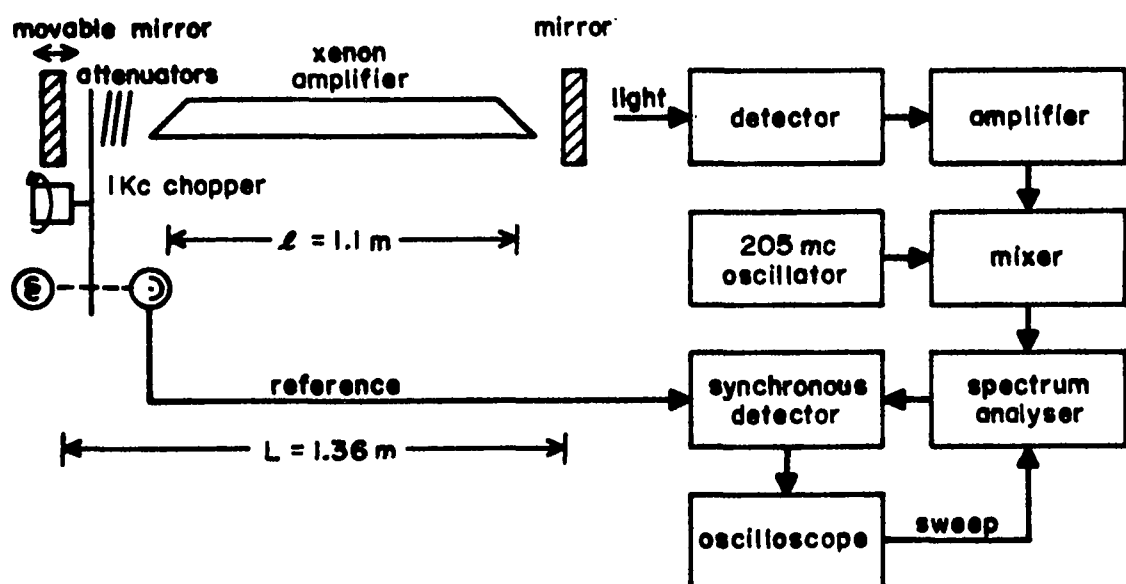


Figure 6.7 Experimental setup for frequency domain measurements.

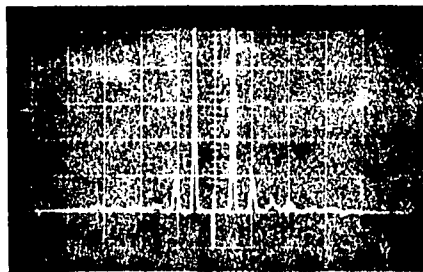


Figure 6.8 Beat spectrum at 40 ma with 5 mc per division dispersion.
Zero frequency is at the center of the display.

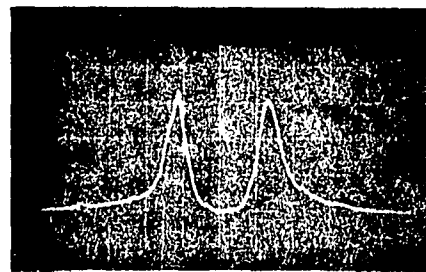


Figure 6.9 Beat spectrum of strongly damped pulsations with 5 MHz per division dispersion.

However, scanning the output with a small aperture showed no change in the pulsing behavior. Moreover, introducing an aperture inside of the cavity was found to reduce the pulsation frequency in exactly the same fashion as introducing a uniform attenuator, so the laser was believed to be operating in a single transverse mode.

The importance of the beat spectra data is that the width of the beat lines should be related to the damping predicted by the rate equations if the oscillations are driven by broadband noise. In the simplest linear homogeneous approximation the line width should be given by equation (6.3-23). The experimental line width data for zero attenuation are summarized in Figure 6.10. When the pulsing is non-linear we use the width of the fundamental beat. This is not rigorously correct, of course, but it should be all right qualitatively.

Both the homogeneous result and the general result from equation (6.2-26) are plotted in Figure 6.10 for $\tau = 1.2$ microseconds and using values of g determined from Figure 6.6. The data agree well with the theory only for small currents. For strong saturation the damping is greater than anticipated. The general theoretical result provides a slightly better fit than the homogeneous result showing that inhomogeneous broadening effects (spectral hole burning) are probably important as expected from the discussion in Section 6.3. The remaining discrepancy may be due partly to the spatial nonuniformity of the fields which we have neglected here^(6.3,6.4), low frequency fluctuations (power supply), or the limited cavity linewidth. Since the observed spectra agree at least approximately with the theory, we conclude that

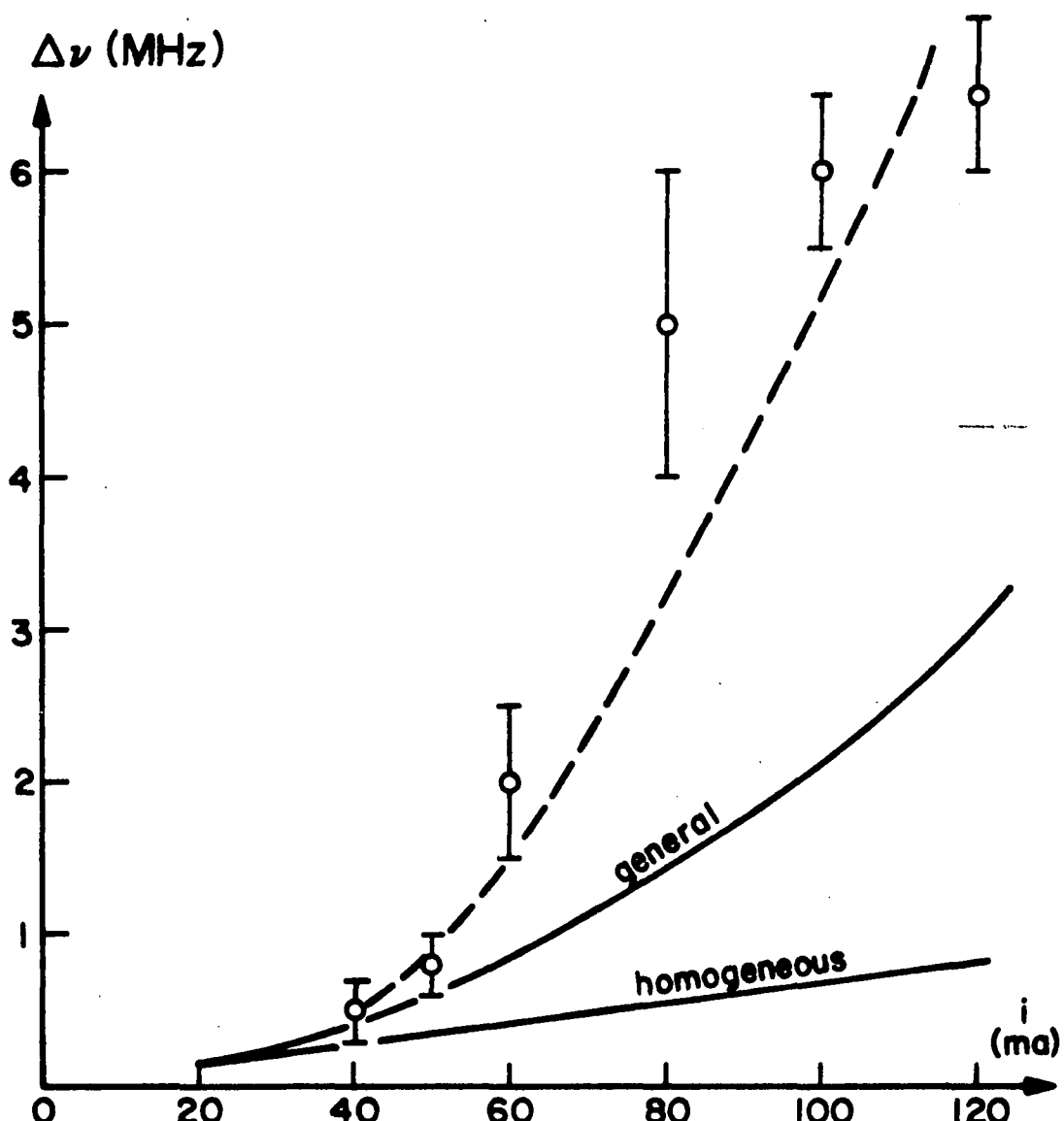


Figure 6.10 Pulsation line width as a function of discharge current.
The solid lines are theoretical results and the dashed line is drawn roughly through the data.

the inhomogeneous rate equation model driven by broadband noise provides an adequate explanation for the experimentally observed intensity fluctuations in a xenon laser.

6.6 Coherence effects

The purpose of this section is to investigate theoretically the effects of the coherence time on the relaxation of transients in lasers. As our starting point we use equations (2.2-18) and (2.2-19). To keep the mathematics tractable we make the approximation that the medium is effectively homogeneously broadened. Then for radiation at gain center the governing equations may be written

$$\frac{dn}{dt} = P - B \sqrt{q(t)} \int_{-\infty}^t e^{-\frac{t-t'}{T_2}} \sqrt{q(t')} n(t') dt' - \frac{n}{T_1} \quad (6.6-1)$$

$$\frac{dq}{dt} = B \sqrt{q(t)} \int_{-\infty}^t e^{-\frac{t-t'}{T_2}} \sqrt{q(t')} n(t') dt' - \frac{q}{t_c} \quad (6.6-2)$$

where T_1 and T_2 are the phenomenological spontaneous decay time and transverse coherence time respectively.

Equations (6.6-1) and (6.6-2) may be differentiated^(6.12) and combined with the original equations to obtain the pair of nonlinear second order equations

$$\frac{d^2n}{dt^2} + \left(\frac{1}{T_2} + \frac{1}{T_1} - \frac{1}{2q} \frac{dq}{dt} \right) \frac{dn}{dt} + \left(\frac{1}{T_2 T_1} + Bq - \frac{1}{2q} \frac{dq}{dt} \right) n = \left(\frac{1}{T_2} - \frac{1}{2q} \frac{dq}{dt} \right) P \quad (6.6-3)$$

$$\frac{d^2q}{dt^2} + \left(\frac{1}{T_2} + \frac{1}{2t_c} - \frac{1}{2q} \frac{dq}{dt} \right) \frac{dq}{dt} + \left(\frac{1}{T_2 t_c} - Bn \right) q = 0 \quad (6.6-4)$$

It is useful to introduce the additional parameters $m = \frac{dn}{dt}$ and $p = \frac{dq}{dt}$. Then equations (6.6-3) and (6.6-4) may be written as the system of four first order equations

$$\frac{dm}{dt} = -\left(\frac{1}{T_2} + \frac{1}{T_1} - \frac{p}{2q}\right)m - \left(\frac{1}{T_2 T_1} + Bq - \frac{p}{2q} \frac{1}{T_1}\right)n + \left(\frac{1}{T_2} - \frac{p}{2q}\right)p$$

$$\frac{dp}{dt} = -\left(\frac{1}{T_2} + \frac{1}{t_c} - \frac{p}{2q}\right)p - \left(\frac{1}{T_2 t_c} - Bn\right)q$$

$$\frac{dn}{dt} = m$$

$$\frac{dq}{dt} = p \quad (6.6-5)$$

Equations (6.6-5) can't be solved in general, and we only obtain here the solutions to the linearized equations. These solutions yield the behavior of the population inversion and photon density in the vicinity of an equilibrium point of the system. With the substitutions $m = m'(t)$, $p = p'(t)$, $n = n_o + n'(t)$, $q = q_o + q'(t)$, and the retention of only the terms through first order in the primed quantities, equations (6.6-5) are changed into the linear system

$$\frac{dm'}{dt} = -\left(\frac{1}{T_2} + \frac{1}{T_1}\right)m' + \left(\frac{n_o}{2q_o} \frac{1}{T_1} - \frac{1}{2q_o}\right)p' - \left(\frac{1}{T_2 T_1} + Bq_o\right)n' - (Bn_o)q' + \left(\frac{p}{T_2} - \frac{n_o}{T_2 T_1} - Bq_o n_o\right)$$

$$\frac{dp'}{dt} = -\left(\frac{1}{T_2} + \frac{1}{2t_c}\right)p' + (Bq_o)n' + (Bn_o - \frac{1}{T_2 t_c})q' + (Bn_o q_o - \frac{q_o}{T_2 t_c})$$

$$\frac{dn'}{dt} = m'$$

$$\frac{dq'}{dt} = p' \quad (6.6-6)$$

Thus the steady state results are

$$P = \frac{n_o}{T_1} + BT_2 q_o n_o$$

$$\frac{1}{t_c} = BT_2 n_o \quad (6.6-7)$$

Combining equations (6.6-7) with equations (6.6-6) yields the array

	m'	p'	n'	q'
$\frac{dm'}{dt}$	$-(\frac{1}{T_2} + \frac{1}{T_1})$	$-(\frac{1}{2t_c})$	$-(\frac{a}{T_1 T_2})$	$-(\frac{1}{T_2 t_c})$
$\frac{dp'}{dt}$	0	$-(\frac{1}{T_2} + \frac{1}{2t_c})$	$\frac{a-1}{T_1 T_2}$	0
$\frac{dn'}{dt}$	1	0	0	0
$\frac{dq'}{dt}$	0	1	0	0

(6.6-8)

where the parameter $a = PBT_2 T_1 t_c$ has been introduced. This parameter indicates the operating point of the laser with respect to threshold. From equations (6.6-7) the threshold condition ($q_o = 0$) is clearly $a = 1$.

The natural frequencies of equations (6.6-8) are obtained as the eigenvalues of the corresponding matrix or

$$\begin{vmatrix} -\left(\frac{1}{T_2} + \frac{1}{T_1}\right)s & -\frac{1}{2t_c} & -\frac{a}{T_1 T_2} & -\frac{1}{T_2 t_c} \\ 0 & -\left(\frac{1}{T_2} + \frac{1}{2t_c}\right)s & \frac{a-1}{T_1 T_2} & 0 \\ 1 & 0 & -s & 0 \\ 0 & 1 & 0 & -s \end{vmatrix} = 0$$

(6.6-9)

Expanding equation (6.6-9) in cofactors leads to the quartic equation

$$s^4 + s^3 \left(\frac{2}{T_2} + \frac{1}{T_1} + \frac{1}{2t_c} \right) + s^2 \left(\frac{1}{T_2 T_2} + \frac{a+1}{T_2 T_1} + \frac{1}{2T_2 t_c} + \frac{1}{2T_1 t_c} \right) + s \left(\frac{2a-1}{2T_2 T_1 t_c} + \frac{a}{T_2 T_2 T_1} \right) + \frac{a-1}{T_2 T_2 T_1 t_c} = 0 \quad (6.6-10)$$

One finds (eventually) that this equation may be factored into

$$\left[s + \frac{1}{T_2} \right] \left[s^3 + s^2 \left(\frac{1}{T_2} + \frac{1}{T_1} + \frac{1}{2t_c} \right) + s \left(\frac{a}{T_2 T_1} + \frac{1}{2T_1 t_c} \right) + \frac{a-1}{T_2 T_1 t_c} \right] = 0 \quad (6.6-11)$$

The first factor represents a strongly damped real solution which we need not consider further. Thus, the equation governing the

natural relaxation frequencies is the cubic

$$s^3 + s^2 \left(\frac{1}{T_2} + \frac{1}{T_1} + \frac{1}{2t_c} \right) + s \left(\frac{a}{T_2 T_1} + \frac{1}{2T_1 t_c} \right) + \frac{a-1}{T_2 T_1 t_c} = 0 \quad (6.6-12)$$

Equation (6.6-12) cannot be factored simply, so we consider instead two important limiting cases. First of all, if the transverse relaxation time is short, $T_2 \ll t_c$ (and $t_c \ll T_1$), then equation (6.6-12) may be factored approximately into

$$\left(s + \frac{1}{T_2} \right) \left(s^2 + \frac{a}{T_1} s + \frac{a-1}{T_1 t_c} \right) \approx 0 \quad (6.6-13)$$

Again we discard the damped real solution and are left with the quadratic

$$s^2 + \frac{a}{T_1} s + \frac{a-1}{T_1 t_c} = 0 \quad (6.6-14)$$

But equation (6.6-14) is the same as equation (6.3-3), and one may regard this result as the "incoherent" limit of equation (6.6-12). It is solved in section 6.3. That this result should be obtained in the limit of small T_2 is, of course, to be expected and represents a check on the preceding mathematics.

Now we consider the "coherent" limit. If the transverse relaxation time is long, $T_2 \gg at_c$, then equation (6.6-12) may be factored approximately into

$$\left[s + \frac{1}{2t_c} \right] \left[s^2 + \frac{1}{T_1} s + \frac{2(a-1)}{T_1 T_2} \right] \approx 0 \quad (6.6-15)$$

The strongly damped real factor may be discarded and one is left with the quadratic

$$s^2 + \frac{1}{T_1} s + \frac{2(a-1)}{T_1 T_2} = 0 \quad (6.6-16)$$

The solutions are

$$s = \frac{1}{2T_1} \pm \frac{i}{2T_1} \sqrt{\frac{8(a-1)T_1}{T_2} - 1} \quad (6.6-17)$$

Equation (6.6-17) is qualitatively similar to the incoherent solution given by equation (6.3-13). In both results the frequency increases as the laser is operated farther above threshold. However, in equation (6.6-17) the damping is independent of the operating point. In a low pressure gas laser pressure broadening is unimportant and the two lifetimes are approximately related by $T_2/2 \sim T_1 = \tau$ provided that the displacement of the atoms in one lifetime is unimportant. Then equation (6.6-17) simplifies to

$$s = \frac{1}{2\tau} \pm \frac{i}{\tau} \sqrt{2a - \frac{9}{4}} \quad (6.6-18)$$

In most laser systems which exhibit relaxation phenomena the coherence time is much shorter than the cavity lifetime t_c , so that the incoherent approximation given in equation (6.6-14) is valid. Possible exceptions might be the high gain semiconductor or gas lasers where the cavity lifetime may be comparable to T_2 and the condition $T_2 \ll t_c$ will fail. This derivation was included here primarily as a simple application of the coherent

rate equations. The techniques of this chapter could be generalized in a straightforward fashion to include both inhomogeneous broadening and a finite coherence time, but the mathematics would be more complicated.

In our experiments with a xenon laser it was found that equation (6.3-13) provides a much better fit to the data than does equation (6.6-18) using the calculated values for the lifetime τ (6.8, 6.9). The reason for this result is presumably that at thermal velocities (~ 200 meters per second) the atoms move a half wavelength in a time much shorter than the natural lifetime, and the coherence time T_2 is reduced accordingly.

6.7 Conclusion

In this chapter general theoretical results have been derived for relaxation oscillations in inhomogeneously broadened lasers. The behavior of the oscillations is conveniently classified as either "homogeneous" or "inhomogeneous" depending on the level of saturation. Relaxation phenomena have been observed experimentally in a high gain xenon laser at 3.51 microns. At low current levels there are regular undamped pulsations while with large currents and strong saturation the pulsations are damped. The period of these pulsations agrees well with the results of the rate equation theory. In the frequency domain the beat spectrum changes gradually from several discrete lines in the nonlinear pulsation regime to a single broad line as the saturation increases. This behavior is in qualitative agreement with the model if a broadband noise source is included. The effects of a long coherence time on the pulsation behavior have also been studied theoretically for a homogeneously broadened laser. It turns out that even in this limit the pulsations should be qualitatively similar to those in a simple incoherent homogeneous system.

Bibliography

6. 1 R. Dunsmuir, Journal of Electronics and Control 10, page 453, 1961.
6. 2 C. L. Tang, Journal of Applied Physics 34, page 2935, 1963.
6. 3 M. E. Globus, Yu. V. Naboikin, A. M. Ratner, I. A. Rom-Krichevskaya, and Yu. A. Tiunov, Soviet Physics JETP 25, No. 4, Page 562, October 1967.
6. 4 R. Polloni and O. Svelto, Journal of Quantum Electronics QE-4, No. 8, page 481, August 1968.
6. 5 H. Bateman, Tables of Integral Transforms, Volume 1 (New York: McGraw-Hill 1954) Page 136, No. 4.2.25.
6. 6 This expression is similar to the denominator factor of equations (6.6) and (6.10) of D. E. McCumber, Physical Review 141, No. 1, Page 306, January 1966.
6. 7 D. R. Armstrong, Journal of Quantum Electronics QE-4, No. 11, page 968, November 1968.
6. 8 P. O. Clark, R. A. Huback, and J. Y. Wada, JPL Contract No. 950803, Final Report, April 1965.
6. 9 L. Allen, D. G. C. Jones, and D. G. Schofield, Journal of the Optical Society of America 59, No. 7, page 842, July 1969.
- 6.10 W. Kaplan, Ordinary Differential Equations, Addison-Wesley, Reading Massachusetts, Page 433, August 1962.
- 6.11 T. L. Paoli and J. E. Ripper, Physical Review Letters 22, No. 21, page 1085, 26 May 1969.
- 6.12 F. B. Hildebrand, Methods of Applied Mathematics, Prentice-Hall, Inc., Englewood Cliffs, New Jersey, Section 4.1,

- 217 -

equation (5), December 1961.

VII. Oscillation Line Width

7.1 Introduction

The purpose of this chapter is to investigate theoretically and experimentally the effects of a high gain laser medium on the output radiation line width of a laser oscillator. The results for the oscillation line width of low gain lasers are well known. Typically the calculations are carried out by analogy with a resonant electrical circuit^(7.1). One finds that the line width is proportional to the square of the empty cavity line width and inversely proportional to the energy in the laser field.

In a high gain laser the results may be significantly different. Under some conditions the line width may increase with increasing power, which is the opposite of the low gain behavior. The cause of these new effects is the dispersion which is associated with a narrow high gain laser transition. We begin with a general analysis of the oscillation conditions which must be satisfied in a one dimensional laser independent of any dispersion considerations. In the limit of low gain and no dispersion the theoretical line width reduces to the well known value.

The oscillation line width in unsaturated high gain lasers is then treated including dispersion effects. The oscillation line may be much broader or narrower than the nondispersed value depending on the relation of the oscillation center frequency to the gain center frequency. If saturation is substantial in an inhomogeneously broadened medium, then hole burning effects must also be considered. In a laser with a very intense oscillation line the

dispersion associated with the burned hole may make it possible for the cavity to support new oscillation frequencies in the wings of the hole. The overall effect is believed to be a strong broadening of the laser line whenever the gain is high and hole burning is important. This conclusion is supported by an experiment which shows a broadening of the oscillation line in a xenon laser by a factor of about five as saturation is increased.

7.2 Oscillation line width

In this section general expressions are obtained for the oscillation conditions and the oscillation line width of a laser oscillator containing a high gain amplifying medium. The analysis is essentially one dimensional. It is based on the transmission characteristics of a plane parallel Fabry-Perot resonator.

We assume that an electromagnetic wave of amplitude E_i is incident on the resonator from the left and a wave of amplitude E_t is transmitted through the resonator. The propagation of the wave is governed by a relation of the form

$$E = E_0 e^{-i \int k dz} \quad (7.2-1)$$

where k is the slowly varying complex propagation constant. The transmission and reflection coefficients of the right and left mirrors of the resonator are respectively t_ℓ , r_ℓ , t_r , and r_r . One can write down immediately that the transmitted field is related to the incident field by

$$E_t = t_\ell t_r E_i e^{-i \int_0^L k dz} \left(1 + (r_\ell r_r) e^{-i \int_0^L k dz} + (r_\ell r_r)^2 e^{-2i \int_0^L k dz} + \dots \right) \quad (7.2-2)$$

where L is the length of the resonator and the closed integral indicates one loop through the resonator. The first term in the parentheses represents light which travels directly through the resonator, the second term represents light which makes one extra

loop through the resonator, and so on.

Equation (7.2-2) is a geometric series which may be readily summed. The result may be written

$$\frac{E_t}{E_i} = \frac{T_e \int_0^L k dz}{1 - Re \int_0^L k dz} \quad (7.2-3)$$

where the net transmission coefficient T is defined by $T = t_l t_r$ and the net reflection coefficient R is defined by $R = r_l r_r$. Experimentally the intensity is a more useful quantity than the electric field. But the intensity is proportional to the square of the absolute magnitude of the electric field. Therefore, the Fabry-Perot intensity transmission coefficient may be found as the product of equation (7.2-3) and its complex conjugate or

$$\frac{I_t}{I_i} = \frac{E_t E_t^*}{E_i E_i^*} = \left(\frac{T_e \int_0^L k dz}{1 - Re \int_0^L k dz} \right) \left(\frac{T_e \int_0^L k^* dz}{1 - Re \int_0^L k^* dz} \right)^* \quad (7.2-4)$$

The constant k is separated into its real and imaginary parts according to

$$k = \gamma + i\alpha \quad (7.2-5)$$

Then equation (7.2-4) simplifies to

$$\frac{I_t}{I_i} = \frac{T^2 e^{-2 \int_0^L \alpha dz}}{\left(1 - \operatorname{Re} \int_0^L \alpha dz - i \int_0^L \gamma dz\right) \left(1 - \operatorname{Re} \int_0^L \alpha dz + i \int_0^L \gamma dz\right)}$$

$$= \frac{T^2 e^{-2 \int_0^L \alpha dz}}{1 + R^2 e^{2 \int_0^L \alpha dz} - 2 \operatorname{Re} \int_0^L \alpha dz - \cos \int_0^L \gamma dz} \quad (7.2-6)$$

Using a half-angle formula this becomes

$$\frac{I_t}{I_i} = \frac{T^2 e^{-2 \int_0^L \alpha dz}}{\left(1 - \operatorname{Re} \int_0^L \alpha dz\right)^2 + 4 \operatorname{Re} \int_0^L \alpha dz \sin^2 \frac{\int_0^L \gamma dz}{2}} \quad (7.2-7)$$

Oscillation may be defined as the condition wherein there is an output from the Fabry-Perot resonator in the absence of any input. This is only possible when the denominator of equation (7.2-7) vanishes. The denominator is zero if the gain condition

$$1 - \operatorname{Re} \int_0^L \alpha dz = 0 \quad (7.2-8)$$

and the phase condition

$$\int_0^L \gamma dz = 2\pi m \quad (7.2-9)$$

with m an integer are both satisfied. This phase condition was the basis of the discussion of longitudinal modes in Chapter IV.

The preceding analysis neglected the effects of spontaneous emission. In any real laser oscillator spontaneous emission adds energy to the oscillation field. As a consequence, neither the gain condition nor the phase condition of equations (7.2-8) and (7.2-9) are rigorously satisfied. Equation (7.2-9) determines only the center frequency of the oscillation field (Chapter IV), but it is also possible for nearby frequencies to exist in the resonator. In other words, the radiation field has a nonzero frequency width.

To find the oscillation line width, we consider again equation (7.2-7). The Fabry-Perot transmission falls to one half of its line center value when γ is determined by

$$\left(1 - \operatorname{Re} \int_0^L \alpha dz\right)^2 = 4 \operatorname{Re} \int_0^L \alpha dz \sin^2 \left(\int_0^L \frac{\gamma_{12}}{2} dz - m\pi \right) \quad (7.2-10)$$

If spontaneous emission is relatively weak, then the sine function in equation (7.2-10) must be small. In this case the sine may be replaced by its argument and equation (7.2-10) becomes

$$\int_0^L \gamma_{12} dz - 2m\pi = 1 - \operatorname{Re} \int_0^L \alpha dz \quad (7.2-11)$$

This equation may also be written

$$\int_0^L \Delta \gamma_{12} dz = 2 \left(1 - \operatorname{Re} \int_0^L \alpha dz \right) \quad (7.2-12)$$

where $\Delta\gamma_{12}$ is the full width of the resonance in units of γ .

The factor in parentheses represents the fraction of the field which was not fed back by the mirrors and amplifying medium and must therefore be due to spontaneous emission.

If the index of refraction is nearly independent of frequency over the oscillation line width, equation (7.2-12) is

$$\Delta\nu = \frac{c \left(1 - \text{Re} \int \alpha dz \right)}{\pi \int n dz} \quad (7.2-13)$$

This is the general result for the oscillation line width of a laser provided that the spontaneous emission per pass is small compared to the total laser field and dispersion effects are unimportant. In a low gain laser equation (7.2-13) reduces to

$$\Delta\nu = \frac{c \left(1 - R - \int \alpha dz \right)}{\pi \int n dz} \quad (7.2-14)$$

If there is no gain at all we have simply

$$\Delta\nu_c = \frac{c(1 - R)}{\pi \int n dz} \quad (7.2-15)$$

where $\Delta\nu_c$ is referred to as the cavity line width.

Equation (7.2-13) is a general expression for the oscillation line width, but it is not useful unless the detailed z

dependence of the saturated gain α is known. This result can be obtained, in principle, from the equation

$$\frac{dI}{dz} = 2\alpha I + 2\eta\alpha \quad (7.2-16)$$

where the saturated gain α is a function of the intensity I . Throughout this chapter distributed losses are assumed to be negligible. The generalization to lasers with large distributed losses is elementary and only clutters the mathematics. The last term in equation (7.2-16) represents the contribution of spontaneous emission, which is proportional to the population inversion and hence to the gain also. The factor η measures the relative importance of spontaneous and stimulated emission. Some geometrical considerations are necessary in determining η since in typical lasers only a small fraction of the total spontaneous emission is directed in such a way as to contribute to the total laser field. We do not need numerical results so η isn't evaluated here.

Equation (7.2-16) can be divided by I and "integrated" to obtain

$$I(z_2) = I(z_1) e^{2 \int_{z_1}^{z_2} \alpha (1 + \frac{\eta}{I}) dz} \quad (7.2-17)$$

The oscillation gain condition for the intensity is that the field reproduce itself after one round trip so that

$$1 - R^2 e^{2 \int \alpha(1 + \frac{\eta}{I}) dz} = 0 \quad (7.2-18)$$

Factoring this equation yields the amplitude condition

$$1 - \text{Re} \int \alpha(1 + \frac{\eta}{I}) dz = 0 \quad (7.2-19)$$

or

$$1 - \text{Re} \int \alpha dz = \text{Re} \int \alpha dz \left(e^{\int \frac{\eta}{I} dz} - 1 \right) \quad (7.2-20)$$

Far above threshold the spontaneous emission is relatively weak and equation (7.2-20) simplifies to

$$1 - \text{Re} \int \alpha dz = \eta \int \frac{\alpha}{I} dz \quad (7.2-21)$$

Then from equation (7.2-13) the oscillation line width of a high gain laser is given by

$$\Delta v = \eta \frac{\int \frac{\alpha}{I} dz}{\int \alpha dz} \quad (7.2-22)$$

To evaluate equation (7.2-22), it is still necessary to know the z dependences of α and I . Less accuracy is needed, however, than for evaluation of the small difference term in equation (7.2-13). In particular, α and I can be determined from the equation

$$\frac{dI}{dz} = 2\alpha(I)I \quad (7.2-23)$$

which is the same as equation (7.2-16) with spontaneous emission neglected. The boundary conditions are provided by the laser mirrors. Some solutions of equation (7.2-23) for specific types of saturation are discussed in Chapter X, and they needn't be considered further here.

In a low gain laser these results simplify. The intensity is approximately constant and equation (7.2-22) can be written

$$\Delta v = \frac{n}{I} \frac{\int c o d z}{\pi \int o d z} \quad (7.2-24)$$

The loop gain is nearly equal to the mirror transmission losses so that equation (7.2-24) becomes

$$\Delta v = \frac{n}{I} \frac{c(1-R)}{\pi \int o d z} \quad (7.2-25)$$

Using equation (7.2-15), this is simply

$$\Delta v = \frac{n \Delta v_c}{I} \quad (7.2-26)$$

This result has the same intensity dependence as the solution of the circuit model laser analogue^(7.1). This comparison with the circuit model would probably provide the simplest means of evaluating

the coefficient η .

In this section the gain and phase oscillation conditions have been derived for a one dimensional Fabry-Perot resonator containing a high gain laser medium. General expressions have also been obtained for the oscillation line width of such a resonator. In the limit of a low gain medium with no dispersion the line width is proportional to the square of the cavity line width and inversely proportional to the energy in the laser cavity. This well known result is ordinarily derived indirectly from a circuit model analogy. The circuit model, however, is basically a zero dimensional approximation, which is incapable of accurately treating the high gain lasers of interest here.

7.3 Dispersion effects

In this section we consider the effects of anomalous dispersion on the oscillation line width of an unsaturated laser. The general implicit expression for the oscillation line width is given, according to equation (7.2-12) by

$$\int \Delta\gamma_2 dz = 2 \left(1 - \text{Re} \int \alpha dz \right) \quad (7.3-1)$$

Also, the general expression for the longitudinal mode spacing, equation (7.2-9), may be written

$$\int \Delta\gamma dz = 2\pi \quad (7.3-2)$$

These two equations are essentially identical in form provided that the gain α in equation (7.3-1) is independent of frequency over the oscillation line width. Thus, we have the reasonable result that changes in mode spacing due to dispersion are accompanied by proportionate changes in line width. In other words, the Fabry-Perot finesse is unaffected by dispersion in any frequency interval which is small compared to the overall gain line width.

We consider first the case of a Doppler broadened inhomogeneous gain line. For this purpose one may adapt the mode pulling results of section 4.2 since the mode spacing is proportional to the line width. Expansion of equation (4.2-5) to first order in a Taylor series for a narrow line yields

$$\Delta x_0 = \left| \frac{d}{dx} (\beta F(x) + x) \right| \Delta x$$

or

$$\Delta x = \frac{\Delta x_0}{\left| 1 + \beta \frac{dF}{dx} \right|} \quad (7.3-3)$$

which expresses the relationship between the actual oscillation line width Δx and the nondispersed line width Δx_0 . $F(x)$ is Dawson's integral and β is the dispersion parameter defined by Equation (4.2-6).

The factor $|1 + \beta(dF/dx)|^{-1}$ is plotted as a function of frequency for three values of β in Figure 7.1. For $\beta = 0$ the line width has its nondispersed value. At higher values of β the lines are narrowed near gain center and broadened in the gain wings. When β is greater than 3.51 (by analogy with the mode splitting results of Chapter IV), singularities appear in the dispersion factor of equation (7.3-3). The line width cannot actually go to infinity, of course. To properly study the behavior of the line in the vicinity of a singularity of equation (7.3-3), it is necessary to retain another term in the Taylor series expansion. Solution of the resultant quadratic leads to the expression which is everywhere finite

$$\Delta x = \left| \frac{1 + \beta \frac{dF}{dx} - \sqrt{(1 + \beta \frac{dF}{dx})^2 + 2\beta \frac{d^2F}{dx^2} \Delta x_0}}{\beta \frac{d^2F}{dx^2}} \right| \quad (7.3-4)$$

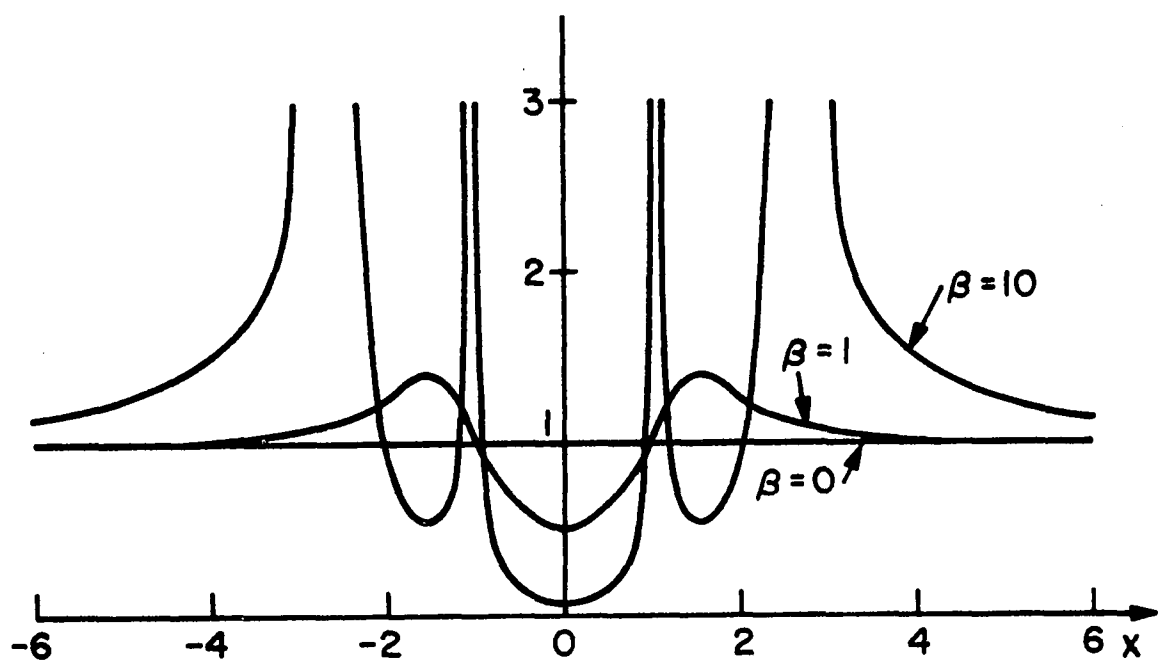


Figure 7.1 Dispersion factor $|1 + \beta \frac{dF}{dx}|^{-1}$ for three values of β .

Equation (7.3-4) is the same as equation (7.3-3) in the limit $\Delta x_0 \rightarrow 0$. The derivative terms in these equations could be simplified using equation (2.6-10). For the degenerate case $\beta = 3.51$ the third derivative term in the Taylor series must be retained to prevent ambiguity at the inflection point $d^2 F/dx^2 = 0$.

So far only Doppler broadened lasers have been considered. The results for homogeneously broadened lasers are qualitatively the same. They may be obtained from equations (7.3-3) and (7.3-4) by replacing Dawson's integral $F(x)$ by $y/(1+y^2)$ and changing β to β' in analogy with the analysis of Section 4.3. Thus equation (7.3-3) becomes

$$\Delta y = \frac{\Delta y_0}{\left| 1 + \beta' \frac{1 - y^2}{(1 + y^2)^2} \right|} \quad (7.3-5)$$

Since these results are similar to those for an inhomogeneously broadened laser, we do not consider them further.

In this section we have considered the dependence of the oscillation line width on the dispersion associated with an unsaturated high gain transition. It was shown that the line width may differ greatly from the line width which would be expected if dispersion effects were neglected. The line width is either increased or diminished depending on the relation of the oscillation frequency to the transition center frequency.

7.4 Saturation effects

By this point it is probably clear that the calculation of the oscillation line width may be quite complicated. In this section we consider in a somewhat qualitative way an additional complication which may result from saturation. The dispersion in a high gain laser depends on the field intensity, and as a result the dispersion sensitive line width may have a strong saturation dependence. This effect is in addition to the basic intensity dependence described in Section 7.2, which was caused by spontaneous emission. We find that in a high gain inhomogeneously broadened laser the oscillation line width may under some conditions be roughly equal to the width of the spectral hole burned by the radiation.

If the oscillation line width is small compared to the homogeneous line width, then the index of refraction of an inhomogeneously broadened medium with a single saturating field at the frequency x_1 is governed by equation (2.7-18)

$$n(x_\ell) - n_0 = \frac{c g}{4\pi\nu_\ell} \left\{ \frac{2F(x_\ell)}{\sqrt{\pi}} + \frac{sI_1 \delta e^{-x_1^2}}{(sI_1 + \delta^2)^2 + 4\delta^2} \left[2 - \frac{2 + sI_1 + \delta^2}{\sqrt{1 + sI_1}} \right] \right\} \quad (7.4-1)$$

To simplify the problem, we assume that the radiation is at gain center. Then $x_\ell = \epsilon\delta$ and using equations (4.2-4) and (4.2-6) one can write

$$x_m - x = \beta \left\{ F(x) + \frac{\sqrt{\pi}}{2} \left(\frac{sI\delta}{(sI + \delta^2)^2 + 4\delta^2} \right) \left(2 - \frac{2 + sI + \delta^2}{\sqrt{1 + sI}} \right) \right\}$$

or

$$\delta_m - \delta = \beta \left\{ \frac{F(\epsilon\delta)}{\epsilon} + \frac{\sqrt{\pi}}{2\epsilon} \left(\frac{sI\delta}{(sI + \delta^2)^2 + 4\delta^2} \right) \left(2 - \frac{2 + sI + \delta^2}{\sqrt{1 + sI}} \right) \right\} \quad (7.4-2)$$

For radiation very near to gain center ($\delta \rightarrow 0$) equation (7.4-2) simplifies to

$$\delta_m - \delta = \beta \delta \left[1 + \frac{\sqrt{\pi}}{2\epsilon sI} \left(2 - \frac{2 + sI}{\sqrt{1 + sI}} \right) \right] \quad (7.4-3)$$

Since the line width $\Delta\nu$ is proportional to $\Delta\delta$, one finds

$$\Delta\nu = \frac{\Delta\nu_0}{1 + \beta \left[1 + \frac{\sqrt{\pi}}{2\epsilon sI} \left(2 - \frac{2 + sI}{\sqrt{1 + sI}} \right) \right]} \quad (7.4-4)$$

The z dependence of the intensity is complicated, and for simplicity we neglect the averaging which appears in equation (7.4-4). The results should still be qualitatively correct.

A plot of the coefficient of $\Delta\nu_0$ from equation (7.4-4) as a function of sI is given in Figure 7.2 for $\beta = 10$. The natural damping ratio ϵ was chosen to be .0083, which is the value roughly appropriate to a xenon laser at 3.51 microns ($\Delta\nu_D \approx 100\text{MHz}$, $\Delta\nu_h \approx 1\text{MHz}$). In the limit of no saturation ($sI = 0$) the line width is reduced by a factor of eleven in agreement with the unsaturated

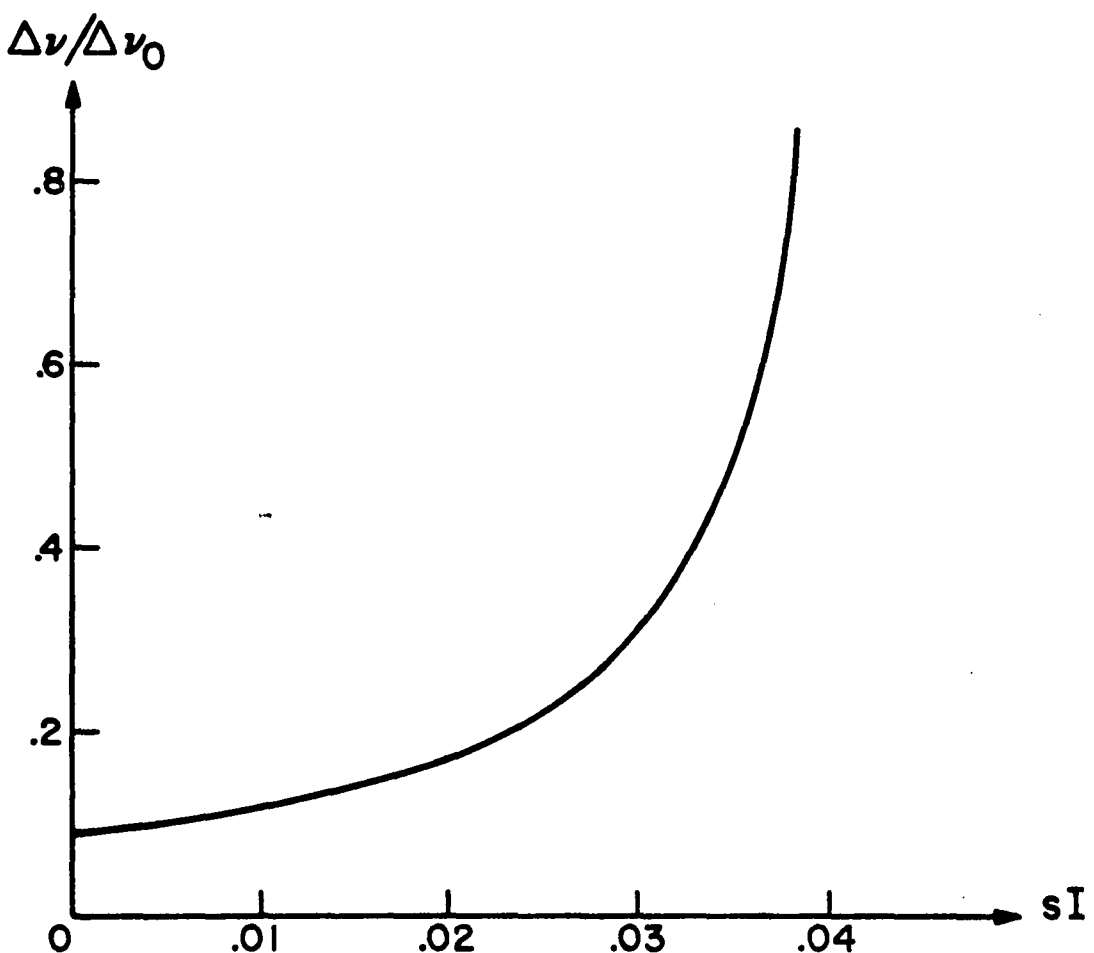


Figure 7.2 Dispersion factor at line center from equation (7.4-4)
versus sI for $\beta = 10$.

line width results of Figure 7.1. As saturation becomes important, the line width increases past its nondispersed value to infinity. The line width doesn't actually go to infinity, of course, because the analysis breaks down when the line width becomes comparable to the radiation broadened homogeneous line width.

To look at the saturation broadening somewhat differently we write equation (7.4-2) as

$$\frac{\delta_m - \delta}{\beta} = \frac{F(\epsilon\delta)}{\epsilon} + \frac{\sqrt{\pi}}{2\epsilon} \left[\frac{sI\delta}{(sI + \delta^2)^2 + 4\delta^2} \right] \left[2 - \frac{2 + sI + \delta^2}{\sqrt{1 + sI}} \right] \quad (7.4-5)$$

Graphical solutions of equation (7.4-5) are shown in Figure 7.3 for various values of sI with $\beta = 10$ and $\epsilon = .0083$. For $sI = 0$ there is no saturation and the figure is the same (except for scale) as Figure 4.1c. As sI increases the slopes of the left and right sides of equation (7.4-5) become more nearly equal and the line broadening shown in Figure 7.2 results. For sufficiently high intensity the right side is steeper than the left and as a consequence the mode splits into three. Thus the presence of an intense monochromatic field makes possible laser oscillation at neighboring frequencies. This situation is not particularly physical because the neighboring lines will themselves saturate causing further modification of the dispersion profile.

The purpose of the preceding discussion has been to make plausible the following assertion. The onset of saturation results in a broadening of the oscillation line from its dispersion-narrowed

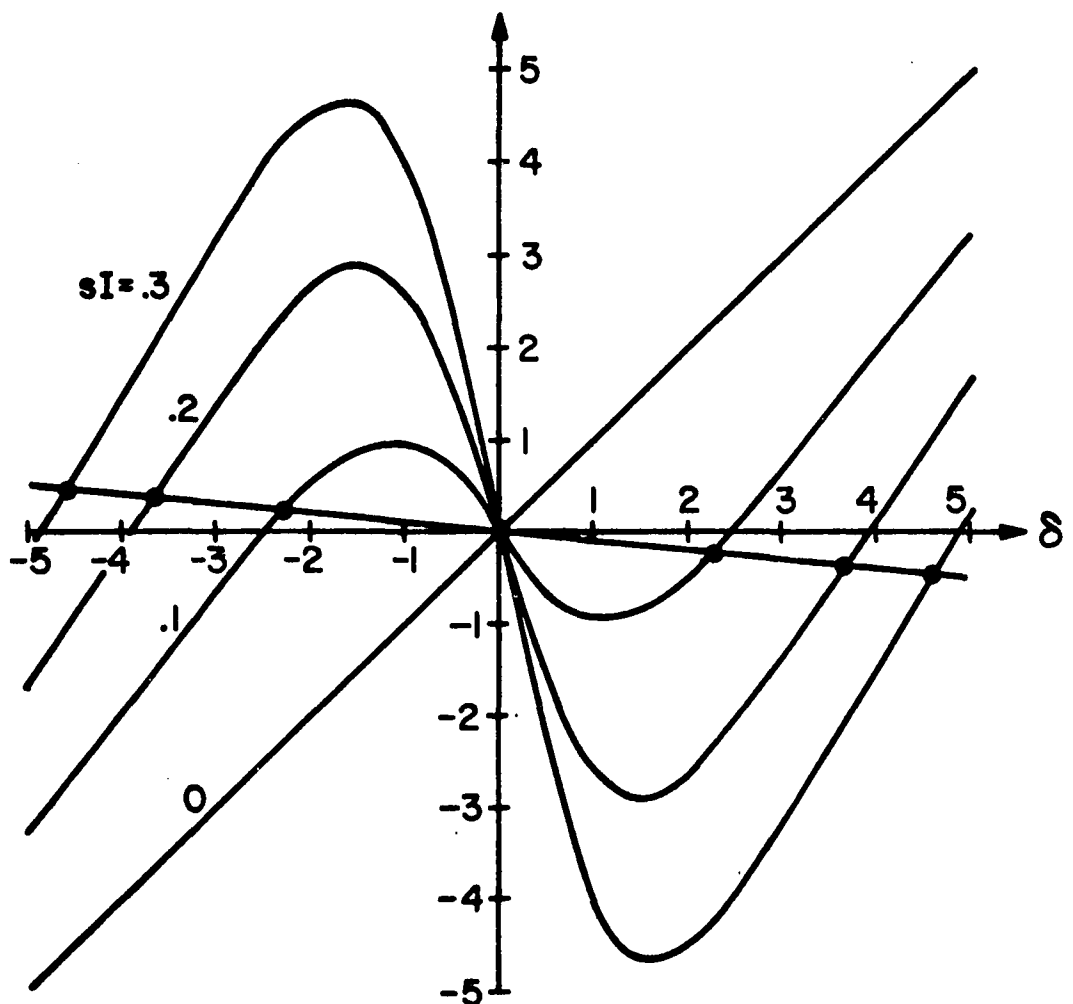


Figure 7.3 Graphical solution for mode splitting caused by a single intense monochromatic field.

value to a value comparable to the width of the hole burned in the gain spectrum. With increasing intensity the line continues to broaden following the increasing hole width. It is the hole width, of course, which characterizes the frequency regime which is affected by the saturation. A rigorous treatment of this problem would require a complicated computer solution which we have not attempted. The considerations given here provide an adequate description of the experimentally observed saturation broadening which is described in the next section. From equation (7.4-4) it is evident that if the natural damping ratio is too large, saturation broadening cannot be important.

For extremely intense fields the entire gain line would be burned down and dispersion effects would vanish. Thus in a very high Q cavity the line width would return to its nondispersed value. This situation is not conveniently attainable in our laser system and we do not consider it further. Also, we have only treated here the case of a strongly inhomogeneous laser transition. For the opposite limit of a homogeneous transition the line remains Lorentzian and the results of the previous section can, with slight modifications, be applied.

In this section we have shown in a nonrigorous fashion that the oscillation line width of a high gain inhomogeneously broadened laser is expected to increase with increasing saturation in contrast to the generally accepted theoretical behavior which predicts a narrowing. The line width increases rapidly until it is roughly equal to the width of the hole in the gain spectrum. It is then expected to increase at the same rate as the average hole

width. The hole width is given by equation (2.7-25) as

$$\Delta v_{\text{hole}} = \Delta v_h (1 + \sqrt{1 + sI}) \quad (7.4-6)$$

Thus for intense fields the line width should grow as the square root of the intensity.

7.5 Experiment

The apparatus used in the line width measurements was identical to that described in Section 4.5 in connection with the mode pulling experiments and the description is omitted here. If the laser were oscillating in a single longitudinal mode, there would be a beat spectrum near D.C. the width of which would be a measure of the oscillation line width. The spectrum analyzer used was insensitive near D.C., however, so the line width measurements could not be made in this way. Instead, the laser was adjusted to operate on two longitudinal modes, and the line width was inferred from the width of the beat between the modes.

The beat spectrum is related to the oscillation spectrum by the convolution integral^(7.2)

$$S(v) \sim \int_0^\infty I(\zeta) I(\zeta + v) d\zeta \quad (7.5-1)$$

In particular, if the oscillation spectrum is roughly Gaussian in shape, one can show that the beat spectrum will also be a Gaussian which is broader by a factor of the square root of two. In our experiments the beat frequency is usually not especially Gaussian-looking, but the width of the beat is nevertheless expected to be a reasonable measure of the oscillation line width. The factor $\sqrt{2}$ is also ignored since only qualitative agreement with the saturation broadening theory is sought.

A typical beat spectrum is shown in Figure 4.3. Thus, the beat in this case occurs at about 46 MHz and has a width of about 1 MHz. Some experimental data are collected in Figure 7.4. The

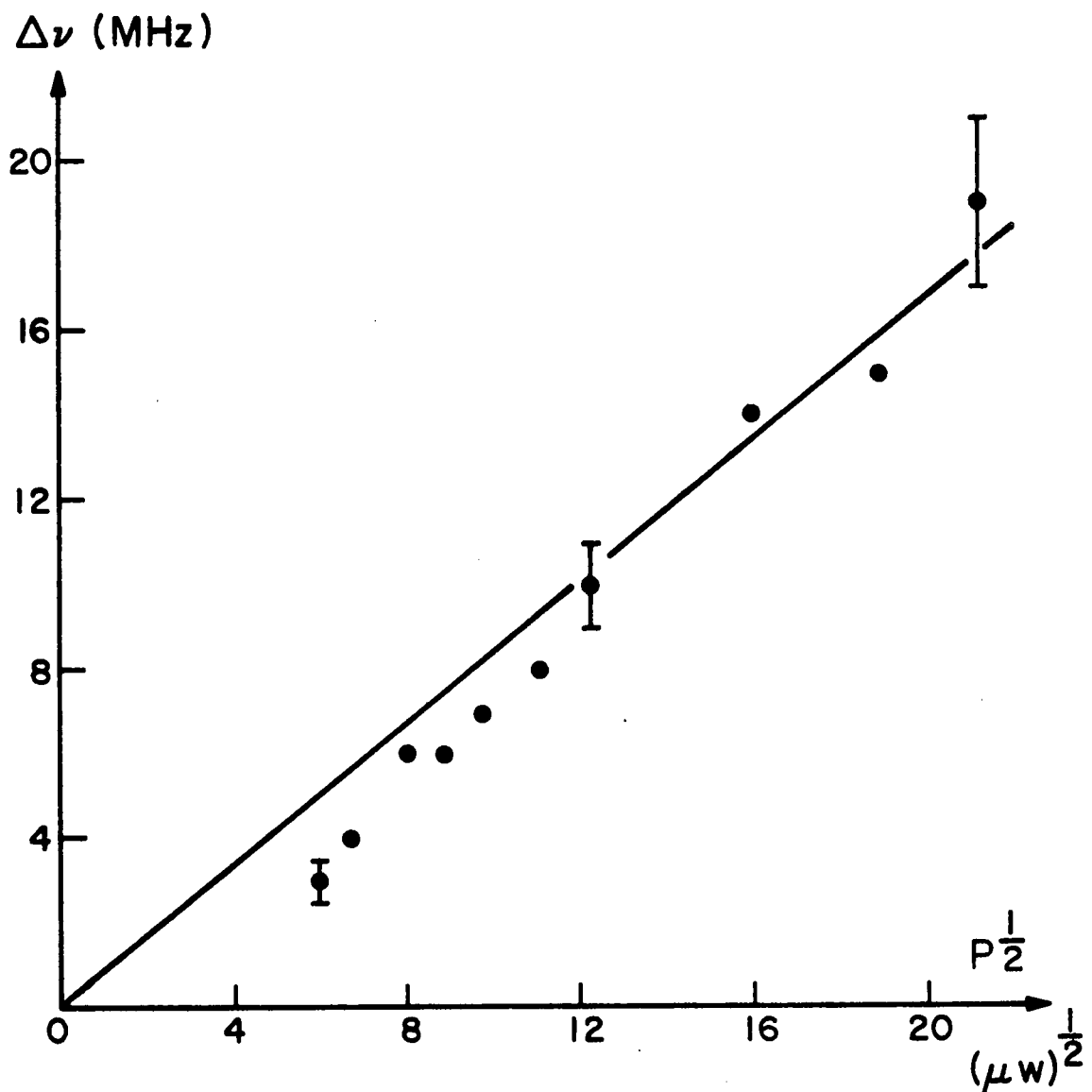


Figure 7.4 Beat line width versus the square root of output power and some typical error brackets.

values were obtained by varying the discharge current (gain) and using no additional attenuation in the cavity. A straight line is roughly fitted to the data in accordance with the high intensity limit of equation (7.4-6).

Errors in the line width data are substantial, particularly when the saturation is strong. The primary cause of these uncertainties is the somewhat irregular shape of the beat spectrum. These irregularities are not well understood. Probable contributors are the non-Gaussian gain line resulting from isotope shifts and hyperfine structure, and relaxation oscillations. It is presumably this broad oscillation line width which makes possible the high frequency relaxation oscillations described in Chapter VI. Additional work on the relation between the line width and the intensity fluctuations would probably be justified.

The good agreement between the theory and the data supports the conclusion that the saturating line width is roughly equal to the hole width. According to equation (6.2-28), the hole width is given by $\Delta\nu_{\text{hole}} = a\Delta\nu_h$ where a is the threshold parameter. With our apparatus values of a of up to six or seven should be obtainable. This factor agrees well with the maximum amount of saturation broadening we have observed. From section 3.2 the homogeneous line width is about 4 MHz, so that the oscillation line width is in semiquantitative agreement with the hole width for strong saturation. For weak saturation the oscillation line width may be less than the homogeneous line width since saturation broadening is then unimportant. Measurements of the line width at intensities far below the saturation level have not been possible

- 243 -

due to insufficient sensitivity of our equipment.

7.6 Conclusion

It was shown in this chapter that the oscillation line width of a high gain laser may differ widely from that expected on the basis of a circuit model treatment, even if dispersion effects are ignored. Dispersion can lead to an additional narrowing or broadening of the laser line. In a strongly saturated laser which is primarily inhomogeneously broadened the line width tends to follow the hole width. An experiment was performed which supports this conclusion.

Bibliography

- 7.1 A. Yariv, Quantum Electronics, Wiley and Sons, New York,
section 24.1 and references, 1967.
- 7.2 A. T. Forrester, Journal of the Optical Society of America
51, No. 3, page 253, equation (5), March 1961.

VIII. Spectral Narrowing

8.1 Introduction

Spectral narrowing refers to the fact that under some circumstances radiation incident on a laser amplifier or generated within an amplifier will emerge with a narrower spectrum than it started with. In high gain lasers spectral narrowing may be substantial. This phenomenon is well known and it has recently found application in high resolution spectroscopy^(8.1). Spectral narrowing can provide a highly stable and monochromatic light source. The applications of such a frequency standard in metrology are well known^(8.2). Comparison of the input and output spectra of a laser amplifier might provide a sensitive indirect measurement of the amplifier gain. The narrowing of transition line profiles due to radiation fields has been considered by Feld and Javan^(8.3). The narrowing of net gain in unsaturated amplifiers has been treated experimentally and theoretically by Hotz^(8.4).

The purpose of this chapter is to study in some detail the influence of an amplifying medium on a spectral continuum including the effects of saturation and distributed loss. Emphasis is placed on the important problem of superradiance, but narrowing in other amplifiers and oscillators is also considered and limiting line widths are determined. It is found that in unsaturated amplifiers the narrowing is essentially independent of the resonance broadening mechanism and the narrowed line approaches a Gaussian. The onset of saturation slows or reverses the narrowing process. Attention is mostly

restricted to illustrative limiting cases when the general solutions become mathematically tedious and of limited practical interest.

8.2 Unsaturated amplifiers

In an unsaturated amplifier the growth of an intensity continuum

$I(y_\ell)$ is governed by

$$\frac{dI(y_\ell, z)}{dz} = g(y_\ell) I(y_\ell, z) - \alpha I(y_\ell, z) + \eta g(y_\ell) \quad (8.2-1)$$

where y_ℓ is the homogeneous frequency difference which is defined following equation (2.5-4) and $I(y_\ell)$ is the intensity per unit frequency range. The unsaturated incremental gain spectrum $g(y_\ell)$ is, for simplicity, assumed to be independent of the distance z . The second term on the right side of equation (8.2-1) represents distributed losses. The last term is the spontaneous emission, which has the same frequency dependence $g(y_\ell)$ as the incremental gain. This one-dimensional approximation is valid in narrow amplifiers. The coefficient η is then proportional to the spontaneous emission rate and to a geometrical factor which depends on the amplifier dimensions.

Solving for an amplifier of length z yields

$$I(y_\ell, z) = I(y_\ell, 0) e^{\frac{[g(y_\ell) - \alpha]z}{g(y_\ell)}} + \frac{\eta g(y_\ell)}{g(y_\ell) - \alpha} (e^{\frac{[g(y_\ell) - \alpha]z}{g(y_\ell)}} - 1) \quad (8.2-2)$$

Superradiance will be considered first. In a superradiant source there is no input, and if losses are negligible equation (8.2-2) simplifies to

$$I(y_\ell, z) = \eta (e^{\frac{g(y_\ell)z}{g(y_\ell)}} - 1) \quad (8.2-3)$$

Defining $f(y_\ell)$ as the fraction of the line center intensity at the

frequency y_ℓ yields

$$f(y_\ell, z) = \frac{I(y_\ell, z)}{I(0, z)} = \frac{g(y_\ell)z}{e^{g(0)z} - 1} \quad (8.2-4)$$

From equation (2.4-9) one has an expression for $g(y_\ell)$ in the limit

$$I(y_\ell) \rightarrow 0$$

$$g(y_\ell) = \frac{k}{\pi} \int_{-\infty}^{\infty} \frac{e^{-\epsilon^2 y_\ell^2}}{1 + (y - y_\ell)^2} dy \quad (8.2-5)$$

where k is the pumping constant. Most lasers can be classed as either homogeneously or inhomogeneously broadened, so these important limiting cases will be considered first.

For homogeneous broadening ($\epsilon \gg 1$) the Lorentzian in equation (8.2-5) may be taken outside of the integral with the result

$$g(y_\ell)_{\text{hom}} = \frac{k}{\sqrt{\pi} \epsilon} \frac{1}{1 + y_\ell^2} \quad (8.2-6)$$

Combining this with equation (8.2-4) for $f = 1/2$ leads to an expression for the line width as a function of z

$$\Delta y_{\text{hom}} = 2y_\ell \ln 2 = 2 \sqrt{\frac{kz}{\sqrt{\pi} \epsilon} \frac{1}{\ln \frac{1}{2} \left(e^{\frac{kz}{\sqrt{\pi} \epsilon}} + 1 \right)}} - 1 \quad (8.2-7)$$

or

$$\Delta v_{\text{hom}} = \Delta v_h \sqrt{\frac{kz}{\sqrt{\pi} \epsilon} \frac{1}{\ln \frac{1}{2} \left(e^{\frac{kz}{\sqrt{\pi} \epsilon}} + 1 \right)}} - 1 \quad (8.2-8)$$

For short distances ($\frac{kz}{\sqrt{\pi} \epsilon} \ll 1$) the line width given by equation (8.2-8) is just the homogeneous line width Δv_h . For long distances

$(\frac{kz}{\sqrt{\pi} \epsilon} \gg 1)$ where the narrowing effect becomes important, equation (8.2-8) simplifies to

$$\Delta v_{hom} \approx \Delta v_h \sqrt{\frac{\sqrt{\pi} \epsilon}{kz} \ln 2} \quad (8.2-9)$$

$\frac{\Delta v_{hom}}{\Delta v_h}$ is plotted versus the normalized distance $Z_{hom} = \frac{kz}{\sqrt{\pi} \epsilon \ln 2}$ in Figure 8.1. The approximate result given by equation (8.2-9) becomes valid after the width is narrowed to about one half of its initial value.

For an inhomogeneously broadened amplifier ($\epsilon \ll 1$) the Gaussian in equation (8.2-5) may be taken outside of the integral with the result

$$g(y_\lambda)_{inhom} = ke^{-\epsilon^2 y_\lambda^2} \quad (8.2-10)$$

Combining this with equation (8.2-4) for $f = 1/2$ yields

$$\Delta y_{inhom} = \frac{2}{\epsilon} \sqrt{\ln kz - \ln \ln \frac{1}{2}(e^{kz} + 1)} \quad (8.2-11)$$

or

$$\Delta v_{inhom} = \Delta v_D \sqrt{\ln kz - \ln \ln \frac{1}{2}(e^{kz} + 1)} \quad (8.2-12)$$

For short distances ($kz \ll 1$) the width of the emission is equal to the Doppler width Δv_D . For long distances ($kz \gg 1$) one finds

$$\Delta v_{inhom} \approx \Delta v_D \frac{1}{\sqrt{kz}} \quad (8.2-13)$$

A plot of $\Delta v_{inhom}/\Delta v_D$ versus the dimensionless distance $Z_{inhom} = kz$ also appears in Figure 8.1.

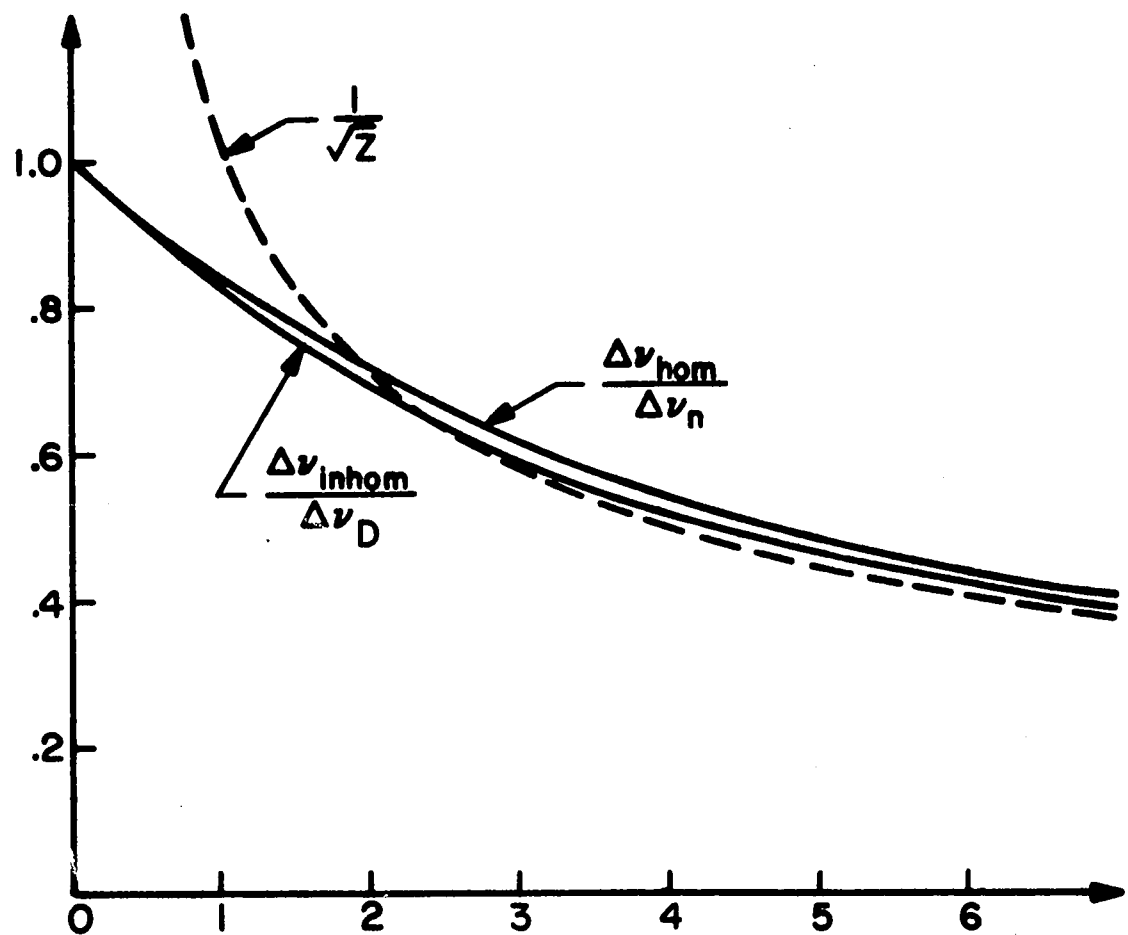


Figure 8.1 Superradiant narrowing versus distance.

The similarity of the plots in Figure 8.1 suggests the non-intuitive result that narrowing proceeds in about the same fashion independent of the line broadening mechanisms. In fact, if the coefficient f had been carried through the algebra, both equations (8.2-9) and (8.2-13) could have been written in the form

$$v - v_0 \sim \sqrt{\frac{-\ln f}{z}} \quad (8.2-14)$$

where v is the frequency at which the spectrum is down to the fraction f of its line center value. Solving equation (8.2-14) for $f(v-v_0)$ shows that at large distances the spectrum becomes Gaussian for both homogeneous and inhomogeneous broadening in contrast to a conclusion of Parks et al^(8.1). The reason for this behavior is that the narrowed line interacts only with the center of the resonance line. For both the Lorentzian and Gaussian lines the center of the line is roughly quadratic in frequency and a quadratic gain supports a narrowing Gaussian spectrum.

To verify the preceding conclusions, one may consider a completely general incremental gain function $g(y_\ell)$ with a maximum at the frequency $y_0 = 0$. Assuming that $g(y_\ell)$ is differentiable in the neighborhood of zero, it may be expanded as

$$g(y_\ell) = g_0 - g_2 y_\ell^2 + g_3 y_\ell^3 + g_4 y_\ell^4 + \dots \quad (8.2-15)$$

where g_0 and g_2 are positive. The spectrum of the superradiance is given by equation (8.2-4) as

$$f(y_\ell) = \frac{e^{[g_0 - g_2 y_\ell^2 + g_3 y_\ell^3 + \dots]z} - 1}{e^{g_0 z} - 1}$$

$$= \frac{e^{g_0 z} e^{-\left(\frac{y_\ell}{\Delta_2}\right)^2} e^{\left(\frac{y_\ell}{\Delta_3}\right)^3} e^{\dots}}{e^{g_0 z} - 1} \quad (8.2-16)$$

where $\Delta_n = (zg_n)^{-1/n}$.

At large distances the zero order terms cancel, leaving

$$f(y_\ell) \approx e^{-\left(\frac{y_\ell}{\Delta_2}\right)^2} e^{\left(\frac{y_\ell}{\Delta_3}\right)^3} e^{\dots} \quad (8.2-17)$$

Also, at very large distances one finds that $\Delta_n \ll \Delta_{n+1}$ so that the Gaussian factor is much narrower than the others. Consequently, all of the factors but the first may be replaced with their value at line center. Therefore,

$$f(y_\ell) \approx e^{-\left(\frac{y_\ell}{\Delta_2}\right)^2}, \quad \Delta_2 = \frac{1}{\sqrt{g_2 z}} \quad (8.2-18)$$

This is in agreement with the previous results for homogeneous and inhomogeneous broadening as may be verified by expanding $g(y_\ell)$ of equations (8.2-6) and (8.2-10) in power series in y_ℓ to obtain g_2 .

The expression for the incremental gain $g(y_\ell)$ in a laser with an arbitrary amount of Doppler broadening given by equation (8.2-5) contains only even terms as can be seen by writing it as

$$g(y_\ell) = \frac{k}{\pi} e^{-\epsilon y_\ell^2} \int_{-\infty}^{\infty} \frac{e^{-\epsilon^2 t^2}}{1+t^2} \cosh(2\epsilon^2 t y_\ell) dt \quad (8.2-19)$$

with $t = y - y_\ell$. The first terms in the expansion for $g(y_\ell)$ can then be written as

$$g_0 = \frac{k}{\pi} \int_{-\infty}^{\infty} \frac{e^{-\epsilon^2 t^2}}{1+t^2} dt , \quad g_2 = \epsilon^2 (g_0 + \epsilon \frac{dg_0}{d\epsilon}) \quad (8.2-20)$$

This form for the quadratic may be useful when the integral for g_0 can be approximated. Equation (8.2-20) can be shown to agree with equation (8.2-6) in the homogeneous limit ($\epsilon \gg 1$) and with equation (8.2-10) in the inhomogeneous limit ($\epsilon \ll 1$) near line center. More generally if the incremental gain has several maxima, we expect the emission to eventually resolve itself into narrowing Gaussian lines centered on the gain maxima. This resolving effect has been observed by Parks et al^(8.1).

So far only superradiance has been considered. If an amplifier has an input $I(y_\ell, 0)$ and negligible spontaneous emission, equation (8.2-4) for the output light spectrum is replaced by

$$f'(y_\ell, z) = \frac{I(y_\ell, 0)}{I(0, 0)} \frac{e^{g(y_\ell)z}}{e^{g_0 z}} \quad (8.2-21)$$

At large distances this is

$$f'(y_\ell, z) \approx \frac{I(y_\ell, 0)}{I(0, 0)} e^{-\left(\frac{y_\ell}{\Delta_2}\right)^2}, \quad \Delta_2 = \frac{1}{\sqrt{g_2 z}} \quad (8.2-22)$$

If the input is reasonably smooth the output spectrum is simply

$$f'(y_\ell, z) \approx e^{-\left(\frac{y_\ell}{\Delta_2}\right)^2} \quad (8.2-23)$$

If the input is a narrow Gaussian of width Δ_{in} , the output will be a Gaussian of width Δ_{out} such that

$$\left(\frac{1}{\Delta_{out}}\right)^2 = \left(\frac{1}{\Delta_{in}}\right)^2 + \left(\frac{1}{\Delta_2}\right)^2 \quad (8.2-24)$$

The concept of gain narrowing is sometimes useful instead of spectral narrowing. The two are obviously closely related. If one assumes that the input spectrum in equation (8.2-21) is white, then the intensity factors cancel and $f'(y_\ell)$ is a general expression for the gain spectrum of an amplifier normalized to unity on line center. Expressions for the gain line width, for example, are then obtained by setting f equal to one half and solving equation (8.2-21) for y_ℓ 1/2. For an inhomogeneously broadened amplifier the results may be made to conform with those of Hotz^(8.4).

In summary, one may conclude that in an unsaturated amplifier the width of the amplified spectrum decreases with distance. The shape of the spectrum approaches a Gaussian as the effective part of the gain approaches a quadratic. As an example, in a helium-xenon discharge the gain may be 400 dB/m^(8.5) or nearly $k = 100$ so that the spectrum of a superradiant source one meter long would be narrowed according to equation (8.2-13) by a factor of ten provided saturation did not occur. From Section 3.3 the Doppler width of xenon at room temperature is about $\Delta\nu_D = 100$ MHz so the narrowed radiation would

have a width of about 10 MHz. Since the frequency of the 3.51 micron transition is about 10^8 MHz, the light would be monochromatic to a part in 10^7 . Jaseja et al^(8.6) claim a better stability of one part in 10^9 for a stabilized helium-neon oscillator near threshold over long times. Collimation in a long high gain gas laser is taken care of by the gain profile of the medium itself (Chapter V), and there should not be much difficulty in constructing a gas discharge amplifier of arbitrary length. However, care is necessary to prevent saturation as will be shown in the next section.

8.3 Saturation effects

As saturation sets in, the behavior of the spectrum becomes considerably more complicated and for a completely general treatment computer solutions are required. The details of the general problem may be of limited practical interest, so only certain important limiting situations will be considered here. The qualitative features of the intermediate regions will be apparent.

For a homogeneously broadened amplifier the saturation is governed by equation (2.5-5) which may be written

$$\frac{dI(y_\ell)}{dz} = \frac{kI(y_\ell)}{\sqrt{\pi} \epsilon h(z)} \frac{1}{1 + y_\ell^2} \quad (8.3-1)$$

where

$$h(z) = 1 + s \int_{-\infty}^{\infty} \frac{I(y_n) dy_n}{1 + y_n^2} \quad (8.3-2)$$

and distributed losses are ignored. Thus the gain profile remains Lorentzian even with saturation, although its amplitude decreases. The quadratic term in the expansion of the gain decreases in magnitude and hence a narrow Gaussian beam will continue to narrow, but at a reduced rate as saturation becomes important. Solving as before yields for large distances

$$\Delta\nu_{\text{hom}} = \Delta\nu_h \sqrt{\frac{\sqrt{\pi} \epsilon \ln 2}{k \int dz / h(z)}} \quad (8.3-3)$$

To proceed, expressions for $h(z)$ must be obtained.

For a narrow spectrum equation (8.3-2) becomes

$$h(z) \approx 1 + s \int_{-\infty}^{\infty} I(y_n) dy_n = 1 + sI_t \quad (8.3-4)$$

where I_t is the total intensity. Therefore, it is first necessary to obtain expressions for I_t . Equation (8.3-1) may be integrated over frequency yielding approximately

$$\frac{dI_t}{dz} = \frac{kI_t}{\sqrt{\pi} \epsilon (1 + sI_t)} \quad (8.3-5)$$

Thus in an unsaturated amplifier the intensity grows according to

$$I_t = I_{to} e^{kz/\sqrt{\pi} \epsilon} \quad (8.3-6)$$

while in a highly saturated amplifier the intensity is governed by

$$I_t = I_{to} + \frac{kz}{\sqrt{\pi} \epsilon s} \quad (8.3-7)$$

Eventually distributed losses in the amplifier may become important so that the intensity is determined from

$$\frac{dI_t}{dz} = \frac{kI_t}{\sqrt{\pi} \epsilon (1 + sI_t)} - \alpha I_t = 0 \quad (8.3-8)$$

If the unsaturated gain is much greater than the loss, the steady state intensity is

$$I_t = \frac{k}{\sqrt{\pi} \epsilon \alpha s} \quad (8.3-9)$$

These results may be collected as

$$I_t = \begin{cases} I_{to} e^{\frac{kz}{\sqrt{\pi} \epsilon}} & \text{unsaturated} \\ I_{to} + \frac{kz}{\sqrt{\pi} \epsilon s} & \text{saturated} \\ \frac{k}{\sqrt{\pi} \epsilon \alpha s} & \text{high loss} \end{cases} \quad (8.3-10)$$

They are similar to Rigrod's solutions^(8.7) for monochromatic radiation at gain center.

Using equations (8.3-4) and (8.3-10), equation (8.3-3) may be written for large distances as

$$\frac{\Delta v_{hom}}{\Delta v_h} = \begin{cases} \sqrt{\frac{\sqrt{\pi} \epsilon}{kz} \ln 2} & \text{unsaturated} \\ \sqrt{\frac{\ln 2}{\ln \frac{kz}{\sqrt{\pi} \epsilon}}} & \text{saturated} \\ \sqrt{\frac{\ln 2}{\alpha z}} & \text{high loss} \end{cases} \quad (8.3-11)$$

As the gain is pulled down by saturation, the narrowing rate is slowed. When losses become important, the gain curve is clamped and narrowing speeds up again. In a practical situation it is possible that these regimes of narrowing might not be distinct, but this simplest situation is at least instructive. In a homogeneously broadened amplifier neither saturation nor losses stop the narrowing process.

For an inhomogeneously broadened amplifier ($\epsilon \ll 1$) it will be assumed that the intensity is nearly uniform over a natural line width

so that the governing equation is (2.6-23) or

$$\frac{1}{I(y_\ell)} \frac{dI(y_\ell)}{dz} = \frac{k e^{-\epsilon^2 y_\ell^2}}{1 + \pi s I(y_\ell)} \quad (8.3-12)$$

The spectral density $I(y_\ell)$ is found in the various regions from equation (8.3-12) in a manner essentially identical to the homogeneous case. The results are

$$I(y_\ell) = \begin{cases} I(y_\ell, 0) e^{ke^{-\epsilon^2 y_\ell^2} z} & \text{unsaturated} \\ I(y_\ell, 0) + \frac{k}{\pi s} e^{-\epsilon^2 y_\ell^2 z} & \text{saturated} \\ \frac{k}{\pi \alpha s} e^{-\epsilon^2 y_\ell^2} & \text{high loss} \end{cases} \quad (8.3-13)$$

and consequently the spectral width for large distances is

$$\frac{\Delta v_{inhom}}{\Delta v_D} = \begin{cases} \frac{1}{\sqrt{Kz}} & \text{unsaturated} \\ 1 & \text{saturated} \\ 1 & \text{high loss} \end{cases} \quad (8.3-14)$$

It is evident that the effects of saturation on narrowing in an inhomogeneously broadened amplifier are significantly different from the effects in a homogeneously broadened amplifier. In the inhomogeneous case the onset of saturation reverses the narrowing process and restores the radiation to its Doppler line shape. This occurs because the center of the line saturates first, while the wings continue to grow exponentially.

The minimum line width for a simple inhomogeneous superradiant source may be readily calculated. From equation (8.3-12) it is evident that saturation becomes important when $I(y_0) = 1/\pi s$. Then, using equation (8.2-3), one finds that saturation occurs at a distance z_{sat} given by

$$\begin{aligned} g_0 z_{\text{sat}} &= kz_{\text{sat}} = \ln(1 + \frac{1}{\pi s \eta}) \\ &\approx -\ln \pi s \eta \end{aligned} \tag{8.3-15}$$

Use of this expression in equation (8.2-13) yields the minimum line width

$$\Delta v_{\text{inhom min}} = \frac{\Delta v_D}{\sqrt{-\ln \pi s \eta}} \tag{8.3-16}$$

Thus if, for example, $\eta \approx 10^{-10}$ watts and $s \approx 3 \times 10^{-4}$ watts $^{-1}$, then the Doppler line can be narrowed by at most a factor of about 5.5 before saturation becomes important at a distance in xenon ($k \approx 15$) of about 2.0 meters. These values for η and s are judged to be reasonably valid for our xenon laser based on the data of Clark^(8.8) (assuming that I in our theory is the total power in units of watts.) This narrowing is not too impressive, and decreasing η by orders of magnitude doesn't help much, since the dependence on η involves a logarithm and a square root.

A possible scheme for reducing the ultimate line width is to place attenuators between sections of the amplifying medium. These would cut down the intensity to prevent saturation without affecting the narrowing process. Even in such a system, however, the spectral

line width could never approach zero because there is always broadband background noise being added to the beam by spontaneous emission. The result of the background is that the spectrum must eventually approach a narrow limiting line shape.

The narrowest possible line would be obtained in a long amplifier with distributed losses which are just sufficient to keep the line center intensity somewhat below the saturation intensity $1/\pi s$. To get an estimate of this limiting line shape one can write equation (8.2-1) for steady state with $I = 1/\pi s$ as

$$0 = \frac{g_o}{\pi s} - \frac{\alpha}{\pi s} + \eta g_o \quad (8.3-17)$$

Thus, the appropriate value for the loss constant α is

$$\alpha = g_o(1 + \pi s \eta) \quad (8.3-18)$$

Using this result, equation (8.2-1) away from line center can be written at steady state as

$$0 = g(y_\ell) I(y_\ell) - g_o(1 + \pi s \eta) I(y_\ell) + \eta g(y_\ell) \quad (8.3-19)$$

with the solution

$$I(y_\ell) = \frac{\eta g(y_\ell)}{g_o(1 + \pi s \eta) - g(y_\ell)} \approx \frac{\eta}{1 + \pi s \eta - \frac{g(y_\ell)}{g_o}} \quad (8.3-20)$$

Keeping the second order term in the power series expansion of $g(y_\ell)$ leads finally to the intensity spectrum

$$I(y_\ell) = \frac{1/\pi s}{1 + \frac{g_2}{\pi s n} y_\ell^2} \quad (8.3-21)$$

Therefore, the narrowest possible line is a Lorentzian of width

$$\Delta\nu_{\min} = \Delta\nu_h \sqrt{\frac{\pi s n g_o}{g_2}} \quad (8.3-22)$$

where we have used the definition $y = \frac{2(v_\ell - v_o)}{\Delta\nu_h}$.

If the gain profile is the Gaussian given by equation (8.2-10) then $g_2 = g_o \epsilon^2$ and the line width is simply

$$\Delta\nu_{\min} = \frac{\Delta\nu_h}{\epsilon} \sqrt{\pi s n} = \Delta\nu_D \sqrt{\frac{\pi s n}{\ln 2}} \quad (8.3-23)$$

Using the approximate numbers given previously for s and n , one finds that the Doppler line would be narrowed by a factor of about 4×10^{-7} . A Doppler width of $\Delta\nu_D \approx 10^8$ Hz could yield an intensity spectrum of about 40 Hz width. If the oscillation frequency were about 10^{14} Hz as in xenon, the output could be used as an absolute frequency standard with a stability of about four parts in 10^{13} . Similar calculations can be carried out for the limiting line shape in a laser incorporating discrete rather than continuous losses.

The preceding discussion suggests that a superradiant helium-xenon laser could be useful as an extremely stable frequency standard. Some practical limitations on such a system should be emphasized. The intensity only approaches its limiting form at a rate given by equation (8.2-13). Thus to obtain a line width of 40 Hz for a gain constant of $k \approx 100 \text{ m}^{-1}$ the overall length of the laser would have to be

greater than 10^5 meters which would be awkward in the laboratory. Nevertheless, superradiant lasers of more reasonable lengths should be competitive with stabilized laser oscillators as absolute frequency standards.

We have described a scheme for obtaining extreme spectral narrowing which consisted of a sequence of narrow band amplifiers separated by absorbing filters. An obvious alternate construction would consist of a sequence of narrow band resonant filters separated by laser amplifiers. In this case the narrowing would be accomplished by the filters rather than by the amplifiers. This problem is also straightforward and the details are omitted.

There is an interesting analogy between focussing of beams in amplifiers and spectral narrowing which will conclude this section on amplifiers. It has been shown here that a gain profile which is quadratic in frequency supports a beam with a narrowing Gaussian spectrum. It is also true that a gain profile which is quadratic in space supports a Gaussian beam profile (Chapter V). In fact, starting with the beam matrix for a general lenslike medium in the limit of negligible diffraction (Figure 5.1g), one can show that the spot size of a narrowing plane Gaussian beam in a medium with a gain profile is governed at large distances by

$$w \sim \frac{1}{\sqrt{\alpha_2 z}} \quad (8.3-24)$$

where α_2 is the quadratic term in the gain profile. This expression is the same as equation (8.2-18) governing spectral narrowing.

In this section we have studied the effects of saturation on spectral narrowing in laser amplifiers. It turns out that the narrowing is slowed by saturation in homogeneously broadened amplifiers and reversed in amplifiers which are inhomogeneously broadened. Schemes involving losses have been discussed for eliminating the saturation effects.

8.4 Oscillators

In conventional laser oscillators the resonant frequencies are determined by the resonator configuration, and the line widths are determined mostly by motion of the mirrors. The only effect of the amplifying medium on the output spectrum is to perhaps shift the resonant frequencies and scale the line widths as shown in Chapters IV and VII. This situation is not of interest here. It is possible, however, to design oscillators in which the output spectrum is determined primarily by the amplifying medium, and the resonator geometry is unimportant. Such a system would have obvious frequency stability advantages and is the subject of this discussion.

In the previous section it was shown that narrowing effects are most pronounced in an unsaturated amplifier. Consequently it will be assumed here that the oscillator is operated very near to threshold. Then spatial hole burning and other saturation effects are unimportant and the propagation "constant" may be assumed to be a constant.

The empty cavity mode spacing of a one-dimensional gas laser is $c/2L$. Then the actual mode spacing near line center is given by equation (4.2-8) as

$$\Delta\nu = \frac{c/2L}{1 + \beta} \quad (8.4-1)$$

where β is the dispersion parameter. If the mode spacing is much less than the spectral width of the laser radiation, then the fact that there are discrete modes becomes unimportant for the purposes of this discussion and the cavity is effectively nonresonant. This

clearly is accomplished by making the cavity long according to

$$L \gg \frac{c}{2(1+\beta)\Delta\nu} \quad (8.4-2)$$

where $\Delta\nu$ is now the minimum spectral width. Thus to achieve a line width of one megacycle (for $\beta \ll 1$) the cavity length should be somewhat more than one hundred meters. This is quite long, but lasers have been built much longer^(8.9). Moreover, it is only the cavity which must be long. The amplifying medium may be much shorter.

The previous paragraph described a necessary condition on the cavity in order for any particular amount of narrowing to be possible. The gain and mirror reflectivities must then be chosen so as to maintain the laser intensity just below the strong saturation level. If the medium were homogeneously broadened, saturation would not be so disastrous because it was shown that narrowing continues even in a saturated amplifier. Narrowing could be limited by the Doppler shift due to the velocity of the reflectors. Such motion might be reduced by careful construction and perhaps cooling of the entire cavity. The actual positions of the mirrors are unimportant, in contrast to the situation in an ordinary resonant oscillator. Thus long term stability and resettability are limited only by variations in the laser medium's composition or operating point.

Another possibility for obtaining "nonresonant" feedback in an oscillator has been described by Ambartsumyan et al^(8.10). In it one of the mirrors is replaced by a large number of scatterers. As a result there are many closely spaced resonant frequencies and again the radiation spectrum is determined mostly by the amplifying medium

instead of by the cavity. These authors also report the application of such a scattering mirror to a high gain helium-xenon laser. The spectral narrowing by a factor of five or six which they have observed is about the same, however, as should be obtainable in a similar simple helium-xenon superradiant amplifier.

Throughout this chapter it has always been assumed that the laser was operating at steady state. To study the dynamics of narrowing in oscillators, it is necessary to include time dependence. The simplest possible case is the time dependent, spatially independent intensity in a nonresonant oscillator. Then if there is no saturation, it is clear from equation (2.3-9) that one need only replace z by ct/n_0 in the results which have been obtained to get the time dependence of the spectral width. For example, the spectrum of an abruptly started inhomogeneously broadened laser would narrow as

$$\Delta\nu(t)_{inhom} = \Delta\nu_D \sqrt{\frac{n_0}{kct}} \quad (8.4-3)$$

according to equation (8.2-13).

In this section we have considered briefly some possible applications of the theory of spectral narrowing to nonresonant laser oscillators. The advantage of these schemes is that narrowing which could otherwise only be obtained in unreasonably long amplifiers may perhaps be possible in laboratory sized oscillators.

8.5 Conclusion

It has been shown in this chapter that a gain profile which is quadratic in frequency near its maximum can support a narrowing Gaussian radiation spectrum. The spectral width varies inversely as the square root of distance at long distances. In a homogeneously broadened amplifier saturation slows the narrowing process, while in an inhomogeneously broadened amplifier saturation restores the line to its original inhomogeneous line shape. Narrowed amplifiers and oscillators are potentially useful in spectroscopy, gain measurements, and anywhere a stable absolute frequency standard is needed.

Bibliography

- 8.1 Parks, Ramachandra Rao, and Javan, Applied Physics Letters 13, No. 4, page 142, August 1968.
- 8.2 A review of the methods and applications of laser frequency stabilization is given by G. Birnbaum, Proceedings IEEE 55, page 1015, June 1967.
- 8.3 Feld and Javan, Physical Review 177, No. 2, page 540, 10 January 1969.
- 8.4 Hotz, Applied Optics 4, No. 5, page 527, May 1965.
- 8.5 J. W. Klüver, Journal of Applied Physics 37, No. 8, page 2987, July 1966.
- 8.6 Jaseja, Javan and Townes, Physical Review Letters 10, No. 5, page 165, 1 March 1963.
- 8.7 Rigrod, Journal of Applied Physics 34, No. 9, page 2602, September 1963.
- 8.8 P. O. Clark, Journal of Quantum Electronics QE-1, No. 3, page 109, June 1965.
- 8.9 C. K. N. Patel, "Gas Lasers", in Lasers, ed. Levine, 2, Dekker, 1968.
- 8.10 R. V. Ambartsumyan, N. G. Basov, P. G. Kryukov, and V. S. Letokhov, Progress in Quantum Electronics 1, Part 3, Pergamon Press, page 107 (1970).

IX. Ultrashort Pulses

9.1 Introduction

There are basically two types of transient effects which can occur in laser oscillators. The first of these are the relaxation oscillations. Relaxation oscillations may be considered to include all transients which have characteristic times which are long compared to the laser cavity loop time. The other transients are the ultrashort pulsations, which are fast compared to the cavity loop time. We have discussed relaxation oscillations in Chapter VI, and ultrashort pulses are the subject of this chapter.

Ultrashort pulses result from the phase locking of a large number of longitudinal cavity modes. There are various well known techniques for producing mode locking in lasers. Active mode locking may be achieved by modulating the cavity losses at a frequency equal to the intermode frequency spacing. Passive mode locking may result from the presence in the cavity of suitable nonlinear absorbing or refracting media.

Some lasers mode lock spontaneously. Helium-neon^(9.1) and argon lasers^(9.2), for example, are known to exhibit this behavior. We present in Sections 9.2 and 9.3 some theoretical and experimental considerations relevant to the observation of spontaneous mode locking in a high gain xenon laser^(9.3). Extremely stable pulsations at repetition rates between 5 and 50 MHz have been obtained. The gain dependent pulse width varied from about 5 to 50 nanoseconds. Following completion of this work we found that spontaneous mode locking of

the 3.51 micron xenon laser had been reported previously by Kim and Marantz (9.4).

In Section 9.4 the propagation of these ultrashort pulses through the laser is discussed. It is found experimentally that the pulses travel through the amplifying medium at a velocity less than the vacuum speed of light by as much as a factor of 2.5. The pulse velocity is a function of the gain and agrees with the group velocity.

9.2 Mode locking theory

In this section we present some elementary considerations regarding the mode locking of a high gain xenon laser. No rigorous analysis is attempted. The most basic features of mode locking are assumed to be well known. The mode spacing and pulse repetition rate are equal to $c/2L$ where L is the cavity length (if dispersion is negligible). Consequently, the first problem is the choice of cavity length. There are some basic reasons why the cavity must be a good deal longer than the 1.4 meter length which was used for most of our experiments. In such a short laser only two or three modes at most will be able to oscillate because the Doppler line width is only about 100 MHz (Section 3.3). The modes could probably not be phase locked anyway because of the very strong mode pulling effects described in Chapter IV. Mode pulling makes the mode spacings unequal.

With a much longer laser, on the other hand, the mode spacing is reduced and the laser can support many more longitudinal modes. Moreover, mode pulling effects become less important because, according to equation (4.2-6), the dispersion parameter vanishes for a long laser. There is no reason, of course, why the amplifying medium should be as long as the optical cavity. It turns out to be convenient to place a short (1.1 meters) amplifier tube at one end of the cavity. The amplifier partially recovers between pulses.

Another reason for making the cavity long is to ensure that there is a strong coupling between the longitudinal modes. In a short inhomogeneously broadened laser the modes would be so widely spaced compared to the homogeneous line width that no mode locking could be

expected. The left and right travelling wave components of each mode interact with atoms on opposite sides of the gain spectrum. Thus, with a sufficiently long cavity, it was anticipated that all of the modes should be strongly coupled. There are some obvious practical reasons for making the cavity no longer than necessary. First, the size of the laboratory is finite. Also, alignment becomes more difficult in a long laser.

The width of the ultrashort pulses is approximately equal to the reciprocal of the frequency width of the mode locked spectrum. Thus if a spectrum 100 MHz wide could be mode locked, then the output pulse width would be about 10 nanoseconds. If only two modes were locked, the output would clearly have a sinusoidal envelope. In a high gain laser the width of the spectrum may effectively be varied. The higher the gain, the greater the number of modes which can oscillate in a cavity of fixed length. Therefore, the output pulse width is variable. Increasing the gain should narrow the pulse width.

A rough idea of the total lasing frequency width can be obtained by setting the frequency dependent Doppler intensity gain equal to the loss or line center gain at threshold g_{th} as

$$g_e = \frac{-(\frac{\Delta v}{\Delta v_D})^2 \ln 2}{= g_{th}} \quad (9.2-1)$$

The solution of this equation is

$$\Delta v = \frac{\Delta v_D}{\ln 2} \sqrt{\ln g - \ln g_{th}} \quad (9.2-2)$$

Near threshold the line width is approximately

$$\Delta v \sim \frac{\Delta v_D}{\ln 2} \frac{\sqrt{g - g_{th}}}{\sqrt{g_{th}}} \quad (9.2-3)$$

Therefore, the pulse width should be

$$\Delta t \sim \frac{\ln 2}{\Delta v_D} \frac{\sqrt{g_{th}}}{\sqrt{g - g_{th}}} \quad (9.2-4)$$

This result is compared with some experimental data in the following section.

In this section we have discussed in a qualitative way some theoretical considerations relevant to the mode locking of a high gain 3.51 micron xenon laser. It was shown that mode locking might be expected if the laser is of the appropriate length.

9.3 Mode locking experiment

Phase locking has been observed experimentally in a high gain 3.51 micron xenon laser. Experiments have been performed in both the time domain and the frequency domain. The apparatus used in the time domain studies is shown schematically in Figure 9.1. The discharge was 5.5 millimeters in diameter and the pressure was maintained at about 5 microns by means of a liquid nitrogen trap^(9.5). Flat front surface aluminum mirrors were used, and the beam splitter was a quartz flat.

Extremely stable pulses were observed, and the intensity of the light goes essentially to zero between the pulses. A typical pulse train is shown in Figure 9.2 for a cavity length of 10.7 meters. The pulses were found to get shorter as the gain (discharge current) is increased. This is in agreement with the discussion of the previous section, where it was indicated that increasing the gain increases the number of modes which reach threshold. Some pulse width data are collected in Figure 9.3 for this cavity. The gain was determined from Figure 6.6. The threshold gain was about $g_{th} = 6.8m^{-1}$ and the rough proportionality of equation (9.2-4) was found to be fairly well satisfied. The proportionality constant is about twice as large as expected indicating that, as usual, the Doppler width has effectively been increased by isotope shifts or hyperfine structure.

The shortest pulses observed had a width of only about 8 nanoseconds for a discharge current of 100 ma. The actual pulse width is probably somewhat less than this value because of equipment limitations. The risetime of the amplifier (H.P. model 462A) was specified

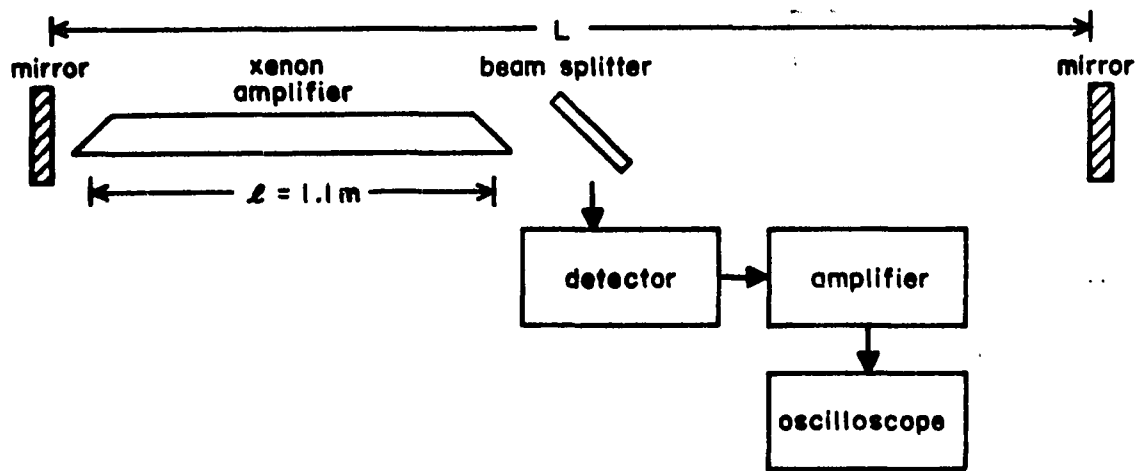


Figure 9.1 Experimental setup for time domain measurements.

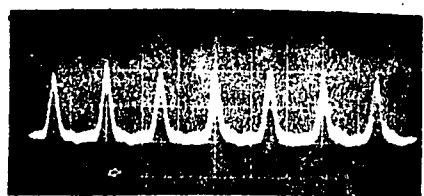


Figure 9.2 Ultrashort pulses at 68 ma. and 50 nanoseconds per division.

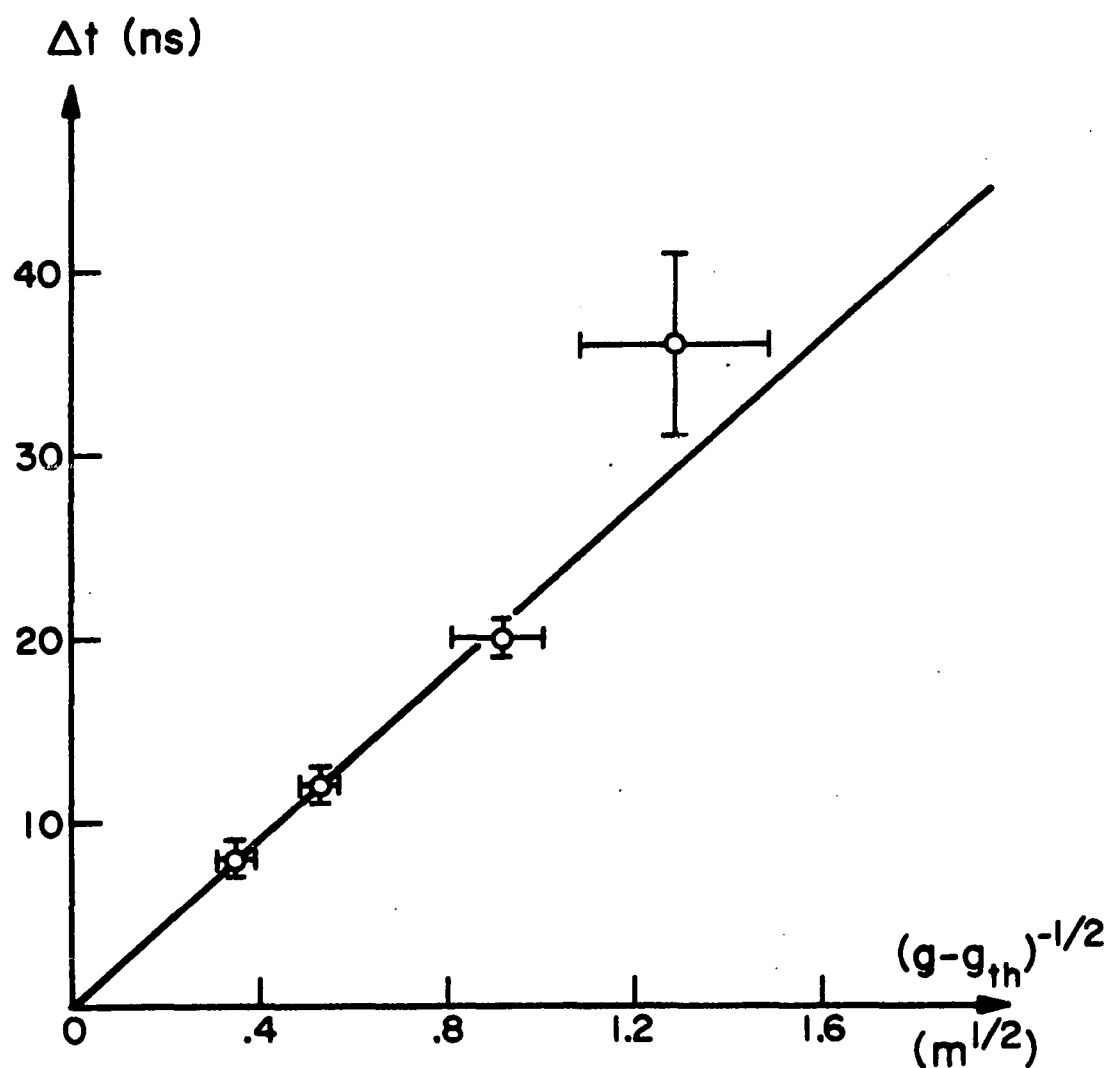


Figure 9.3 Pulse width versus $(g - g_{th})^{-\frac{1}{2}}$

as less than 4 nanoseconds and the risetime of the oscilloscope (Tektronix type 585A with type 82 plug-in) was about 4 nanoseconds. The room temperature InAs detector (Philco L4530) is alleged to have a bandpass of several GHz. The average output power with a 100 ma discharge and a cavity length of 10.7 meters was about 85 μ w as determined with an Eppley thermopile. Therefore, the peak power is on the order of a milliwatt. Near threshold the output is sinusoidal in time as shown in Figure 9.4. Altogether we have obtained pulses in the range of about 5 to 50 nanoseconds pulse width.

The pulse repetition rate has been varied from 5 to 50 MHz by varying the cavity length. With a very long cavity there is some indication of double pulsing. This effect is shown in Figure 9.5 for a cavity length of 33 meters. A small irregular pulse occurs half-way between the dominant pulses indicating that for such a long cavity the medium has time to partially recover between pulses.

With a "short" cavity of 5 or 6 meters length both relaxation oscillations and ultrashort pulsations may be observed simultaneously. The output then consists of a train of relaxation oscillations which is itself modulated by the ultrashort pulses. An example of this situation is shown in Figure 9.6.

The apparatus used in the frequency domain experiments is the same as that shown in Figure 9.1 except that, as usual, the light beam was chopped and a spectrum analyzer and synchronous detector were inserted between the amplifier and oscilloscope. A typical spectrum is shown in Figure 9.7 for a cavity length of 10.7 meters. The dispersion is 5 MHz per division and zero frequency is at the right side

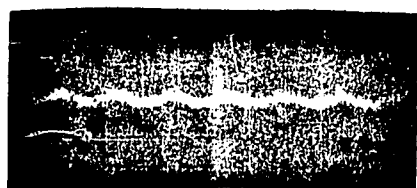


Figure 9.4 Sinusoidal output at 50 nanoseconds per division with a
47 ma. discharge.

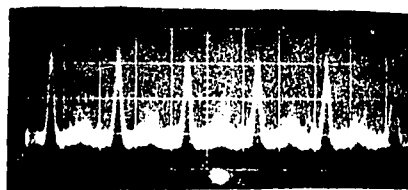


Figure 9.5 Double pulsing at 100 nanoseconds per division with a
79 ma. discharge.



Figure 9.6 Relaxation oscillations and ultrashort pulses at .2 microseconds per division with a discharge of 61 ma.

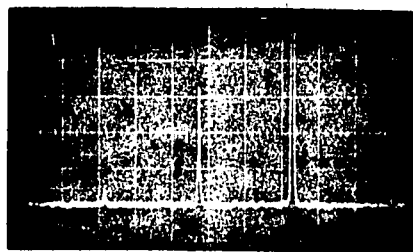


Figure 9.7 Ultrashort pulse spectrum at 5 MHz per division.

of the display. Excellent agreement has been obtained between the form of the mode spectrum and the pulsing in time, which indicates that all of the oscillating modes are locked in phase. Near threshold with only two modes oscillating the sinusoidal output shown in Figure 9.4 was obtained. With ten or twenty modes oscillating the pulse widths are reduced appropriately.

9.4 Pulse propagation

It has been argued theoretically (9.6,9.7) that the velocity of pulse propagation in amplifying or absorbing media is equal to the classical group velocity dw/dk and is thus larger (in an absorbing medium) or smaller (in a gain medium) than the phase velocity.

Experiments designed to verify this prediction (9.8,9.9,9.10) utilized the weak 6328 \AA transition in neon, and the observed changes in velocity were less than a part in a thousand.

In what follows we report on the pulse velocity in a xenon discharge near its amplifying 3.51 micron transition. In this case the combination of high optical gain and narrow linewidth result in extremely large dispersion. The observed pulse velocity is less than $c/2$. Furthermore, using an analytic expression for the gain dependence of the index of refraction of the Doppler broadened transition, we show that the pulse propagation velocity agrees with the group velocity.

The group velocity may be written

$$v_g = \frac{c}{n + v \frac{dn}{dv}} \quad (9.4-1)$$

The frequency dependent index of refraction of a Doppler broadened medium has been given in Section 2.6. If saturation is unimportant and if the homogeneous linewidth is negligible compared to the Doppler width $\Delta\nu_D$, the appropriate expression is equation (2.6-14)

$$n(v) = 1 + \frac{cg F(x)}{2\pi^{3/2} v} \quad (9.4-2)$$

where $F(x)$ is Dawson's integral

$$F(x) = e^{-x^2} \int_0^x e^{t^2} dt \quad (9.4-3)$$

The frequency is measured by $x = [2(v-v_0)/\Delta v_D](\ln 2)^{1/2}$ and g is the small-signal incremental intensity gain constant at line center.

Equations (9.4-1) and (9.4-2) can in principle be combined to obtain the frequency dependent group velocity. We are most interested in the behavior near line center where $F(x) \approx x$. Then equation (9.4-2) may be written

$$n(v) = 1 + \frac{cg(v-v_0)(\ln 2)^{1/2}}{\pi^{3/2}v \Delta v_D} \quad (9.4-4)$$

From equation (9.4-1) the group velocity is then given by

$$\frac{v_g}{c} = \frac{1}{1 + \beta} \quad (9.4-5)$$

where β is the dispersion parameter,

$$\beta = \frac{cg(\ln 2)^{1/2}}{\pi^{3/2} \Delta v_D} \quad (9.4-6)$$

It was shown in Section 4.2 that β can be much greater than unity in xenon amplifiers, so a significant slowing of the pulses should be possible. Equations (9.4-5) and (9.4-6) bear an obvious relation to equations (4.2-7) and (4.2-6) respectively if $\lambda = L$, because the pulse repetition rate must equal the mode spacing.

The apparatus used in our experiment consisted of an optical resonator of length $L = 5.5$ m containing an amplifying xenon discharge section of length $\lambda = 1.1$ m. Other details of the apparatus

are discussed in Section 9.3. A measurement of the pulsation period as a function of gain for a fixed cavity length provides a direct indication of the pulse velocity in the xenon amplifier. The velocity v of the pulses in the amplifying medium is related to the experimentally measured pulsation period T by the expression

$$\frac{v}{c} = \frac{1}{1 + \frac{c}{2L} (T - T_0)} \quad (9.4-7)$$

where $T_0 = \frac{2L}{c} = 37$ nanoseconds would be the pulsation period if the dispersive medium were not present in the cavity. The pulse retardation effects are so strong in xenon that T_0 can be determined to sufficient accuracy by simply measuring the cavity length.

Some experimental results are collected in Figure 9.8 using equation (9.4-7) and the measured values of the pulsation period. The gain calibration was obtained from Figure 6.6. The theoretical curve in the figure is a plot of equation (9.4-5) with the Doppler width taken as $\Delta v_D = 270$ MHz. This value is about twice as large as that resulting from pure Doppler broadening and, as noted in Chapter III, is probably due in part to isotope shifts and hyperfine structure of the transition. The data were obtained by operating very near threshold in order to minimize saturation, which would tend to reduce the pulse retardation. The good agreement between the data points and the theoretical plot shows that the pulse propagation velocity is indeed given by the group velocity.

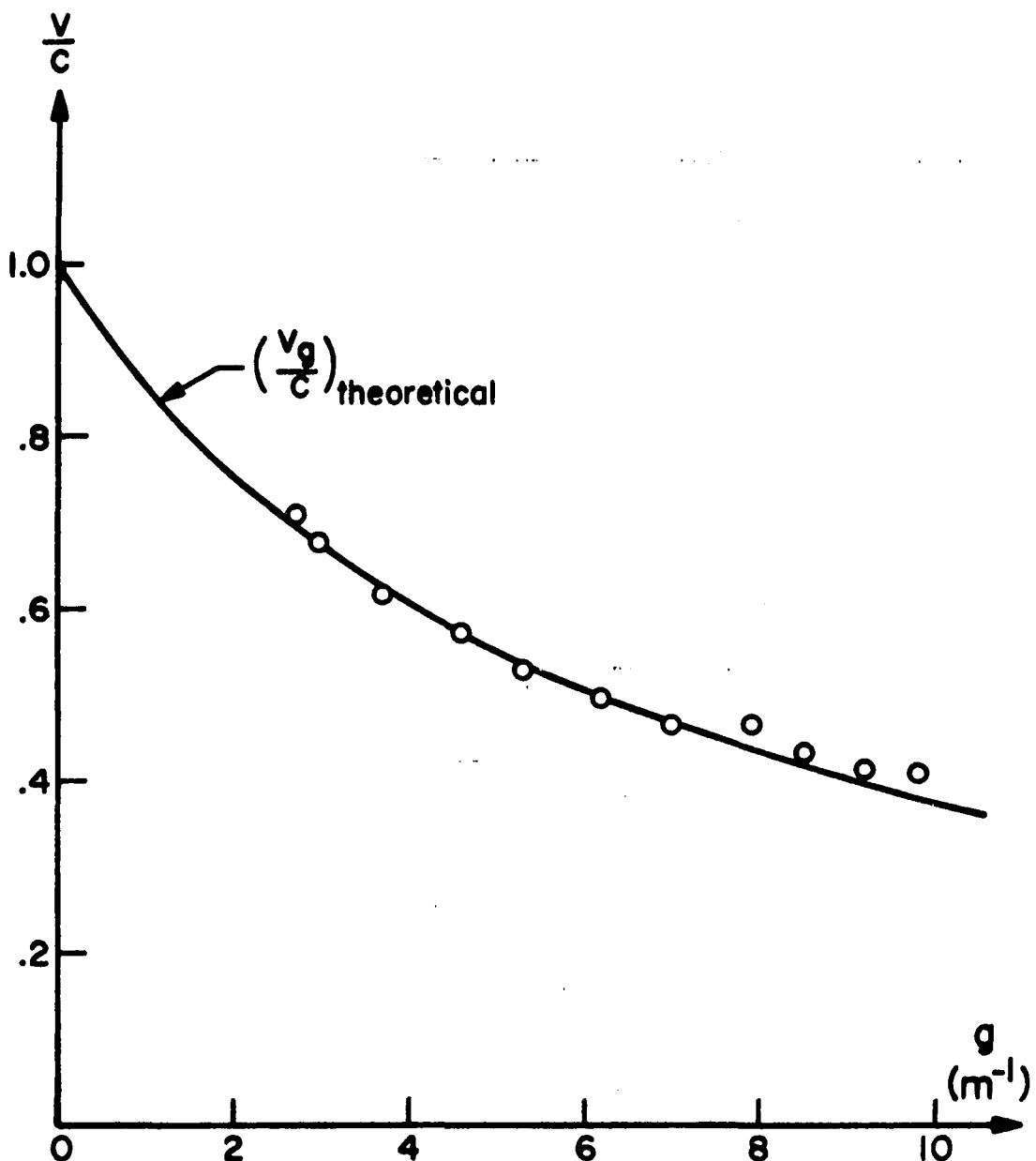


Figure 9.8 Gain dependence of the relative pulse velocity.
Experimental data are indicated by circles.

9.5 Conclusion

We have discussed here the observation of extremely regular pulses in a continuous high gain xenon laser. The results indicate a complete phase locking of all the modes which are above threshold. The time domain and frequency domain results are in good agreement with qualitative theoretical considerations. The theory does not give a rigorous explanation of how the phase locking occurs, but it provided sufficient incentive for us to undertake the experiments.

The pulses which we have observed have repetition rates between about 5 and 50 MHz, depending on the cavity length. The pulse widths were readily varied from about 5 to 50 nanoseconds by varying the discharge current. It is expected that much shorter pulses could be obtained by increasing the amplifier gain and reducing the cavity losses. This should also lead to higher power pulses.

For most of the experiments described in this thesis it would have been advantageous to use monoisotopic xenon. The ultrashort pulse width, on the other hand, is minimized by maximizing the overall gain line width. Consequently to obtain the shortest possible pulses, it would probably be desirable to use an appropriately enriched combination of isotopes. According to Figure 3.4, the hyperfine components of the odd isotopes are scattered over a frequency range of about 1.4 GHz. Therefore, the narrowest pulses possible in xenon would have a width of about .7 nanoseconds.

We have also observed a reduction by a factor of about 2.5 in the propagation velocity of optical pulses due to the dispersion associated with the 3.51 micron transition in xenon. These results are in

agreement with theoretical considerations. The pulse slowing is, in fact, the time domain manifestation of the strong mode pulling discussed in Chapter IV. The slowing effect could be enhanced by using monoisotopic xenon because of its higher gain and narrower linewidth. The incorporation of a xenon absorbing section into the optical resonator should make possible the observation of values of v_g/c considerably in excess of unity.

Bibliography

- 9.1 M. H. Crowell, Journal of Quantum Electronics QE-1, page 12, 1965.
- 9.2 O. L. Gaddy and E. M. Schaefer, Applied Physics Letters 9, No. 8, page 281, 15 October 1966.
- 9.3 L. W. Casperson and A. Yariv, Physical Review Letters 26, page 293, 8 February 1971.
- 9.4 H. H. Kim and H. Marantz, IEEE Journal of Quantum Electronics QE-6, page 749, November 1970.
- 9.5 D. R. Armstrong, Journal of Quantum Electronics QE-4, No. 11, page 968, November 1968.
- 9.6 E. O. Schulz-DuBois, Proceedings of the IEEE 57, No. 10, page 1748, October 1969.
- 9.7 C. G. B. Garrett and D. E. McCumber, Physical Review A1, No. 2, page 305, February 1970.
- 9.8 J. A. Carruthers and T. Bieber, Journal of Applied Physics 40, page 426, 1969.
- 9.9 A. Frova, M. A. Duguay, C. G. B. Garrett and S. L. McCall, Journal of Applied Physics 40, No. 10, page 3969, September 1969.
- 9.10 F. R. Faxvog, C. N. Y. Chow, T. Bieber and J. A. Carruthers, Applied Physics Letters, page 192, 1 September 1970.

X. Power in Laser Oscillators

10.1 Introduction

Conventional treatments of power and coupling in laser oscillators assume that the radiation intensity is uniform throughout the resonator. Typically, the cavity losses are lumped together into a single photon lifetime. For many applications this is a serious approximation and, as a consequence, only qualitative agreement with experiments can be obtained. In high gain lasers the assumption of uniform intensity is especially inappropriate. We refer to the neglect of all spatial variations as the zero dimension approximation. It is considered first for reference purposes.

The next level of sophistication is the one dimension laser approximation. A basic reason why the intensity cannot be uniform in any practical laser is that there must be a power flow toward the mirrors. Thus the energy density is necessarily higher near the ends of a laser than near its center. The one dimension approximation takes account of this variation and is expected to provide satisfactory results for high gain lasers. Some consequences of the theory are verified with a high gain 3.51 micron xenon laser.

The laser beam may also have an intensity profile. Typically, the intensity is higher near the axis of a laser medium than near its outside surface. Modifications of the basic one-dimensional saturation equations are obtained for the important special case of beams with Gaussian intensity profiles. Another type of spatial variation results from the periodic standing wave nature of the electromagnetic fields. If the spatial cross relaxation is "slow", there may result

spatial hole burning or small scale variations in the population inversion density. Some consequences of spatial hole burning have been considered by Tang et al^(10.1) and we assume here that these effects are unimportant.

10.2 Zero dimensions

The purpose of this section is to derive the output power of a laser oscillator in the simplest possible approximation. This involves the assumption that all of the parameters of the laser including the radiation fields are uniform throughout the cavity. This is the approximation which is usually used in the treatment of oscillator problems. The results will be compared with those obtained by more accurate treatments in the following sections.

The basic relation, equation (2.4-7), governing the saturation at a point in a Doppler broadened laser medium which is illuminated by several discrete lines at the frequencies y_n may be written

$$\frac{dI_i}{dz} = \frac{gI_i}{\pi} \int_0^{\infty} \frac{-\epsilon^2 y^2 e^{-dy}}{[1 + (y-y_i)^2][1 + s \sum_{n=1}^{\infty} \frac{I_n}{1 + (y-y_n)^2}]} - \alpha I_i \quad (10.2-1)$$

Here g , s , and α are respectively the gain, saturation and loss parameters of the medium, I_n is the intensity of the n^{th} line, $y_n = \frac{2(v_n - v_o)}{\Delta v_h}$ is the normalized frequency, and $\epsilon = \frac{\Delta v_h}{\Delta v_D} \sqrt{\ln 2}$ is the natural damping ratio. If ϵ is sufficiently large, one obtains the homogeneous limit given by equation (2.5-3)

$$\frac{dI_i}{dz} = g' I_i \frac{1}{[1 + y_i^2][1 + s \sum_{n=1}^{\infty} \frac{I_n}{1 + y_n^2}]} - \alpha I_i \quad (10.2-2)$$

where $g' = g/\sqrt{\pi} \epsilon$.

We consider here only the simplest case of a single mode having equal intensities travelling to the left and to the right. If the radiation is at gain center and the one way intensity is I , then equation (10.2-2) becomes

$$\frac{dI}{dz} = \frac{g'I}{1 + 2sI} - \alpha I \quad (10.2-3)$$

If the radiation were not at gain center, g' and s should be replaced by

$$g^* = \frac{g'}{1 + y_1^2}, \quad s^* = \frac{s}{1 + y_1^2} \quad (10.2-4)$$

The intensity gained in a loop through the cavity is

$$\Delta I = \frac{2g'IL}{1 + 2sI} - 2\alpha IL \quad (10.2-5)$$

where it is assumed that the single pass gain is very small and L is the length of the medium.

This intensity gain must equal the intensity lost at the mirrors. If the reflectivities of the left and right mirrors are R_L and R_R respectively, then the intensity is governed by

$$(1 - R_L)I + (1 - R_R)I = \frac{2g'IL}{1 + 2sI} - 2\alpha IL \quad (10.2-6)$$

The solution of this equation is

$$I = \frac{1}{s} \left[\frac{g'L}{(1 - R_L) + (1 - R_R) + 2\alpha L} - \frac{1}{2} \right] \quad (10.2-7)$$

The output intensities at the right and left ends of the laser are

$$I_o^+ = \frac{T_r}{s} \left[\frac{g'L}{(1 - R_\ell) + (1 - R_r) + 2\alpha L} - \frac{1}{2} \right] \quad (10.2-8)$$

$$I_o^- = \frac{T_\ell}{s} \left[\frac{g'L}{(1 - R_\ell) + (1 - R_r) + 2\alpha L} - \frac{1}{2} \right] \quad (10.2-9)$$

The plus and minus sign superscripts here denote beams travelling to the right and left respectively and T_r and T_ℓ are the mirror transmission coefficients. For comparison with later work we also write the obvious relation between the outputs at the two ends of the laser

$$\frac{I_o^+}{T_r} = \frac{I_o^-}{T_\ell} \quad (10.2-10)$$

All spatial variations were neglected in deriving equations (10.2-7) to (10.2-10), and we refer to these results as the zero dimension approximation for a single mode homogeneously broadened laser oscillator.

If ϵ is sufficiently small, equation (10.2-1) reduces to the inhomogeneous limit

$$\frac{dI_1}{dz} = \frac{qI_1}{\pi} e^{-\epsilon^2 y_i^2} \int_{-\infty}^{\infty} \frac{dy}{1 + (y - y_i)^2 + sI_1 + s \sum_{n \neq 1} I_n \left[\frac{1}{1 + (y - y_n)^2} \right]} - \alpha I_1 \quad (10.2-11)$$

This integration cannot be performed in general. A qualitative approximation can be obtained, however, by observing that the integrand is nonzero only for y nearly equal to y_i . Setting $y = y_i$ in the last term in the denominator leads to

$$\begin{aligned} \frac{dI_i}{dz} &= \frac{gI_i}{\pi} e^{-\epsilon^2 y_i^2} \int_{-\infty}^{\infty} \frac{dy}{1 + (y-y_i)^2 + sI_i + s \sum_{n \neq i} \frac{I_n}{1 + (y_i - y_n)^2}} - \alpha I_i \\ &= \frac{gI_i e^{-\epsilon^2 y_i^2}}{(1 + sI_i + s \sum_{n \neq i} \frac{I_n}{1 + (y_i - y_n)^2})^{1/2}} - \alpha I_i \end{aligned} \quad (10.2-12)$$

This approximation becomes rigorous in the limit of weak saturation.

In a Doppler broadened laser a single mode corresponds in effect to two travelling wave fields on opposite sides of the gain curve. This is because the right and left travelling waves interact with atoms having opposite axial components of thermal velocity. For this case the equation for the right travelling beam is

$$\frac{dI^+}{dz} = \frac{gI^+ e^{-\epsilon^2 y^2}}{(1 + sI^+ + \frac{sI^-}{1 + 4y^2})^{1/2}} - \alpha I^+ \quad (10.2-13)$$

If the gain is small, $I^+ \approx I^- \approx I$ and equation (10.2-13) reduces to

$$\frac{dI}{dz} = \frac{gI e^{-\epsilon^2 y^2}}{[1 + sI(1 + \frac{1}{1 + 4y^2})]^{1/2}} - \alpha I \quad (10.2-14)$$

The double pass intensity gain is

$$\Delta I = \frac{2gIL e^{-\epsilon^2 y^2}}{[1 + sI(1 + \frac{1}{1 + 4y^2})]^{1/2}} - 2\alpha IL \quad (10.2-15)$$

In terms of the mirror reflectivities this is

$$(1 - R_L) + (1 - R_R) = \frac{2gL e^{-\epsilon^2 y^2}}{\left[1 + sI\left(1 + \frac{1}{1+4y^2}\right)\right]^{1/2}} - 2\alpha L \quad (10.2-16)$$

Therefore, the one way intensity in the cavity is

$$I = \frac{1}{s\left(1 + \frac{1}{1+4y^2}\right)} \left[\left(\frac{2gL e^{-\epsilon^2 y^2}}{(1 - R_L) + (1 - R_R) + 2\alpha L} \right)^2 - 1 \right] \quad (10.2-17)$$

We refer to this result as the zero dimension approximation for an inhomogeneously broadened laser. When y goes to zero the output clearly drops by a factor of two (neglecting the Gaussian). This effect is, of course, the well known Lamb dip.

We have obtained here some approximate results for the intensity in homogeneous and inhomogeneous lasers in which all spatial variations can be neglected. This approximation is only valid if the gain per pass is very small and if the beam and gain profiles are uniform. In the next section we relax the condition of small gain, and in Section 10.4 some profile effects are considered.

10.3 One dimension

The solutions of some one-dimensional amplifier problems have been obtained by Rigrod^(10.2) and others. In this section we consider the problem of a laser oscillator with arbitrarily large single pass gain. At first sight this problem would seem to be quite complicated because the left and right travelling waves may interact with the same atoms. It turns out, however, that some simple and useful analytical results can be obtained for the output intensity of a high gain laser. In many situations it is found that the product of the right and left travelling waves is a constant independent of position in the laser.

As our starting point we use again equation (10.2-1). We consider the situation where the light travelling to the right interacts with precisely the same atoms as the light travelling to the left. This is the case for a homogeneously broadened transition and also for one in which the inhomogeneous broadening is due to the Stark or Holzmark effects. It is, of course, not valid for Doppler broadened transitions. The Gaussian factor should be replaced by the appropriate inhomogeneous spectrum for nonDoppler broadening.

Equation (10.2-1) for a line propagating to the right may be rewritten

$$\frac{dI_1^+}{dz} = \frac{gI_1^+}{\pi} \int_{-\infty}^{\infty} \frac{e^{-\epsilon^2 y^2}}{[1 + (y-y_1)^2][1 + s \sum_n \frac{I_n^+ + I_n^-}{1 + (y-y_n)^2}]} dy - \alpha I_1^+ \quad (10.3-1)$$

where the superscripts + and - label the beams travelling to the right and left respectively. A similar equation can be written for the corresponding beam travelling to the left

$$\frac{dI_i^-}{dz} = -\frac{g I_i^-}{\pi} \int_{-\infty}^{\infty} \frac{e^{-\epsilon^2 y^2} dy}{[1 + (y - y_i)^2][1 + s \sum_n \frac{I_n^+ + I_n^-}{1 + (y - y_n)^2}]} + \alpha I_i^- \quad (10.3-2)$$

The signs in equation (10.3-2) are different from those in equation (10.3-1) because by definition the left travelling beam grows in the minus z direction.

By comparing equations (10.3-1) and (10.3-2) one obtains the relation

$$\frac{1}{I_i^+} \frac{dI_i^+}{dz} = -\frac{1}{I_i^-} \frac{dI_i^-}{dz} \quad (10.3-3)$$

This equation may be expressed in terms of the logarithm as

$$\frac{d}{dz} \ln(I_i^+ I_i^-) = 0 \quad (10.3-4)$$

The solution of this equation is the simple theorem

$$I_i^+ I_i^- = \text{const.} \equiv a_i \quad (10.3-5)$$

Thus we have the important result that the product of the intensity to the right and the intensity to the left for a single laser line is a constant throughout the amplifying medium. Summing over all of the lines yields

$$\sum_n I_n^+ I_n^- = \text{const.} \quad (10.3-6)$$

Equations (10.3-5) and (10.3-6) hold even for resonators containing more than one amplifying (or absorbing) medium. This is so

because the intensity product at the right end of one medium must be the same as the product at the left end of the next, and from equation (10.3-5) the product is a constant throughout each medium. By letting the segments of amplifying material become arbitrarily short, one can conclude that equations (10.3-5) and (10.3-6) hold even if g , s , and α are functions of z . This result is also evident by giving g , s , and α a z dependence in equations (10.3-1) and (10.3-2).

It is perhaps worthwhile to make equation (10.3-5) a little more plausible by considering two special cases. If the "medium" consists of free space, then the intensity each way is a constant and so is the intensity product. In a nonsaturating absorber the fields decay exponentially for propagation in either direction. But the product of these two exponentials is a constant as required by equation (10.3-5). That this equation should hold also in saturating medium is a non-trivial consequence of the basic laser saturation equations.

Equation (10.3-5) has immediate consequences for the laser output. A potentially important practical problem in a high gain laser is the question of what fraction of the energy output comes out of each end of the resonator. Assume that the transmission and reflection of the left and right mirrors are given respectively by T_L , R_L and T_R , R_R . The usual assumption that the intensity is uniform throughout the resonator yields a simple relation between the output intensity at the left of the resonator I_o^- and the output intensity at the right end I_o^+ .

$$\frac{I_o^-}{T_L} = \frac{I_o^+}{T_R} \quad (10.3-7)$$

which we have given in equation (10.2-10). This result holds only when the reflectivities of both mirrors are nearly equal to unity. The correct expression follows simply from equation (10.3-5) as we now show.

The mirrors define relationships between the intensity to the right and to the left at the ends of the resonator

$$I_{il}^+ = R_l I_{il}^- \quad I_{ir}^- = R_r I_{ir}^+ \quad (10.3-8)$$

The notation may be clarified by Figure 10.1. As a consequence of equations (10.3-8),

$$I_{il}^+ I_{il}^- = R_l (I_{il}^-)^2 \quad I_{ir}^- I_{ir}^+ = R_r (I_{ir}^+)^2 \quad (10.3-9)$$

But from equation (10.3-5)

$$I_{il}^+ I_{il}^- = I_{ir}^- I_{ir}^+ \quad (10.3-10)$$

Combining equations (10.3-9) and (10.3-10) yields the relation

$$R_l (I_{il}^-)^2 = R_r (I_{ir}^+)^2 \quad (10.3-11)$$

In terms of the output intensity this is

$$R_l \left(\frac{I_{io}}{T_l} \right)^2 = R_r \left(\frac{I_{io}}{T_r} \right)^2 \quad (10.3-12)$$

Taking the square root of both sides gives

$$\frac{\sqrt{R_l}}{T_l} I_{io}^- = \frac{\sqrt{R_r}}{T_r} I_{io}^+ \quad (10.3-13)$$

Equation (10.3-13) may be summed over all of the modes to obtain as a

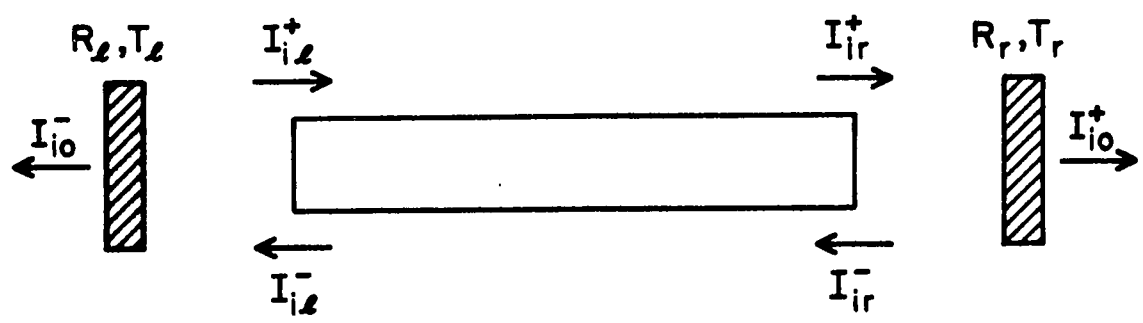


Figure 10.1 Schematic of one dimensional laser.

corollary of equation (10.3-5) the final result

$$\frac{\sqrt{R_L}}{T_L} I_o^- = \frac{\sqrt{R_R}}{T_R} I_o^+ \quad (10.3-14)$$

where $I_o = \sum_n I_{no}$. Equation (10.3-14) is the same as the approximate low gain result, equation (10.3-7), in the limit that the mirror reflectivities approach unity, as we should expect. It describes the relation between the outputs at the left and right ends of a laser having arbitrary mirror properties and unknown gain.

So far, of course, the actual values of the constants a_i , or more generally, the intensities $I_i^-(z)$ and $I_i^+(z)$ have not been determined. To obtain them, a detailed solution of the simultaneous equations (10.3-1) and (10.3-2) is required. Needless to say, this is in general an exceedingly difficult problem. Nevertheless, some important practical problems can be solved. We consider the homogeneous limit of equations (10.3-1) and (10.3-2). For sufficiently large values of ϵ these equations become

$$\frac{dI_i^+}{dz} = \frac{g'I_i^+}{[1+y_i^2][1+s \sum_n \frac{I_n^- + I_n^+}{1+y_n^2}]} - \alpha I_i^+ \quad (10.3-15)$$

$$\frac{dI_i^-}{dz} = - \frac{g'I_i^-}{[1+y_i^2][1+s \sum_n \frac{I_n^- + I_n^+}{1+y_n^2}]} + \alpha I_i^- \quad (10.3-16)$$

where $g' = g/\sqrt{\pi}\epsilon$ is the line center unsaturated gain constant. To simplify the problem we assume that the laser is oscillating in only a

single mode at gain center and distributed losses are negligible.

Then equations (10.3-15) and (10.3-16) reduce to

$$\frac{dI^+}{dz} = \frac{g'I^+}{1+s(I^- + I^+)} \quad (10.3-17)$$

$$\frac{dI^-}{dz} = -\frac{g'I^-}{1+s(I^- + I^+)} \quad (10.3-18)$$

If the radiation were not at gain center, new frequency dependent gain and saturation parameters should be introduced as

$$g^* = \frac{g'}{1+y^2} \quad s^* = \frac{s}{1+y^2} \quad (10.3-19)$$

To find the intensity everywhere in the laser, equations (10.3-17) and (10.3-18) must be solved simultaneously. By using equation (10.3-5), some symmetry arguments, and a little hindsight, one may be led to try a substitution of the form

$$I^+ = \sqrt{a} e^{u(z)} \quad I^- = \sqrt{a} e^{-u(z)} \quad (10.3-20)$$

With $I^+ = I^-$ at $z = 0$. This reduces equations (10.3-17) and (10.3-18) to the single equation

$$\frac{du}{dz} = \frac{g'}{1+2s\sqrt{a} \cosh u} \quad (10.3-21)$$

This equation can be integrated, and the result is

$$z = \frac{1}{g'} [u(z) - u(0) + 2s\sqrt{a} (\sinh u(z) - \sinh u(0))] \quad (10.3-22)$$

This is a transcendental equation from which the z dependence of I^+

and I^- can in principle be determined. These implicit results do not have much intuitive appeal. It turns out, however, that often one is not interested in the intensity everywhere in the laser medium, but only at the ends. A simple explicit solution is possible for the intensity at the ends of the laser.

Using equation (10.3-5), equation (10.3-17) may be rewritten

$$\frac{dI^+}{dz} = \frac{s'I^+}{1 + s(I^+ + \frac{a}{I^+})} \quad (10.3-23)$$

For an amplifying medium of length L this yields

$$g'L = s(I_r^+ - I_\lambda^+) + \ln \frac{I_r^+}{I_\lambda^+} - \frac{sa}{I_r^+} + \frac{sa}{I_\lambda^+} \quad (10.3-24)$$

Using equation (10.3-5) again to eliminate a , this becomes

$$g'L - \ln \frac{I_r^+}{I_\lambda^+} = s[(I_r^+ - I_r^-) + (I_\lambda^- - I_\lambda^+)] \quad (10.3-25)$$

But $I_r^+ - I_r^-$ is just the net power flowing toward the right mirror $I_o^+(1 - R_r)/T_r$, and similarly $I_\lambda^- - I_\lambda^+ = I_o^-(1 - R_\lambda)/T_\lambda$. Therefore, equation (10.3-25) becomes

$$I_o^+ \frac{(1 - R_r)}{T_r} + I_{io}^- \frac{(1 - R_\lambda)}{T_\lambda} = \frac{1}{s}(g'L - \ln \frac{I_r^+}{I_\lambda^+}) \quad (10.3-26)$$

Now if the ratio I_r^+/I_λ^+ were known, equation (10.3-26) together with equation (10.3-14) would determine explicitly the output intensity at both ends of the laser oscillator. Equation (10.3-5) implies

$$\frac{I_r^+}{I_\lambda^+} = \frac{I_\lambda^-}{I_r^-} = \frac{I_\lambda^+/R_\lambda}{R_r^- I_r^+} \quad (10.3-27)$$

Therefore, one obtains

$$\frac{I_r^+}{I_\lambda^+} = \frac{1}{\sqrt{R_\lambda R_r}} \quad (10.3-28)$$

and equation (10.3-26) is

$$I_o^+ \frac{(1 - R_r)}{T_r} + I_o^- \frac{(1 - R_\lambda)}{T_\lambda} = \frac{1}{s} (g'L + \frac{1}{2} \ln R_\lambda R_r) \quad (10.3-29)$$

Combining equations (10.3-14) and (10.3-29) gives the final expressions for the output intensities

$$I_o^+ = \frac{\frac{(T_r/s)}{(1 - R_r) + \sqrt{\frac{R_r}{R_\lambda}(1 - R_\lambda)}}}{(g'L + \frac{1}{2} \ln R_\lambda R_r)} \quad (10.3-30)$$

$$I_o^- = \frac{\frac{(T_\lambda/s)}{(1 - R_\lambda) + \sqrt{\frac{R_\lambda}{R_r}(1 - R_r)}}}{(g'L + \frac{1}{2} \ln R_\lambda R_r)} \quad (10.3-31)$$

Thus we have the nonintuitive result that the output of a one-dimensional high gain laser varies linearly with the unsaturated gain. If g' varies with z due, for example, to nonuniform pumping, then $g'L$ in the preceding equations should be replaced by $\int_0^L g'dz$. If s varies with z or if α is not negligible, then a simple explicit solution is not possible.

Equations (10.3-30) and (10.3-31) are the principle results of this section, and it is instructive to check them against known results. At threshold, for example, the output must go to zero. Then from equation (10.3-30) one finds

$$g'L = -\frac{1}{2} \ln R_L R_R \quad (10.3-32)$$

or

$$\frac{1}{R_L R_R} = e^{2g'L} \quad (10.3-33)$$

But this is just the well known threshold condition for an oscillator with exponential gain. Next one may consider the opposite limit of an oscillator with small single pass gain. In this case the mirror reflectivities must be nearly equal to unity. Then the logarithm in equation (10.3-30) may be expanded and one obtains

$$I_o^+ = \frac{(T_r/s)}{(1 - R_r) + (1 - R_L)} [g'L - \frac{1}{2}(1 - R_r) - \frac{1}{2}(1 - R_L)] \quad (10.3-34)$$

But this is the same as equation (10.2-8) for the zero dimension approximation provided that distributed losses are negligible, as we should expect. Clearly the usual zero dimension approximation ceases to be valid as soon as the mirror reflectivities are significantly less than unity.

We have derived here expressions for the output of high loss one-dimensional lasers in which the waves travelling to the right interact with the same atoms as the waves travelling to the left. The output from the right end of such a laser is found to be always proportional to the output from the left end as the gain is varied. In a

low gain laser one expects the output to vary linearly with the unsaturated gain as shown in Section 10.2. It was shown here that a linear variation is obtained even in lasers with arbitrarily large gain. Rate equations for a high gain laser have been written by Hope^(10.3). However, that author has only obtained analytic solutions in the limit of no saturation.

10.4 Gaussian modes in three-dimensional lasers

Ordinarily when calculating the growth of power in a laser amplifier, one assumes that the intensity is roughly uniform over some cross section. Then the usual one-dimensional saturation results are used. In actual lasers, however, it is often the case that the pump rate and beam intensity have a spatial dependence. Here the possibility of extending the saturation equations to three dimensions will be investigated. The principle assumption made is that the form of the laser beam is known and that only the total power growth is to be determined. In some high gain systems the form of the beam is, of course, affected strongly by saturation. For those cases analytic solutions are generally impossible to obtain. Emphasis here will be on the important and relatively simple problem of Laguerre-Gaussian beam modes. The validity of the one-dimension approximation will be checked. The new three-dimensional saturation equations could be applied in the usual fashion to amplifier and oscillator problems, and the solutions are mostly omitted here.

In most practical lasers the beams are nearly plane waves. Thus the intensity at any point in the laser can be factored into two parts as

$$I(r, \theta, z) = P(z) f(r, \theta, z) \quad (10.4-1)$$

$P(z)$ describes the z dependence of the power and $f(r, \theta, z)$ is a normalized function giving the variation of intensity over any cross section of the beam. For this discussion $f(r, \theta, z)$, the mode structure, is presumed known while $P(z)$ is to be determined.

From equations (2.5-7) and (2.6-13) the saturation equations for a single laser line may be written in their simplest form as

$$\frac{dI}{dz} = \frac{gI}{1 + sI} \quad \text{homogeneous} \quad (10.4-2)$$

$$\frac{dI}{dz} = \frac{gI}{\sqrt{1 + sI}} \quad \text{inhomogeneous} \quad (10.4-3)$$

where here g is the unsaturated line center gain and s is a saturation parameter. If the line is not on the center of the resonance, both g and s will be frequency dependent as indicated previously. In general g will depend on the radius r . For example, in a low pressure gas discharge the dependence is often given approximately by the Bessel function^(10.4)

$$g = g_o J_o \left(\frac{2.40r}{r_o} \right) \approx g_o \left(1 - \frac{1.44r^2}{r_o^2} \right) \quad (10.4-4)$$

where r_o is the radius of the discharge.

In an ordinary axially symmetric low gain laser oscillator with spherical mirrors, the modes are given by the well known Laguerre-Gaussian functions. For the case of axial degeneracy the intensity in a mode may be written in the form of equation (10.4-1) as

$$I(r, z) = P(z) \underbrace{\frac{2p!}{\pi w^2 (\ell+p)!} \left(\frac{2r^2}{w^2} \right)^\ell \left(L_p^\ell \left(\frac{2r^2}{w^2} \right) \right)^2 e^{-\frac{2r^2}{w^2}}}_{f(r, z)} \quad (10.4-5)$$

The spot size w is governed by diffraction and provides the z dependence in $f(r, z)$. Equation (10.4-5) was obtained by normalizing the

intensity distribution, which is given by the square of equation (5.3-7) ^(10.5).

In the absence of saturation, equation (10.4-1) becomes

$$\frac{d}{dz} [P(z) f(r, \theta, z)] = g(r) P(z) f(r, \theta, z) \quad (10.4-6)$$

Integrating equation (10.4-6) over the cross section of the beam yields

$$\frac{d}{dz} P(z) = P(z) \int_0^{2\pi} \int_0^{\infty} r g(r) f(r, \theta, z) dr d\theta \quad (10.4-7)$$

since by definition $f(r, \theta, z)$ is normalized. If the gain is assumed to be the quadratic $g(r) = g_0 - \frac{1}{2} g_2 r^2$ and $f(r, \theta, z)$ is given by equation (10.4-5), the integral in equation (10.4-7) may be performed ^(10.6) with the result

$$\frac{dP}{dz} = P \left[g_0 - \frac{g_2 w^2}{4} (2p + l + 1) \right] \quad (10.4-8)$$

Thus a Laguerre-Gaussian beam grows exponentially (for constant w), but the gain is reduced because of the profile. Moreover, the lowest order (smallest diameter) mode grows fastest. In the case of a laser oscillator this means that because of the profile the fundamental mode ($p = l = 0$) will reach threshold first. Equation (10.4-8) could also have been obtained using the techniques of Chapter V. The spot size w appearing in equation (10.4-8) may vary with z . For instance, in free space it is governed by equation (5.4-31)

$$w^2(z) = \frac{\lambda z_0}{\pi} \left[1 + \left(\frac{z}{z_0} \right)^2 \right] \quad (10.4-9)$$

If losses are important they can be included by subtracting the term

$$P \int_0^{2\pi} \int_0^{\infty} \alpha(r, \theta, z) f(r, \theta, z) r dr d\theta \quad (10.4-10)$$

from the right side of equation (10.4-7) where α is the loss coefficient.

For inhomogeneous saturation one finds from equation (10.4-3)

$$\frac{dP}{dz} = P \int_0^{2\pi} \int_0^{\infty} \frac{rg(r) f(r, \theta, z) dr d\theta}{\sqrt{1 + sf(r, \theta, z)P}} \quad (10.4-11)$$

This integral is of course considerably more complicated than the no saturation expression, equation (10.4-7). For the case of the fundamental Gaussian beam one finds^(10.7), for example,

$$\begin{aligned} \frac{dP}{dz} = & \frac{g_0 \pi w^2}{s} \left[\left(1 + \frac{2sp}{\pi w^2} \right)^{1/2} - 1 \right] + \frac{g_2 \pi w^4}{4s} \left[\ln \left(\frac{\left(1 + \frac{2sp}{\pi w^2} \right)^{1/2} + 1}{\left(1 + \frac{2sp}{\pi w^2} \right)^{1/2} - 1} \right) \right. \\ & \left. - 2 \left(1 + \frac{2sp}{\pi w^2} \right)^{1/2} + \ln \frac{sp}{2\pi w^2} \right] \end{aligned} \quad (10.4-12)$$

This expression is too complicated to be of much use. For a uniform gain it becomes simply

$$\frac{dP}{dz} = \frac{g_0 \pi w^2}{s} \left[\left(1 + \frac{2sp}{\pi w^2} \right)^{1/2} - 1 \right] \quad (10.4-13)$$

The one dimension approximation for a beam of area πw^2 would be from equation (10.4-3)

$$\frac{dP}{dz} = \frac{g_0 P}{\sqrt{1 + \frac{sp}{\pi w^2}}} \quad (10.4-14)$$

The last two equations are compared in Figure 10.2. We see that they agree well at low power levels (to second order in P) but differ for strong saturation. Equation (10.4-13) can be used in the same way as equation (10.4-14). For example, in an amplifier of length L with an approximately constant Gaussian beam the output power is found to be related to the input by

$$g_o L = \sqrt{1 + 2x_0} - \sqrt{1 + 2x_1} + \ln \frac{\sqrt{1 + 2x_0} - 1}{\sqrt{1 + 2x_1} - 1} \quad (10.4-15)$$

where $x = \frac{SP}{\pi w^2}$.

For homogeneous saturation one finds from equation (10.4-2)

$$\frac{dP}{dz} = P \int_0^{2\pi} \int_0^\infty \frac{rg(r) f(r, \theta, z) dr d\theta}{1 + sf(r, \theta, z)P} \quad (10.4-16)$$

For uniform gain and a Gaussian beam this is^(10.8)

$$\frac{dP}{dz} = \frac{g_o \pi w^2}{2s} \ln(1 + \frac{2SP}{\pi w^2}) \quad (10.4-17)$$

The one dimension approximation would be

$$\frac{dP}{dz} = \frac{g_o P}{1 + \frac{SP}{\pi w^2}} \quad (10.4-18)$$

These expressions are also compared in Figure 10.2 and again they agree to second order in P . It is evident from the graph that in general the one dimension approximation overestimates the effects of saturation.

In summary, the elementary one dimension saturation equations have been extended to three dimensions for some simple but important

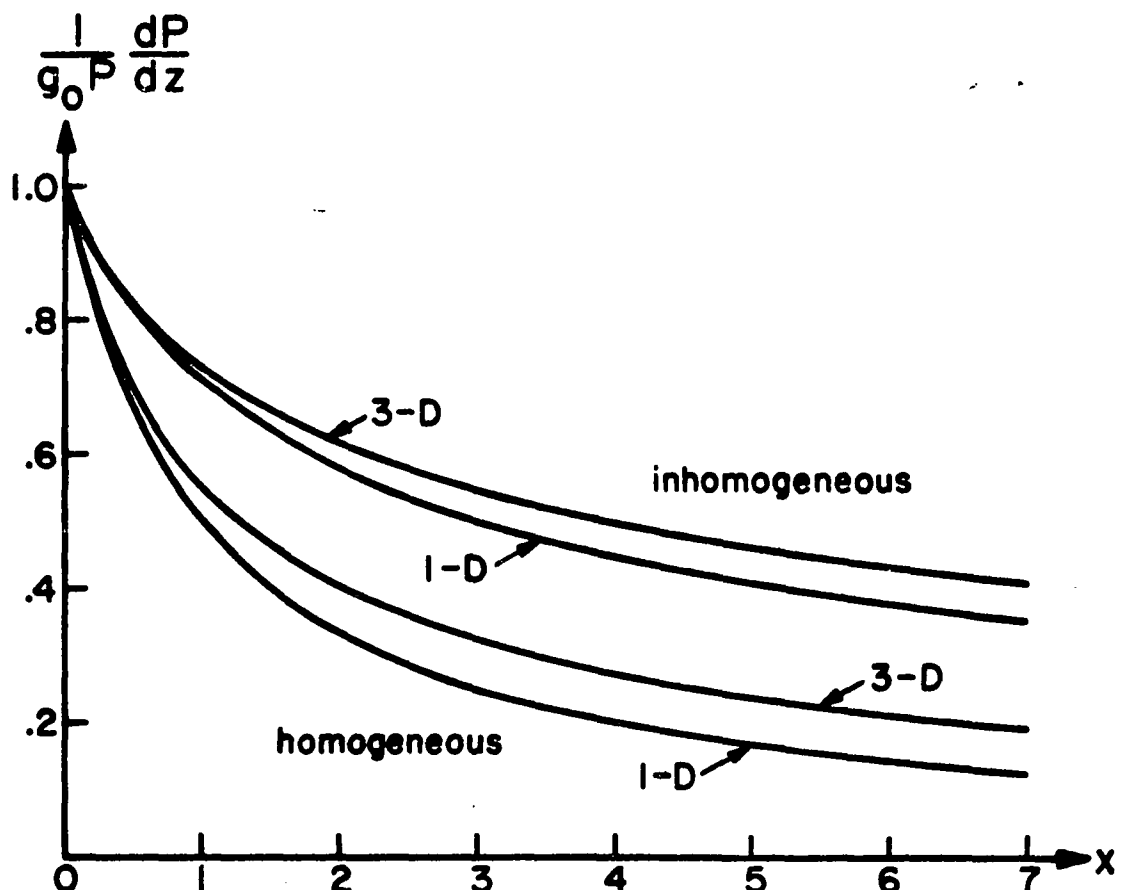


Figure 10.2 $\frac{I}{g_0 P} \frac{dP}{dz}$ versus $x = \frac{sP}{\pi\omega^2}$ for homogeneous and inhomogeneous saturation in one and three dimensions.

- 317 -

laser situations. The results differ significantly when the saturation is severe. Thus, in a saturated laser with a Gaussian transverse mode one should use the new equations even if the gain per pass is small.

10.5 Experiment

In Section 10.3 expressions were obtained for the power output of a laser having an arbitrarily large single pass gain. Here we describe an experiment which has been performed in an effort to verify the theoretical results. The laser used a high gain xenon amplifier at a wavelength of 3.51 microns. Xenon is inhomogeneously broadened, so it is not necessarily true that the light travelling to the right interacts with the same atoms as the light travelling to the left. However, if the laser cavity is made sufficiently long, the mode spacing becomes comparable to the saturation broadened homogeneous line width. Then the light spectrum is effectively continuous and the saturation is identical to homogeneous saturation (Section 2.6). If the laser is operated well above threshold, the addition of new modes with increasing gain will have a negligible effect on the output power. Then the output should be given approximately by equations (10.3-30) and (10.3-31).

For our experiments a cavity length of 10.7 meters was used. The resulting mode spacing was about $c/2L \approx 14$ MHz. The results of Section 10.3 should be applicable except near threshold. The apparatus is shown in Figure 10.3. The D.C. discharge was 5.5 millimeters in diameter and the pressure was maintained at about 5 microns by means of a liquid nitrogen trap^(10.9).

Some typical data are shown in Figure 10.4. Figure 6.6 was used for the gain calibration, and the power was calibrated with an Eppley thermopile. A straight line is drawn through the data in accordance with equation (10.3-30). The agreement is good except close to

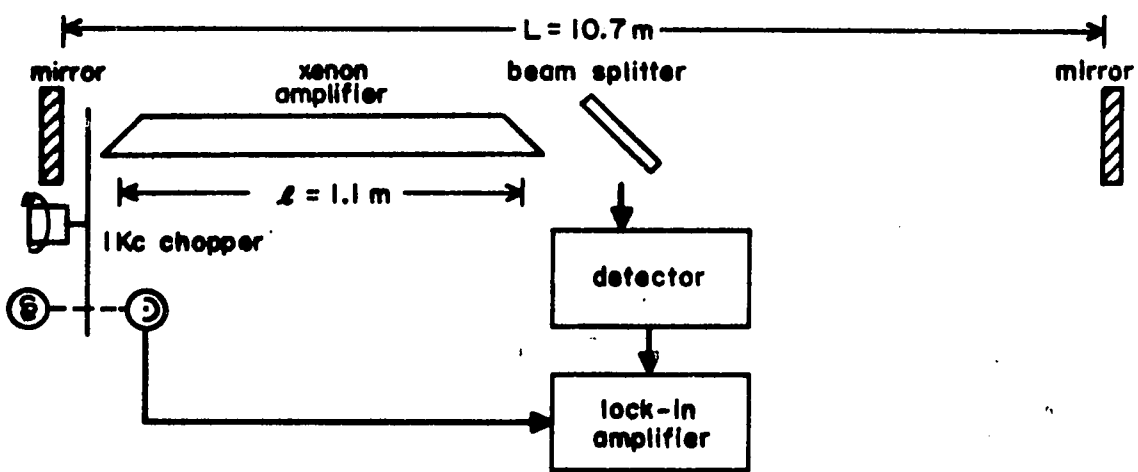


Figure 10.3 Experimental setup

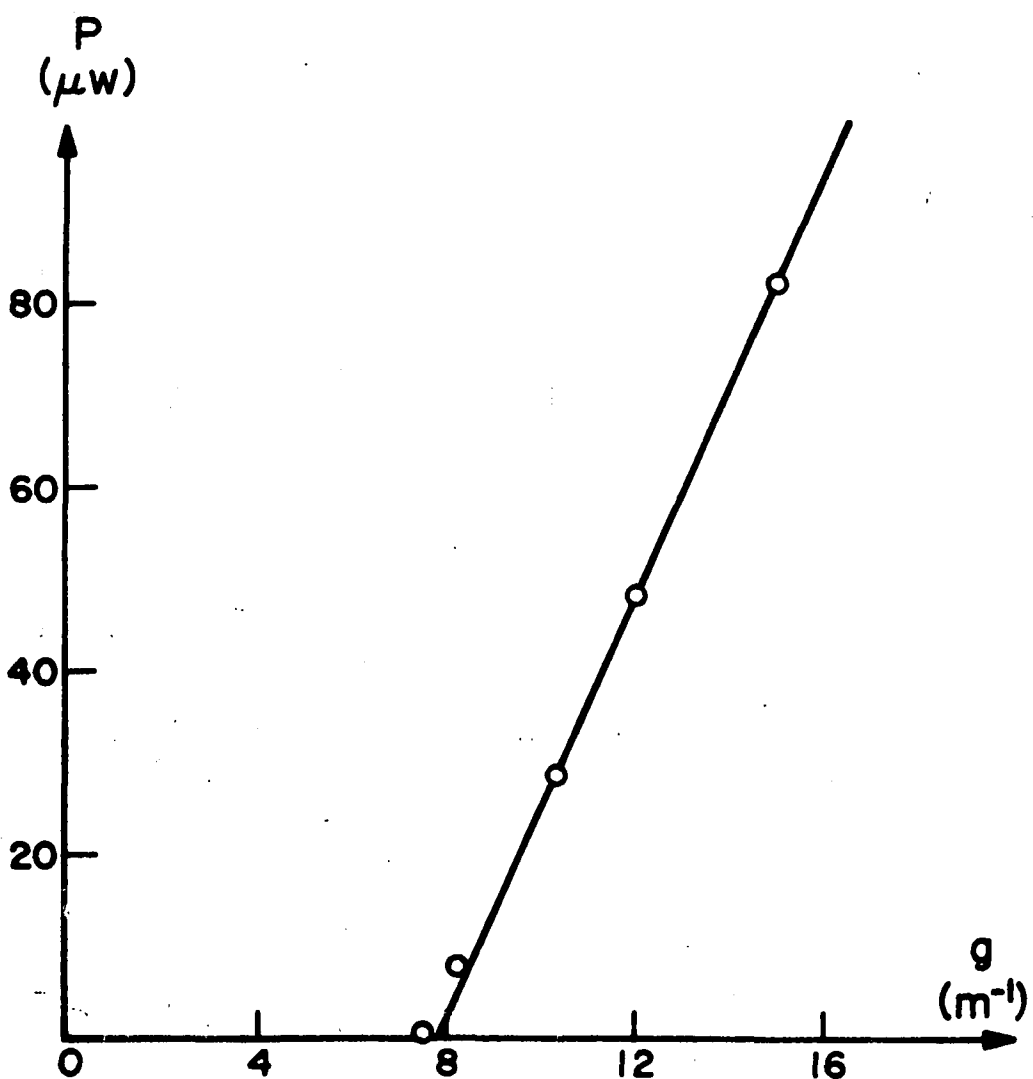


Figure 10.4 Output power versus unsaturated gain for fixed losses.

threshold. The slight discrepancy there probably results from the addition of new modes with increasing gain. This effect becomes unimportant with strong saturation. In any case the agreement between theory and experiment is regarded as satisfactory. For a more rigorous test of the one-dimensional theory a high gain homogeneously broadened laser should be used, but none was available to us.

10.6 Conclusion

Spatial variations of the electromagnetic fields and gain are often neglected in calculating the saturated power in laser amplifiers and oscillators. As a consequence of these approximations, one can at best hope for qualitative agreement between theory and experiment. In this chapter we have obtained some generalizations of the usual zero dimensional theory which include spatial variations. Simple expressions have been derived for the output of a one-dimensional laser with arbitrarily large gain, and experimental verification has been obtained. The basic saturation formulas have also been generalized to include the effects of a Gaussian beam profile. The analysis in this chapter is not exhaustive. The purpose has been to introduce some simple generalizations and solutions which should extend the usefulness of the familiar saturation results.

Bibliography

- 10.1 C. L. Tang, H. Statz and G. deMars, Journal of Applied Physics 34, No. 8, page 2289, August 1963.
- 10.2 W. W. Rigrod, Journal of Applied Physics 34, No. 9, page 2602, September 1963.
- 10.3 L. L. Hope, IEEE Journal of Quantum Electronics QE-4, No. 11, page 888, November 1968.
- 10.4 W. R. Bennett, Applied Optics Supplement 2, Chemical Lasers, page 3, 1965.
- 10.5 A useful integral for obtaining the normalization is 7.414-3 of I. S. Gradshteyn and I. M. Ryzhik, Table of Integrals, Series and Products, Academic Press, New York, 1965.
- 10.6 A useful integral is equation (21) of Section 12.2 of H. Buchholz, The Confluent Hypergeometric Function, Springer, New York, 1969.
- 10.7 This integral can be evaluated by making the substitution $y = e^{-2r^2/w^2}$ and using equation 2.727-5 of Gradshteyn and Ryzhik, op. cit.
- 10.8 This integral is elementary after the substitution $y = e^{-2r^2/w^2}$.
- 10.9 D. Armstrong, IEEE Journal of Quantum Electronics QE-4, page 968, 1968.